2013

A History of Sea Ice in the Cenzoic Arctic Ocean

Cristin Ashmankas
University of Rhode Island, igo2cea@gmail.com

A HISTORY OF SEA ICE IN THE CENOZOIC ARCTIC OCEAN

BY

CRISTIN ELIZABETH ASHMANKAS

A THESIS SUBMITTED IN PARTIAL FULFILLMENT

OF THE REQUIREMENTS FOR THE DEGREE OF

MASTER OF SCIENCE

IN

OCEANOGRAPHY

UNIVERSITY OF RHODE ISLAND

2013

MASTER OF SCIENCE THESIS

OF

CRISTIN E. ASHMANKAS

APPROVED:

Thesis Committee:

Major Professor

Kathryn Moran

_____

Steve D'Hondt

_____

Christopher Baxter

_____

Nasser Zawia

_____

DEAN OF THE GRADUATE SCHOOL

UNIVERSITY OF RHODE ISLAND
2013

ABSTRACT

The body of this work focuses on the use and revelations of grain size distributions combined with age models and physical properties of sediments, expanding our understanding of the central Arctic Ocean in the Cenozoic Era. The Integrated Ocean Drilling Program's (IODP) Expedition 302, Arctic Coring Expedition (ACEX), recovered sediment cores from the Lomonosov Ridge, providing the most extensive geologic record of the region ever recovered. This record provides the first opportunity for scientists to directly determine the paleo- ice history of the region, one of high importance to understanding global climate.

Grain size distribution analyses reveal a more consistent ice presence than previously believed possible for the region. The implication suggests a simultaneous transition to a strong cryo-state occurring at both poles. This differs from the previous paradigm of the Antarctic's cryo-state strengthening millennia earlier than the Arctic. A simultaneous transition to a stronger cryo-state implies a global climatic driver, disavowing theories of current and continental shifts driving one pole than the other.

Due to the premiere opportunity to study the cryo-state of the central Arctic Ocean over a significant portion of the Cenozoic, proxies and analysis techniques needed to be developed and updated. A series of proxies for determining the type and intensity of the cryo-state are presented and employed in paleo- analyses. In addition, predictive relationships between grain size distributions and the physical properties of the sediments developed for these glacio-marine sediments allows more extensive analysis that can be used in the future to determine regions of interest non-destructively to the cores. This will be of significant benefit to future expeditions to

the region. Finally, the use of grain size to determine and remove the effects of paleo-currents was updated for the unique depositional environment. Interconnecting other elements of the global climate system to the central Arctic's cryo-state demonstrates the true interconnectedness of the global system.

ACKNOWLEDGEMENTS

"The greatest glory of living lies not in never falling, but in rising every time you fall."

-Nelson Mandela

My deepest, sincerest thanks to everyone who has been there when I've fallen; ready to support me as I've risen.

My thanks to the advice and assistance provided by: Steve D'Hondt, Chris Baxter, John King, and Becky Robinson. It was with their push that I worked harder and went farther, gaining the knowledge and confidence I needed to pursue my own path. I would also like to thank Harold Bibb, Rob Pockalny, Meredith Clark, and Peter August for their invaluable support, aid, and direction along the way.

The research in this thesis was completed with the samples, data and work of the Integrated Ocean Drilling Program (IODP) and the ACEX scientists. I was supported with a series of funding from the U.S. National Science Foundation (NSF), University of Rhode Island, and the Discovery Channel. It is with such support that the next generation of science is able to progress.

To my graduate associates on bay campus, Meghan, Meghan, Oliver, Julie, Katy, Junsheng, and others, I owe all of you so many small kindnesses. I have been blessed to have so generous colleagues. To my friends, Gretchen, Andria, Rob, Kerri and the rest, thank you for my sanity, which would have been lost with out you. You were there each and every time I needed you.

Thank you to my family who have agonized with me every step of the way. Your belief and pride in me has provided me the freedom and love to see my dreams through to wherever they may lead. Most children are talked out of their youthful dreams and fancies. You not only never questioned them, you encouraged them. I can't even begin to describe what kind of gift that is or the impact it has made. This thesis is as much yours as it is mine.

PREFACE

Expedition 302, Arctic Coring Expedition (ACEX), of the Integrated Ocean Drilling Program (IODP) was the initial attempt at a mission specific platform expedition. It was successfully completed in the summer of 2004, retrieving ~420 m of core from the Lomonosov Ridge, central Arctic Ocean, recovering a substantial portion of the Cenozoic Era. This was the first such extensive recovery of the region's sedimentary history. I have been investigating the sea ice history of those cores, looking predominantly at the < 2000 μm grain size fractions.

The following thesis is presented in a manuscript format, comprising of three chapters outlining much of the research I have completed on the ACEX cores sediment samples. This work both answers some of the questions concerning the central Arctic's paleo- cryo-state as well as raising new avenues of investigation. It is my hope that the following chapters will provide a solid foundation for future Arctic cryo-state investigations, the importance of which cannot be understated to understanding the global climate system.

Chapter 1 of this thesis formulates proxies for various aspects of the cryo-state, particularly the form of ice and intensity of the climate's frozen state. These proxies are utilized along with published age models to determine the ages of various climate states. There is particular focus on the different cryo-states present in the neogene and paleogene.

Chapter 2 of this thesis focuses on relationships between the grain size distributions and the non-destructive measurements of a multi-sensor core logger

(MSCL) or the physical properties of the sediments. These relationships were utilized in the creation of predictive equations, translating the sediment's physical properties into cryo-state proxies. This permits us to investigate through the high- resolution nature of MSCL data, the precise timing of major cyro-state transitions. These transitions are compared to the transitions in the SST record. The methods formulated in this chapter are of particular interest to the conduction of future glacio-marine expeditions.

Chapter 3 of this thesis utilizes a method set forth by others for the investigation of paleo- current intensity. The method commonly referred to as 'sortible silt', uses the mean diameter of the silt fraction in a sample as a measure of current strength. Employing this method, I was able to minimize the winnowing effect of a sample, translating it to a distribution more similar to that found at the original time of deposition. This eliminates much of the high- frequency changes in samples' grain size distributions. It also provided a means of comparing transitions in current strength to those of cryo- state, demonstrating the inter-connected quality of the global system. This interconnected nature was particularly examined in the late Pleistocene.

TABLE OF CONTENTS

LIST OF TABLES

LIST OF FIGURES

Chapter 1

"Arctic Coring Expedition, IODP 302, Grain Size Analyses, Revealing Arctic Paleo- Cryo Environments"

by

Cristin E. Ashmankas[1,2]

written for submission to Journal of Paleoceanography

[1] Graduate School of Oceanography, The University of Rhode Island, Narragansett, RI 02882.
[2] Assistant Professor, Natural Science and Mathematics Division, Lesley University, Cambridge, MA 02138. Email: cashmank@lesley.edu

Chapter 1. Arctic Coring Expedition, IODP 302, Grain Size Analyses, Revealing Arctic Paleo- Cryo Environments.

ABSTRACT

Summer 2004 hosted an unprecedented event in Arctic research; the successful coring of Arctic sediments to obtain a paleo-ice record that extends through the Cenozoic Era. Low-resolution grain size analyses of samples taken during the Arctic Coring Expedition (ACEX), IODP 302, reveal five ice rafted debris (IRD) relationships, which we hypothesize to correspond to five distinct Arctic paleo-ice environments. This study defines IRD as the percentage of terrigenous grains > 63 μm. IRD is comprised of both sea-ice rafted debris (SIRD) and iceberg rafted debris (IBRD). IBRD is defined as the percentage of terrigenous grains > 250 μm. Grain size analyses were completed using a laser diffraction type analyzer (a Malvern Mastersizer 2000). The five relationships and their corresponding environments are: 1) low sand percentage and low coarse sand percentage, indicating a seasonally cold environment with little ice of glacial origin, 2) high sand percentage and low coarse sand percentage, an indication of a sea-ice dominated environment, 3) low sand percentage and high coarse sand percentage, indicative of conditions of considerable iceberg expulsion and low sea-ice production, 4) no sand present, corresponding to a warm ice-free Arctic climate, and 5) an extremely high coarse sand contribution, which supports a river ice dominated site. The earliest indication of IRD in the ACEX record occurs in the Eocene, a time much earlier than the intensification of Northern Hemisphere glaciation of ~3 Ma. Throughout the Neogene, IRD remains an important component of the sedimentary record. Differentiating modes of IRD in terms of SIRD

and IBRD is an important step in reconstructing Arctic paleo-environments and the Arctic paleo- albedo contribution.

INTRODUCTION

The Arctic Ocean is a relatively shallow ocean basin roughly centered on the northern pole of the Earth, with water exchange between the Arctic and the Atlantic Ocean through both the Fram and Davis Straits and with the Pacific Ocean through the Bering Strait (Herman, 1974; Coachman and Aagaard, 1974; Aagaard, 1981) (Figure 1.1). This ocean has a major contributing influence on the Atlantic, Pacific Oceans, and global thermohaline circulation, and is strongly influenced by the Atlantic and Pacific intermediate and surface waters, and the production/dissolution of sea ice (Aagaard, 1981). The Arctic Ocean has two key roles in the Earth's climate system. It acts as a climate regulator by controlling solar insulation at high latitudes with changes of the ocean's albedo through the presence or absence of ice cover and by influencing thermohaline circulation (Singarayer et al., 2006; Dethloff et al., 2006; Curry et al., 1995; Holland and Bitz, 2003; Broecker, 1997; Holland et al., 2001, Rennermalm et al., 2006). It is this quality of the Arctic Ocean that makes it a dynamic location with global implications and of key importance to fully understanding global climate. One of the goals of the Integrated Ocean Drilling Program (IODP) Expedition 302, the Arctic Coring Expedition (ACEX), a multi-national study funded through the National Science Foundation (NSF), the IODP, and others is to investigate the paleo sea ice dynamics of the Arctic Ocean's central region (Backman et al., 2004).

Processes within the Arctic Ocean act as controlling mechanisms for heat and freshwater (Coachman and Aagaard, 1974; Aagaard, 1981; Aagaard and Carmack, 1989). The dominating presence of sea ice across the Arctic Ocean greatly increases the region's albedo and facilitates the redirection of solar radial heat/energy back into space (Singarayer et al., 2006; Dethloff et al., 2006; Curry et al., 1995; Holland and Bitz, 2003). The loss of heat feeds into the formation of ice in the region, sequestering freshwater and feeding back into strengthening the albedo. This strengthening albedo can be the result of exclusively sea ice, whose formation has only a temperature dependence. It can also be the result of continental glaciation, whose formation is dependent on both low temperatures and high humidity. Sea ice formation isolates much of the local sources of humidity needed for glacier formation. Alternatively, glacier formation sequesters water onto the continents, lowering sea level, raising salinities, and thus lowering the temperature required for sea ice production. This means that while at the climate extremes, there can exist no ice or an abundance of both forms of ice, it is likely that in periods of transition or average climate the production of one form of ice may negatively impact the production of the other. With open water having a much lower albedo than ice-free terrain, the greater presence of sea ice has a larger effect on the Earth's albedo than a greater presence of glaciers. Through its links to the global ocean system and its considerable effect on the global solar insolation, the Arctic Ocean is a key component of the global climate system.

Various authors had determined the transition to a perennially glaciated Northern Hemisphere as occurring roughly, 2.6-3.1 Ma (Shackleton et al., 1988;

Maslin et al., 1998; Zachos et al., 2001). The presence of IRD in the North Atlantic and mid-latitude $\delta^{18}O$ records are the evidence used for assigning the transition to the late Pliocene (Shackleton et al., 1988; Maslin et al., 1998; Knight et al., 2002; Raymo et al., 2006; Reeh, 2004; Ruddiman, 1977 a, b; Zachos et al., 2001). The advent of the ACEX's ability to retrieve deep cores from beneath the Arctic's ice-covered waters, allows us to redefine the paleoclimate transition to a cold Arctic without the reliance upon these external Arctic proxies.

The cores recovered during ACEX were from locations on the Lomonosov Ridge (Figure 1.2). The Lomonosov Ridge is a rifted portion of the Eurasian continent, separated ~57 Ma by the formation of the Gakkel Ridge (Backman et al., 2006). Subsequently, sediments have been captured on the ridge, providing a record for much of the Cenozoic Era. The sites cored were situated high on the Lomonosov Ridge, above the limit of the turbidite zone, providing for a usable ice rafted debris record. While this record proved to be incomplete with sediment record hiatuses from 9.4 to 11.6 Ma and 18.2 to 44.4 Ma (Backman et al., 2007), we are able to use it to distinguish periods of sea ice and or glacier intensity, subsequently inferring changes in the Arctic's albedo contribution.

METHODS

Grain Size Analyses

The initial step to determining the paleo-ice environment of the Cenozoic Arctic Ocean is to determine the grain size distribution of the cores. To accomplish this, each of the sediment samples was analyzed for the individual grain size

distribution of terrigenous material. The samples were chemically cleaned of biological components in order to isolate the terrigenous portion of each sample. The cleaning process is adapted from a combination of the processes employed by Dr John King's lab (personal communication) and Mortlock and Froelich (1989). The process involved using acetic acid to rid the samples of biogenic carbonate, hydrogen peroxide to remove the lipids in each sample and sodium carbonate to eliminate the biogenic silicate. Approximately 20% of the samples were visually examined to ensure that only terrigenous material remained. The samples were then steeped in a solution of sodium hexametaphosphate for at least 48 hours to ensure that the clay particles were neutralized and no flocculation would occur, skewing the grain size results. Each of the biologically cleaned samples were then run on the Malvern Mastersizer 2000, a laser diffraction particle sizing system. The Mastersizer operates using both a red light laser and a blue light laser. By operating with lasers at two different wavelengths of light the Mastersizer increases the accuracy and precision of the results. The Mastersizer was set to analyze each sample in a general mode and not material specific, since each sample contained multiple mineral components, which could change from sample to sample. These data were then compiled into half phi size bins (phi being a scale of grain size equal to $-\log_2$(diameter of grain)). The Mastersizer sub-sampled each sediment sample three times, determined the grain size distribution and then averaged the three sub-samples. The averaged data set was then transferred into a Microsoft Excel worksheet.

The entire grain size distribution from clay through sand was collected with this method. The focus of this study is on the sand portion, using the finer sediments

as a means of normalizing the sand contribution. The presence of any sand sized grain (>63μm) is indicative of a frozen environment, whether it is sea-ice or iceberg (Bischof, 2000; Lisitzin, 2002). The absence of any sand is suggestive of an Arctic environment where the climate was, on average, above freezing annually.

Ice Rafted Debris and the Glacial Environment

Ice rafted debris (IRD) present in sediment records reveals the presence of ice at a deep ocean location at some time in the geologic past (Jakobsson et al., 2001; Poore et al., 1993; Phillips and Grantz, 1997; Thiede et al., 1989; Gyllencreutz, 2005; Prins et al., 2002; Clark, 1996; Ruddiman, 1977a, b; Sakamoto et al., 2005; Lisitzin, 2002; Eldrett et al., 2007; Bischof and Darby, 1997: 1999; Darby et al., 2002; Bischof et al., 1996; Krissek et al., 1989; Norgaard-Pedersen et al., 1998; Heinrich, 1988; Hald et al., 2004; Nam et al., 1995; Bischof et al., 1999; Bischof, 2000; Winter et al., 1997). Ice is capable of rafting the complete range of sediment sizes from clay to boulder and releases them onto the seafloor in undifferentiated deposits, distinguishing them from turbidite deposits. However, the entire suite of sediment sizes is not useful when determining the cryo- history of an ocean basin. The fine component of sediments, clay and silts, may be corrupted by fluvial and eolian sources. Kotlyakov and Gordienko (1982) found at the Camp Century Station, a modern research station located on the Greenland ice sheet that the aerosol contribution to the site was 0.04 to 8 μm in size and contributed 0.24% of the sediments entrained in the glacier core. Ruddiman (1977a, b), in studies of ice rafted debris in the North Atlantic, determined that an insignificant portion of the coarse component of sediments, gravel to boulder,

are included in 6 to 9 cm diameter cores, excluding them as a reliable indicator or the presence of ice. This leaves the sand component (63 μm to 2000 μm) as the reliably collected and uncorrupted component of sediments to be used in the determination of paleo- ice presence and subsequently –cryo environments (Ruddiman, 1977a,b; Ruddiman and Glover, 1972; Ruddiman and JOIDES, 1991; Smythe et al., 1985; Ruddiman and McIntyre, 1976, 1977, 1981, 1984; Ruddiman et al., 1986). A study by Vanney and Dangeard (1976), examining the sediment size ranges entrained in icebergs and iceberg-related deposits in Baffin Bay, determined that silt comprised 40-60%, clay 20-40% (the higher values found at sites in current-protected depressions), and gravel/pebble 1-10%. The combined contributions of silt and sand typically comprise 50-80% of both the icebergs and their deposits, showing cryo- sediments to be predominately laden with silt and sand size IRD. Nurnberg et al. (1994) studied the sand, silt, and clay fractions of sea ice and icebergs taken in the central Arctic Ocean region during a 1991 research cruise. The analyses showed similar ranges as the Vanney and Dangeard (1976) study (Figure 1.3). This also shows that when analyzing the sand component in its totality there is no significant difference in the sand percentage entrained in sea ice and icebergs, illustrating the need for a method to reliably determine the sea ice and iceberg contributions.

Ruddiman (1977 a, b) found that the sand fraction (63 μm to 2000 μm), representing ice rafted debris from sea ice and icebergs, increases during glacials and decreases during inter-glacials (Figure 1.4). In response to the Ruddiman (1977a, b) study, a number of more modern studies have adopted the use of 63 μm to 2000 μm for determining the Arctic's cryo- strength (Jakobsson et al., 2001; Poore et al., 1993;

Phillips and Grantz, 1997; Thiede et al., 1989; Gyllencreutz, 2005; Prins et al., 2002; Clark, 1996; Sakamoto et al., 2005; Lisitzin, 2002; and Eldrett et al., 2007). The 63 μm barrier for defining ice rafted debris is also supported by analyses of the individual grain size distributions of the ACEX core samples (Figure 1.5). All of the samples analyzed contained sediments for the entire silt range (4 to 63 μm), this included the samples that contained no sand contribution. In those samples, there is consistently sediment up to 63 μm in size, but no larger.

Lisitzin (2002) and Madureira et al. (1997) employed the ratio of the number of ice rafted grains to total number of grains counted to normalize the IRD analysis (Figure 1.6). While this particular study looked at iceberg rafted debris (IBRD), by defining the ice rafted grains as those particles >125 μm, the use of the ratio enhances small differences in the sand fraction percentages.

In this study of the ACEX cores, we employ a similar approach to Madureira et al. (1997). Instead of a grain point count, we use the 63 μm to 2000 μm sand fraction percentage in a ratio to the finer sediment (silt and clay) percentage to interpret glacials and inter-glacials or times of more intense cryo- environments and less intense cryo- environments.

Sea Ice versus Iceberg Rafted Debris

The occurrence of IRD permits us to study the possible ice environment at the time of deposition. This can be achieved with the stipulation that coarser sands characterize an environment dominated by icebergs and finer sands by sea-ice (Bischof et al., 1999; Bischof, 2000; Winter et al., 1997; Lisitzin, 2002). The

understanding that icebergs carry coarser sand material led Bischof and Darby (1997, 1999), Darby et al. (2002), Bischof et al. (1996), and Krissek et al. (1989) to choose to utilize a minimum grain size of 250 μm in their studies of iceberg rafted debris (IBRD). Icebergs carry a complete suite of sediment sizes. However, Kotlyakov and Gordienko (1982) determined at the Camp Century Station, Greenland (a location of Arctic iceberg origin) that sediments entrained in the glacier ice typically ranged from 2 μm to 2000 μm, a silt- sand dominance. Ruddiman and McIntyre (1976) assigned sediments with >2% of particles >550 μm as iceberg rafted debris (IBRD) after directly investigating the sediment load of Arctic icebergs. Lisitzin (2002) subsequently determined that IBRD samples have ~2.9% in the >500 μm and <1% in pebble or greater. Bellair et al. (1964) found the median diameter of sediments from icebergs calved from Adelie Land, Antarctica to be 35 μm, this value includes the silt and clay fraction. Mulholland (1976) found studying Massachusetts' glacial till that the statistical mode of sediments was 125- 177 μm, this range of values is typically reduced in clay and silt, the finer fractions having been transported away. These mean values are larger than that of sea ice (Table 1.1).

Reimnitz et al. (1993a, b, 1998) compared in the Beaufort Sea sediments in sea ice to bottom sediments. They found that sea ice lacked coarse material, sand represented <2% of any given sample, and that the samples were dominated by silt and clay. Due to the circulation pattern and direction of ice drift in the Arctic Ocean (Figure 1.7), the ACEX IODP 302 sites in the central Arctic Ocean, Lomonosov Ridge, typically are covered with sea ice originating from the Siberian shelf. Modern studies of the Siberian shelf sediments entrained in sea ice lack coarse-grained

material and are characterized by fine-grained glacial material, rarely exceeding 250 μm in diameter (Lisitzin, 2002). Based on these earlier studies, recent studies, (Bischof et al., 1999; Bischof, 2000; Winter et al., 1997) have broken the sand size fraction into a >63 to <250 μm portion to represent sea ice and a >250 μm portion to represent glacial ice.

Additional studies of the granulometric composition of sea ice compared to icebergs supports the use of the coarser sand fraction to represent IBRD and the finer sand fraction to represent sea ice rafted debris (SIRD). Dreimanis and Vagners (1971) found that as one moves from a moraine (a region of sediment entrainment for icebergs) out over the continental shelf (a region of sediment entrainment for sea ice) less sand is present and more silt dominates. Lisitzin and Chernyshova (1970) and Lisitzin (1961a) working in the North Pacific and Bering Sea determined the coarse sand in cores to be glacial in origin and the fine sand-silt sediments (missing coarser sand material) were sea ice in origin.

Finally, these determinations have been further enforced through sediment trap studies in both the Arctic and Antarctic (Wefer et al., 1982, 1990; Honjo 1980; Lisitzin et al. 1994). By examining Antarctic grain distributions from the region around McMurdo Bay, we can more clearly see the grain size distribution differences for icebergs and sea ice (Figure 1.8). The grain size distributions of the icebergs are clearly skewed to the coarser sand fractions, while the sea ice is skewed to the finer sand fractions. One can distinguish in the bottom sediment samples, which sample sites are predominately influenced by sea ice and which are influenced by icebergs (Barrett and Treves, 1981). The use of 250 μm as a division between sea ice and

iceberg rafted debris is further supported by analysis of individual ACEX grain size distributions (Figure 1.9). A number of ACEX samples with significant percentages of fine sand (63 to 250 μm), have either no sand contribution or diminished sand contributions >250 μm.

Goldstein (1983) presents and defines a term R which is the ratio of iceberg (I) to sea ice (SI) and claims iceberg material is distinguished by particles > 500 μm and that Arctic Siberian sea ice is classified by finer material with ~90% of particles being <100 μm in size. He subsequently found that samples from Alpha Ridge, Arctic Ocean, showed that around the white-pink layers, enriched in carbonates, corresponded to periods of greater iceberg presence as represented by high R values.

By dividing the sand sized particles into sea-ice dominated contribution (63-250μm) and iceberg dominated contribution (250μm-2000μm) and by analyses of one contribution compared to the other, this study of central Arctic paleo- ice environments classifies the type of paleo-ice environment. These analyses are normalized and enhanced by using the R- value (I/SI).

RESULTS

The ACEX cores are the initial attempt of the Integrated Ocean Drilling Program (IODP) to utilize a mission specific platform, which allowed the coring ship to remain on site in a dense ice flow. This methodology allowed the recovery of multiple sediment cores, retrieving much of the present lithology. ACEX attempted core recovery at four sites on the Central Lomonosov Ridge, recovering ~420 m of sediment (Figure 1.10). The four sites were chosen along a previously retrieved seismic line, AWI-91090. Sediments from these sites were used to create a composite

record, representing the paleo-environments of the Cenozoic Central Arctic Ocean (Moran et al., 2006). The composite record was ultimately comprised of ~ 67% of the sediment present at the sites. The majority of the recovered sediment (78%) was from the upper 271 m of the 428 m sediment sequence. The recovered cores were visually sequestered into four lithologic units and numbered sequentially from shallowest to deepest. Samples from three of the sites (sites: 2, 3, 4) were used in this study, plotted using a common composite depth (Figure 1.11) and configured using the established age model (Figure 1.12).

Grain size analyses of the ACEX cores reveal similar classifications as those found in the modern ice rafting mechanisms (sea ice, iceberg). The ACEX grain size classifications from 18.2 Ma to present are similar to the distribution of the modern grain size classifications taken directly from central Arctic Ocean sea ice samples in 1991 (Figure 1.13). The similarities between the deposited material and the modern sea ice rafted debris suggests a common sea ice environment for the last 18.2 Ma. The samples are narrowly banded in the silt:clay ratio but vary significantly in the sand percentage. Due to the averaging nature of sedimentation, it is not surprising that the geological proxy does not show any of the potential 'extremes' shown by the modern sea ice measurements.

The ACEX grain size distributions from 44.4 to 50.4 Ma are comparable to the modern classification of grain size of the central Arctic Ocean sea ice and iceberg samples taken in 1991 (Figure 1.14). The similarities of the Paleocene deposited material to the modern combination of grain size directly taken from modern icebergs and sea ice indicate a cryo-environment in the Paleocene with significant contributions

from both ice-rafting mechanisms. The samples are widely banded in the silt:clay ratio, while remaining in the silt and sandy silt classifications. The Eocene samples vary less significantly in the sand percentage than the Neogene samples. The ACEX cores yielded a single sample during the Eocene that has a silty sand classification and is similar to the river ice grain size distribution taken in the Laptev Sea in 1992 (Figure 1.14).

Grain size and Lithology

The ACEX record reveals the consistent presence of central Arctic ice through much of the Cenozoic by the regular occurrence of sand. The intensity and type of ice environment is indicated by changes in the grain size distributions and are fairly consistent within lithologic sub-units (Figure 1.15). ACEX lithology sub-units 1/1 – 1/4 have low organic contributions (<1% wt) and were defined by color and texture. Lithologic sub-unit 1/2 is characterized by elevated coarse sand percentages. Lithologic sub-unit 1/3 is comprised almost entirely of diminshed sand contributions. Lithologic sub-unit 1/4 has a higher coarse sand contribution, while the unit directly below (Lithologic sub-unit 1/5), which incorporates a significant hiatus, has a more moderate coarse sand contributions. Lithologic sub-units 1/6, 2, and 3 are characterized by organic carbon rich sediments (1-3% wt). Units 1/6, 2, and 3 are distinguished predominately by their microfossil assemblages rather than visual changes in color (Backman et al., 2006). Lithologic sub-units 1/6 and 2 are undifferentiated in their terrigenous grain size distributions, with lower sand values and coarse sand values that rapidly fluctuate between extremely high and low values.

Finally, the few samples present in lithology unit 3 show an increase in sand deposition.

Closer analyses of the individual sub-units show samples that depart from the predominant grain size relationship, ice environment, and relative albedo contribution (Table 1.1). Lithologic sub-unit 1/2 yielded 4 samples between 0 and 4 m that show significantly elevated sand contributions with decreased coarse sand contributions, which we interpret as being a vast sea ice environment (Figure 1.16). Sub-unit 1/2 also has 6 samples, which show elevated coarse sand components compared to the majority pf the unit, suggesting an iceberg influence. The majority of this unit is categorized as high sand and low coarse sand contributions compared to the rest of the sub-unit, which we interpret as a perennial sea ice environment. Lithologic sub-unit 1/3 has 6 points that show significantly elevated sand contributions with decreased coarse sand contributions, which we interpret as being a perennial sea ice environment (Figure 1.17). The majority of this unit is categorized as low sand and coarse sand contributions, which we interpret as being a seasonal sea ice presence. Lithologic unit 1/6 has 9 samples between 204 and 220 m that show no sand contributions, which we interpret as being an ice-free environment (Figure 1.18, Table 1.2). Unit 1/5 has 2 samples, which show elevated sand components with low coarse sand contributions, suggesting a vast sea ice environment. The majority of these units are categorized as alternating between low sand- low coarse sand contributions, which we interpret as being a sea ice environment, and low sand- high coarse sand contributions, which we interpret as being iceberg influenced (Figure 1.18). Lithologic unit 2 is categorized as alternating between low sand- low coarse sand contributions, which we interpret as a

sea ice environment, and low sand- high coarse sand contributions, which we interpret as being iceberg influenced (Figure 1.19). Lithologic unit 3 has one sample that shows extremely elevated sand contributions with extremely coarse sand contributions, which with further investigation for this time period may prove to be a river ice environment (Figure 1.20, Table 1.3). The unit has two samples, which show low sand and coarse sand contributions, which we interpret as a sea ice environment. The unit also has one sample with an elevated coarse sand component, suggesting an iceberg influence.

Grain Size and Age

ACEX grain size distributions can be interpreted in the context of time. The ACEX age model as determined by Backman et al. (2007) defines two hiatuses of sediment retention in the cores. The earliest sedimentation in the ACEX cores (44.4-51 Ma), preceding the early, longer hiatus, shows a diminished sand component, and a widely varying coarse sand component. The calculated mass accumulation rates (MAR) for the percentage of IRD in this region of core ranges from 0.0 to 0.23 $g*ka^{-1}*cm^{-2}$, while the range of MAR for SIRD is 0.0 to 0.49 $g*ka^{-1}*cm^{-2}$. Sedimentation between the hiatuses (11.6- 18.2 Ma) shows again a relatively steady sand component, but with an increasing coarse sand component. MAR ranges for this region of core range from 0.01 to 0.11 $g*ka^{-1}*cm^{-2}$ for IRD and 0.01 to 0.29 $g*ka^{-1}*cm^{-2}$ for SIRD. Sedimentation from present to the more recent hiatus (0- 9.4 Ma) shows a relatively consistent sand component, with a decreasing coarse sand component (Figure 1.21). IRD MAR values for these samples ranged from 0.04 to 0.24 $g*ka^{-1}*cm^{-2}$, while SIRD ranged from 0.04 to 0.49 $g*ka^{-1}*cm^{-2}$. The MAR ranges are consistent and similar to

the values determined by St. John (2008). The general shape distribution is also similar t the one published in that study (St. John, 2008).

44.4- 51 Ma has one period that shows a significantly extreme of elevated sand contribution with a corresponding elevated coarse sand contribution, which may prove to be a river ice environment (Figure 1.22). The time range also has a period, which shows an elevated sand component with low coarse sand, suggesting an elevated sea ice environment. The time range has three periods with no sand contribution, corresponding to an ice-free environment. The majority of the time range is categorized as alternating between samples having low sand- low coarse sand contributions, indicating a sea ice environment, and low sand- high coarse sand contributions, interpreted as an elevated iceberg influence.

The time range from 11.6- 18.2 Ma has two periods that show significantly elevated sand contributions with decreased coarse sand contributions, a sea ice environment (Figure 1.23). The majority of the time range alternates between, low sand- elevated coarse sand components, suggesting an iceberg influence, and low sand- low coarse sand contributions, a diminished, but perennial sea ice environment. The switch between the two regimes took place around 14.5 Ma.

The time range of 0- 9.4 Ma has six periods that show significantly elevated sand contributions with decreased coarse sand contributions, which we interpret as being a sea ice environment (Figure 1.24). This time range also contains samples, which show elevated coarse sand components, suggesting an iceberg influence. The majority of the time range is categorized as having low sand and coarse sand contributions, a diminished, but perennial sea ice environment.

Principle Component Analysis

Principle Component Analysis (PCA) is a popular statistical regression model, commonly used to find variable relationships in seemingly unrelated and independent variables. After extensive use of PCA, it was found no statistically significant variables could be isolated from the ACEX grain size data set (Figure 1.25). There was a slight, non-significant, reliance on the variation in the data towards coarser grain sizes. This is due to the nature of grain size percentages skewing towards coarser grain sizes with the presence of only a few grains. The overall lack of significant variables is most likely a product of the inherent inter-dependence of grain size distributions. When a single grain size bin increases, all other bins naturally decrease. The lack of unrelated, independent variables makes grain size distributions poor candidates for PCA.

DISCUSSION

The interpretation of the overall grain size from the central Arctic Ocean supports a mid-Cenozoic transition to a perennial cyro-state. Diminished sand deposits between 44.4 and 51 Ma is supportive of a seasonal ice presence (Figure 1.21). This interpretation is further supported by the presence of a sea ice dependant diatom *Synedropsis* in the core stratigraphy from 45.5 to 46.97 Ma (Stickley et al., 2009). The percentage of *Synedropsis* has a positive correlation with the IBRD/SIRD, in a relationship determined between IBRD/SIRD and the diatom sampling that were within a centimeter in the core (Figure 1.26). (Additional data are not available for this relationship determination at this time, due to sampling periodicity differences,

SIRD differences in Stickley et al. (2009) from this study, and fundamental differences in methodology.) The relationship suggests that while the Arctic at this time was seasonally sea ice covered with occasional periods of iceberg presence, the icebergs appear at times of particularly strong seasonal sea ice (ergo strong *Synedropsis* deposition). Since the seasonal ice presence, supported by both studies, would have corresponded to the winter or dark season in the Northern Hemisphere, the sea ice in the Early Cenozoic would have a minimal effect on global albedo. Any albedo contribution would have likely been isolated to the spring season, when the waters had not warmed above freezing and the light had returned to the region. The albedo contribution drops to essentially non-existent during the time period from 44.6 to 45.3 Ma, a time period in the ACEX cores containing sand-free samples (Table 1.2). After the ACEX cores' major hiatus (18.6- 44.4 Ma), the sediment deposited in the late-Cenozoic supports the theory of a perennial ice environment (Figure 1.22, Figure 1.23). The year-round presence of sea ice in the central Arctic in the late Cenozoic would have contributed to the global albedo, particularly during the Northern Hemisphere's summer season, resulting in a cooler summer season further reducing summer ablation. The even greater contribution of ice in the Central Arctic during the earliest part of the Cenozoic would have enhanced these effects. While the transition from seasonal sea ice to perennial sea ice is not present in the sediments collected on IODP Expedition 302, we are able to limit the transition as some point during the hiatus, 18.6- 44.4 Ma.

While the exact strengthening of the transition to a perennial sea ice cover most likely occurred some time during the 18.6-44.4 Ma hiatus, we do have a

transition from a mix of perennial ice and high iceberg influence (18.6-14.5 Ma) to a perennial sea ice with little to no iceberg influence (14.5 to 11.6 Ma) (Figure 1.21 and 1.23). This may indicate a switch at 14.5 Ma to a perennial sea ice cover of such extent as to make iceberg passage difficult. This strengthening of perennial sea ice extent would correspond to the initiation of North Atlantic Deep Water (NADW) formation, global increased cooling, and the expansion of the E. Antarctic Ice Sheet, all occurring at ~14.5 Ma (Woodruff and Savin, 1989; Hodell and Woodruff, 1994; Pagani et al., 2000). The seemingly synchronicity of all these events suggests either a single global driver, or a domino effect between them (i.e strengthening of Arctic perennial sea ice leads to formation of NADW, which causes global cooling that leads to the ice sheet strengthening). Our interpreted timing of perennial sea ice and Middle Miocene Climate Transition (15-14 Ma) strengthening corresponds to the timing determined by other non-grain size distribution variables such as ice provenance and drift rates, $^{10}Be/^{9}Be$ ratios, and the presence of IRD at lower latitudes (Krylov et al., 2008; Darby, 2008; Haley et al., 2008a, 2008b; Frank et al., 2008, Knies and Gaina, 2008; O'Regan et al., 2010).

The timing of the central Arctic's cryo- state transition, being during the Mid-Cenozoic Era, corresponds to the cryo-state transition of the Antarctic (Zachos, 2001). While the exact timing of the central Arctic's transition can not be determined with out more extensive coring efforts, the work completed in this study supports the theory of a simultaneous cryo-state transition in both polar regions. The glaciation of the Antarctic is associated with a benthic $\delta^{18}O$ value transition from a value of 1 to a value of 2. The transition in the Arctic, being initially predominately sea ice would not

impact the benthic $\delta^{18}O$ value. However, using that as a proxy for global temperatures, it is likely that the Arctic transition is associated with a global temperature of 4- 8° C (Figure 1.25).

Enhanced sand presence is typically interpreted as enhanced sea ice presence; contain an anomalous sample that is the exception to this rule. The sample from ~50 Ma has an extreme percentage of both sand and coarse sand when compared to the rest of the core. We have associated this with river ice, which is most likely seasonal. The river ice presence supports the theorized paleogeography and surface-water circulation proposed by Backman et al. (2006) for 50 Ma. They propose a strong riverine discharge close to the IODP Expedition 302 site.

CONCLUSION

Differentiating sea ice and iceberg contributions and cryo-state enhancements is essential for understanding the dynamics of the Arctic environment. From this study of sediments from the central Arctic Ocean, we can determine and date 5 cryo-states. Once a cyro-state is determined, the relative albedo contribution can be theorized. The Early Cenozoic is dominated by ice- free, seasonal sea ice, and riverine ice cryo- states, or relatively low albedo contribution. The Late Cenozoic is dominated by perennial sea ice and iceberg/perennial sea ice cyro-states, or a relatively high albedo contribution. This transition from low albedo contribution in the Arctic to high takes place much earlier than previous studies had determined. We are now able to establish a transition point as having occurred at some point between 18.6 and 44.4 Ma. Additional, sediment retrieval in the central Arctic region is necessary to precisely date the transition.

REFERENCES

Aagaard, K., 1981. On the Deep Circulation in the Arctic Ocean. Deep-Sea Research, Vol. 28, No. 3, pp. 251-268.

Aagaard, K., E.C. Carmack, 1989. The Role of Sea Ice and Other Fresh Water in the Arctic Circulation. Journal of Geophysical Research, Vol. 94, No. C10, pp. 14485-14498.

Backman, J., M. Jakobsson, M. Frank, F. Sangiorgi, H. Brinkhuis, C. Stickley, M. O'Regan, R. Lovlie, H. Palike, D. Spofforth, J. Gattacecca, K. Moran, and C. Heil, 2007. "Age Model and Core-Seismic Integration for the Cenozoic ACEX Sediments from the Lomonosov Ridge." *Paleoceanography*,

Backman, J., K. Moran, and D. Evans, 2004. "ACEX Arctic Coring Expedition: Paleoceanographic and tectonic evolution of the central Arctic Ocean." *IODP Expedition 302 Scientific Prospectus,* Edinburgh (Integrated Ocean Drilling Program Management International, Inc.).

Backman, J., K. Moran, D.B. McInroy, L.A. Mayer, 2006. *Proceedings of the Integrated Ocean Drilling Program, 302*, Edinburg (Integrated Ocean Drilling Program Management International, Inc.).

Barrett, L., and S.B. Treves, 1981. "Sedimentology and Petrology of Core from DVDP-15, Western McMurdo Sound." *Antarctic Research Series*, Vol. 33, pp. 281-314.

Bischof, J., 2000. *Ice Drift, Ocean Circulation, and Climate Change*. Springer, NY.

Bischof, J., D.L. Clark, and J.S. Vincent, 1996. "Origin of Ice-Rafted Debris: Pleistocene paleoceanography in the western Arctic Ocean." *Paleoceanography*, Vol. 11, No. 6, pp. 743-756.

Bischof, J.F. and D.A. Darby, 1997. "Mid- to Late Pleistocene Ice Drift in the Western Arctic Ocean: Evidence for a different circulation in the past." *Science*, Vol. 277, pp. 74-77.

Bischof, J.F. and D.A. Darby, 1999. "Quaternary Ice Transport in the Canadian Arctic and Extent of Late Wisconsinan Glaciation in the Queen Elizabeth Islands." *Canadian Journal of Earth Science*, Vol. 36, pp. 2007-2022.

Bischof, J.F., D.A. Darby, and C. Majer, 1999. "Very High Resolution Record of Late Pleistocene to Holocene Ice Rafting and Glacio-Fluvial Meltwater Discharge from the Northern Chukchi Sea." *EOS*, AGU, Vol. 80, No. 46.

Broecker, W.S., 1997. "Thermohaline Circulation, the Achilles Heel of our Climate System: Will man-made CO2 upset the current balance?" *Science*, Vol. 278, pp. 1582-1588.

Clark, D.L., 1996. "The Pliocene Record in the Central Arctic." *Marine Micropaleontology*, Vol. 27, pp. 157-164.

Coachman, L.K. and K. Aagaard, 1974. Physical Oceanography of Arctic and Subarctic Seas. Marine Geology and Oceanography of the Arctic Seas, Springer-Veriag, NY.

Curry, J.A., J. Schramm, and E.E. Ebert, 1995. On the Sea-Ice Albedo Climate Feedback Mechanism. Journal of Climate, Vol. 8, pp. 240-247.

Darby, D.A., 2008. "Arctic Perennial Ice Cover Over the Last 14 Million Years." *Paleoceanography,* Vol. 23, PA1S07. doi:10.1029/2007PA001479.

Darby, D.A., J.F. Bischof, R.F. Spielhagen, S.A. Marshall, and S.W. Herman, 2002. "Arctic Ice Export Events and their Potential Impact on Global Climate during the Late Pleistocene." *Paleoceanography*, Vol. 17, No. 2.

Dethloff, K, et al., 2006. A Dynamical Link Between the Arctic and the Global Climate System. Geophysical Research Letters, Vol. 33, L03703.

Dreimanis A., and V.J. Vagners, 1971. "Bimodal Distribution of Rock and Mineral Fragments in Basal Tills." In: R.P. Goldthwait (ed) *A Symposium on Till*, Univ. Press, Ohio, pp. 237-250.

Eldrett, J.S., I.C. Harding, P.A. Wilson, E. Butler, and A.P. Roberts, 2007. "Continental Ice in Greenland during the Eocene and Oligocene." *Nature.*

Frank, M., Backman, J., Jakobsson, M., Moran, K., O'Regan, M., King, J., Haley, B.A., Kubik, P.W., Garbe–Scho¨nberg, D., 2008. "Beryllium Isotopes in Central Arctic Ocean Sediments Over the Past 12.3 Million Years: Stratigraphic and paleoclimatic Implications." *Paleoceanography* , Vol. 23, PA1S02. doi:10.1029/2007PA001478.

Goldstein, R.H., 1983. "Stratigraphy and Sedimentology of Ice-Rafted and Turbidite Sediment, Canadian Basin, Arctic Ocean." In: B Molnia (ed) *Glacial Marine Sedimentation*. Plenum Press, New York, pp. 367-401.

Gyllencreutz, R., 2005. "Late Glacial and Holocene Paleoceanography in the Skagerrak from High-Resolution Grain Size Records." *Paleogeography, Paleoclimatology, Paleoecology*, Vol. 222, pp. 344-369.

Hald, M., H. Ebbesen, M. Forwick, F. Goftliebsen, L. Khomenko, S. Korsun, L.R. Olsen, and T.O. Vorren, 2004. "Holocene Paleoceanography and Glacial History of the West Spitsbergen Area, Euro-Arctic Margin." *Quaternary Science Reviews*, Vol. 23, pp. 2075-2088.

Haley, A.B., Frank, M., Spielhagen, R.F., Eisenhauer, A., 2008a. "Influence of Brine Formation on Arctic Ocean Circulation Over the Past 15 Million Years." *Nature Geoscience*, Vol. 1, pp. 68–72.

Haley, B.A., Frank, M., Spielhagen, R.F., Fietzke, J., 2008b. "Radiogenic Isotope Record of Arctic Ocean Circulation and Weathering Inputs of the Past 15 Million Years." *Paleoceanography* , Vol. 23, PA1S13. doi:10.1029/2007PA001486.

Heinrich, H., 1988. "Origin and Consequences of Cyclic Ice Rafting in the Northeast Atlantic Ocean during the Past 130,000 Years." *Quaternary Research*, Vol. 29, pp. 142-152.

Herman, Y., 1974. Topography of the Arctic Ocean. Marine Geology and Oceanography of the Arctic Seas, Springer-Veriag, NY.

Hodell, D.A., Woodruff, F., 1994. "Variation in the Strontium Isotope Ratio of Seawater during the Miocene: stratigraphic and geochemical implications." *Paleoceanography*, Vol. 9, pp. 405-426.

Holland, M.M., et al., 2001. "The Role of Ice-Ocean Interactions in the Variability of the North Atlnatic Thermohaline Circulation." *Journal of Climate*, Vol. 14, pp. 656-675.

Holland, M.M., and C.M. Bitz, 2003. Polar Amplification of Climate Change in Coupled Models. Climate Dynamics, Vol. 21, pp. 221-232.

Honjo, S., 1980. "Material Fluxes and Mode of Sedimentation in Mesopelagic and Bathypelagic Zones." *Journal of Marine Research*, Vol. 38, pp. 53-97.

Jakobsson, M., R. Lovlie, E.M. Arnold, J. Backman, L. Polyak, J.O. Knutsen, and E. Musatov, 2001. "Pleistocene Stratigraphy and Paleoenvironmental Variation from Lomonosov Ridge Sediments, Central Arctic Ocean." *Global and Planetary Change*, Vol. 31, pp. 1-22.

Knies, J., Gaina, C., 2008. "Middle Miocene Ice Sheet Expansion in the Arctic: views from the Barents Sea". *Geochemistry, Geophysics, and Geosystems*, Vol. 9, Q02015. doi:10.1029/2007GC001824.

Knight, P.G., R.I. Waller, C.J. Patterson, A.P. Jones, and Z.P. Robinson, 2002. "Discharge of Debris from Ice at the Margin of the Greenland Ice Sheet." *Journal of Glaciology*, Vol. 48, No. 161, pp. 192-198.

Kotlyakov, V.M., and F.G. Gordienko, 1982. "Isotopic and Geochemical Glaciology." *Gidrometeoizdat*, Moscow.

Krissek, L.A., 1989. "Late Cenozoic Records of Ice-Rafting at ODP Sites 642, 643, and 644, Norwegian Sea: onset, chronology, and characteristics of glacial/interglacial fluctuations." *Proceedings of ODP, Scientific Results*, Edinburgh (Ocean Drilling Program Management International, Inc.).

Krylov, A.A., Andreeva, I.A., Vogt, C., Backman, J., Krupskaya, V.V., Grikurov, G.E., Moran, K., Shoji, H., 2008. "A Shift in Heavy and Clay Mineral Provenance Indicates a Middle Miocene Onset of a Perennial Sea Ice Cover in the Arctic Ocean." *Paleoceanography* , Vol. 23, PA1S06. doi:10.1029/2007PA001497.

Lisitzin, A.P., 2002. *Sea-Ice and Iceberg Sedimentation in the Ocean*. Springer, NY.

Lisitzin, A.P., 1961. "Ice-Rafted Deposits and Glacial Epochs on the Polar Areas and their Importance for Paleogeography." *International Geography Congress in Stockholm*, pp. 33-43.

Lisitzin, A.P., and V.I. Chernyshova, 1970. "Rock Material from Bottom Sediments of the North Pacific." In: *The Pacific Ocean*, Nauka, Moscow, pp. 237-296.

Lisitzin, A.P., V.P. Shevchenko, M.E. Vinogradov, O.V. Severina, V.V. Vavilova, I.N. Mitzkevich, 1994. "Particle Fluxes in the Kara Sea and Ob and Yenisei Estuaries." *Oceanology*, Vol. 34, pp. 748-759.

Madureira, L.A.S., S.A. Kreveld, G. Eglington, H. Maureen, G. Ganssen, J.E. Hinte, J.J. Ottens, 1997. "Late Quaternary High-Resolution Biomarker and other Sedimentary Climate Proxies in a Northeast Atlantic Core." *Paleoceanography*, Vol. 12, pp. 255-269.

Maslin, M.A., X.S. Li, M.F. Loutre, and A. Berger, 1998. The Contribution of Orbital Forcing to the Progressive Intensification of Northern Hemisphere Glaciation. Quaternary Science Reviews, Vol. 17, pp. 411-426.

Moran, K., J. Backman, H. Brinkhuis, S.C. Clemens, T. Cronin, G.R., Dickens, et al., 2006. "The Cenozoic Palaeoenvironment of the Arctic Ocean." *Nature*, Vol. 441, pp. 601-605.

Mortlock, R.A., and P.N. Froelich, 1989. "A Simple Method for the Rapid Determination of Biogenic Opal in Pelagic Marine Sediments." *Deep-Sea Research*, Vol. 36, No. 9, pp. 1415-1426.

Mulholland, J.W., 1976. "Texture of Tills, Central Massachusetts." *Journal of Sedimentary Petrology*, Vol. 46, pp. 778-787.

Nam, S.I., R. Stein, H. Grobe, and H. Hubberten, 1995. "Late Quaternary Glacial-Interglacial Changes in Sediment Composition at the East Greenland Continental Margin and their Paleoceanographic Implications." *Marine Geology*, Vol. 122, pp. 243-262.

Norgaard-Pedersen, N., R.F. Spielhagen, J. Thiede, and H. Kassens, 1998. "Central Arctic Surface Ocean Environment during the Past 80,000 Years." *Paleoceanography*, Vol. 13, No. 2, pp. 193-204.

Nurnberg, D., I. Wollenburg, D. Dethleff, H. Eicken, H. Kassens, T. Letzig, E. Reimnnitz, and J. Thiede, 1994. "Sediments in the Arctic Sea Ice: Implications for entrainment, transport, and release." *Marine Geology*, Vol. 119, pp. 185-214.

Pagani, M., Arthur, M.A., Freeman, K.H., 2000. "Variations in Miocene Phytoplankton Growth Rates in the Southwest Atlantic: Evidence for changes in ocean circulation." *Paleoceanography*, Vol. 15, pp. 486-496.

Phillips, R.L., and A. Grantz, 1997. "Quaternary History of Sea Ice and Paleoclimate in the Amerasia Basin, Arctic Ocean, as Recorded in the Cyclical Strata of Northwind Ridge." *GSA Bulletin*, Vol. 109, No. 9, pp. 1101-1115.

Prins, M.A., L.M. Bouwer, C.J. Beets, S.R. Troelstra, G.J. Weltje, R.W. Kruk, A. Kuijpers, and P.Z. Vroon, 2002. "Ocean Circulation and Iceberg Discharge in the Glacial North Atlantic: Inferences from unmixing of sediment size distributions." *Geology*, Vol. 30, No. 6, pp. 555-558.

Poore, R.Z., R.L. Phillips, and H.J. Rieck, 1993. "Paleoclimate Record for Northwind Ridge, Western Arctic Ocean." *Paleoceanography*, Vol. 8, No. 2, pp. 149-159.

Raymo, M.E., L.E. Lisiecki, and K.H. Nisancioglu, 2006. "Pli-Peistocene Ice Volume, Antarctic Climate, and the Global $\delta^{18}O$ Record." *Science*,

Reeh, N., 2004. "Holocene Climate and Fjord Glaciations in Northeast Greenland: implications for IRD deposition in the North Atlantic." *Sedimentary Geology*, Vol. 165, pp. 333-342.

Reimnitz, E., M. McCormick, K. McDougall, and E. Brouwers, 1993a. "Sediment Export by Ice-Rafting from Coastal Polynya, Arctic, Alaska, USA." *Arctic and Alpine Research*, Vol. 25, pp. 83-89.

Reimnitz, E., J.R. Clayton, E.W. Kempema, J.R. Payne, W.S. Wefer, 1993b. "Interaction of Rising Frazil with Suspended Particles: Tank experiments with application to nature." *Cold Regions Science and Technology*, Vol. 21, pp. 117-135.

Reimnitz, E., M. McCormick, J. Bischof, D.A. Darby, 1998. "Comparing Sea-Ice Sediment Load with Beaufort Sea Shelf Deposits: Is entrainment selective?" *Journal of Sedimentary Research*, Vol. 68, pp. 777-787.

Rennermalm, A.K., E.F. Wood, S.J. Dery, A.J. Weaver, and M. Eby, 2006. Sensitivity of the Thermohaline Circulation to Arctic Runoff. Geophysical Research Letters, Vol. 33, L12703.

Ruddiman, W.F., 1977a. "Late Quaternary Deposition of Ice Rafted Sand in the Subpolar North Atlantic (Lat. 40º to 65º N)." *Geological Society of America Bulletin*, Vol. 88, pp. 1813-1827.

Ruddiman, W.F., 1977b. "North Atlantic Ice Rafting: a major change at 75000 years before present." *Science*, Vol. 196, pp. 1208-1211.

Ruddiman, W.F., and L.K. Glover, 1972. "Vertical Mixing of Ice-Rafted Volcanic Ash in North Atlantic Sediments." *Geological Society of America Bulletin*, Vol. 83, pp. 2817-2836.

Ruddiman, W.F., and JOIDES NAAG-DPG, 1991. "North Atlantic-Arctic Gateways." *JOIDES Journal*, Vol. 17, pp. 38-50.

Ruddiman, W.F., and A. McIntyre, 1976. "Northeast Atlantic Paleoclimatic Changes over the Past 60000 Years." *Geological Society of America Mem*, Vol. 145, pp. 111-146.

Ruddiman, W.F., and A. McIntyre, 1977. "Late Quaternary Surface Ocean Kinematics and Climatic Change in the High-Latitude North Atlantic." *Journal of Geophysical Research*, Vol, 82, pp. 3877-3887.

Ruddiman, W.F., and A. McIntyre, 1981. "The North Atlantic Ocean during the Last Deglaciation." *Palaeogeography Palaeoclimatology Palaeoecology*, Vol. 35, pp. 145-214.

Ruddiman, W.F., and A. McIntyre, 1984. "Ice-Age Thermal Response and Climatic Role of the Surface Atlantic Ocean, 40ºN to 63ºN." *Geological Society of America Bulletin*, Vol. 95, pp. 381-396.

Ruddiman, W.F., N.J. Shackleton, and A. McIntyre, 1986. "North Atlantic Sea-Surface Temperatures for the Last 1.1 Million Years." In: M. Smmaerhayes, N.J. Shackleton (eds) *North Atlantic Palaeoceanography*. Geological Society Special Publications, Vol. 21, pp. 155-173.

Sakamoto, T., M. Ikehara, K. Aoki, K. Iijima, N. Kimura, T. Nakatsuka, and M. Wakatsuchi, 2005. "Ice-Rafted Debris (IRD)- Based Sea-Ice Expansion Events during the Past 100 kyrs in the Okhotsk Sea." *Deep-Sea Research*, Vol. 52, pp. 2275-2301.

Shackleton, N.J., J. Imbrie, and N.G. Pisias, 1988. The Evolution of Oceanic Oxygen-Isotope Variability in the North Atlantic Over the Past Three Million Years. Phil. Trans. R. Soc. Lond. B, Vol. 318, pp. 679-688.

Singarayer, J.S., J.L. Bamber, and P.J. Valdes, 2006. Twenty-First Century Climate Impacts from a Declining Arctic Sea Ice Cover. Journal of Climate, Vol. 19, pp. 1109-1124.

Smythe, F.W., W.F. Ruddiman, and D.N. Lumsden, 1985. "Ice-Rafted Evidence of Long-term North Atlantic Circulation." *Marine Geology*, Vol. 64, pp. 131-141.

Stickley, C.E., K. St John, N. Koc, et al., 2009. "Evidence for Middle Eocene Arctic Sea Ice from Diatoms and Ice-Rafted Debris." *Nature*, Vol. 460, pp. 376-390.

St. John, K., 2008. "Cenozoic Ice-Rafting History of the Central Arctic Ocean: Terrigenous Sands on the Lomonosov Ridge." *Paleoceanography*, Vol. 23.

Thiede, J., O. Eldholm, E. Taylor, 1989. "Variability of Cenozoic Norwegian-Greenland Sea Paleoceanography and Northern Hemisphere Paleoclimate." *Proceedings of ODP, Scientific Results*, Vol. 104.

Vanney, J., and L. Dangeard, 1976. "Les deposits glacio-marins actuels et anciens." *Rev Geogr Montr*, Vol. 30, pp. 9-50.

Wefer, G., E. Suess, W. Balzer, et al., 1982. "Fluxes of Biogenic Components from Sediment Trap Deployment in Circumpolar waters of the Antarctic sector." In: U. Bleil and J. Thiede (eds) *Geological History of the Polar Oceans: Arctic versus Antarctic*, Kluwer Academic Publishing, Dordrecht, pp. 245-254.

Wefer, G., G. Fisher, D. Futterer, R. Gersonde, S. Honjo, D. Osterman, 1990. "Particle Sedimentation and Productivity in Atlantic waters of the Atlantic sector." In: U. Bleil and J. Thiede (eds) *Geological History of the Polar Oceans: Arctic versus Antarctic*, Kluwer Academic Publishing, Dordrecht, pp. 363-380.

Woodruff, F., Savin, S.M., 1989. "Miocene Deepwater Oceanography." *Paleoceanography*, Vol. 4, pp. 87-140.

Woods Hole Oceanographic Institution, 2008. "Image: Arctic Ocean Circulation Primer." Polar Research, <www.whoi.edu/page.do?pid=12317&tid=441&cid=41043&ct=61&article=23446>. (March 3, 2008).

Winter, B.L., C.M. Johnson, and D.L. Clark, 1997. "Strontium, Neodymium, and Lead Isotope Variations of Authigenic and Silicate Sediment Components from the Late Cenozoic Arctic Ocean: Implications for Sediment Provenance and the Source of Trace Metals in Seawater." *GSA*, Vol. 61, No. 19, pp. 4181-4200.

Zachos, J., M. Pagani, L. Sloan, E. Thomas, and K. Billups, 2001. "Trends, Rhythms, and Aberrations in Global Climate 65 Ma to Present." *Science*, Vol. 292, pp. 686-693.

Study	Defined size range of Iceberg Rafted Debris	Size range of debris in Iceberg material	Size range of debris in Sea Ice	Defined size range of Sea Ice Rafted Debris
Bischof and Darby (1997, 1999)	> 250 µm			
Darby et al. (2002)	> 250 µm			
Bischof et al. (1996)	> 250 µm			
Krissek et al. (1989)	> 250 µm			
Kotlyakov and Gordienko (1982)		2 µm to 2000 µm		
Ruddiman and McIntyre (1976)		2 % > 550 µm		
Lisitzin (2002)	2.9% > 500 µm		<250 µm	
Bellair et al. (1964)		average = 35 µm		
Mulholland (1976)		mode = 125 - 177 µm		
Winter et al. (1997)				>63 - < 250 µm
Bischof et al. (1999)				>63 - < 250 µm
Bischof (2000)				>63 - < 250 µm

Table 1.1: A reference comparison of various studies cited in this paper, outlining the given size ranges for icebergs, sea ice, iceberg rafted debris (IBRD), and sea ice rafted debris (SIRD).

Ice Environment	Sand vs. Fine Sediment Ratio	Coarse Sand vs. Fine Sand Ratio	Relative Albedo
Ice Free Arctic	Null Value	Null Value	Extremely Low
River Deposit	Very High	Very High	Extremely Low
Seasonal Sea Ice	Low	Low	Medium
Iceberg Presence	Low	High	Low
Perennial Sea Ice	High	Low	High

Table 1.2: Table outlining the 5 proposed central Arctic ice environments in this study, their criteria, the various color combinations are how they are identified through the remainder of this study, and their relative albedo contribution.

Sample ID	Depth (mcd)	Age (Ma)
302-2A-47X-3W-114	204.34	44.6609
302-2A-48X-3W-44	210.09	44.8975
302-2A-48X-4W-50	211.66	44.9621
302-2A-49X-2W-44	212.91	45.0136
302-2A-49X-2W-114	213.61	45.0424
302-2A-49X-3W-44	214.41	45.0753
302-2A-49X-4W-114	216.62	45.1663
302-2A-49X-5W-58	217.57	45.2054
302-2A-50X-1W-114	219.02	45.2650

Table 1.3: Table indicating samples containing no sand contribution to the grain size distribution. The sample identification, depths, and ages are provided. The 'no sand' samples are found in a narrow depth and age range. We maintain that these samples represent an ice-free environment.

Sample ID	Depth (mcd)	Age (Ma)
302-4A-19X-1W-44	320.97	50.2512

Table 1.4: Table indicating the sample containing an extremely high sand and coarse sand contribution to the grain size distribution. The sample identification, depth, and age are provided. We maintain that this sample represents a river ice environment.

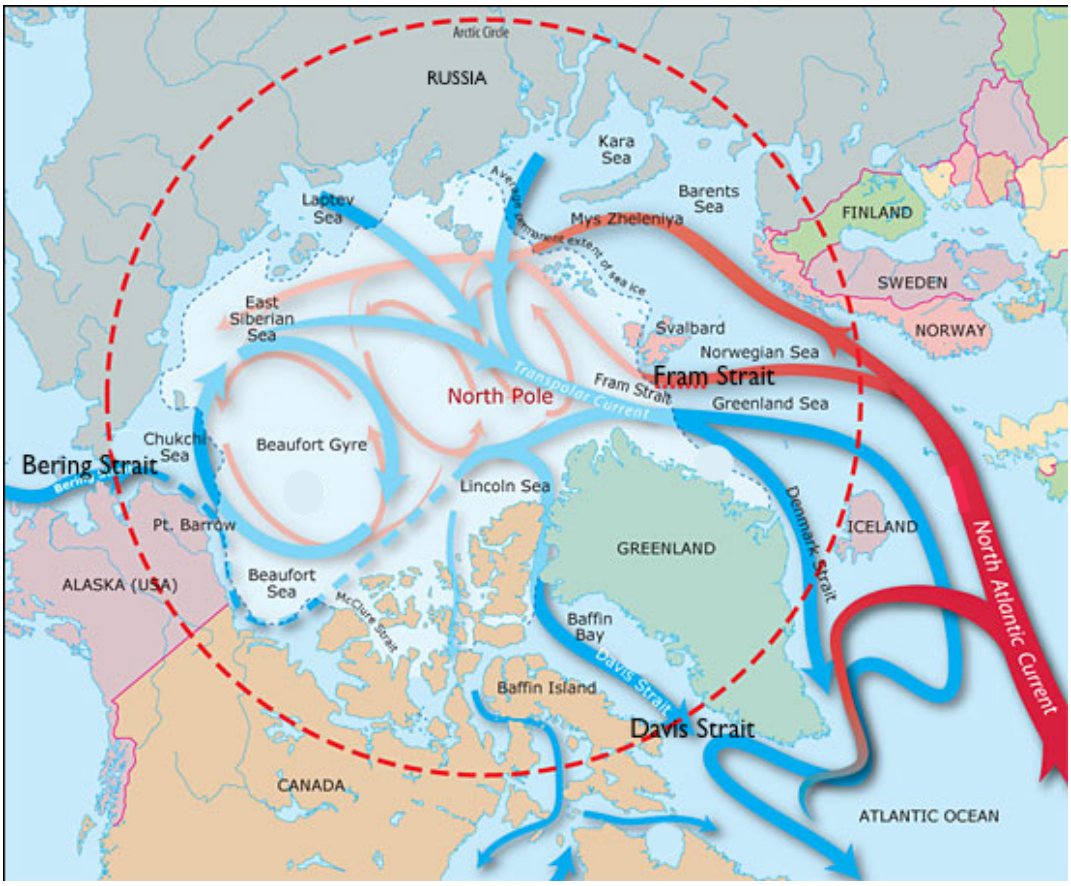

Figure 1.1: Map of the Arctic Ocean showing modern ocean circulation patterns. There is ocean water and heat exchange between the Atlantic and Arctic Oceans through the Fram and Davis Straits. Ocean water exchanges from the Pacific Ocean into the Arctic Ocean through the Bering Strait. The Arctic Ocean itself is roughly centered on the North Pole and is almost entirely contained within the Arctic Circle. (Woods Hole Oceanographic Institution, 2008)

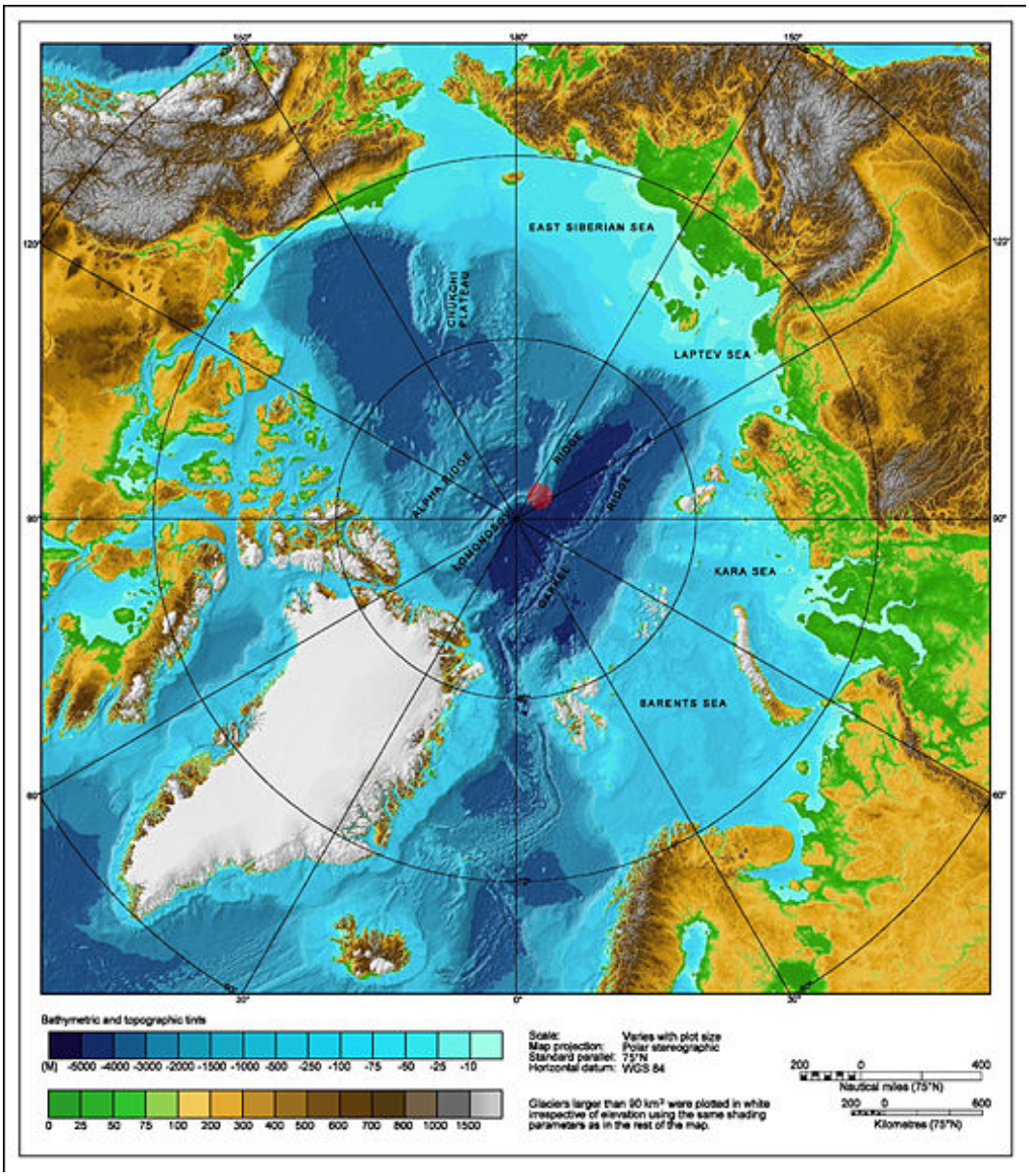

Figure 1.2: Bathymetric and topographic map of the Arctic. The IODP Expedition 302, ACEX, core sites were on the Lomonosov Ridge, central Arctic Ocean (red dot). The Lomonosov Ridge separated from the Barents/Kara shelf due to the formation of the Gakkel Ridge. By being elevated from the abyssal plain and separated from the continental shelf, the Lomonosov Ridge is an ideal setting for paleo- sea ice investigations of the Arctic. (IBCAO, 2008)

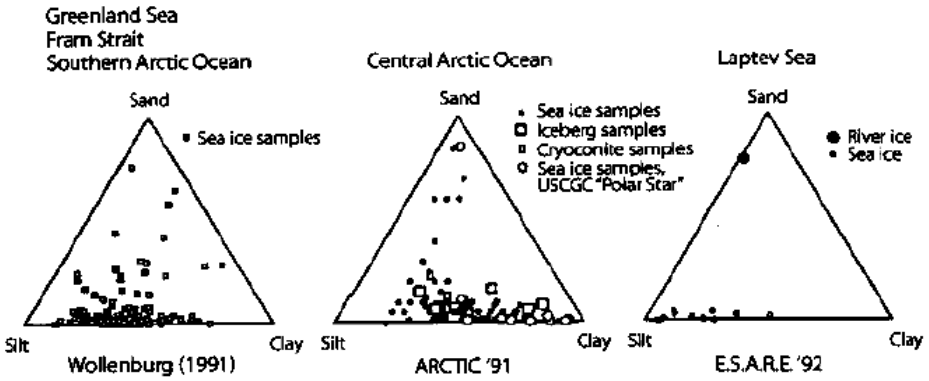

Figure 1.3: Tertiary diagrams taken from Lisitzin (2002) showing grain size distributions determined directly from sea ice, iceberg, and river ice samples on three different Arctic studies. The location of the ARCTIC '91 study (central diagram) is geographically the closest to the ACEX study. The sea ice samples show widely varying grain size distributions, while icebergs typically show lower sand contributions.

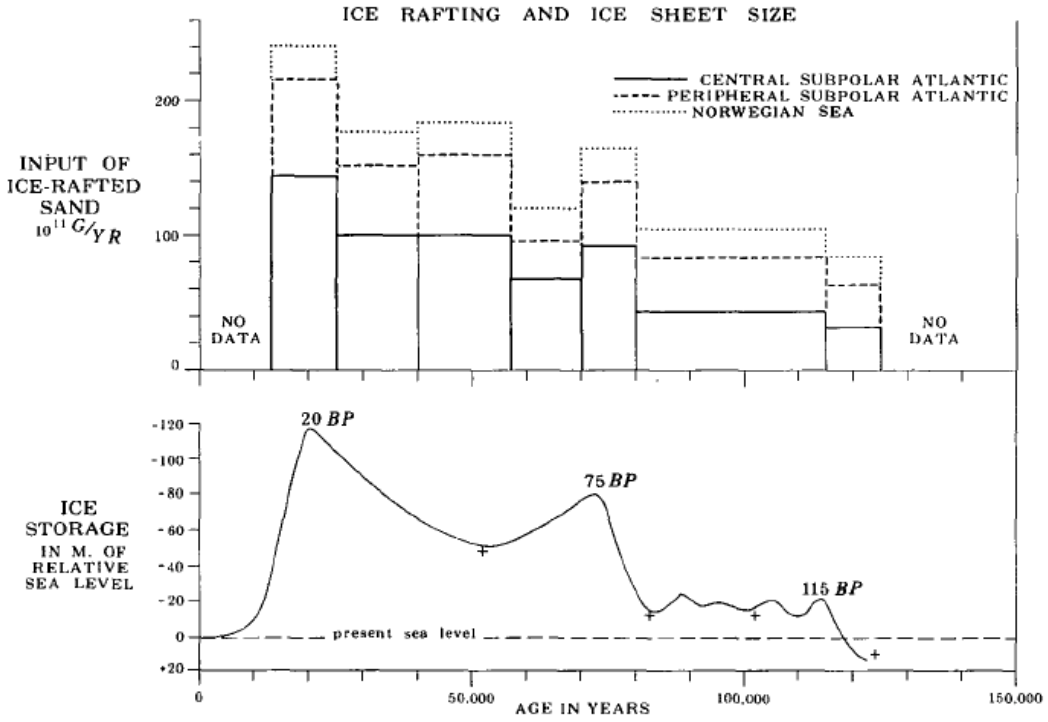

Figure 1.4: Upper graph shows variation in IRD input for the last 125,000 years at 3 locations. Lower graph shows the variation in sea level for the same time period. Sea level can be interpreted as a proxy for glacial ice extent. Periods of lower sea level, greater ice extent (glacial) correspond to periods of increased IRD deposition. (Ruddiman, 1977a)

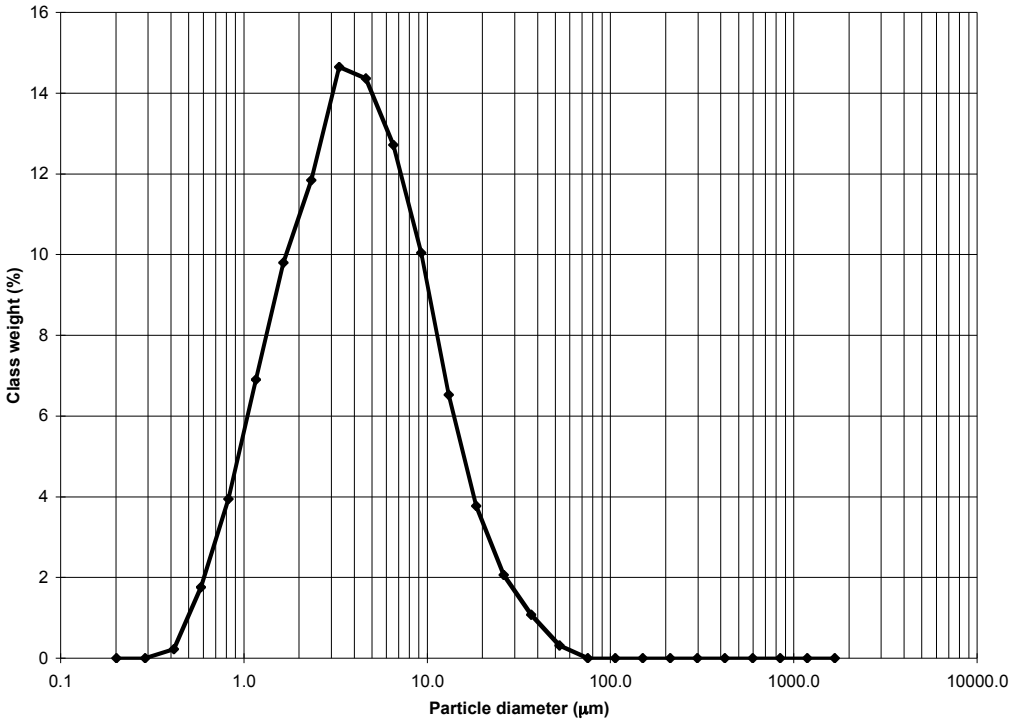

Figure 1.5: The grain size distribution of ACEX sample, 302-2A-48X-3W-44. This sample is an example showing a sediment range up to 63 μm with no > 63 μm contribution. No sand presence indicates no ice rafting contribution, and therefore representing an ice-free Arctic environment. Similar samples with no sand contribution also show sediment up to 63 μm in size.

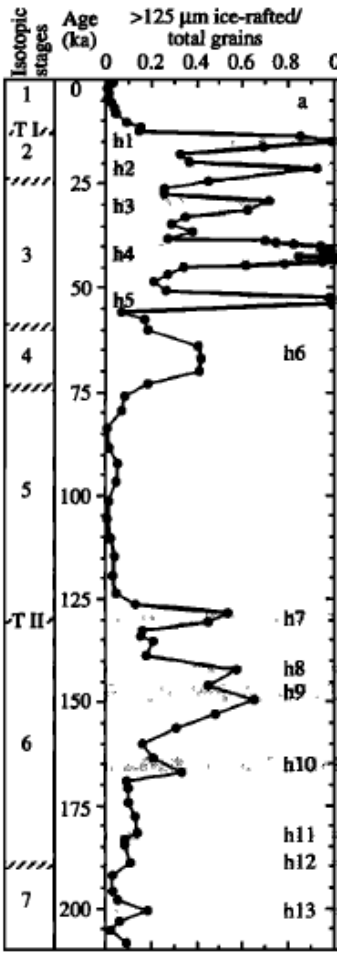

Figure 1.6: In the graph above, the IRD component was normalized and emphasized by plotting the ratio of IRD to finer sediments. (Madureira et al., 1997)

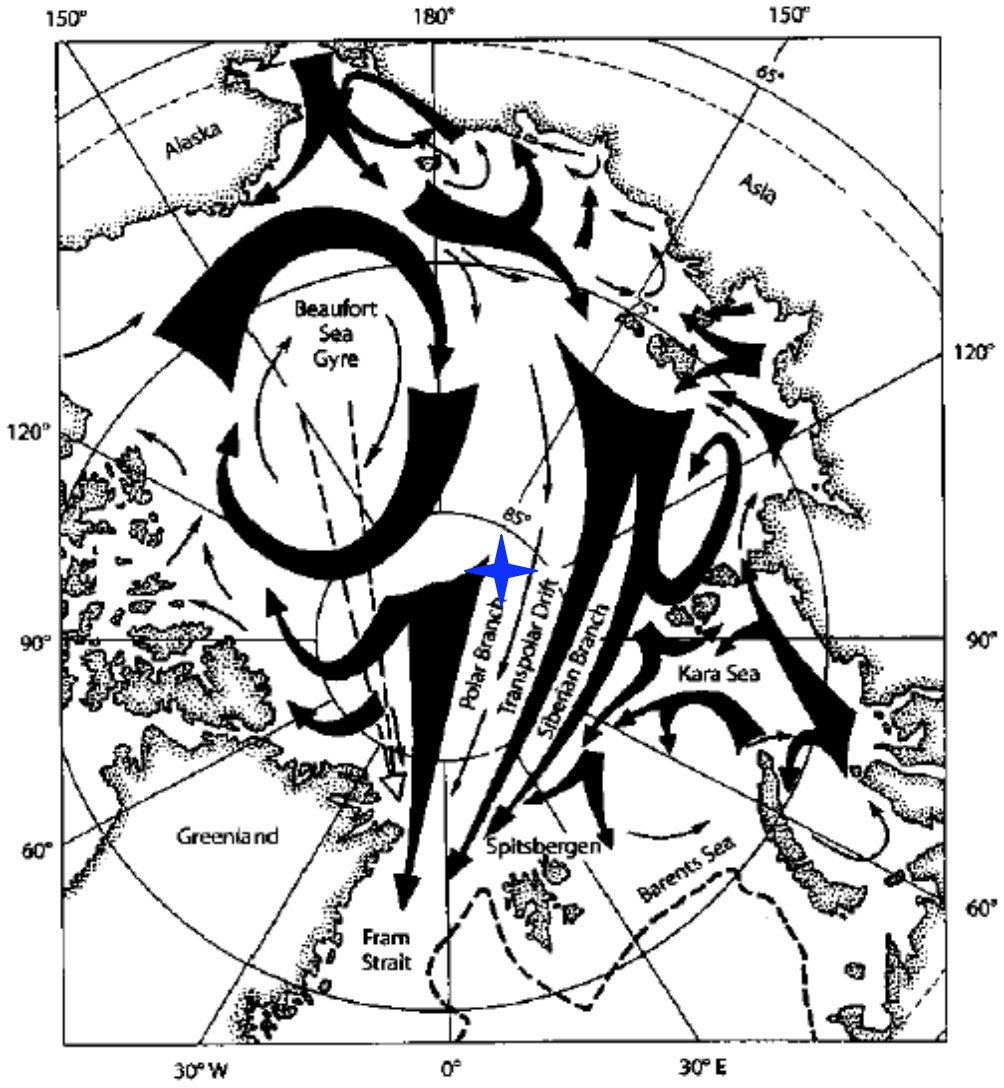

Figure 1.7: Map of Arctic Ocean showing circulation gyres and drift directions for sea ice transport (Lisitzin ,2002). The ACEX, IODP 302, site (indicated by a star) experiences deposition from Arctic ice in the Transpolar Drift. This sea ice originated and entrained sediment from the Siberian shelf. Siberian shelf sediments are typically fine sand, silt, and some clay.

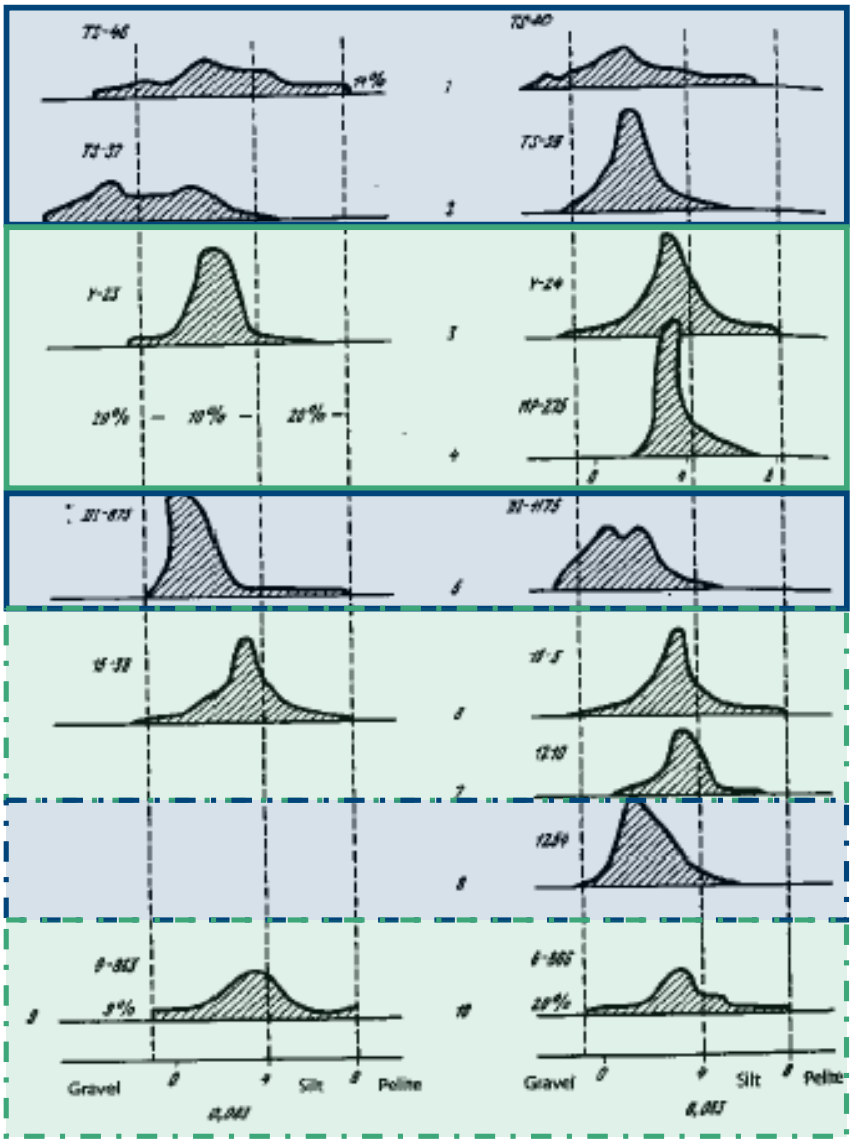

Figure 1.8: Grain size distributions for samples taken from the McMurdo Sound, Antarctica region (Barrett and Treves, 1981). Samples in boxes a and c are taken directly from glacial ice material. Samples in box b are taken directly from sea ice. Samples in boxes d, e, and f are from offshore cores. Box a and c, representing iceberg material, show coarse sand averages. Box b, sea ice, shows fine sand averages. Employing the ratio of coarse sand to fine sand (I/SI), box d and f are interpreted as being a sea ice dominated depositional environment, and box e as iceberg dominated. This shows the I/SI is viable for determining ice environments even in Antarctica where the grain sizes are generally coarser and less distinctive between the two transport mechanisms than they are in the Arctic Ocean.

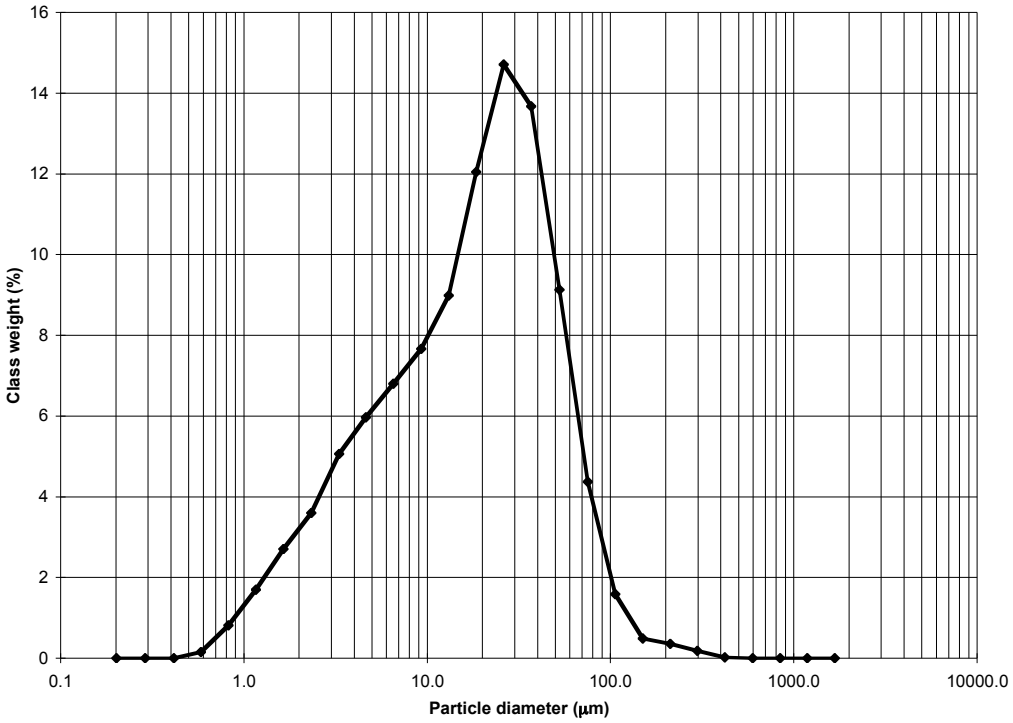

Figure 1.9: The grain size distribution of ACEX sample, 302-2A-56X-2W-114. This sample is an example showing a sediment range up to 250 μm with no > 250 μm contribution. No coarse sand presence indicates no iceberg rafting contribution, and therefore representing a sea ice environment. Similar samples with dominantly fine sand contributions also show sediment either not exceeding or considerably diminishing at 250 μm in size.

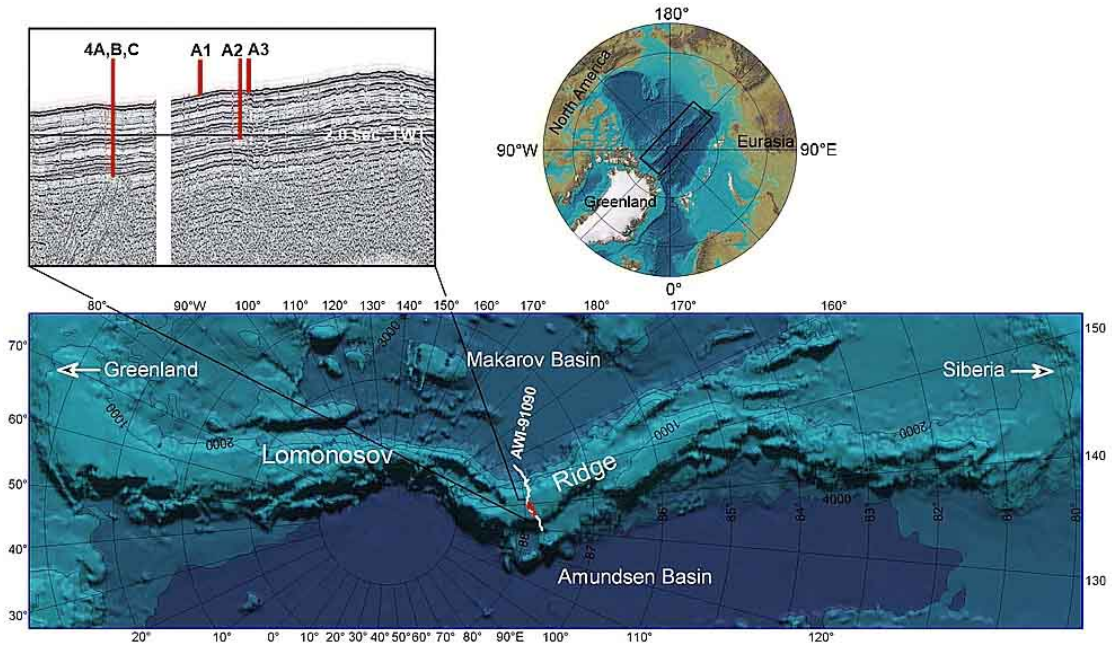

Figure 1.10: Bathymetric map showing the location of the four ACEX drill sites on the Lomonosov Ridge. Along with depth penetration of each site shown in the seismic reflection profile AWI-91090. Over 420 m of sediments from the Lomonosov Ridge were drilled. (Backman et al., 2007)

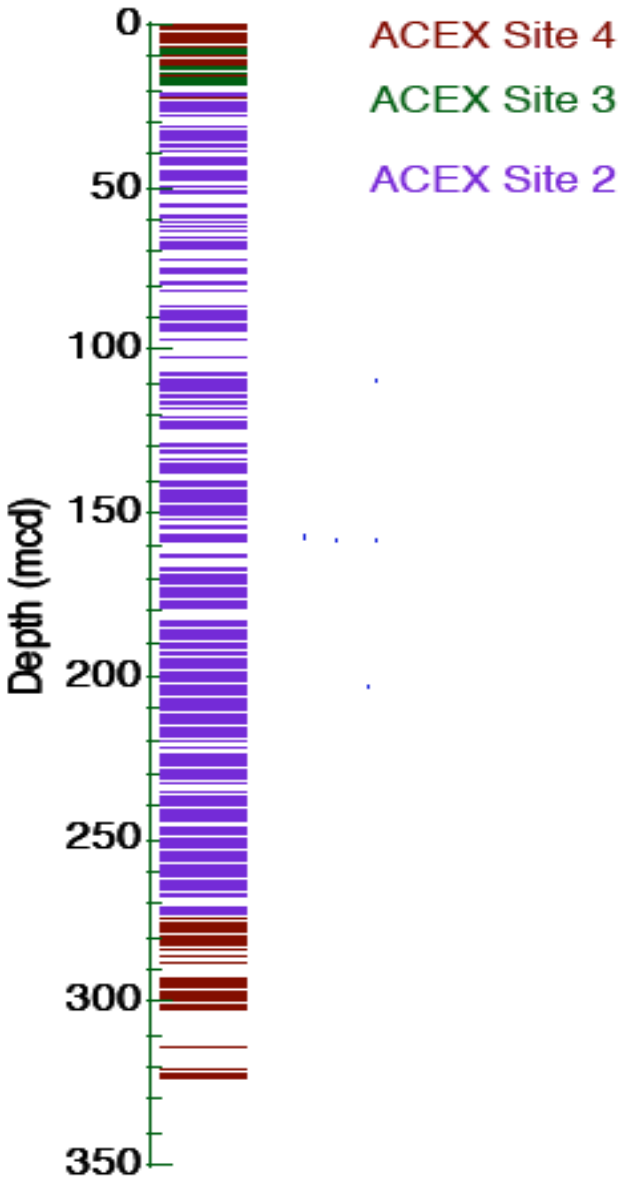

Figure 1.11: Samples for this study came from three of the four ACEX sites. The sample locations are plotted on the composite depth scale. Samples plotted in red came from cores taken at site 4. Samples plotted in green came from cores taken at site 3. Samples plotted in purple came from cores taken at site 2. The samples from the three sites combined make a more compete history of the central Arctic Ocean during the Cenozoic. Using the composite depth scale eliminates differences in accumulation rates between the three sites.

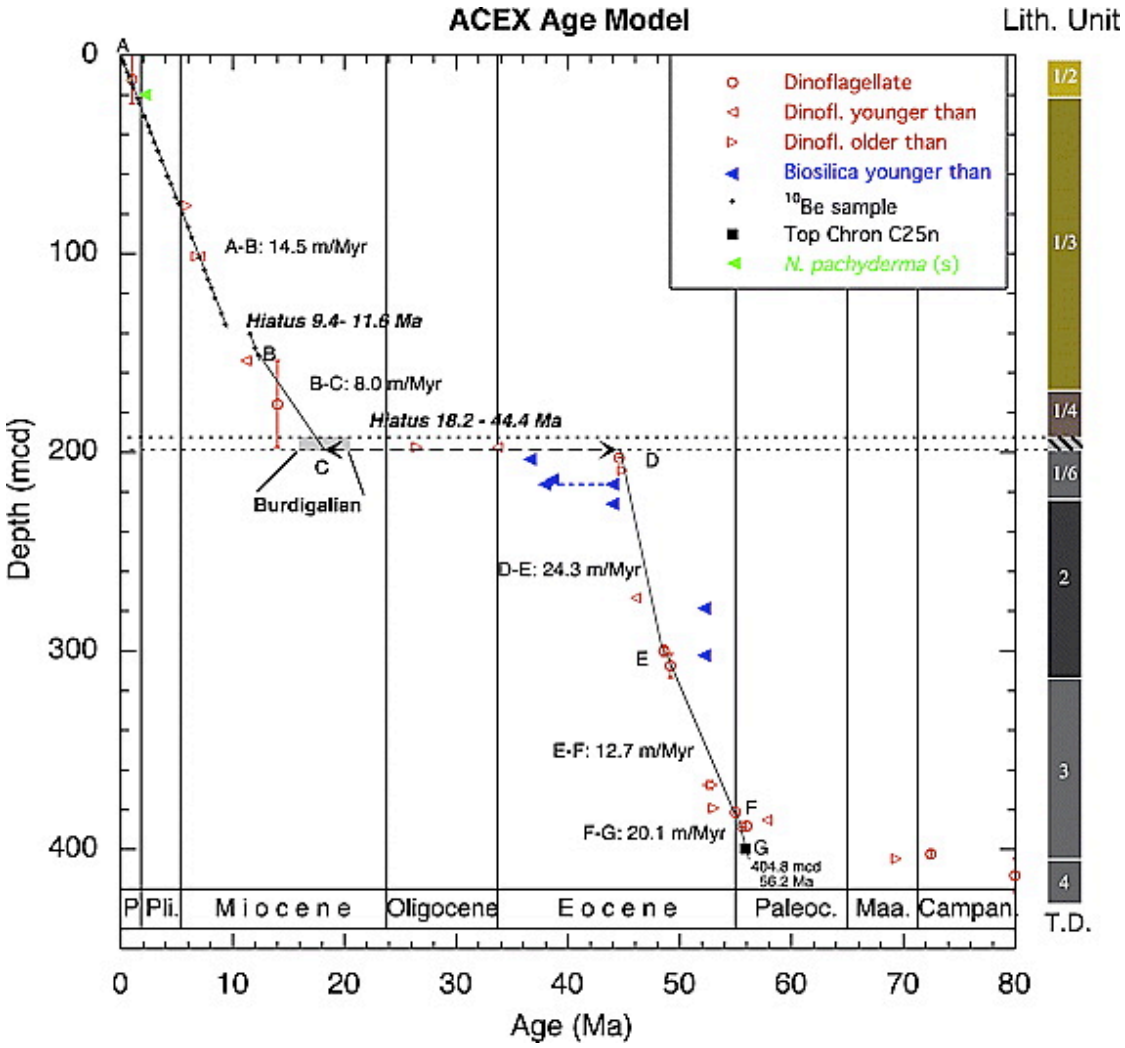

Figure 1.12: Age model for the ACEX cores as determined by Backman et al. (2007). Two hiatuses were found in the record, one from 9.4-11.6 Ma and the other from 18.2-44.4 Ma. This age model was applied to all samples used in this study.

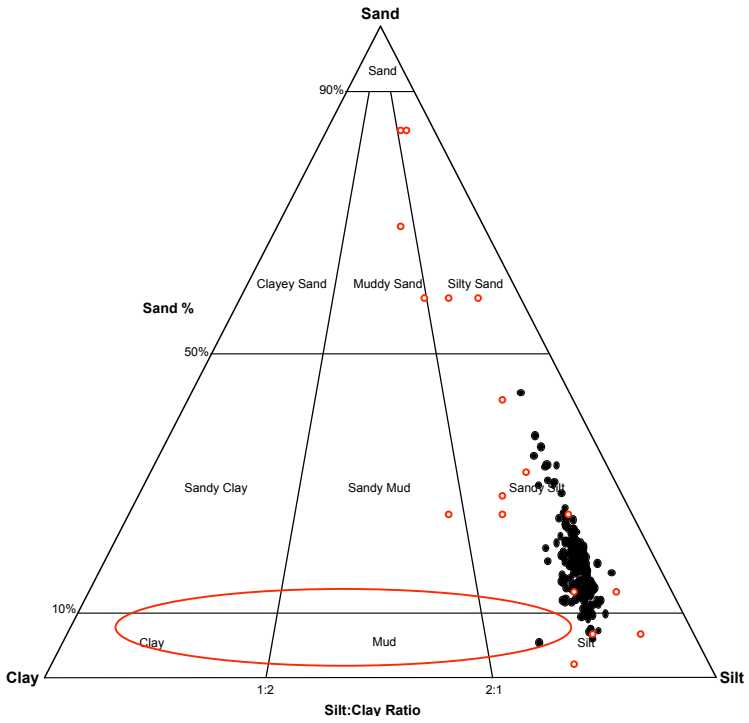

Figure 1.13: The ACEX grain size distributions from 18.2 Ma to present are plotted on a tertiary graph (solid black dots). This distribution compares to the distribution of the grain size of the central Arctic Ocean sea ice samples taken in 1991 (hallow red dots, large red oval represents region of many data points). The samples are narrowly banded in the silt:clay ratio but vary significantly in terms of the sand percentage.

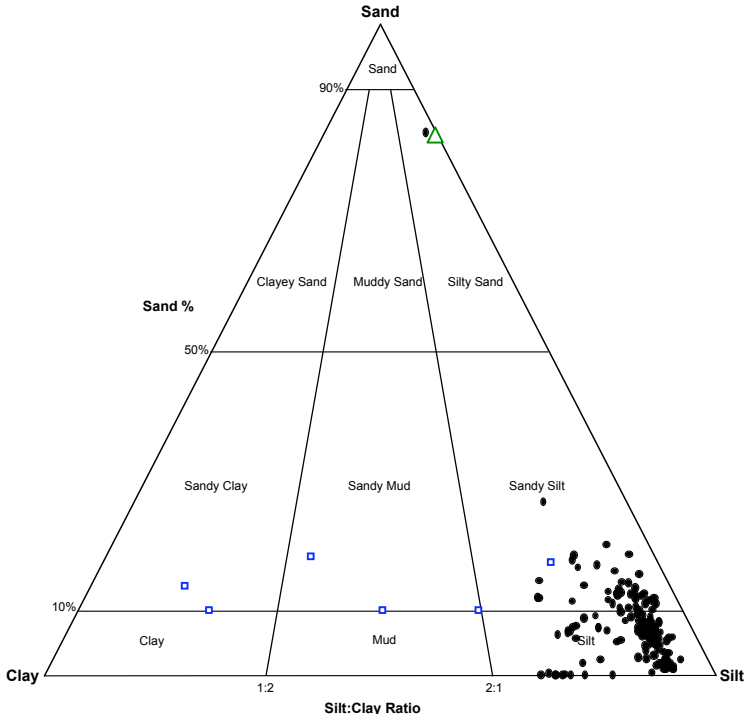

Figure 1.14: The ACEX grain size distributions from 44.4 to 50.4 Ma are plotted on the tertiary graph above (solid black dots). This distribution compares to the distribution of the grain size of the central Arctic Ocean sea ice and iceberg samples taken in 1991 (square blue dots- icebergs). The samples are widely banded in the silt: clay ratio, while remaining in the silt and sandy silt distinctions. They vary more in the sand percentage than the direct iceberg samples. The notable outlier for this time range is a single sample, which has a silty-sand distinction and is comparable to the river ice grain size distribution taken in the Laptev Sea in 1992 (triangle green dot- river ice).

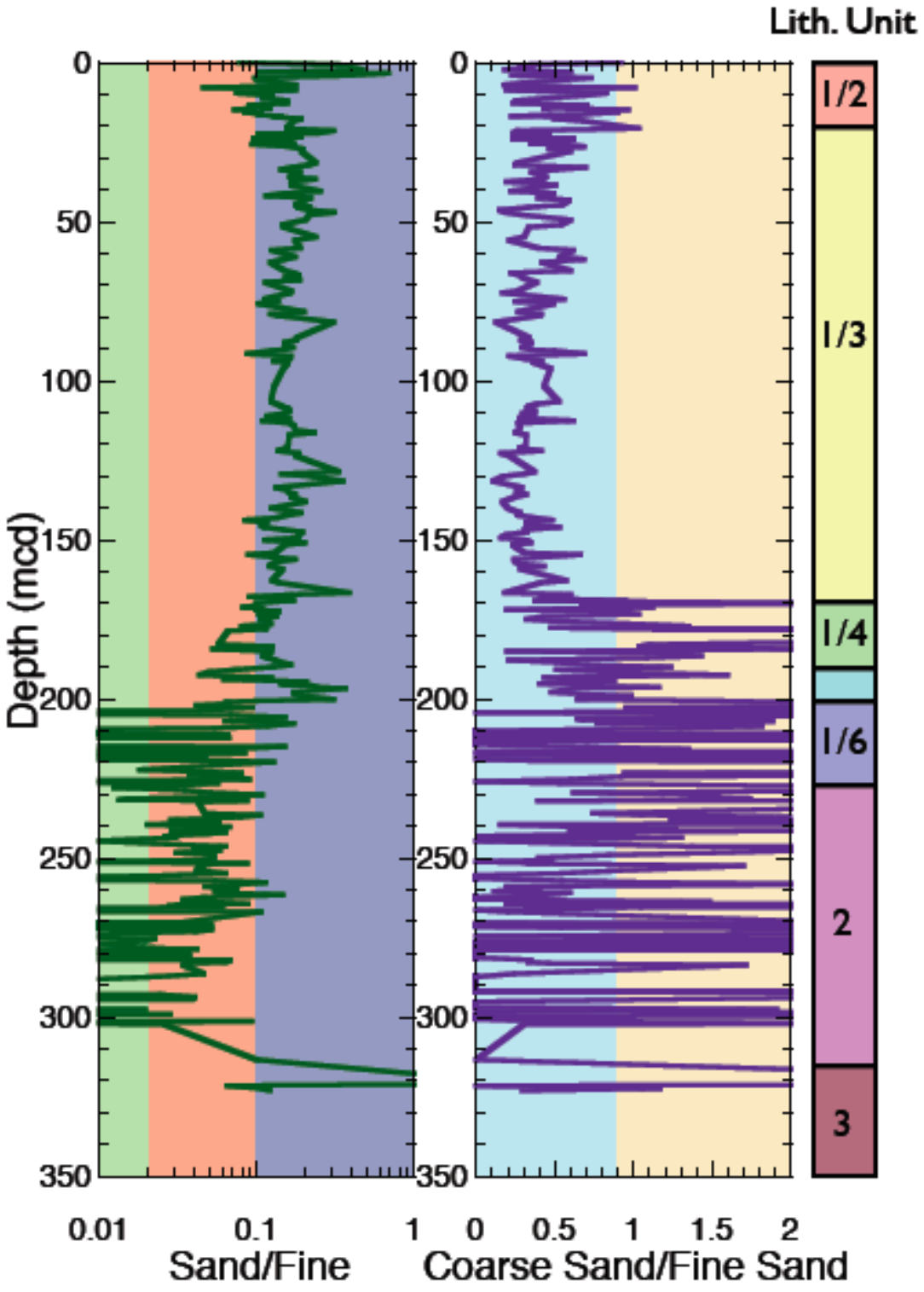
Lith. Unit
I/2
I/3
I/4
I/6
2
3
Depth (mcd)
0
50
100
150
200
250
300
350
0.01
0.1
1
Sand/Fine
0
0.5
1
1.5
2
Coarse Sand/Fine Sand

Figure 1.15: Grain size distributions of the ACEX cores are plotted here using the ratios of sand to fine sediments and coarse sand to fine sand. Changes in the grain size distributions correspond to changes in lithology. Unit 1/2 is dominated by high coarse sand percentages. Unit 1/3 is characterized by moderate sand contributions. Unit 1/4 has significant coarse sand contributions, while the unit directly below, which incorporates a significant hiatus, returns to more moderate coarse sand levels. Units 1/6 and 2 are undifferentiated in regard to grain size distribution, with low sand values and coarse sand values that fluctuate between extremely high and low values. The few samples from Unit 3 show an increase in sand deposition.

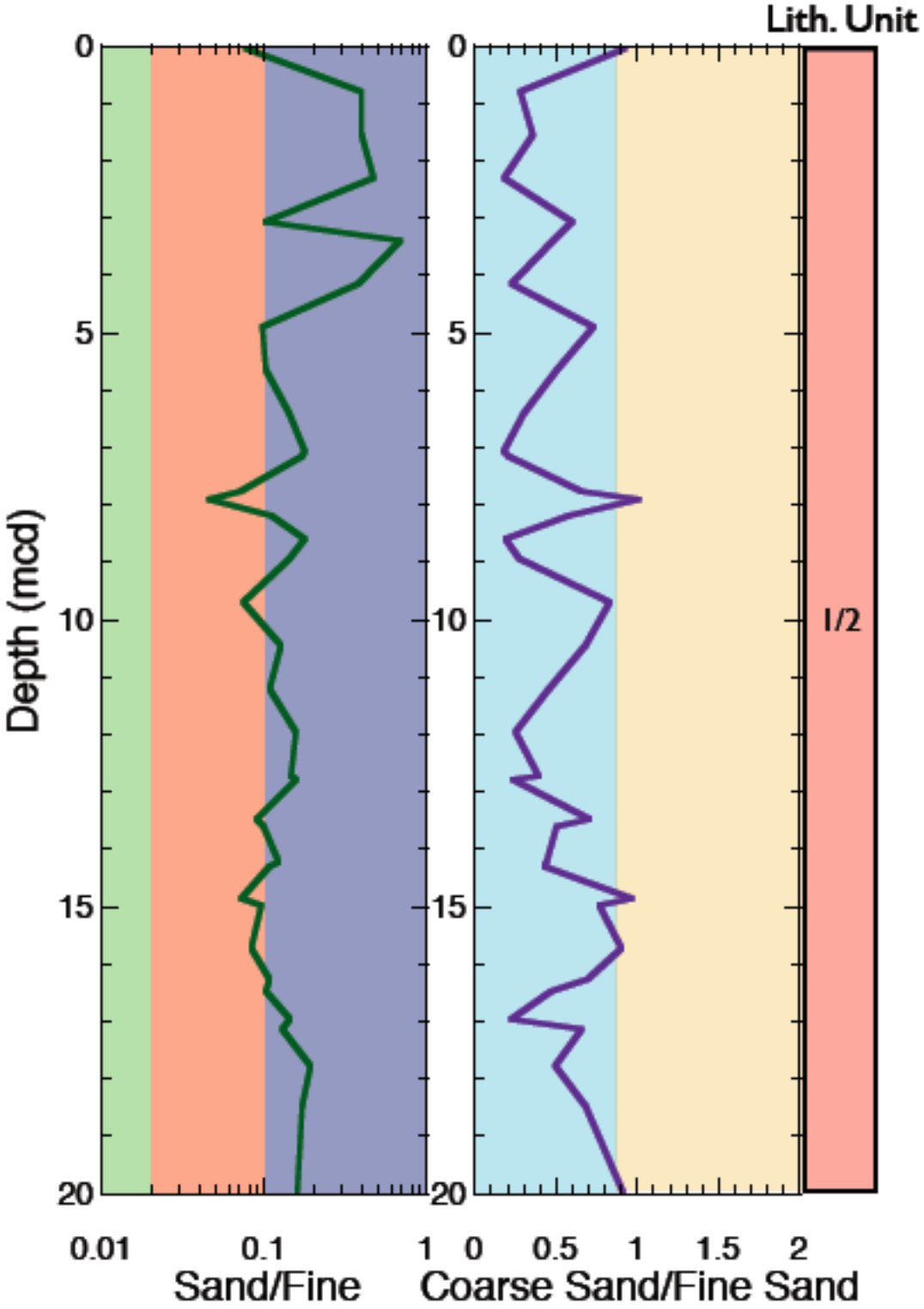
Lith. Unit
0
5
10
15
20
Depth (mcd)
I/2
0.01
0.1
1
Sand/Fine
0
0.5
1
1.5
2
Coarse Sand/Fine Sand

Figure 1.16: The plotted grain size distribution ratios are for the ACEX Lithology Unit 1/2. Four samples show elevated sand percentages and decreased coarse sand contributions, indicative of a sea ice environment. Numerous samples show elevated coarse sand components, suggesting an iceberg influence. Overall this unit is categorized as low sand and coarse sand contributions.

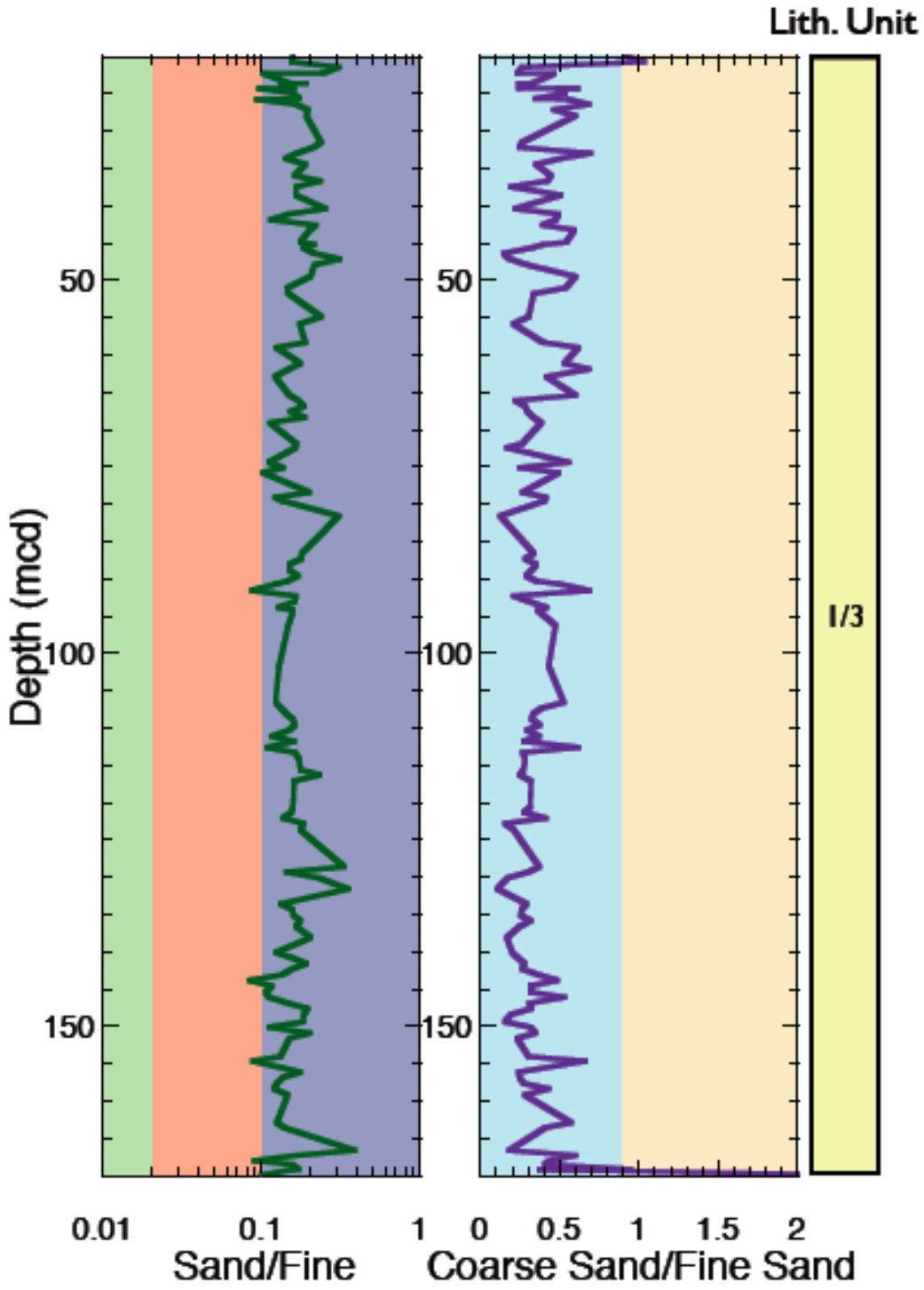
Lith. Unit
Depth (mcd)
50
100
150
50
100
150
I/3
0.01
0.1
1
Sand/Fine
0
0.5
1
1.5
2
Coarse Sand/Fine Sand

Figure 1.17: The plotted grain size distribution ratios are for the ACEX Lithology Unit 1/3. Six samples show elevated sand with decreased coarse sand contributions, which we interpret as being a sea ice environment. The majority of this unit is categorized as low sand and coarse sand contributions, a diminshed sea ice presence.

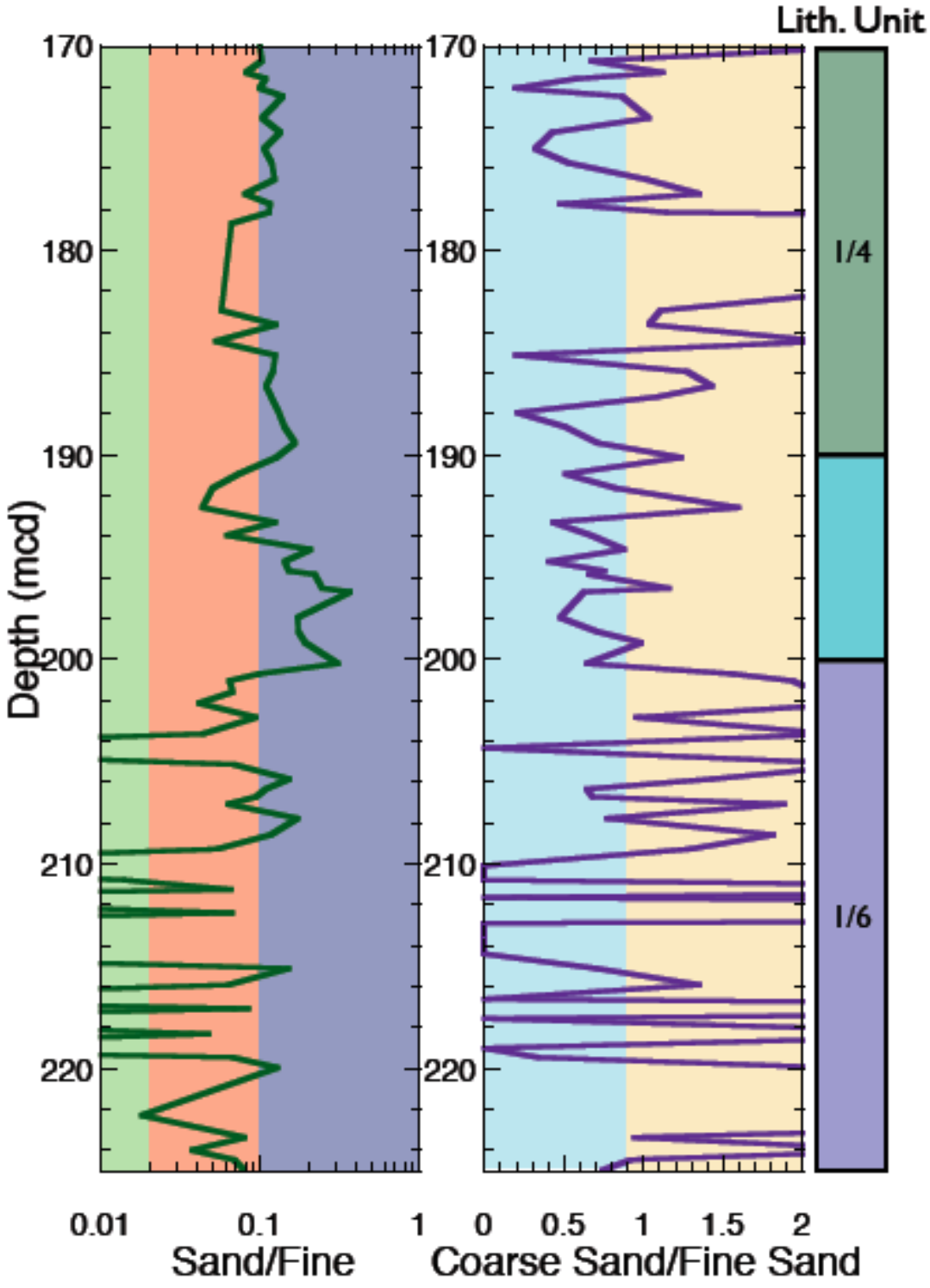
Lith. Unit
170
180
190
200
210
220
Depth (mcd)
I/4
I/6
0.01
0.1
1
Sand/Fine
0
0.5
1
1.5
2
Coarse Sand/Fine Sand

Figure 1.18: The plotted grain size distribution ratios are for the ACEX Lithology Units 1/4- 1/6. Unit 1/6 has nine samples between 204 and 220 m with no sand, indicative of an ice-free environment (Table 1.2). Unit 1/5 has two samples, with elevated sand and low coarse sand contributions, a sea ice environment. Most samples alternate between low sand- low coarse sand contributions, and low sand- high coarse sand contributions, going from sea ice to periods of iceberg influence.

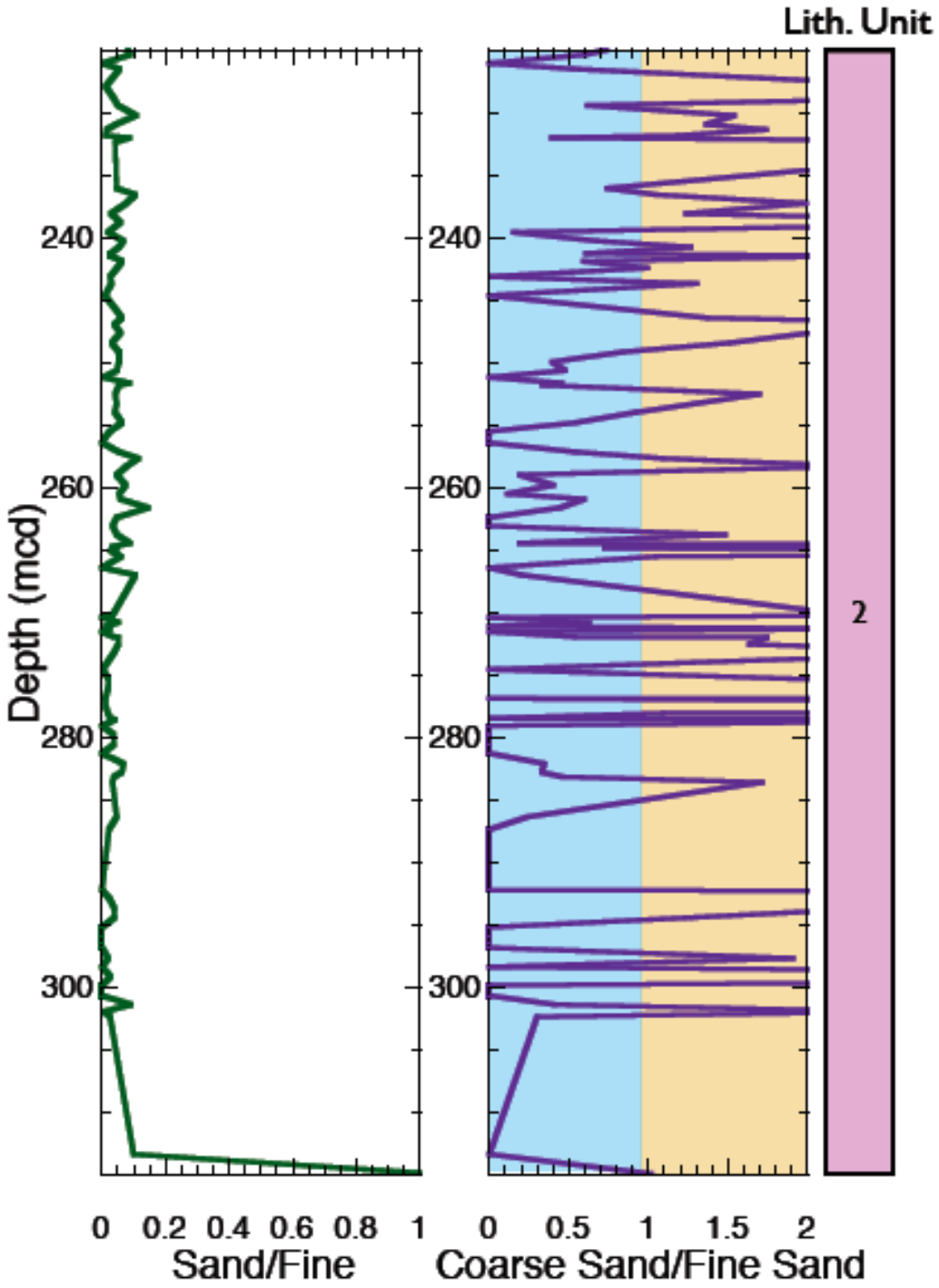

Figure 1.19: The plotted grain size distribution ratios are for the ACEX Lithology Unit 2. This region alternates between low sand- low coarse sand, and low sand- high coarse sand contributions, iceberg inclusions.

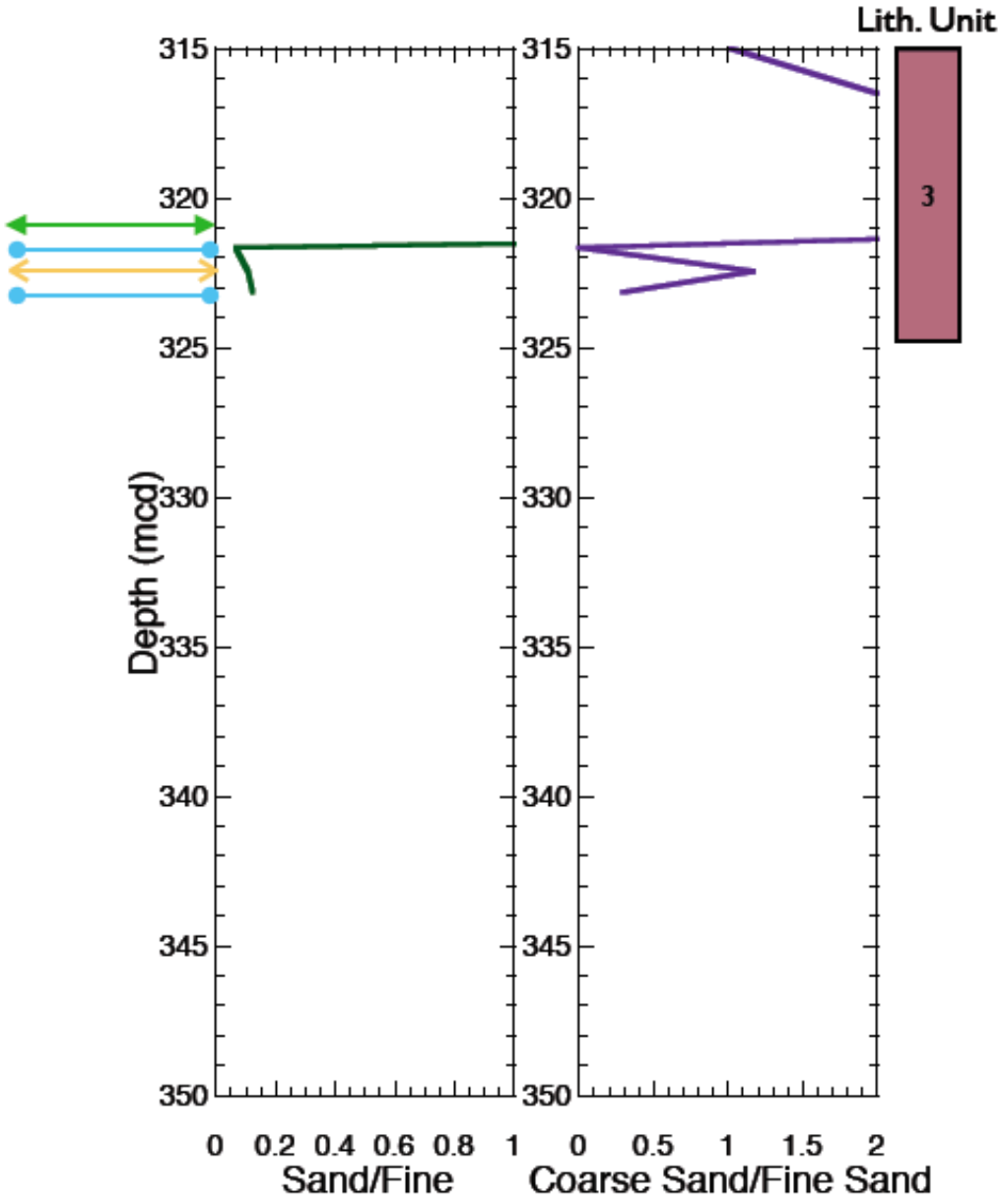

Figure 1.20: The plotted grain size distribution ratios are for the ACEX Lithology Unit 3. This unit has a sample that shows elevated sand with extremely coarse sand contributions. This may be a river ice environment (Table 1.3). There are two samples with low sand and coarse sand contributions, a seasonal sea ice presence. The sample with elevated coarse sand, suggests iceberg influence.

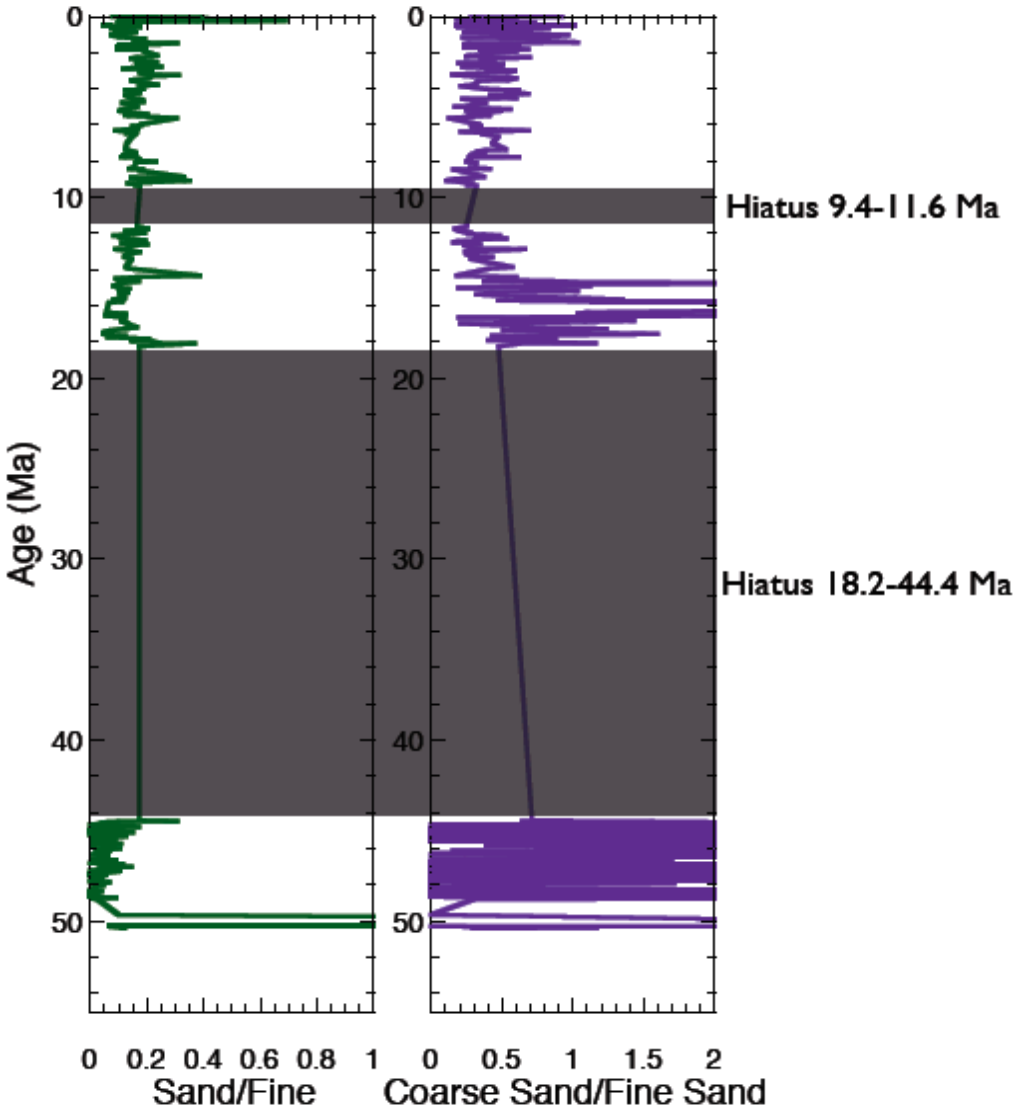

Figure 1.21: The ACEX grain size distribution ratios are plotted in time. The darkened portions of the graphs represent hiatuses in the deposition record. 0- 9.4 Ma shows a relatively steady sand component, with a decreasing coarse sand component. 11.6- 18.2 Ma shows again a relatively steady sand component, but with an increasing coarse sand component. 44.4- 51 Ma shows a diminished, but present sand component, and a widely varying coarse sand component.

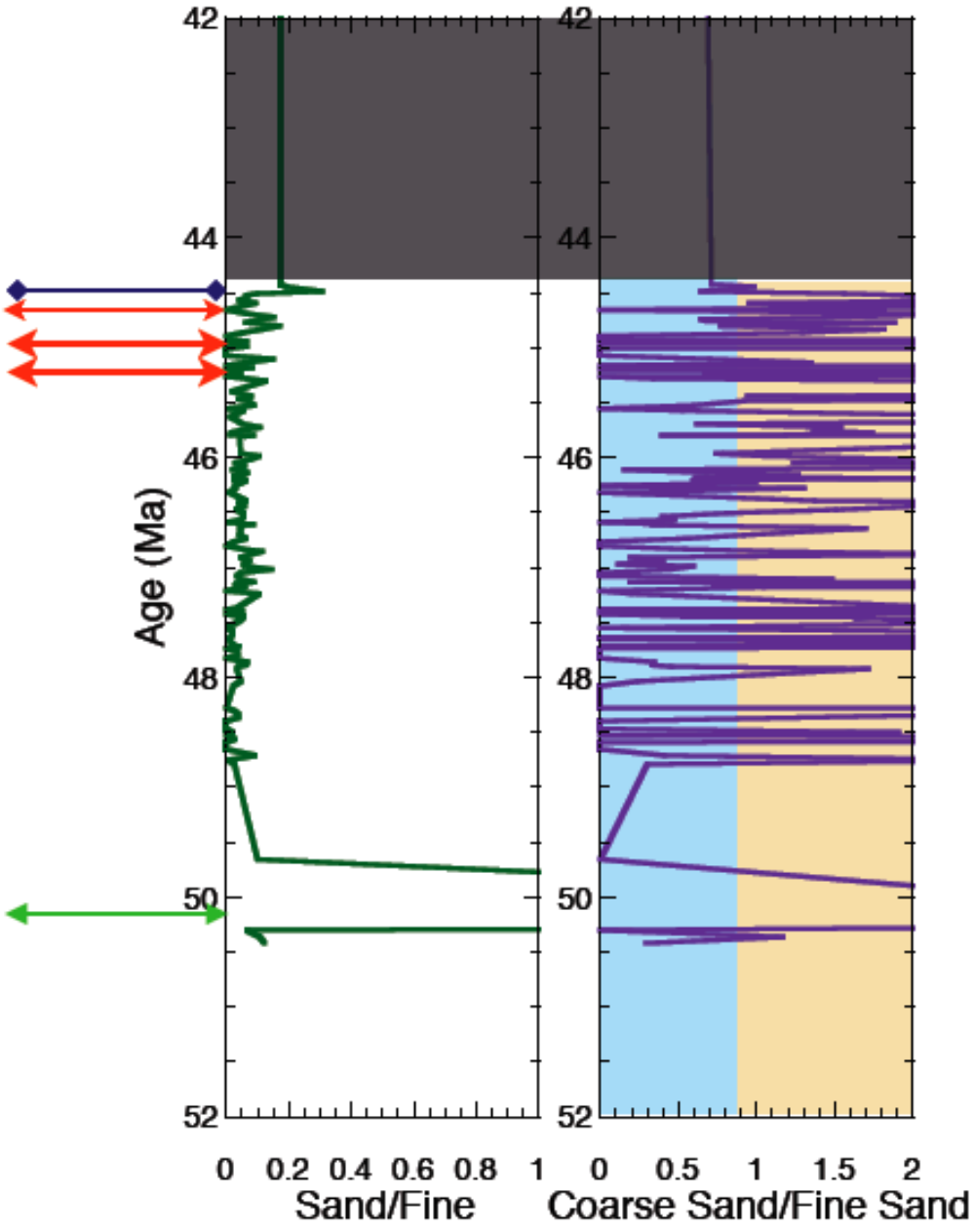
42
44
46
48
50
52
Age (Ma)
0 0.2 0.4 0.6 0.8 1
Sand/Fine
0 0.5 1 1.5 2
Coarse Sand/Fine Sand

Figure 1.22: The plotted grain size distribution ratios are for the ACEX cores 44.4- 51 Ma. This time range has a period that shows a significantly extremely elevated sand contribution with a corresponding elevated coarse sand contribution, possibly a river ice environment (Table 1.3). This time has a period with elevated sand component, low coarse sand, a sea ice environment. The time range has three periods with no sand, an ice-free environment (Table 1.2). The majority of the time range is categorized as alternating between having low sand- low coarse sand contributions, seasonal sea ice, and low sand- high coarse sand contributions, iceberg influenced.

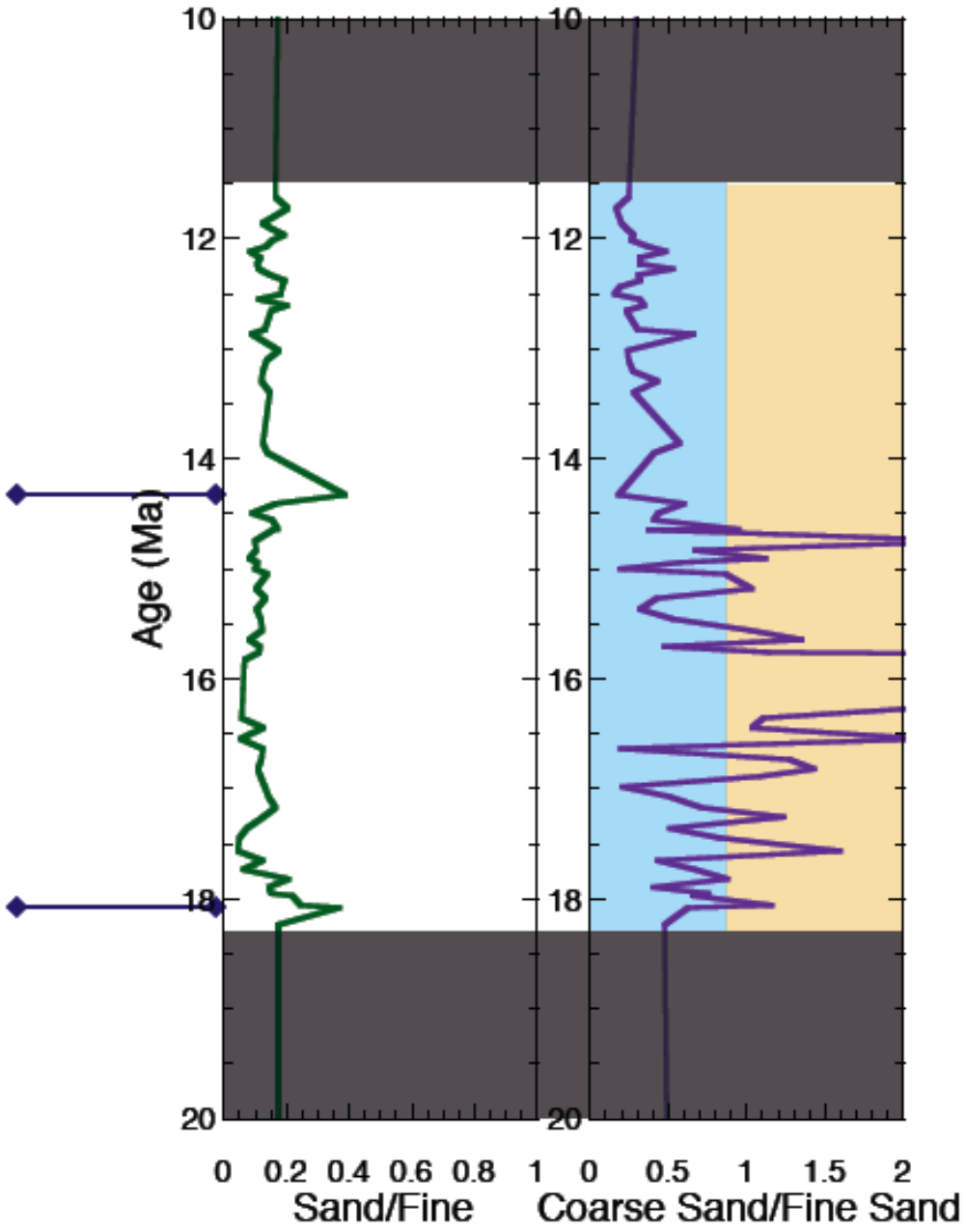

Figure 1.23: The plotted grain size distribution ratios are for the ACEX cores 11.6-18.2 Ma. This time range has two periods that have elevated sand, decreased coarse sand contributions, a sea ice environment. The majority of the time range alternates between, low sand- elevated coarse sand components, suggesting an iceberg influence, and low sand- low coarse sand contributions, diminished sea ice presence.

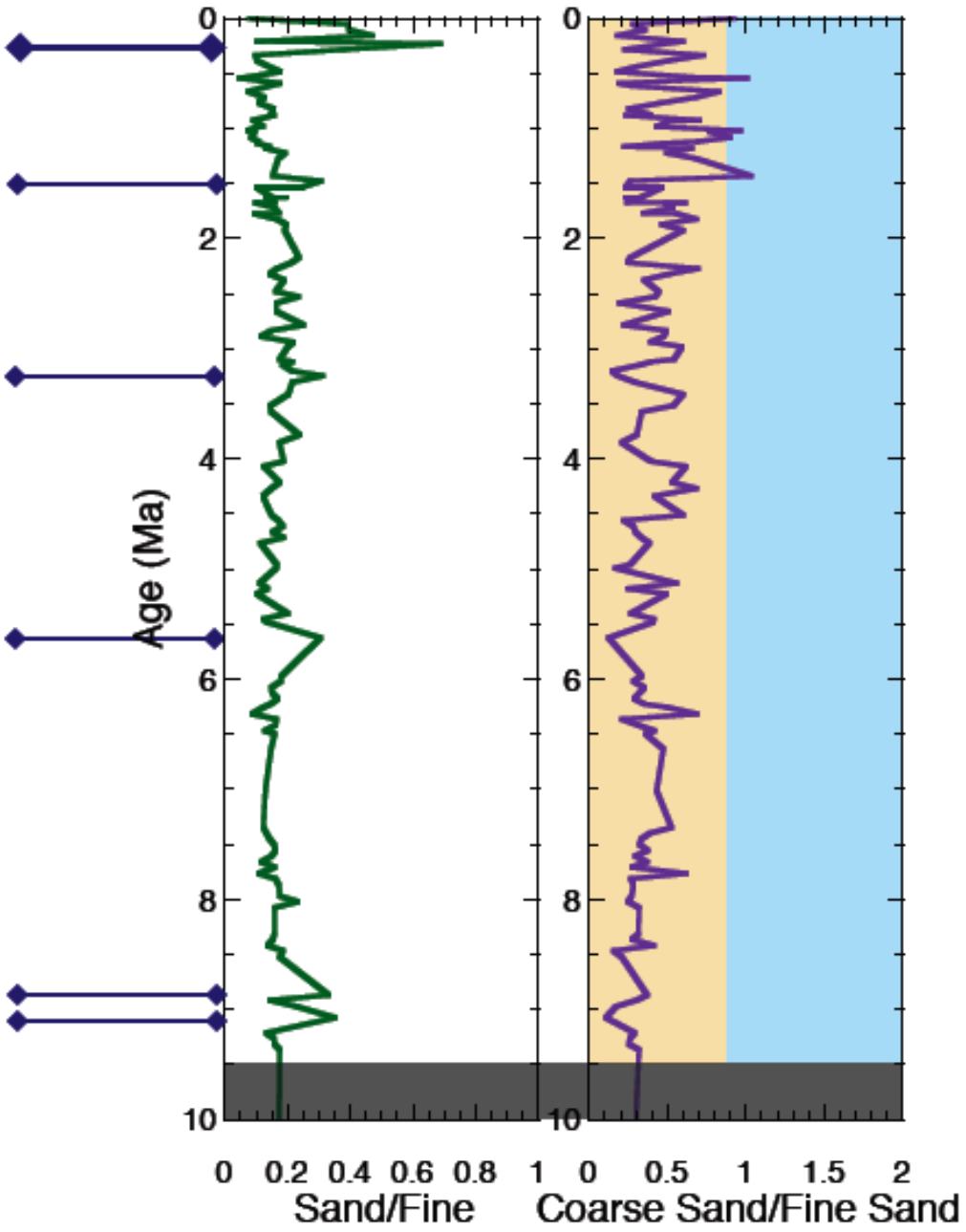

Figure 1.24: The plotted grain size distribution ratios are for the ACEX cores 0- 9.4 Ma. This time range has six periods of elevated sand, decreased coarse sand contributions, a sea ice environment. The time range also has samples that display elevated coarse sand components, suggesting an iceberg influence. The majority of the time range is categorized as having low sand and coarse sand contributions, a seasonal sea ice presence.

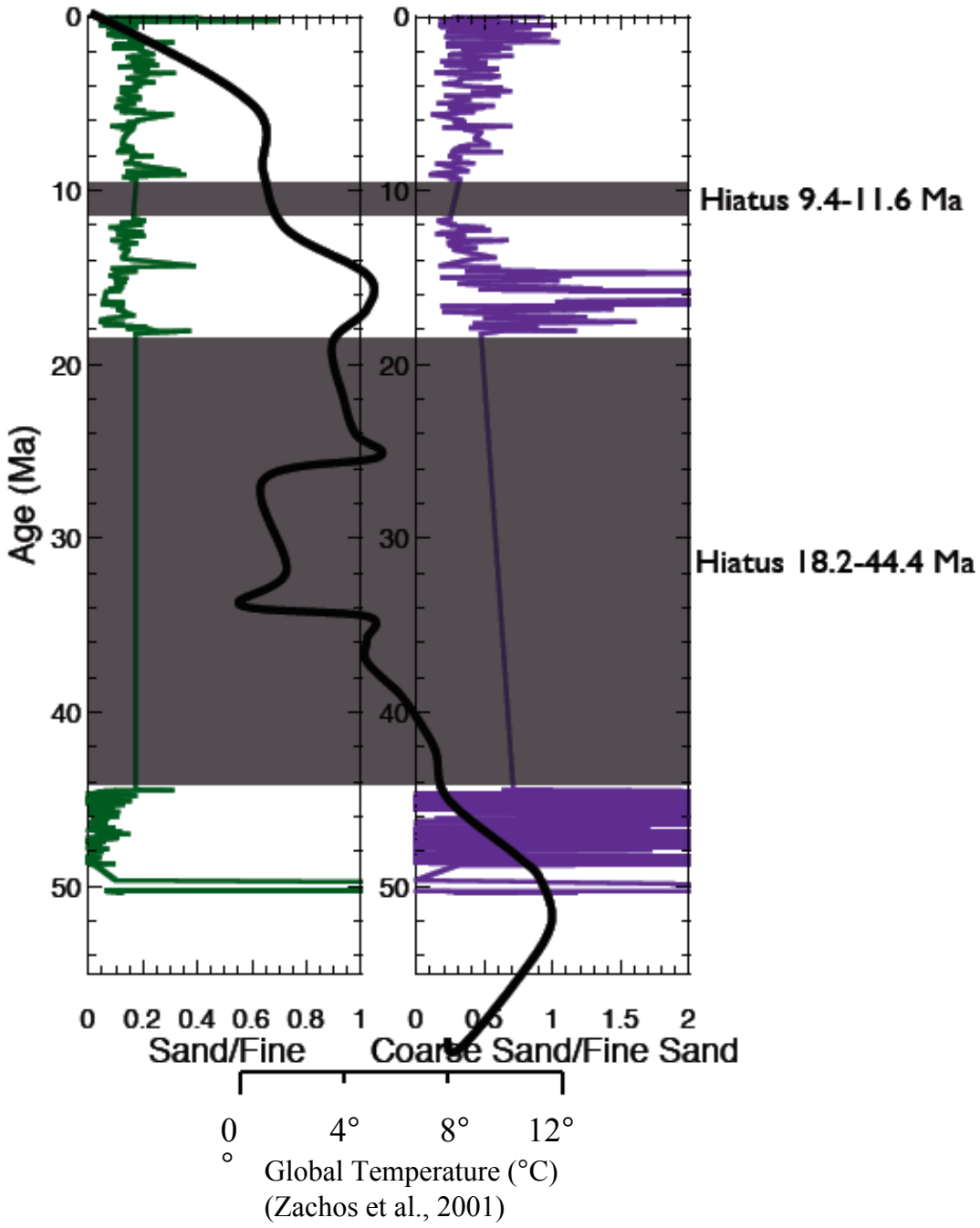

Figure 1.25: The solid black line superimposed on the grain size distributions of this study, is the global benthic $\delta^{18}O$ compiled by Zachos et al. (2001) and interpreted as global mean temperature. There has been an overall decrease in global mean temperature for the Cenozoic Era. The transition from seasonal sea ice to perennial sea ice took place at a time when the global mean temperature was between 4° and 8° C.

Principle Component	Fraction of variance explained
1	0.439665
2	0.247123
3	0.139087
4	0.0647166
5	0.0466547

Table 1.5: The first 5 principle components (components of greatest significance) for the ACEX grain size distribution data set. For statistically significant principle components, the fraction of variance explained by the first principle component needs to exceed 0.5. None of the principle components for the ACEX grain size data set meet the requirements of being statistically significant. The principle component analysis was completed using the Molegro Data Modeller software.

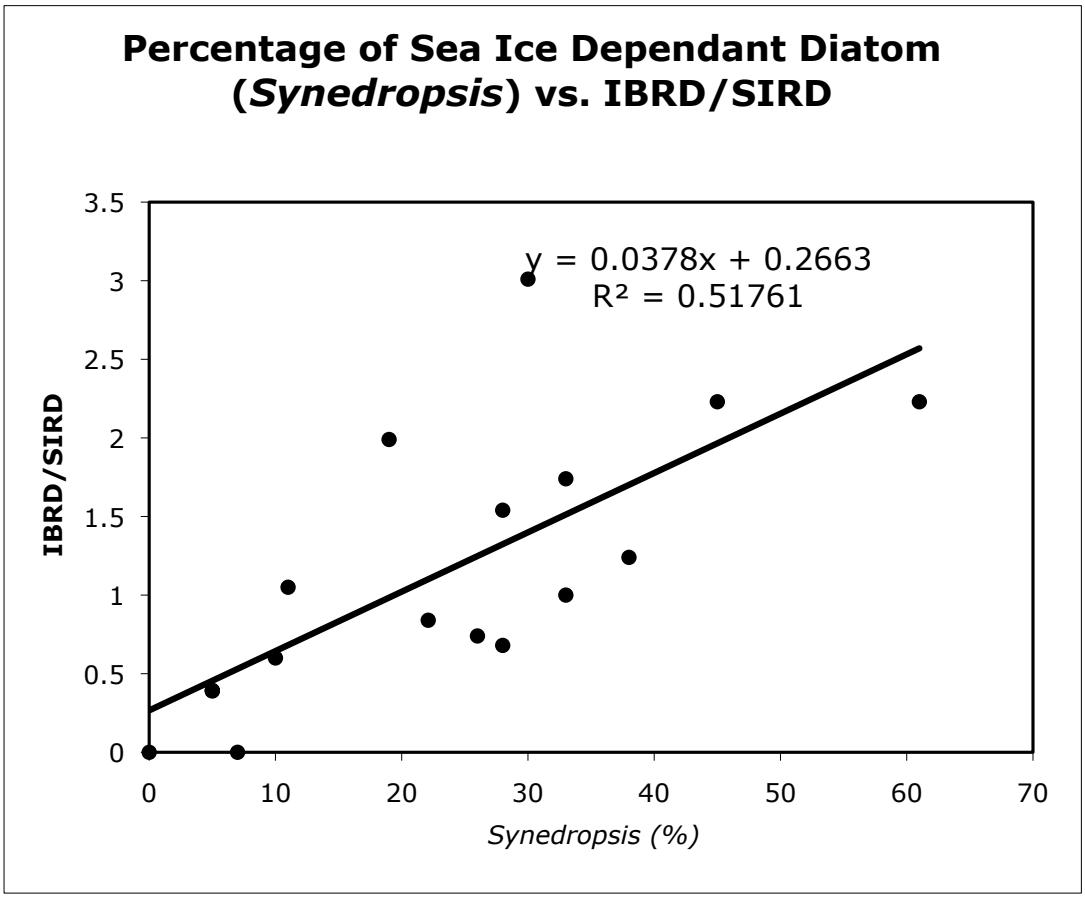

Figure 1.26: Samples of lithography unit 2 where both the determination of the percentage of sea ice dependant diatom, *Synedropsis*, and grain size profiles from this study were taken within 10 centimeters (± 4,115 yrs) of each other graphed showing a positive correlation. This relationship suggests that at periods in unit 2 when icebergs were present there was also a strengthening in the presence of seasonal sea ice. The *Synedropsis* percentages were obtained from Stickley et al. (2009).

Chapter 2

"Physical Properties and Grain Size of Glacio-marine Sediment as Predictors of Cryo-States in the Arctic Ocean"

by

Cristin E. Ashmankas[3,4]

written for submission to Geophysical Research Letters

[3] Graduate School of Oceanography, The University of Rhode Island, Narragansett, RI 02882.
[4] Assistant Professor, Natural Science and Mathematics Division, Lesley University, Cambridge, MA 02138. Email: cashmank@lesley.edu

Chapter 2. Physical Properties and Grain Size of Glacio-marine Sediment as Predictors of Cryo-States in the Arctic Ocean

ABSTRACT

We present the results of grain size analyses performed on glacio-marine sediment from IODP Expedition 302, Arctic Coring Expedition (ACEX), at the Lomonosov Ridge and the relationships to physical properties determined from nondestructive measurements. Analyses of the sand (>63 μm), silt (<63 μm, >4 μm), and clay (<4 μm) fractions show varying relationships to the physical properties of acoustic compressional wave velocity, bulk density, and color reflectance. Sand percentages were found to have relationships to density, acoustic compressional wave velocity and color. Silt percentages were found to have relationships to color, and density. Clay percentages were also found to only have relationships to density, and color. Equally weighting these relationships can be utilized to predict a ratio of sand (>63 μm) to fine grained material (<63μm) that shows regions of significant differences in grain size distributions. These differences in the ratio have been previously determined (Chapter 1) to indicate major changes in the cryo-state of the Arctic polar region. The prediction of the sand to fine-grained material ratio from the physical properties better resolves the ages of the climate transitions than is possible with the coarse resolution of the direct grain size analyses, permitting increased correlation with other high resolution factors. Utilizing the method we outline would aid future coring expeditions to high latitudes to determine nondestructively sections of core of particular climatic interest.

INTRODUCTION

Physical properties of glacio- marine sediments are practically employed in determining grain size distributions. Grain size distributions have been linked in past studies to porosity, permeability, bulk density, and acoustic compressional wave velocity (Bachman, 1985; Boggs, 1995; Fetter, 2001; Hamilton, 1970; Hein, 1991; Schreiber, 1968; Steurer and Underwood, 2003; Moran et al., 2007). These physical properties, as well as gamma-ray attenuation, electrical resistivity, magnetic susceptibility, are measurements that can be completed in minimal time and at low cost, shipboard, and in a manner that does not destructively impact the core.

The nature of the physical properties obtained from a multi-sensor core track, while continuous; act as a smoothing filter to the contributions of grain size distribution changes. This reduces the potential for misinterpretation from aliasing inherent in discrete sampling at low frequency (Bendat and Piersol, 2000). This also highlights low frequency changes or modifications to the deposited grain size distributions.

Grain size distributions can be particularly helpful in the interpretation of high-latitude, paleo- cryo-climate in marine sediments (Chapter 1). The ability to predict low frequency modifications of grain size distributions in field would aid in reducing the cost and time associated in the analysis of such cores. To this end, we investigated the empirical relationships between the grain size distributions of the glacio- marine cores of Integrated Ocean Drilling Program (IODP) Expedition 302 and the physical properties of those cores. This was then extended out to the reinterpretation of other high- latitude, glacio- marine cores. Thus developing reliable, predictive, empirical

equations that can be utilized for the interpretation of other such cores. IODP Expedition 302, Arctic Coring Expedition (ACEX), targeted the Lomonosov Ridge, central Arctic Ocean, for the interpretation of the dynamics of the deposited sediments found at that location and are used as the glacio- marine sediments that are the basis of this study.

Geologic Setting

The Lomonosov Ridge is a rifted section of the Eurasian continental shelf dividing the Arctic Basin. Drilling during ACEX focused on four sites, recovering sediments from three of the sites, penetrating ~420 m (Figure 2.1). The sediments recovered at the three sites reveal much of the Cenozoic Era, with the noticeable exclusion of two depositional hiatuses.

Following the coring process, three major units of lithology were identified (Backman et al., 2004). The upper lithology unit was composed mainly of sandy silt, devoid of most biological deposition. The bottom two lithologies are composed mainly of clayey silt and are richly abundant in biological material. They are distinguished from each other by changes in biological components. The sites were influenced by drifting ice, as evidenced by the presence of sand for most of the recovered record.

METHODS

Grain Size Analyses

Samples were collected and sealed aboard ship and refrigerated until grain size analyses could be performed. Sediment samples were analyzed for the individual grain size distribution of terrigenous material. To isolate the terrigenous material, the

samples were placed in a beaker and treated with acetic acid to rid the samples of biogenic carbonate, hydrogen peroxide to remove the lipids in each sample and sodium carbonate to eliminate the biogenic silicate (Dr John King, personal communication; Mortlock and Froelich, 1989). The samples were then dispersed using a solution of sodium hexametaphosphate for a minimum of 48 hours; further dispersion was achieved by exposing the samples to an ultrasonic bath for 10 minutes.

Grain size distributions from the samples were obtained on a Malvern Mastersizer 2000, a laser diffraction particle sizing system. The system determined the sand, silt, and clay fractions present in each sample. These data were compiled into half phi size bins (phi being a scale of grain size equal to $-\log_2$(diameter of grain)). These data and the subsequent physical properties used in this study can be found in Table 2.1.

Acoustic Compressional Wave Velocity

Acoustic compressional wave velocity (Vp) was measured utilizing a Geotek Multi Sensor Core Track (MSCL) p-wave logger. A p-wave logger generates an ultrasonic wave pulse. The pulse's dominant frequency is 500 kHz. The pulse is transmitted through an unopened, undisturbed core. The p-wave logger records the travel time. The diameter of the core is divided by the travel time, determining the velocity. The p-wave velocity was corrected for transducer and core liner time delays and core diameter deviations (Schulthesis and McPhail, 1989). The data were then run through a detrending program to remove the influence of depth.

Bulk Density

Bulk density was measured utilizing a gamma-ray attenuation porosity evaluator (GRAPE) on the MSCL (Evans, 1965). The measurement of bulk density in this matter is based on the concept of Compton scattering and attenuation. A parallel, monoenergetic beam of gamma rays produced from a sample of ^{137}Cs pass though the core and is detected on the opposite side by a scintillation counter. During passage gamma rays are absorbed and or scattered, loosing energy and direction. The energy loss and the attenuation are used to determine the bulk density (Boyce, 1976).

Color Reflectance

Color reflectance was measured utilizing a high-resolution color image camera on the MSCL. The image was then processed to determine both the percentage of color contribution from every 10-nm wavelengths (from 400 nm to 700 nm) and the color coefficient for each of the red, green, blue (RGB) contributions.

Approach

We investigated correlation relationships between physical properties of sediments, determined nondestructively from core logging techniques, and grain size distributions, determined from discrete samples. From these relationships, we were able to formulate predictive empirical equations for grain size distributions, ultimately determining changes in cryo-state.

Principle component analysis (PCA), a multi-variable statistical regression model, was initially employed to determine possible relationships for this study. However, due to the often-strong correlation of the nondestructive physical properties of the cores to each other, correlations to a particular grain size were indistinguishable

and mostly insignificant (Tables 2.2-2.6). PCA proved to be an analysis tool of limited usefulness for this data set due to its over-all interdependent nature. PCA requires a complete independent variable data set. It lacks usefulness for grain size and direct measurements of the physical properties of those grains analysis. Ultimately, the relationships reported in this study were determined by direct one-to-one comparison of various grain size ranges to their corresponding physical properties. This is a longer, but much more reflective, accurate, and revealing process that ensures no significant relationship is missed.

RESULTS

A previous study of grain size distributions and physical properties (Steurer and Underwood, 2003) compared clay fraction percentages and the physical properties of bulk density and porosity (Figure 2.2). Since porosity is calculated from the GRAPE-derived bulk density, assuming a specific gravity of 2.7, any relationship that exists for bulk density also exists for porosity. Therefore, in this study, we ignored the porosity relationships as a redundancy, focusing only on the bulk density. Additional studies (Bachman, 1985; Hamilton, 1971) compared the grain size distribution in terms of median grain diameter to the physical properties of compressional wave velocity and impedance. Again, since the impedance is calculated by multiplying velocity and bulk density, any relationship that exists for either one, should also result in a relationship with impedance. Therefore, in this study, we ignored the impedance relationships as a redundancy, focusing on the velocity and bulk density only. Studies of color and glacial/interglacial cycles have been completed on similar Arctic

sediments (Jakobsson et al., 2000; Jakobsson et al., 2001; Poore et al., 1993; Phillips and Grantz, 1997). The studies claimed that brown sediments, made so by additional Manganese content, were interglacial periods and contained an absence of larger grain size distributions. We found color relationships to grain size as well, however, the level of brown did not correspond to any of the size fractions.

In this study, we found relationships with physical properties for all three relevant categories of sediment (clay, silt, and sand). The Udden-Wentworth size classification system was employed for this study. This system defines sand as particles with diameters between 2000 μm and 63 μm. Silt is defined as particles with diameters between 63 μm and 4 μm. Clay is defined as all particles with diameters <4 μm. Using the grain size distribution samples that had reliable MSCL data at the same location (with the exception of the one major outlier in grain size distributions), linear regressions were fit to the various datasets of sand, silt, clay, and fines. The best correlations are used in this study for prediction purposes.

Sand was found to have strong positive correlations to acoustic compressional wave velocity (Vp; R = 0.79), bulk density (ρ; R = 0.67), and color reflectance at a 570 nm wavelength (570λ; R = 0.55) (Figure 2.3). Multiple color reflectance λs were found to have correlating relationships with the percentage of sand. A λ of 570 nm was chosen for prediction purposes since it produced the highest correlation coefficient (R) (Figure 2.4). Equally weighting all three relationships increases the accuracy of the predictive equation for sand:

$$\text{Sand \%} = -25.6686 + 1/3*(1.1*[570\lambda] + 0.05*[Vp] + 16\rho) \quad (2.1)$$

Silt was found to have strong negative correlations to bulk density (ρ; R = 0.82) and color reflectance at the 660 nm wavelength (660λ; R = 0.73) (Figure 2.5). Again multiple color reflectance λs were found to have a correlating relationship with the percentage of silt. A λ of 660 nm was chosen for prediction purposes since it produced the highest correlation coefficient (R) (Figure 2.6). Equally weighing both relationships increases the accuracy of the predictive equation for silt:

$$\text{Silt \%} = 5*(13 - 4\rho + 11*[660\lambda]^{(-0.32)}) \quad (2.2)$$

Clay was found to have a positive correlation to bulk density (ρ; R = 0.61) and a negative correlation to the green contribution on the RGB scale (G; R = 0.57) (Figure 2.7). All three color contributions (red, green, and blue) were found to have a correlation to the percentage of silt. Green was chosen for prediction purposes since it produced the highest correlation coefficient (R) (Figure 2.8). Equally weighing both relationships increases the accuracy of the predictive equation for clay:

$$\text{Clay \%} = 44.5 - 0.24*[G] + 24\rho \quad (2.3)$$

The predictive equations for silt and clay were added together, resulting in an equation for the prediction of the percentage of fine material in a sample (< 63 μm):

$$\text{Fines \%} = 109.5 + 4\rho + 0.24*[G] + 55*[660\lambda]^{(-0.32)} \quad (2.4)$$

By combining the silt and clay percentages in this manner, we are able to increase the accuracy of the predictions (Figure 2.9) and employ the cryo-state ratio of sand percentages to fines percentages (S/F) established in previous studies (Chapter 1). Higher values of the S/F ratio are indicative of a strong, perannial cyro-state with multi year sea ice (of some combination of frozen sea water and or icebergs). Lower values of the S/F ration are indicative of a weak, seasonal cryo-state with a diminished sea ice presence (of either frozen sea water and or icebergs).

While the individual relationships inherently missed percentage changes present in the samples, compounding relationships decreased these occurrences (Figure 2.9). When the predictive equations are applied to the entire high-resolution MSCL dataset with quality data acquisition, the S/F ratio eliminates the high frequency changes present in the physical samples and highlights the low frequency, major shifts in the central Arctic's cryo-state (Figure 2.10 and 2.11). The extended predicted S/F ratio matches the measured S/F ratio remarkably well. Major shifts in the predicted data occur at ~220mcd or 44.5 Ma, ~300mcd or 48.75 Ma, and ~315mcd or 50 Ma. A drawback of this predictive approach is that short isolated points were no sand was present in the direct sample is missed in the smoothing effect of the prediction. Times between 45.5 and 48 Ma, when through direct grain size analyze there is an ice free Arctic Ocean are predicted as a weakened, seasonal sea ice presence, but not as ice free.

DISSCUSSION

By utilizing the predictive relationships outlined in this study to determine the S/F ratio, future central Arctic coring expeditions will be able to determine if the three

cyro-state shifts found in the Expedition 302 cores are the only major shifts in the Arctic during the Cenozoic Era. Additionally, this can be used as a correlation feature between cores. If the uniqueness of the three cryo-state shifts persists with future exploration and research, it would indicate a fairly consistent cryo-state has existed in the central Arctic Ocean for the last 44.5 Ma. There was a weakened cryo-state previous to the 44.5 Ma transition, with an excursion into a stronger cryo-state from 50 to 48.75 Ma (Figure 2.11).

By comparing the timing and direction of the cryo-state transitions to the published paleogene temperature record of Weller and Stein (2007) for the same cores, we are able to determine a rough estimate for the Sea Surface Temperature that marks the boundary between a strong cryo-state and a weak cryo-state. Weller and Stein (2007) reported a warming of ~7° C across the transition present at 44.5 Ma, a cooling of ~10° C across the transition present at 48.75 Ma, and a warming of ~4° C across the transition present at 50 Ma (Figure 2.14). The transitions in cryo-state occur more rapidly than the warming and cooling periods, indicating a potential "tipping temperature" from one cryo-state to the other. This sea surface temperature appears to be in the 13 to 14° C range. This number can be refined with further SST work, both with increasing frequency of determination and increased accuracy. In addition to the significance of a "tipping temperature" to paleo- Arctic studies, this work can be of importance to the predictions of future Arctic cryo-states.

As of early August 2008, the SST 13° C isotherm was present south of Iceland in the North Atlantic and well south of the Artic Circle in the Pacific Ocean. SST temperatures at the present ice edge are 2-4° C (NCEP, 2008). There remains a

significant amount of energy left to be added to the Arctic surface waters to raise the central Arctic Ocean to the 13-14° C "tipping temperature". A potential avenue of research for ocean modelers will be how and when that threshold of energy reaches the central Arctic Ocean and changes the cryo-state.

CONCLUSIONS

Correlations between the data acquired from the non-destructive Multi- Sensor Core Logger (MSCL) and grain size distributions were developed in this study for the central Arctic region. These correlations can be used to predict core locations that represent shifts in the Arctic's cryo-state. We show that by obtaining acoustic wave velocity, bulk density, and color reflectance from split glacio-marine cores and employing empirical relationships, major shifts in ice presence can be predicted. This prediction can aid in the sampling and study of the cores. The methods outlined in this study have the potential to be developed for additional sedimentary environments, broadening the use and reach of MSCL data.

The utilization of the techniques within the Arctic environment yielded noticeable sharp/fast transitions from one cryo-state to another. All the retrieved transitions from the ACEX cores are older than 44.4 Ma, indicating a reasonably stable cryo-state in the neogene. The possible Sea Surface Temperature associated with the shift from one cryo-state to another may exist around 14 ° C. This study opens multiple avenues for future research in both paleo- and predictive studies.

REFERENCES

Bachman, R.T., 1985. "Acoustic and Physical Property Relationships in Marine Sediments." *Journal of Accoust. Soc. Am.*, Vol. 78, No. 2, pp. 616-621.

Backman, J., K. Moran, and D. Evans, 2004. "ACEX Arctic Coring Expedition: Paleoceanographic and Tectonic Evolution of the Central Arctic Ocean." *IODP Expedition 302 Scientific Prospectus,* Edinburgh (Integrated Ocean Drilling Program Management International, Inc.).

Bendat, J.S., and A.G. Piersol, 2000. Random Data: Analysis and Measurement Procedures. John Wiley & Sons Inc., NY.

Boggs, S., 1995. Principles of Sedimentology and Stratigraphy. Prentice-Hall Inc., NJ.

Boyce, R. E., 1976. "Definitions and Laboratory Techniques of Compressional Sound Velocity Parameters and Wet-Water Content, Wet-Bulk Density, and Porosity Parameters by Gravimetric and Gamma Ray Attenuation Techniques." *Initial Report of the Deep Sea Drilling Program*, Vol. 33, pp. 931-958.

Evans, H.B., 1965. "GRAPE-A Device for Continuous Determination of Material Density and Porosity." *Transactions 6th Annual SPWIA Logging Symposium, Dallas, TX*. Vol. 2, pp. B1-B25.

Fetter, C.W., 2001. Applied Hydrogeology. Prentice-Hall Inc., NJ.

Hamilton, E.L., 1970. "Sound Velocity and Related Properties of Marine Sediments, North Pacific." *Journal of Geophysical Research*, Vol. 75, No. 23, pp. 4423-4446.

Hamilton, E.L., 1971. "Elastic Properties of Marine Sediments." *Journal of Geophysical Research*, Vol. 76, No. 2, pp. 579-604.

Hein, F.J., 991. "The Need for Grain Size Analyses in Marine Geotechnical Studies." *In* Syvitski, J.P.M. (*Ed.*), *Principles, Methods, and Applications of Particle Size Analysis*, Cambridge Univ. Press, NY.

Jakobsson, M., R. Lovlie, H. Al-Hanbali, et al., 2000. "Manganese and Color Cycles in Arctic Ocean Sediments Constrain Pleistocene Chronology." *Geology*, Vol. 28, No. 1, pp. 23-26.

Jakobsson, M., R. Lovlie, E. M. Arnold, et al., 2001. "Pleistocene Stratigraphy and Paleoenvironmental Variation from Lomonosov Ridge Sediments, Central Arctic Ocean." *Global and Planetary Change*, Vol. 31, pp. 1-22.

Moran, K., V. Altmann, M. O'Regan, and C. Ashmankas, 2007. "Acoustic Compressional Wave Velocity as a Predictor of Glacio-marine Sediment Grain Size." *Geotechnical Testing Journal*, Vol. 30, No. 4.

Mortlock, R.A., and P.N. Froelich, 1989. "A Simple Method for the Rapid Determination of Biogenic Opal in Pelagic Marine Sediments." *Deep-Sea Research*, Vol. 36, No. 9, pp. 1415-1426.

NECP, 2008. "Real-time , Global, Sea Surface Temperature Experimental Analysis: Arctic SST." < polar.ncep.noaa.gov/sst/ophi > (July 30, 2008).

Phillips, R. L., and A. Grantz, 1997. "Quaternary History of Sea Ice and Paleoclimate in the Amerasia Basin, Arctic Ocean, as Recorded in the Cyclical Strata of Northwind Ridge." *GSA Bulletin*, Vol. 109, no. 9, pp. 1101-1115.

Poore, R. Z., R. L. Phillips, and H. J. Rieck, 1993. "Paleoclimate Record for Northwind Ridge, Western Arctic Ocean". *Paleoceanography*, Vol. 8, No. 2, pp. 149-159.

Schreiber, B.C., 1968. "Sound Velocity in Deep Sea Sediments." *Journal of Geophysical Research*, Vol. 73, pp. 1259-1268.

Schultheiss, P.J., and S.D. McPhail, 1989. "An Automated P-Wave Logger for Recording Fine-Scale Compressional Wave Velocity Structures in Sediments." *Proc. ODP Sci. Results*, Vol. 108, pp. 407-413.

Steurer, J.F., and M.B. Underwood, 2003. "Data Report: The Relation Between Physical Properties and Grain-Size Variations in Hemipelagic Sediments from Nankai Trough." *In* Mikada, H., G.F. Moore, et al. (*Eds*.), *Proc. ODP Sci. Results*, Vol. 190/196.

Weller, P., and R. Stein, 2008. "Paleogene Biomarker Records from the Central Artic Ocean (IODP Exp. 302): Organic Carbon Sources, Anoxia, and Sea Surface Temperatures. " *Paleoceanography*, Vol. 23.

Table 2.1: Grain size distributions and multi-sensor core logging data from IODP Exp. 302 (ACEX) used in this study.

cruise-hole-core-section	MCD	Sand (vol%)	Silt (vol%)	Clay (vol%)	Bulk Density (g/cc)	Vp (m/s) (depth corrected)	Reflectance at 570 nm wavelength (%)	Reflectance at 660 nm wavelength (%)	RGB Reflec. Coeff. (Green)
302-4-1-1	0.80	28.21	45.56	26.22	1.72	1528.16	20.32	20.59	92
302-4-1-2	1.56	28.35	44.14	27.53	1.68	1494.11	14.33	14.20	70
302-4-3-3	11.21	9.67	52.12	38.21	1.92	1472.11	14.65	14.92	70
302-4-4-3	16.48	9.22	52.11	38.69	1.89	1478.98	16.26	16.58	70
302-2-5-2	22.29	19.50	50.71	29.80	1.91	1483.06	10.29	10.19	87
302-4-3-1	24.27	13.88	54.80	31.33	1.96	1477.63	9.67	9.58	92
302-2-6-1	24.30	8.79	57.17	34.01	1.96	1463.78	9.51	9.42	93
302-4-6-1	24.37	9.26	53.53	37.20	1.86	1474.86	9.72	9.58	94
302-2-6-2	24.97	13.54	54.53	31.94	1.99	1471.94	10.63	10.50	102
302-2-6-2	25.67	14.78	53.93	31.28	1.86	1467.07	17.17	17.06	86
302-4-3-2	25.77	8.53	50.58	40.89	1.82	1449.06	19.03	18.91	77
302-2-7-1	31.51	19.09	52.34	28.55	1.90	1473.62	10.97	10.84	101
302-2-7-1	32.21	17.56	50.30	32.13	1.91	1478.26	11.39	11.26	89
302-2-7-2	33.01	14.34	50.82	34.83	1.91	1480.03	10.83	10.65	89
302-2-7-2	33.71	12.41	54.20	33.38	1.91	1471.51	11.15	11.01	79
302-2-8-2	37.51	14.13	55.49	30.39	1.94	1509.94	10.97	10.82	50
302-2-9-1	40.45	20.10	51.77	28.13	1.96	1522.07	9.47	9.31	81
302-2-9-1	41.15	12.99	52.91	34.10	1.92	1508.90	10.34	10.19	83
302-2-9-2	41.95	10.24	55.02	34.75	1.94	1489.96	9.94	9.81	97
302-2-9-2	42.65	18.00	52.02	30.01	2.06	1505.92	10.27	10.14	93
302-2-9-3	43.26	16.78	49.05	34.18	1.91	1495.89	12.16	11.98	116
302-2-10-1	44.95	14.90	50.96	34.13	1.98	1491.28	11.63	11.48	108
302-2-9-5	45.25	17.69	52.04	30.29	1.98	1491.76	10.88	10.09	93
302-2-10-1	45.65	15.43	53.60	30.96	2.04	1504.93	10.90	10.77	88

302-2-10-2	46.45	17.72	53.76	28.53	1.96	1474.79	9.92	9.81	84
302-2-10-2	47.15	23.77	48.80	27.42	2.05	1502.59	10.83	10.74	83
302-2-10-3	47.95	17.76	51.09	31.16	2.01	1509.00	9.30	9.19	79
302-2-11-1	49.53	16.91	49.74	33.38	1.86	1508.72	18.79	18.69	91
302-2-11-2	51.02	12.66	50.37	36.99	1.86	1483.92	10.69	10.62	71
302-2-11-3	51.83	12.87	52.05	35.08	1.85	1513.98	9.65	9.48	88
302-2-12-2	54.90	19.24	51.11	29.66	1.96	1501.21	11.13	10.99	82
302-2-13-1	58.38	15.85	52.06	32.07	1.88	1508.06	9.73	9.56	82
302-2-13-1	59.04	10.98	50.95	38.07	1.84	1473.34	10.11	9.97	85
302-2-14-1	61.14	14.94	51.87	33.21	1.95	1486.45	8.67	8.57	79
302-2-14-2	61.95	12.91	51.60	35.47	1.95	1510.41	8.77	8.67	71
302-2-14-3	62.95	10.80	52.37	36.83	1.98	1497.58	8.89	8.73	77
302-2-17-1	74.44	9.97	53.15	36.88	1.92	1502.07	9.05	8.94	86
302-2-17-1	75.14	12.04	54.96	33.00	1.93	1501.74	9.61	9.46	82
302-2-18-1	78.44	16.70	52.16	31.15	1.95	1485.28	9.86	9.75	85
302-2-18-1	79.14	10.86	54.37	34.77	1.99	1467.99	10.72	10.56	81
302-2-18-2	79.56	11.86	54.41	33.73	1.94	1494.81	9.31	9.15	58
302-2-19-1	81.64	23.41	48.67	27.92	2.00	1491.80	9.44	9.26	84
302-2-20-3	90.35	12.71	51.77	35.52	2.11	1454.76	8.33	8.22	80
302-2-21-1	91.64	7.93	52.58	39.48	1.97	1474.68	8.43	8.25	73
302-2-21-1	92.34	14.14	54.27	31.58	1.98	1493.79	7.63	7.52	71
302-2-24-2	108.13	12.52	53.40	34.08	1.96	1486.65	10.15	10.05	82
302-2-24-2	108.83	13.57	51.93	34.49	1.96	1450.06	9.58	9.44	89
302-2-25-1	111.14	10.38	53.90	35.73	1.94	1498.99	9.45	9.36	88
302-2-25-2	112.65	9.69	51.33	38.98	1.95	1495.95	10.70	10.60	90
302-2-25-2	113.35	13.93	53.57	32.50	1.97	1492.27	10.22	10.11	81
302-2-26-1	115.64	14.94	51.62	33.42	2.02	1468.62	10.51	10.40	76

302-2-26-1	116.34	18.87	49.90	31.22	2.01	1480.22	9.92	9.78	81
302-2-26-2	117.14	13.78	50.96	35.26	2.07	1480.58	11.02	10.88	92
302-2-27-2	122.84	15.62	55.57	28.81	1.94	1505.79	9.90	9.85	68
302-2-29-1	128.64	24.91	45.60	29.50	1.96	1423.86	9.96	9.84	82
302-2-29-2	130.14	18.66	51.71	29.63	1.92	1463.48	10.14	10.02	79
302-2-32-1	140.14	10.92	53.42	35.65	2.00	1467.97	9.09	8.97	78
302-2-32-1	140.83	13.27	54.50	32.22	2.07	1488.69	10.13	9.99	83
302-2-32-2	141.64	16.15	54.21	29.65	2.02	1489.23	10.42	10.22	90
302-2-32-2	142.34	13.48	54.28	32.24	2.04	1469.65	10.31	10.18	84
302-2-32-3	143.15	11.80	52.77	35.41	2.03	1458.31	11.43	11.28	91
302-2-32-3	143.85	7.72	54.62	37.67	2.00	1447.20	9.58	9.47	89
302-2-33-1	145.44	9.59	54.54	35.88	1.91	1477.76	11.58	9.57	87
302-2-33-1	146.14	10.01	52.98	37.00	1.98	1464.86	10.07	9.97	79
302-2-33-2	146.95	12.83	53.54	33.62	1.95	1460.35	9.95	9.82	84
302-2-33-3	148.47	15.59	53.25	31.14	2.02	1476.49	8.45	8.37	78
302-2-34-2	151.64	13.08	55.00	31.91	2.05	1449.49	11.05	10.90	94
302-2-35-3	156.90	12.03	55.25	32.71	1.90	1442.66	11.81	11.70	73
302-2-35-4	157.71	11.09	55.68	33.22	1.91	1439.44	11.93	11.82	86
302-2-35-4	158.41	10.64	52.49	36.86	1.89	1440.18	12.45	12.29	77
302-2-38-2	167.33	14.27	50.34	35.40	1.88	1398.44	15.02	15.09	91
302-2-38-2	168.03	8.23	49.75	42.01	1.91	1380.11	13.11	13.17	86
302-2-38-3	168.52	13.39	52.84	33.77	1.89	1377.16	14.92	15.16	78
302-2-40-1	173.52	9.29	44.82	45.91	1.83	1385.93	12.04	12.35	62
302-2-40-1	174.22	11.76	45.28	42.98	1.86	1394.09	10.62	11.00	63
302-2-42-2	185.13	11.00	51.57	37.43	1.98	1394.75	10.38	10.64	63
302-2-42-3	186.63	9.74	41.66	48.62	1.91	1385.38	11.46	11.83	66
302-2-43-1	187.93	11.52	49.04	39.45	1.89	1397.75	6.48	6.66	48

302-2-43-1	188.63	12.41	51.49	36.09	1.90	1396.78	10.99	11.21	53
302-2-43-2	189.42	14.16	46.25	39.61	1.88	1390.07	8.21	8.53	46
302-2-43-2	190.12	11.16	47.58	41.26	1.89	1377.19	13.56	13.69	44
302-2-43-3	190.93	6.81	51.56	41.63	1.87	1407.95	6.39	6.58	43
302-2-43-3	191.63	4.76	50.32	44.90	1.88	1400.47	5.36	5.53	37
302-2-45-1	196.71	26.90	40.03	33.08	1.80	1427.55	5.05	5.05	29
302-2-46-1	198.64	14.75	46.18	39.05	1.80	1401.21	7.11	7.11	27
302-2-47-2	202.14	3.93	50.54	45.52	1.91	1346.23	6.68	6.53	39
302-2-47-2	202.84	8.57	64.55	26.88	1.44	1322.12	5.94	5.84	25
302-2-47-3	203.64	4.16	54.85	40.98	1.74	1303.51	7.77	7.76	34
302-2-47-3	204.34	0.00	45.28	52.39	1.90	1292.37	6.86	6.88	45
302-2-47-4	205.15	6.37	35.24	58.38	2.00	1312.07	7.02	7.35	40
302-2-47-4	205.85	13.17	31.25	55.60	2.05	1291.94	6.12	6.65	43
302-2-47-5	206.35	9.71	38.13	52.14	2.10	1323.81	5.50	6.42	50
302-2-48-1	207.08	5.86	47.33	46.80	1.88	1285.00	6.90	6.42	51
302-2-48-1	207.78	14.65	62.16	23.20	1.94	1287.59	6.90	6.42	51
302-2-48-2	208.58	10.37	39.70	49.95	1.96	1302.43	8.17	8.16	51
302-2-48-2	209.28	5.07	38.59	56.31	1.95	1295.34	7.56	7.55	58
302-2-48-3	210.09	0.00	36.31	62.74	1.77	1305.42	8.05	7.99	44
302-2-48-3	210.79	1.37	48.57	50.05	1.77	1306.00	5.68	5.71	35
302-2-49-2	212.91	0.00	36.58	57.92	1.76	1289.80	14.13	12.84	48
302-2-49-2	213.61	0.00	33.09	66.29	1.79	1313.12	8.81	8.82	44
302-2-49-3	214.41	0.00	36.50	62.36	1.77	1296.36	8.02	7.96	42
302-2-49-3	215.11	13.12	47.61	39.28	1.77	1283.47	15.79	15.77	36
302-2-49-4	215.92	5.88	40.43	53.68	1.85	1289.86	9.22	9.18	
302-2-49-4	216.62	0.00	32.99	63.49	1.73	1281.02	6.21	6.19	
302-2-49-5	217.08	7.72	43.31	48.95	1.57	1321.93	8.91	8.92	

302-2-49-5	217.57	0.00	27.77	67.44	1.82	1338.84	10.48	6.46
302-2-50-1	219.02	0.00	37.20	60.66	1.77	1271.10	8.28	8.29
302-2-53-1	227.96	1.21	73.88	24.90	1.40	1297.46	8.24	8.27
302-2-53-2	228.78	3.33	74.70	21.96	1.28	1305.38	8.61	8.65
302-2-53-2	229.48	4.82	75.21	19.98	1.37	1294.58	7.17	7.16
302-2-53-3	230.28	9.73	59.55	30.74	1.44	1302.53	4.93	4.91
302-2-53-3	230.98	4.16	75.08	20.75	1.29	1312.06	4.02	3.98
302-2-53-4	231.88	1.31	69.53	29.15	1.28	1319.55	4.44	3.73
302-2-54-1	232.41	4.05	72.76	23.17	1.40	1321.15	4.39	4.40
302-2-55-2	236.61	9.57	61.07	29.36	1.42	1305.40	4.20	4.16
302-2-55-2	237.31	7.15	62.68	30.16	1.43	1296.26	3.81	3.83
302-2-55-3	238.12	2.75	73.20	24.03	1.38	1304.82	4.02	3.98
302-2-55-4	239.63	1.97	73.84	24.18	1.43	1298.97	3.50	3.50
302-2-55-4	240.33	6.24	64.63	29.12	1.52	1287.84	4.05	4.05
302-2-56-2	242.49	4.57	73.99	21.42	1.34	1305.68	4.17	4.18
302-2-56-2	243.19	2.55	77.63	19.82	1.34	1301.32	4.42	4.46
302-2-56-3	243.74	2.95	75.84	21.22	1.29	1296.29	4.23	4.25
302-2-56-3	244.70	0.98	71.91	27.13	1.36	1290.03	3.77	3.79
302-2-57-2	246.99	3.80	74.94	21.27	1.35	1283.81	3.50	3.51
302-2-57-2	247.69	5.51	68.15	26.34	1.30	1282.79	3.37	3.39
302-2-57-3	248.49	2.96	73.99	23.06	1.35	1286.66	3.73	3.70
302-2-57-3	249.19	5.05	73.89	21.07	1.31	1275.77	3.67	3.70
302-2-57-4	250.00	5.09	72.48	22.42	1.29	1280.45	4.19	4.19
302-2-57-4	250.70	4.55	78.71	16.73	1.31	1286.22	3.45	3.48
302-2-57-5	251.24	0.47	78.41	20.96	1.27	1285.18	3.94	3.96
302-2-57-5	251.70	7.95	72.62	19.46	1.29	1291.35	3.34	3.34
302-2-58-1	251.86	5.16	78.08	16.76	1.25	1302.12	3.82	3.86

302-2-58-1	252.56	4.05	67.80	28.14	1.33	1280.85	3.29	3.29
302-2-58-2	253.36	4.42	67.91	27.68	1.35	1291.03	3.52	3.50
302-2-58-2	254.06	3.95	68.49	27.55	1.27	1292.71	3.34	3.38
302-2-58-3	254.87	5.98	69.65	24.36	1.30	1301.35	3.08	3.09
302-2-58-3	255.57	2.51	85.98	11.50	1.28	1299.51	3.33	3.34
302-2-59-3	259.87	6.99	75.45	17.59	1.36	1269.56	3.66	4.00
302-2-59-3	260.57	5.13	80.75	14.10	1.33	1272.06	4.62	5.93
302-2-60-1	260.98	5.48	70.50	24.01	1.30	1263.34	4.62	5.93
302-2-60-1	261.68	12.71	62.75	24.56	1.37	1260.16	5.10	4.60
302-2-60-2	262.47	4.47	81.66	13.86	1.34	1234.34	3.33	3.36
302-4-4-1	265.15	2.69	77.75	19.56	1.39	1234.15	4.47	4.48
302-2-61-1	265.58	5.69	69.40	24.90	1.42	1238.35	3.61	3.61
302-2-61-2	266.47	0.00	85.05	14.96	1.40	1246.60	3.63	3.59
302-2-61-2	267.06	9.60	76.16	14.21	1.37	1259.00	6.61	6.62
302-2-62-1	270.33	3.23	79.87	16.85	1.37	1235.38	3.14	3.17
302-4-5-1	270.48	0.00	78.21	19.57	1.17	1237.62	4.35	4.35
302-2-62-1	270.87	4.88	70.70	24.40	1.33	1245.85	4.17	4.15
302-4-5-1	271.18	1.25	71.54	27.21	1.38	1231.79	3.72	3.62
302-2-62-2	271.37	2.46	75.53	22.01	1.37	1225.68	3.72	3.62
302-4-5-2	271.62	0.00	77.00	21.36	1.57	1251.00	6.21	6.56
302-4-5-2	272.02	3.61	71.61	24.79	1.57	1246.36	3.32	3.57
302-2-62-2	272.07	4.92	73.58	21.51	1.36	1257.03	4.59	4.90
302-2-62-3	272.63	4.87	79.05	16.07	1.57	1240.89	4.23	4.53
302-2-62-3	273.21	3.88	73.51	22.61	1.58	1253.80	4.23	4.53
302-4-6-1	274.64	0.27	80.89	18.85	1.36	1250.08	5.34	5.38
302-4-6-2	275.44	2.21	73.95	23.81	1.40	1239.04	4.71	4.94
302-4-6-2	276.14	1.92	75.58	22.48	1.41	1239.86	4.81	5.08

302-4-6-3	276.95	1.04	86.04	12.92	1.36	1242.89	5.42	5.67
302-4-6-3	277.65	1.26	76.00	22.73	1.41	1242.64	7.87	8.01
302-4-7-1	279.14	0.00	77.47	21.06	1.35	1249.33	3.30	3.51
302-4-7-1	279.84	3.53	84.72	11.73	1.35	1254.59	3.07	3.35
302-4-7-2	280.66	3.53	70.39	24.37	1.40	1253.55	3.29	3.54
302-4-7-2	281.36	0.00	79.73	20.27	1.40	1253.83	3.66	3.87
302-4-7-3	282.17	6.38	77.23	16.39	1.36	1252.48	3.35	3.55
302-4-7-3	282.87	5.90	75.33	18.76	1.41	1252.31	3.30	3.49
302-4-10-1	292.29	0.00	68.57	31.03	1.46	1246.17	3.20	3.35
302-4-10-1	292.99	2.35	74.09	23.56	1.45	1241.43	3.30	3.35
302-4-10-3	295.29	0.00	73.77	26.24	1.43	1244.01	3.54	3.59
302-4-10-3	295.99	0.00	74.47	22.40	1.44	1242.32	3.52	3.63
302-4-10-4	296.50	0.00	73.28	25.06	1.43	1256.51	5.42	5.39
302-4-10-4	296.92	0.00	72.31	25.19	1.49	1283.69	4.16	4.02
302-4-11-1	297.74	1.92	80.90	17.16	1.34	1242.32	3.32	3.43
302-4-11-1	298.44	0.00	77.44	21.70	1.34	1243.14	3.33	3.39
302-4-11-2	299.24	2.74	73.22	24.05	1.41	1236.92	3.08	3.23
302-4-11-2	299.94	0.00	69.08	29.55	1.48	1241.49	5.52	5.61
302-4-11-3	300.75	0.00	76.69	21.97	1.43	1243.06	4.50	4.66
302-4-11-3	301.45	8.46	67.27	24.23	1.43	1243.85	4.22	4.32
302-4-11-4	302.02	0.70	76.78	22.52	1.41	1234.22	4.48	4.58
302-4-19-1	320.97	82.24	12.51	5.27	1.60	1342.80	2.86	3.10
302-4-19-1	321.67	6.04	57.65	36.31	1.58	1216.32	3.29	3.51
302-4-19-2	322.46	9.62	52.09	38.29	1.60	1225.97	3.75	3.98
302-4-19-2	323.16	10.90	52.73	36.41	1.65	1237.06	4.50	4.69

Table 2.2

Sand	Correlation Coefficient
Acoustic Wave Velocity	0.352
Bulk Density	0.246
Color 570	0.245
Color 580	0.244
Color 590	0.202

Table 2.3

Silt	Correlation Coefficient
Bulk Density	0.626
Acoustic Wave Velocity	0.316
Color 610	0.179
Color 620	0.103
RGB Reflectance (Green)	0.023

Table 2.4

Clay	Correlation Coefficient
Bulk Density	0.368
Acoustic Wave Velocity	0.069
RGB Reflectance (Green)	0.031
RGB Reflectance (Red)	0.027
Acoustic Wave Amplitude	0.002

Table 2.5

Acoustic Wave Velocity	Correlation Coefficient
Color 600	0.806
Color 610	0.803
Bulk Density	0.658
Color 550	0.352
Color 540	0.316

Table 2.6

Bulk Density	Correlation Coefficient
Acoustic Wave Velocity	0.658
Resistivity	0.615
Reflectance at 600	0.558
Reflectance at 610	0.557
Reflectance at 590	0.556

Tables 2.2-2.6: The first principle components (components of greatest significance) for the ACEX MSCL data set and various grain size percentages were all statistically significant (explained more than 0.5 percent of the variance in the data set. For all of the principle component analyses (PCAs) run for each of the sediment sizes of sand, silt, and clay only the first principle component was significant. Once the existence between variables was established, the correlation coefficients were examined for each run. Tables 2.2-2.6 display the correlation coefficients for some of the variables. Too many of the variables qualified as being statistically significant to each other, diminishing the correlation to the grain size. Without any standout variables, this approach prohibited a narrowing down of the variables, which had statistically meaningful relationships with the grain size being analyzed. Tables 2.2-2.6 are the correlation coefficient for sand, silt, and clay respectively and various physical properties. Each of these show significantly lower correlation coefficients than the correlations the physical properties had to each other, examples of which are displayed in table 2.5 for acoustic wave velocity and table 2.6 for bulk density. The noticeable exception to this is the significantly strong correlation silt has with bulk density. The PCA was completed using the Molegro Data Modeller software.

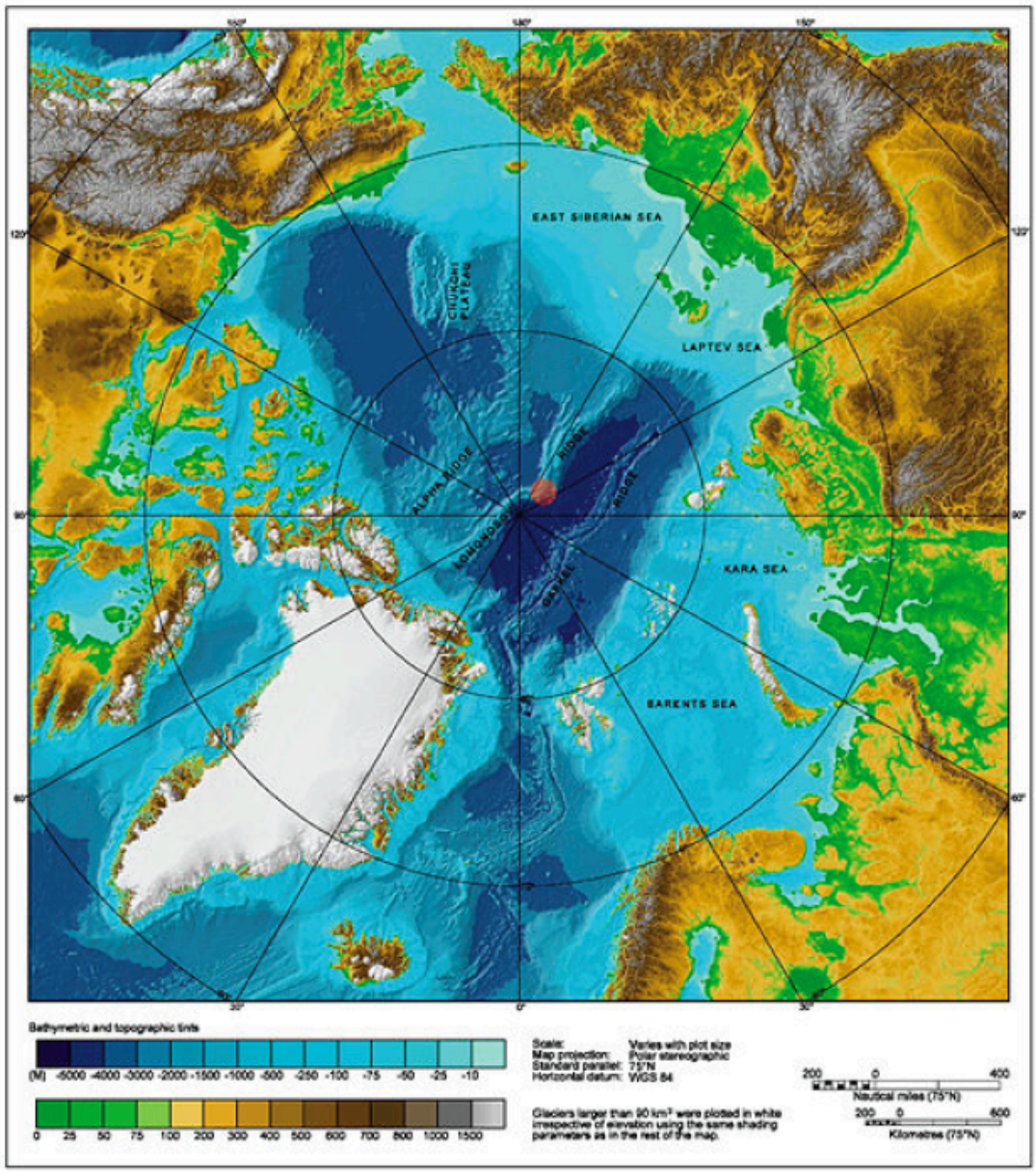

Figure 2.1: IODP Exp. 302 (ACEX) drill sites were located in the central Arctic Ocean, on the Lomonosov Ridge (red dot). These sediments were entirely from the Cenozoic Era and are primarily glacio-marine in origin. (IBCAO, 2008)

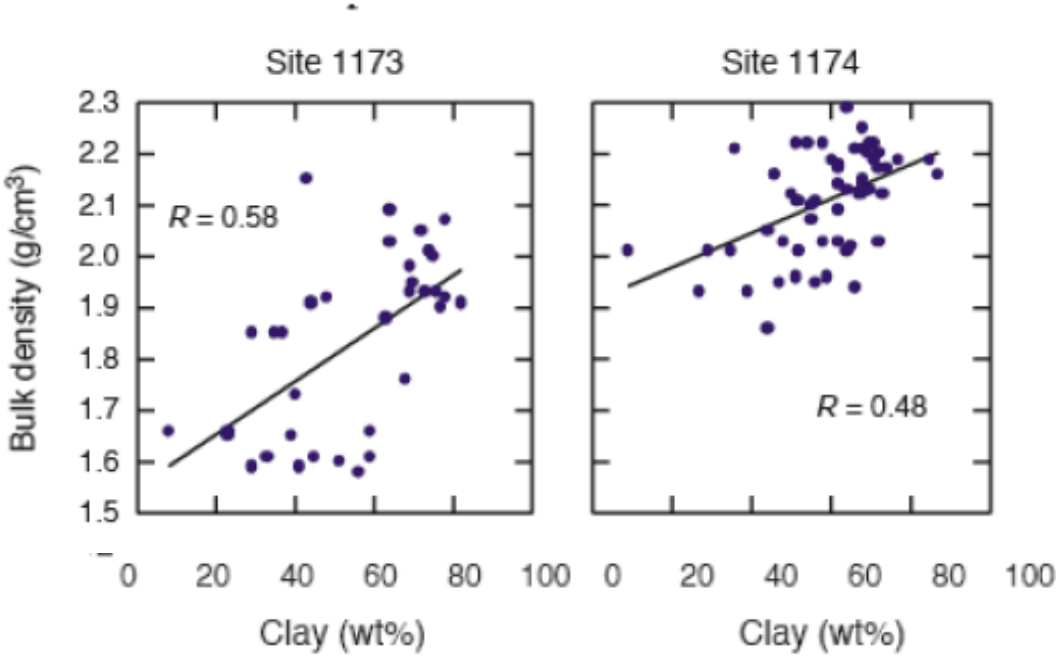

Figure 2.2: Steurer and Underwood (2003) found positive relationships between bulk density and percentage of clay by weight. Sites 1173 and 1174 were located at the Nankai Trench. While a vastly different depositional environment than the sediments analyzed in this study, the positive relationship is true in both studies.

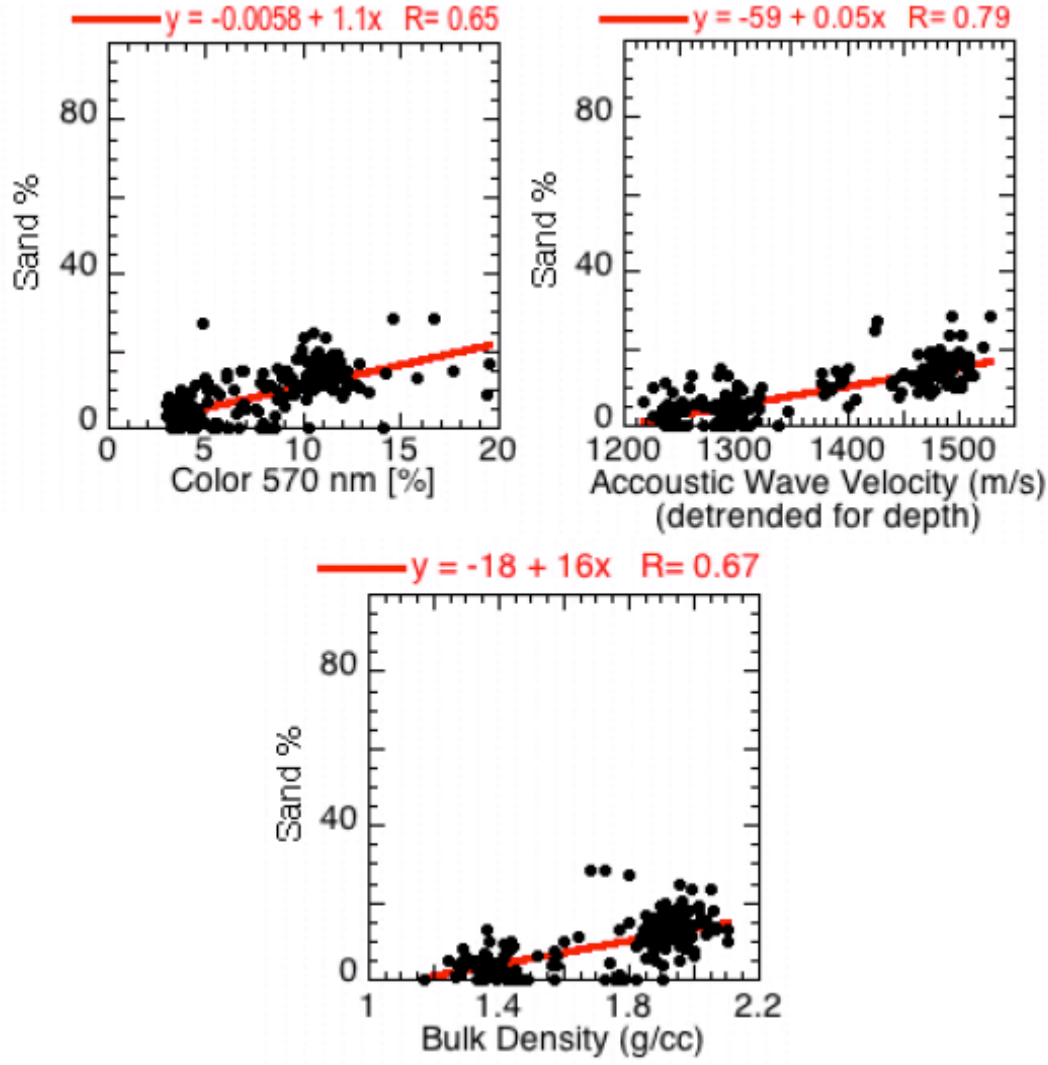

Figure 2.3: The three significant linear relationships between percentage of sand (% volume) and the physical properties of the sediments are color reflectance at the 570 nm wavelength, acoustic wave velocity, and bulk density. The positive linear regressions are combined and used as a predictor of sand contributions.

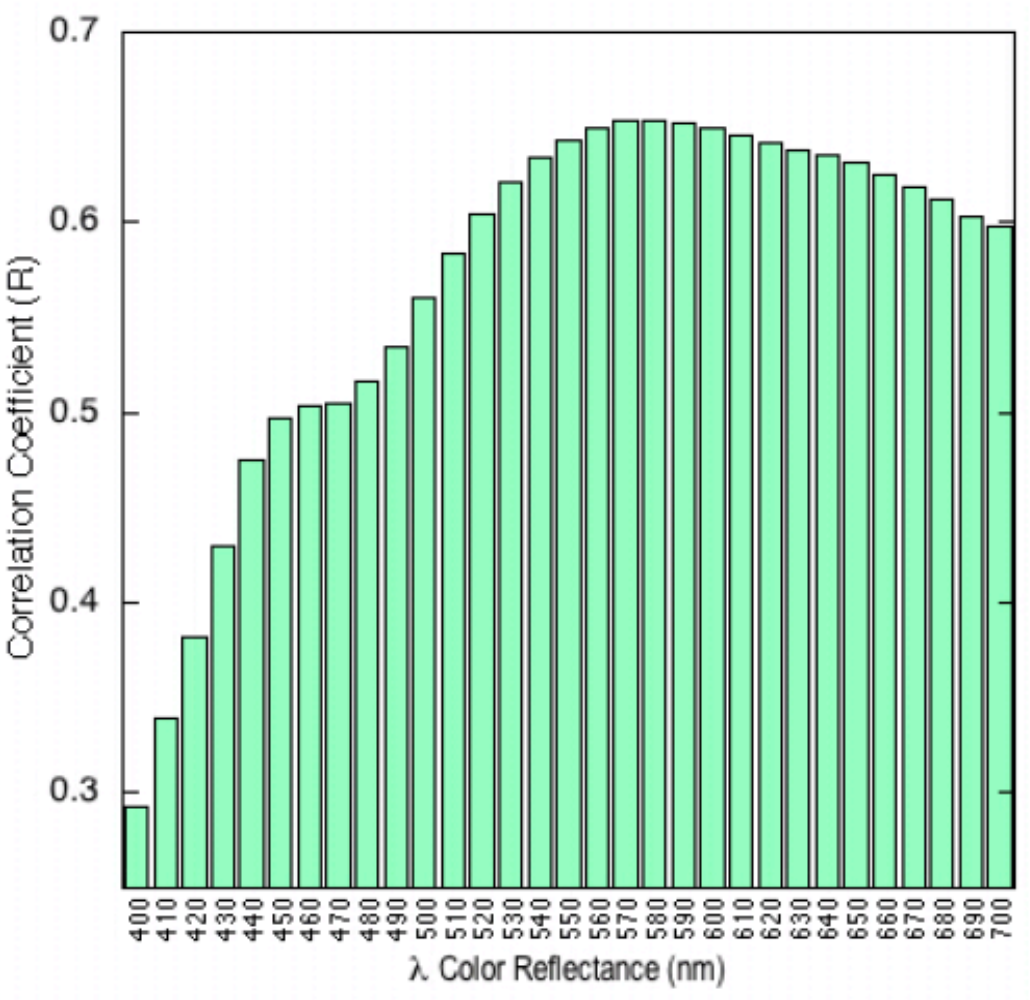

Figure 2.4: Multiple reflectance wavelengths were found to have significant relationships to the percentage of sand (% volume). The wavelength of 570 nm was chosen to be used for prediction purposes since it had the greatest R-value of all the wavelengths.

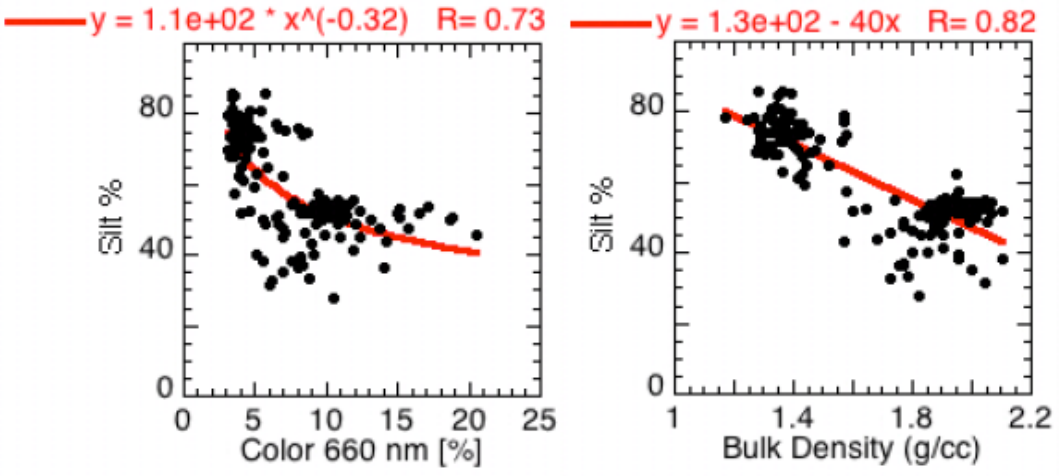

Figure 2.5: Percentage of silt (% volume) has a power relationship with 660 nm wavelength color reflectance and a linear relationship to bulk density. These negative relationships are combined for the purpose of predicting the contribution of silt non-destructively.

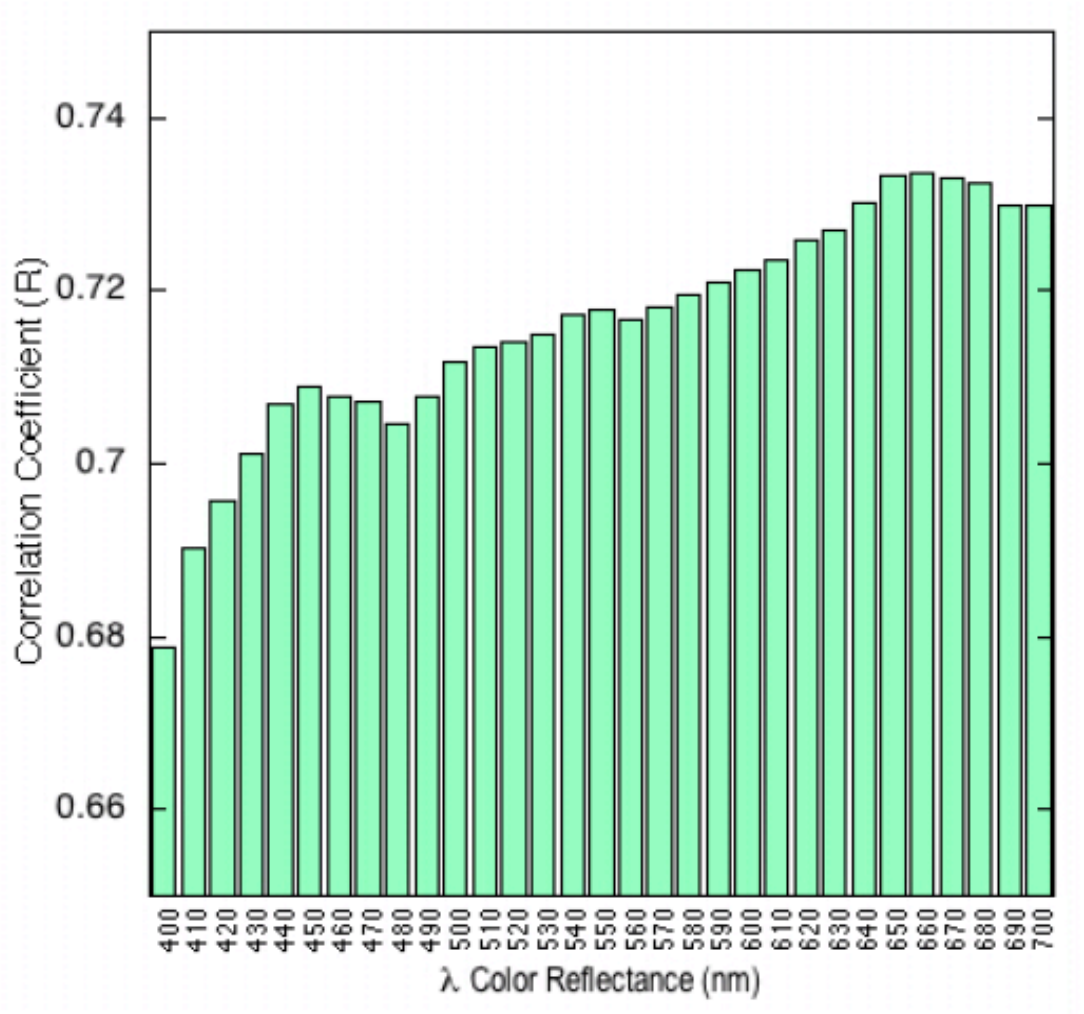

Figure 2.6: All of the color reflectance wavelengths had significant power relationship to the percentage of silt (% volume). The wavelength of 660 nm was chosen for prediction purposes since it had the greatest R-value of all the wavelengths.

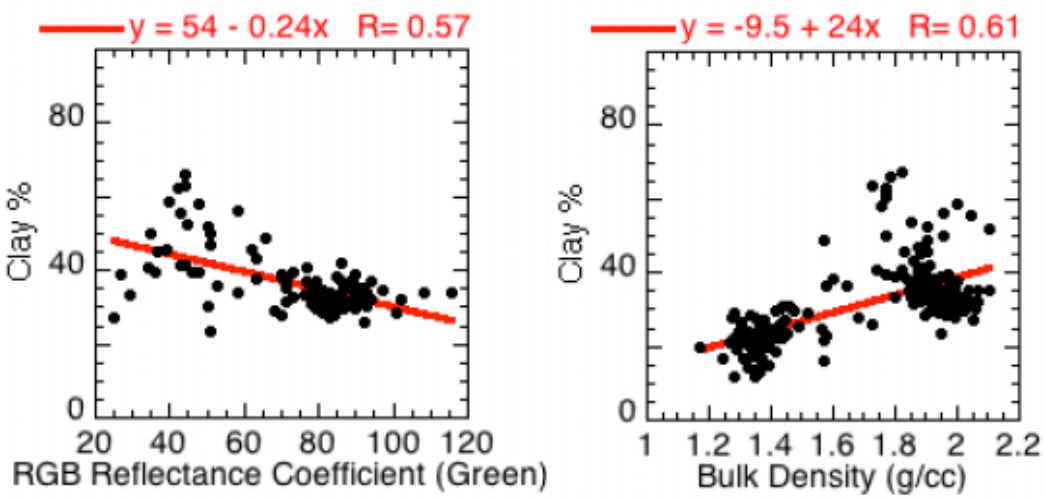

Figure 2.7: The percentage of clay (% volume) has a negative linear relationship with RGB reflectance coefficient of green and a positive linear relationship bulk density. These relationships were combined to establish predicting equations.

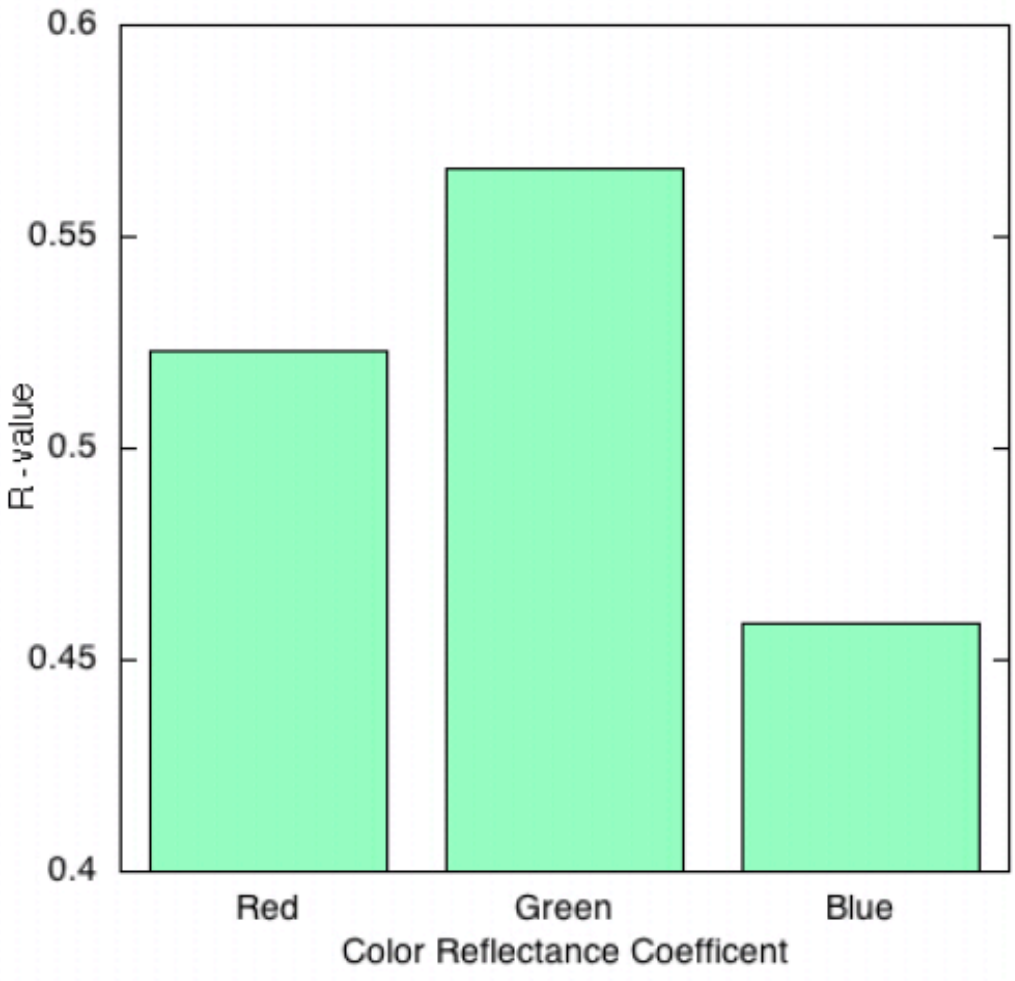

Figure 2.8: Of the three RGB color coefficients, green had the greatest R-value. Green was therefore chosen for the predicting equations.

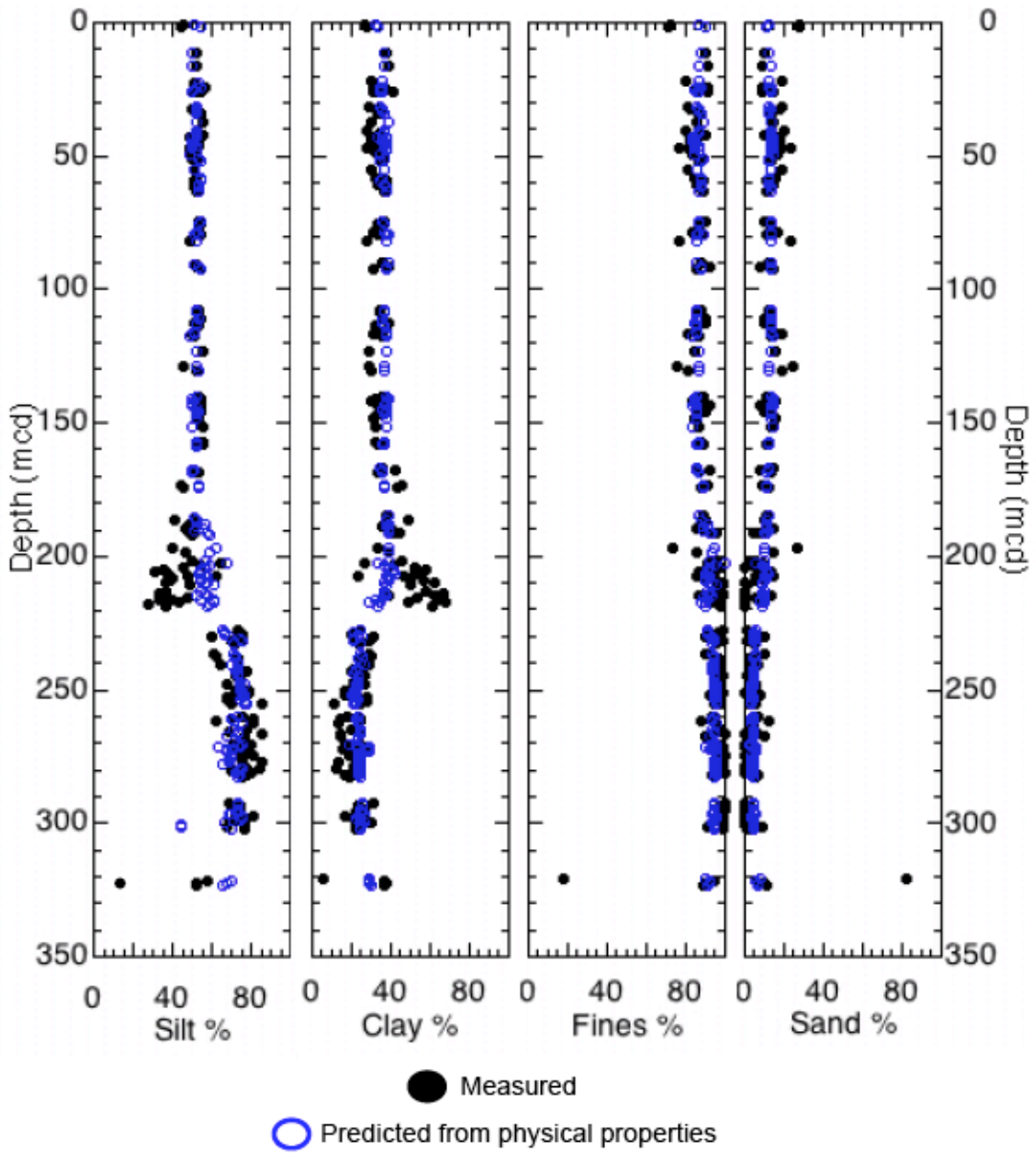

Figure 2.9: The four graphs show the measured percentages (% volume) of silt, clay, fine material (silt + clay), and sand and compares to each locations predicted percentage. The predicted fine material eliminates much of the inaccuracy of the silt and clay predictions.

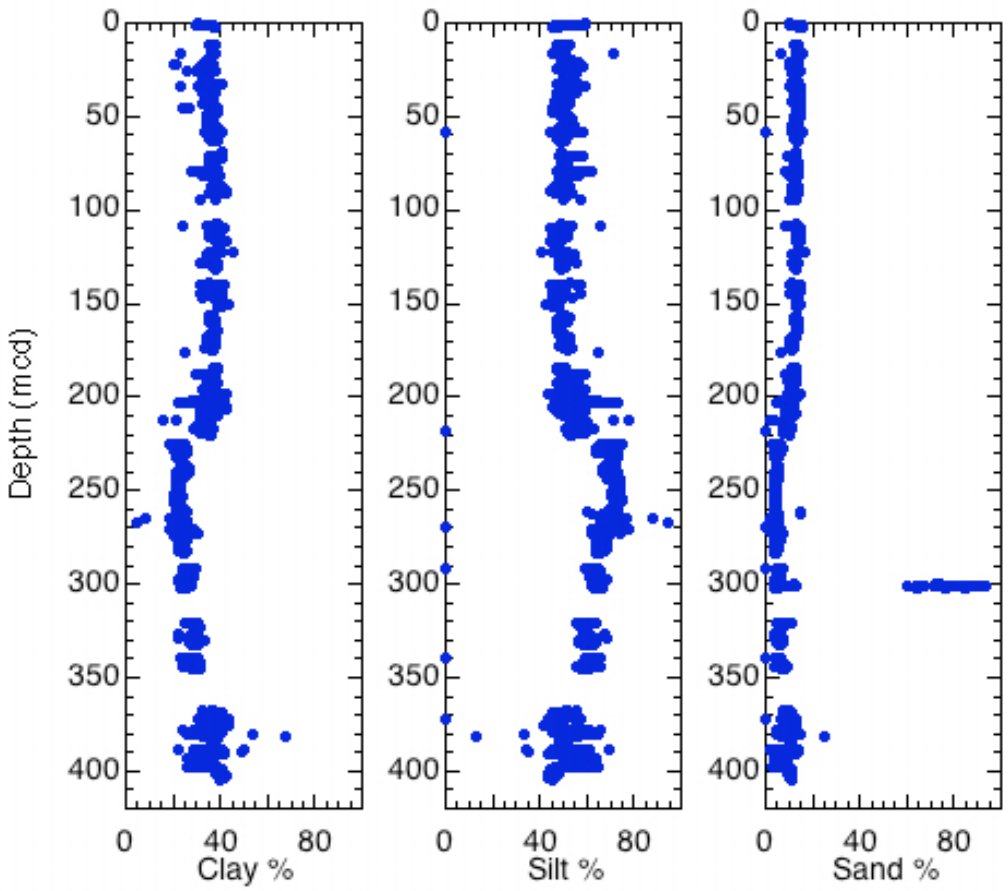

Figure 2.10: The graphs are of the predicted clay, silt, and sand percentages from the high-resolution MSCL data set. Clay, silt, and sand percentages all stay fairly consistent for the top 220 mcd of the ACEX cores. Below 220 mcd, clay percentages decrease (with increases with greater depth), silt percentages increase (with decreases with greater depth), and sand percentages decrease consistently with an exception at ~300 mcd when the sand percentages greatly increases. The changes in percentages above and below 220 mcd are most likely indicative of a change in cryo-state from seasonal sea ice (lower cores) to perennial sea ice. The sharp change in sand percentages may correspond to a strong river influence at that time.

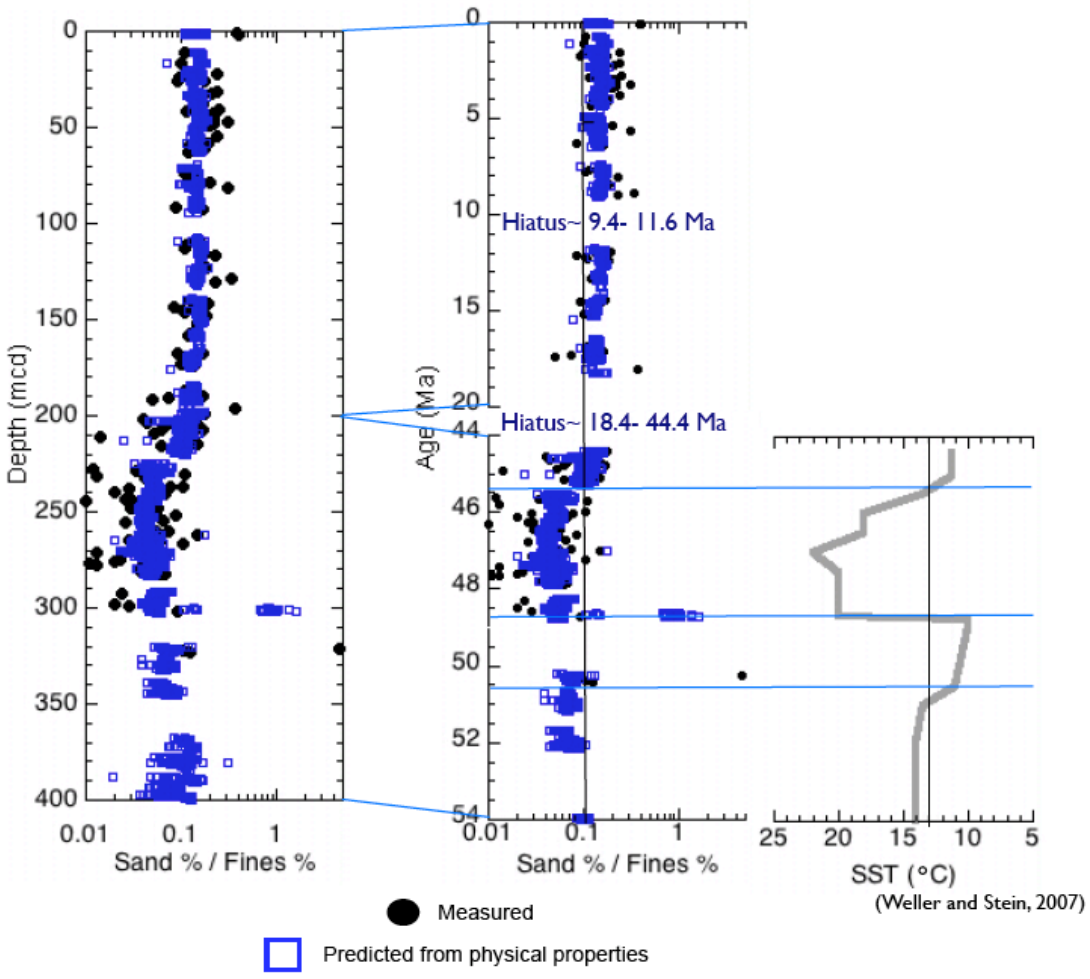

Figure 2.11: The graphs show the predicted sand to fine material ratio (S/F), which is a cryo-state proxy, for all the usable, high-resolution physical properties from the ACEX cores. These are compared to the measured ratio from discrete samples. The predicted ratio is fairly consistent until ~220m, 45.5 Ma. The cryo-state then weakens, with one possible excursion. This analysis of the cryo-state of the central Arctic Ocean correlates well with determined SST from the same cores. The use of high-resolution in the prediction of S/F in these graphs expands and extends the grain size analysis of the cores and helps improve confidence that the discrete samples are not being aliased due to sampling intervals.

Chapter 3

"Late Pleistocene Changes in Ice and Currents from the Central Lomonosov Ridge, Arctic Ocean"

by

Cristin E. Ashmankas[5,6]

written for submission to Journal of Sedimentology

[5] Graduate School of Oceanography, The University of Rhode Island, Narragansett, RI 02882.
[6] Assistant Professor, Natural Science and Mathematics Division, Lesley University, Cambridge, MA 02138. Email: cashmank@lesley.edu

Chapter 3. Late Pleistocene Changes in Ice and Currents from the Central Lomonosov Ridge, Arctic Ocean

ABSTRACT

The Arctic Coring Expedition (ACEX), a milestone research endeavor that took place during the summer of 2004, obtained a sediment core record from the central Lomonosov Ridge, Arctic Ocean. Grain size analyses of samples from the ACEX cores are complemented in the Holocene by high-resolution grain-size sampling taken from an ARCTIC '91 piston core and physical properties from Arctic Ocean-96 cores, both from locations near the ACEX site. This study is concerned with our ability to resolve and decouple paleo-currents from the paleo-ice climate. Relative paleo-current magnitudes can be ascertained using a measure of 'sortable silt' (SS), the mean of the silt fraction in a sample (McCave et al., 1995a,b). Paleo-ice climate can be estimated from the ice rafted debris (IRD), specifically the sand fraction percentage of a sample. The grain size analysis shows a linear relationship between SS and IRD. The linear relationship suggests that paleo-ice climate intensity can be overestimated with higher paleo-current speeds. Employing the linear relationship, the contribution of paleo-currents can be removed from the IRD record and the two paleo-indicators examined separately. The late Pleistocene has a strong paleo-ice climate and a strong, narrow range of paleo- bottom current speeds. There is a strong, noticeable change at the MIS 6 boundary (~200 ka), where the ice climate was significantly strengthened to levels higher than at any other time in the Cenozoic record recovered from ACEX and the central Arctic Ocean, a strengthening not observed in the paleo-current speeds, which stay in the pre-MIS 6 range.

INTRODUCTION

The use of the silt fraction (<63 μm) from grain-size distribution to obtain speeds of paleo- bottom currents is becoming a well-established practice (Prins et al., 2002; McCave et al., 1995a). Silt, which in most glacio- marine influenced regions is deposited from icebergs, bottom currents, and sea ice can not be separated into paleo-climate (IRD) influenced silt deposition and non- paleo-climate influenced deposition in most circumstances due to the multiple deposition mechanisms (McCave et al., 1995b). However, the Lomonosov Ridge, being significantly raised from the Arctic's abyssal plain, removes the influence of bottom-current silt deposition (Clark and Hansen, 1983). This unique bathymetric feature allows for both the interpretation of the paleo-current and –climate. For this reason, the coring study of the Arctic Coring Expedition (ACEX), which took place during the summer of 2004, along with the previous Arctic '91 and Arctic Ocean –96 were ideally suited for examining the paleo-current and –ice climate of the late Pleistocene Arctic Ocean (Figure 3.1).

Aagaard (1981) showed bottom current speeds across the central Lomonosov Ridge that are sufficient for active sediment transport, particularly of the finer grain sizes. Previous studies of the central Lomonosov Ridge have noted that cores from the ridge show increased sand and suggest the effect of bottom currents in winnowing finer sediments from the site (Bjork et al., 2007; Darby et al., 1989, 1997). The measure of paleo-current speed is the mean size of the silt fraction, or 'sortable silt' (SS). Coarser SS sizes indicate stronger current speeds acting on the sediment in both the depositional process and post-deposition winnowing (McCave et al., 1995b; Hall et al., 2001). The work has been further developed by Prins (2002) and Moros et al

(2002) to be used in examining the relationship between the IRD and SS components. The initial work of Prins (2002) and Moros et al. (2002) indicates that the intensity or percentage of IRD in a sample may be increased by the removal of fine-grained sediment by paleo-currents.

Ice Rafted Debris (IRD), commonly considered the sand fraction in glacio-marine sediments, has been well established as a paleo- ice climate indicator (Chapter 1 and 2). Jakobsson et al. (2001), Poore et al. (1993), Phillips and Grantz (1997), Gyllencreutz (2005), Prins et al. (2002), Clark (1996), Ruddiman (1977), and Sakamoto et al. (2005), have all employed a definition of IRD as being the >63 μm grain size component. The use of the 63 μm minimum limit permits the most complete analysis of IRD, specifically including sediment deposited from sea ice along with icebergs.

A number of Arctic studies have evidence of mega-iceburgs originating from the grounded ice shelves of the Laurentide ice sheet (Polyak et al., 2007). These studies place the first erosional horizon of icebergs on the Lomonosov Ridge in MIS 6, ~150 ka (Jakobsson et al., 2001). The collapse of this ice sheet has a chronology of 14-34 ka (Darby et al., 2002). The timing of all this evidence of increased iceberg presence in the central Arctic Ocean correlates to the reconstruction of a massive northern Eurasian ice sheet (Svendsen et al., 2004). The work of this study, by decoupling the influence of winnowing on IRD fractions, provides further evidence for the strengthened paleo- ice climate at the MIS 6 boundary.

METHODS

The sites used in this study can be interpreted to represent the paleo-climate of the central Cenozoic Arctic Ocean because the Lomonosov Ridge separated from the Eurasian shelf, limiting sedimentation influences to those from mid-ocean deposition. All of the core sections were run through a multi-sensor core logger (MSCL) to measure high resolution physical properties, including p-wave velocity, image/color analyses, gamma ray attenuation, magnetic susceptibility, and electrical resistivity. The initial step to determining the paleo-ice environment of the Cenozoic Arctic Ocean is to determine the grain size distribution of the cores. To accomplish this, each of the sediment samples taken from the cores was analyzed for its individual grain size distribution of terrigenous material. The samples were steeped in a solution of sodium hexametaphosphate for at least 48 hours to ensure that the clay particles were neutralized and that no flocculation occurred. Each of the sediment samples was run on the Malvern Mastersizer 2000, a laser diffraction particle sizing system. These data were then compiled into half phi size bins (phi being a scale of grain size equal to – $\log_2$ (diameter of grain)).

The SS of each sample was obtained by determining the mean of each sample's silt component (10 – 63 μm) as a proxy of the paleo-current intensity. Linear regression analysis was performed on the SS and sand % (IRD) components. Once a relationship between the mean silt size and the percentage was established for each data set, the SS contribution to each sand percentage was removed, revealing paleo-ice presence to a greater accuracy.

In addition, an examination of the ability of data from the Malvern Mastersizer 2000 to accurately and precisely determine silt and sand percentages was completed. For the ACEX sediment samples, 10 percent of the samples were compared for their grain size distribution percentages obtained from the Malvern Mastersizer 2000 to a more traditional procedure for determining grain size distributions. For the comparative procedure, samples were prepared in an identical fashion as the sample preparation for the Mastersizer and then hydrometer readings taken at set prescribed times to determine sand and silt percentages (Bouyoucos, 1962). The comparisons between silt and sand grain size distributions obtained by each process show no statistical difference (Figures 3.2-3.3). The small differences that do exist between the two methods (<3% of values) are within the range of error due to rounding differences, human error, and the possible discrepancy in comparing percent volume (Malvern Mastersizer 2000) and percent weight (hydrometer method). Differences in the percentages due to looking at either weight or volume, only exist if there is a difference in the mineral density of the sand, silt, and clay fractions. In addition, 10 percent of the samples were run 3 times on the Malvern Mastersizer 2000 with less than a 1 % difference between the runs. It was suggested by McCave et al. (2006) that laser diffraction was not a reliable means of determining grain size distributions (they used a Malvern Mastersizer 2600 in the study, a previous generation to the 2000 series). Our methodology supports the analyzes of others that have not only demonstrated the accuracy and precision of laser diffraction in grain size distributions, but concluded it as the preferred method for grain size distributions of clay, silt, and sand (Jonkers et al., 2009; Wen et al., 2002; Sperazza et al., 2004; Goossens, 2008).

In fact, the most comprehensive of the studies conducted by Goossens (2008), which examined and compared 10 of the most widely used and accepted methodologies for determining grain size distributions, found that McCave et al.'s (2006) preferred methodology involving the Sedigraph, grossly overestimates the silt fraction due to the nature and assumptions of the methodology.

RESULTS

Sortable Silt- Sand Relationship

Linear regression analysis, performed on both the ACEX and the ARCTIC '91 sediment distributions for the quaternary period, revealed a strong relationship between the mean silt fraction (SS) and the percentage of sand (IRD). The relationship determined for the ACEX quaternary samples is:

$$\text{Sand \%} = 204.65 - 37.572*SS \qquad (3.1)$$

with an R-value of 0.94352, showing highly strong correlation (Figure 3.4). The relationship for the ARCTIC '91 quaternary samples is:

$$\text{Sand \%} = 344.67 - 58.87*SS \qquad (3.2)$$

with an R-value of 0.79399, showing strong correlation (Figure 3.4). The strength of the relationships supports the concept that the measure of the mean silt size (SS) is a proxy for paleo-current intensity for a particular depositional environment. The mechanism that is most likely responsible for both the increased sand presence and the larger mean silt size (lower phi value) is the winnowing of the deposited sediments by paleo-currents. These relationships are then used as projection transforms to reconfigure the sand percentage, as it would have been prior to the winnowing effects.

Changes in Ice and Current Velocities

The transformed sand percentages for the quaternary period of the ACEX samples and the corresponding mean silt sizes (SS) show a dynamic environment in the central Arctic Ocean for the Quaternary period, particularly in the late Pleistocene epoch (Figure 3.5). While prior to MIS 6 in the late Pleistocene (~200 ka), the sand percentage (IRD) is shown to be fairly consistent. This indicates a consistent ice intensity presence. Post-MIS 6, the sand percentage increases by roughly 15%. The implication is a significantly strengthened ice presence following the MIS 6 boundary. This alteration in ice intensity was expected from the physical property analysis for both the ACEX cores and other cores previously taken from the Lomonosov Ridge (Figure 3.6). The physical properties of the sediments all indicated that significant changes in depositional environment took place at the MIS 6 boundary. Bulk density, inclination, and magnetic susceptibility all showed sharp increases at the ~200 ka date. This transition corresponds to a time of global instability in the cryosphere as determined from global benthic $\delta^{18}O$ data that shows a gradual increase in $\delta^{18}O$ values from 4-1.5 Ma (strengthening cryosphere) followed by high frequency changes in the values from 1.5 Ma to present (Zachos et al., 2001; Lisiecki and Raymo, 2005; O'Regan et al., 2010).

While physical properties and sand percentage (IRD) show two distinct regimes pre- and post- MIS 6, the mean silt size (SS), a proxy for current intensity, shows no such pattern (Figure 3.5). Current intensity does vary over the Quaternary period, but with no pre/post MIS6 distinction. There is no discernable pattern in the paleo-current velocities as determined by the SS proxy. This indicates a decoupling

between the climate of the Arctic as indicated by the sand % (IRD) and the physical oceanography of the Arctic Ocean. This supports O'Regan et al. (2010) hypothesis that the increase in IRD at the start of MIS 6 is due to an increase in the amount of heat available for basal ice melt from the opening of the Bering and Fram Straits introducing lower-latitude water bodies to the Arctic.

DISCUSSION

The emerging use of the 'sortable silt' proxy for paleo-currents can be of significant use for raised, isolated, depositional features, such as the Lomonosov Ridge. Further development of the proxy through the analyses of additional samples from multiple sites of similar physical characteristics will lead to a clearer understanding of both paleo-physical and geological oceanography conditions. The use of such methods will prevent future misinterpretations of sand percentage (IRD) strengthening that may have been due to increased current velocities and not to changes in climate. The full potential of such methodologies will develop with time and data volume.

In its limited use, mean silt size (SS) provides intriguing glimpses of the paleo-Arctic, particularly in the ACEX cores' Quaternary samples. They clearly indicate that even with the effects of paleo-current winnowing on sediments, there was a distinct strengthening of the IRD presence in the late Pleistocene. The timing of the sand presence shift corresponds to the MIS 6 boundary and suggests a strengthened ice climate or as suggested by O'Regan et al. (2010) an increase in basal ice melt. The timing of strengthened ice climate observed in this study further support the theory of a pan-Arctic ice sheet (Mercer, 1970; Hughes et al., 1977; Grosswald and Hughes,

1999). There is also a suggestion from the most recent sample and a sample taken at 3 MCD that the Arctic climate may have resumed an ice climate similar to the pan-Arctic ice sheet recently and that there may have been previous decays and regrowths of the pan-Arctic ice sheet (Figure 3.5). Future high-resolution sampling of Arctic cores which date from the period, should reveal whether the pan-Arctic ice sheet was stable or if it was cyclical in nature and we have an unintended sampling bias in the ACEX grain size distribution data set.

Lack of a discernable pattern in the paleo-current intensity may also be a reflection of true Arctic dynamics or a symptom of too few samples. Either way, we have enough samples in this study to determine that while sediments are effected by paleo-currents, paleo-currents are unaffected by the Arctic climate as indicated by sand percentages (IRD). This suggests the paleo-current strengths are also independent of sea level, which is effected by ice volume and surface winds, effected by ice capping. Further investigations in paleo-current strengths along the Lomonosov Ridge may allow for paleo-current mapping. Once paleo-current dynamics in terms of both time and space are resolved, an understanding of the forces driving these currents may be determined.

CONCLUSIONS

Variations in ice intensity can be enhanced through the 'sortable silt' method of removing the winnowing contribution of paleo-currents. By employing the proxy of the mean silt size of a sample (SS) as a measure of relative current velocity, sand percentage variability can be reset to pre- winnowing patterns. By using these proxies and techniques on Quaternary period samples from the ACEX cores, we determine a

consistent ice presence for the early and mid Pleistocene. This ice presence sharply intensified in the late Pleistocene, corresponding to MIS 6. Current velocities remained inconsistent and dynamic throughout the Quaternary era.

The strong correlative relationships between sand percentages (IRD) and mean silt fractions (SS) for the Lomonosov Ridge, show that the methods used in this study will be of further value in future coring endeavors of the ridge and similar depositional sites. The variability found in the paleo-current proxy (SS) suggests the need for high-resolution grain size analyses in future cores to determine if there is a discernable pattern in Arctic Ocean current intensity.

REFERENCES

Aagaard, K., 1981. "On the Deep Circulation in the Arctic Ocean." *Deep-Sea Research*, Vol. 28, pp. 251-268.

Bjork, G., Jakobsson, M., Rudels, B., et al., 2007. "Bathymetry and Deep-Water Exchange Across the Central Lomonosov Ridge at 88-89°N." *Deep-Sea Research I*, Vol. 54, pp. 1197-1208.

Bouyoucos, G.J., 1962. "Hydrometer Method Improved for Making Particle Size Analysis of Soils." *Agronomy Journal*, Vol. 54, pp. 464-465.

Clark, D.L., 1996. "The Pliocene Record in the Central Arctic." *Marine Micropaleontology*, Vol. 27, pp. 157-164.

Clark, D.L., Hansen, A., 1983. "Central Arctic Ocean Sediment Texture: a key to ice-transport mechanism." *In*: B. Molnia (*Ed.*), Glacial-Marine Sedimentation, Plenum, New York, pp. 301-330.

Darby, D.A., Naidu, S.A., Mowatt, T.C., Jones, G.A., 1989. "Sediment Composition and Sedimentary Processes in the Arctic Ocean." *In*: Herman, Y. (*Ed*.), The Arctic Seas: Climatology, Oceanography, Geology, and Biology, Van Nostrand Reinhold Co., New York, pp. 657-720.

Darby, D.A., Bischof, J.F., Jones, G.A., 1997. "Radiocarbon Chronology of Depositional Regimes in the Western Arctic Ocean." *Deep-Sea Research I*, Vol. 44, pp. 1745-1757.

Darby, D.A., Bischof, J.F., Spielhagen, R.F., Marshall, S.A., Herman, S.W., 2002. "Arctic Ice Export Events and their Potential Impact on Global Climate during the Late Pleistocene." *Paleoceanography*, Vol. 17.

Frank, M., J. Backman, M. Jakobsson, K. Moran, M. O'Regan, J. King, B.A. Haley, P.W. Kubik, and D. Garbe-Schonberg, 2008. "Beryllium Isotopes in Central Arctic Ocean Sediments Over the Past 12.3 Million Years: Stratigraphic and Paleoclimatic Implications." *Paleoceanography*, Vol. 23.

Goossens, D., 2008. "Techniques to Measure Grain-Size Distributions of Loamy Sediments: a comparative study of ten instruments for wet analysis." *Sedimentology*, Vol. 55, pp. 65-96.

Grosswald, M.G., Hughes, T.J., 1999. "The Case for an Ice Shelf in the Pleistocene Arctic Ocean." *Polar Geography*, Vol. 23, pp. 23-54.

Gyllencreutz, R., 2005. "Late Glacial and Holocene Paleoceanography in the Skagerrak from High-Resolution Grain Size Records." *Paleogeography, Paleoclimatology, Paleoecology*, Vol. 222, pp. 344-369.

Hall, I.R., McCave, I.N., Shackleton, N.J., Weedon, G.P., Harris, S.E., 2001. "Intensified Deep Pacific Inflow and Ventilation in Pleistocene Glacial Times." *Nature*, Vol. 412, pp. 809-811.

Haley, B.A., M. Frank, R.F. Spielhagen, and J. Fietzke, 2008. "The Radiogenic Isotope Record of Arctic Ocean Circulation and Weathering Inputs of the Past 15 Million Years." *Paleoceanography*, Vol. 23.

Hughes, T.J., Denton, G.H., Grosswald, M.G., 1977. "Was There a Late Wurm Ice Sheet?" *Nature*, Vol. 266, pp. 596-602.

Jakobsson, M., Lovlie, R., Al-Hanbali, H., et al., 2000. "Manganese and Color Cycles in Arctic Ocean Sediments Constrain Pleistocene Chronology." *Geology*, Vol. 28, pp. 23-26.

Jakobsson, M., Lovlie, R., Arnlod, E.M., Backman, J., Polyak, L., Knutsen, J.-O., Musatov, E., 2001. "Pleistocene Stratigraphy and Paleoenvironmental Variation from the Lomonosov Ridge Sediments, Central Arctic Ocean." *Global and Planetary Change,* Vol. 31, pp. 1-22.

Jonkers, L., Prins, M.A., Brummer, G.-J.A., Koner, M., Lougheed, B.C., 2009. "Experimental Insights into Laser Diffraction Particle Sizing of Fine-Grained Sediments for Use in Paleoceanography." *Sedimentology*, Vol. 56, pp. 2192-2206.

Lisiecki, L.E., Raymo, M.E., 2005. "A Pliocene-Pleistocene Stack of 57 Globally Distributed Benthic δ18O Records." *Paleoceanography*, Vol. 20, PA 1003. doi:10.1029/2004PA001071.

McCave, I.N., 2008. "Size Sorting During Transport and Deposition of fine Sediments: Sortable Silt and Flow Speed." In: M. Rebesco, A. Camerlenghi (eds) *Contourites*. Developments in Sedimentology, Vol. 57.

McCave, I.N., and I.R. Hall, 2006. "Size Sorting in Marine Muds:Processes, pitfalls, and prospects for paleoflow-speed proxies." *Geochem. Geophys. Geosyst*., Vol. 7.

McCave, I.N., I.R. Hall, and G.G. Bianchi, 2006. "Laser vs. Settling Velocity Differences in Silt Grainsize Measurements: estimation of palaeocurrent vigour." *Sedimentology*, Vol. 53, pp. 919-928.

McCave, I.N., Manighetti, B., Robinson, S.G., 1995a. "Sortable Silt and Fine Sediment Size/Composition Slicing; Parameters for Paleocurrent Speed and Paleoceanography." *Paleoceanography,* Vol. 10, pp. 593-610.

McCave, I.N., Manighetti, B., Beveridge, N.A.S., 1995b. "Circulation in the Glacial North Atlantic Inferred from Grain Size Measurements." *Nature*, Vol. 374, pp. 149-152.

Mercer, J.H., 1970. "A Former Ice Sheet in the Arctic Ocean." *Palaeogeography, Palaeoclimatology, Palaeoecology*, Vol. 8, pp. 19-27.

Moran, K., Altmann, V., O'Regan, M., Ashmankas, C., 2007. "Acoustic Compressional Wave Velocity as a Predictor of Glacio-Marine Sediment Grain Size." *Geotechnical Testing Journal*, Vol. 30.

Moros, M., Kuijpers, A., Snowball, I., Lassens, S., Backstrom, D., Gingele, F., McManus, J., 2002. "Were Glacial Iceberg Surges in the North Atlantic Triggered by Climatic Warming?" *Marine Geology*, Vol.192, pp. 393-417.

O'Regan, M., St. John, K., Moran, K., Backman, J., King, J., Haley, B.A., Jakobsson, M., Frank, M., Rohl, U., 2010. "Plio-Pleistocene Trends in Ice Rafted Debris on the Lomonosov Ridge." *Quaternary International*, Vol. 219, pp. 168-176.

Phillips, R.L., Grantz, A., 1997. "Quaternary History of Sea Ice and Paleoclimate in the Amerasia Basin, Arctic Ocean, as Recorded in the Cyclical Strata of Northwind Ridge." *GSA Bulletin,* Vol. 109, pp. 1101-1115.

Polyak, L., Darby, D.A., Bischof, J.F., Jakobsson, M., 2007. "Stratigraphic Constraints on Late Pleistocene Glacial Erosion and Deglaciation of the Chukchi Margin, Arctic Ocean." *Quaternary Research*, Vol. 67, pp. 234-245.

Poore, R.Z., Phillips, R.L., Rieck, H.J., 1993. "Paleoclimate Record for Northwind Ridge, Western Arctic Ocean." *Paleoceanography,* Vol. 8, pp. 149-159.

Prins, M.A., Bouwer, L.M., Beets, C.J., Troelstra, S.R., Weltje, G.J., Kruk, R.W., Kuijpers, A., Vroon, P.Z., 2002. "Ocean Circulation and Iceberg Discharge in the Glacial North Atlantic: Inferences from unmixing of sediment size distributions." *Geology*, Vol. 30, pp. 555-558.

Ruddiman, W.F., 1977. "Late Quaternary Deposition of Ice-Rafted Sand in the Subpolar North Atlantic." *GSA Bulletin*, Vol. 88, pp. 1813-1827.

Sakamoto, T., Ikehara, M., Aoki, K., Iijima, K., Kimura, N., Nakatsuka, T., Wakatsuchi, M., 2005. "Ice-Rafted Debris (IRD)- Based Sea-Ice Expansion Events during the Past 100 kyrs in the Okhotsk Sea." *Deep-Sea Research*, Vol. 52, pp. 2275-2301.

Sperazza, M., Moore, J.N., Hendrix, M.S., 2004. "High-Resolution Particle Analysis of Naturally Occurring Very Fine-Grained Sediment Through Laser Diffractometry." *Journal of Sedimentary Research*, Vol. 74, pp. 736-743.

Svendsen, J.I., Alexanderson, H., Astakhov, V.I.,, et al., 2004. "Late Quaternary Ice Sheet History of Northern Euraisa." *Quaternary Science Reviews*, Vol. 23, pp. 1229-1271.

Wen, B., Aydin, A., Duzgoren-Aydin, N.S., 2002. "A Comparative Study of Particle Size Analyses by Sieve-Hydrometer and Laser Diffraction Methods." *ASTM Geotechnical Testing Journal*, Vol. 25, pp. 434-442.

Zachos, J.C., Pagani, M., Sloan, L., Thomas, E., Billups, K., 2001. "Trends, Rhythms, and Aberrations in Global Climate 65 Ma to Present." *Science*, Vol. 292, pp. 686-693.

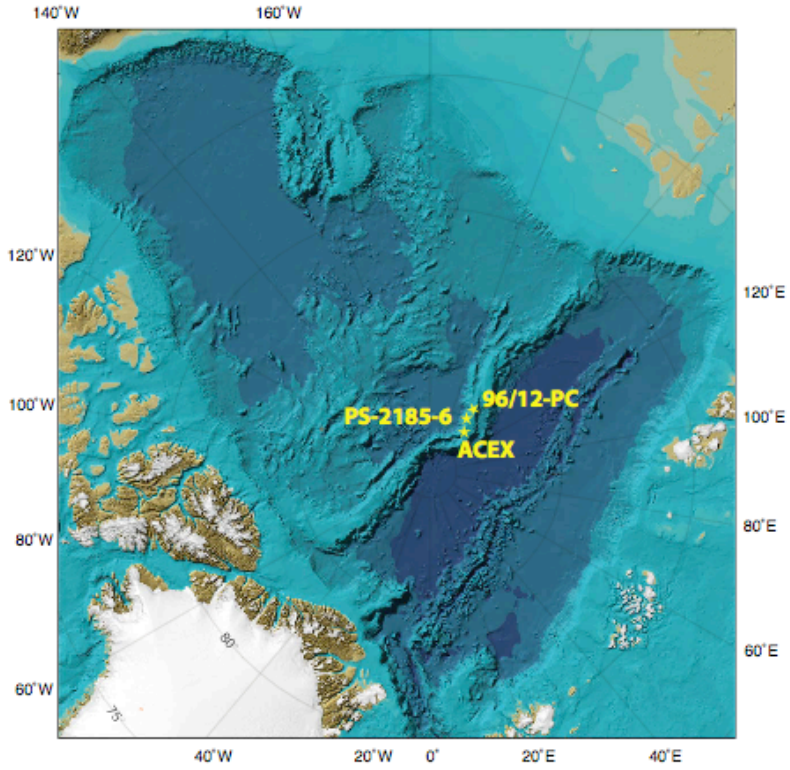

Figure 3.1: A map produced by the IBCAO of the bathymetry of the Arctic Ocean basin. The Lomonosov Ridge is the raised bathymetric feature fractioning the basin in two. The ridge provides a silt deposition site that is uninfluenced by bottom current deposition, while being affected by bottom current winnowing. This provides an ideal location for paleo-studies separating ice climate from bottom current speeds. The central Arctic Ocean coring locations of ACEX, ARCTIC '91, and Arctic Ocean-96 used in this study are identified on the map. PS-2185-6 is the site of the ARCTIC '91 study. 96/12-PC is the site of the Arctic Ocean-96 study.

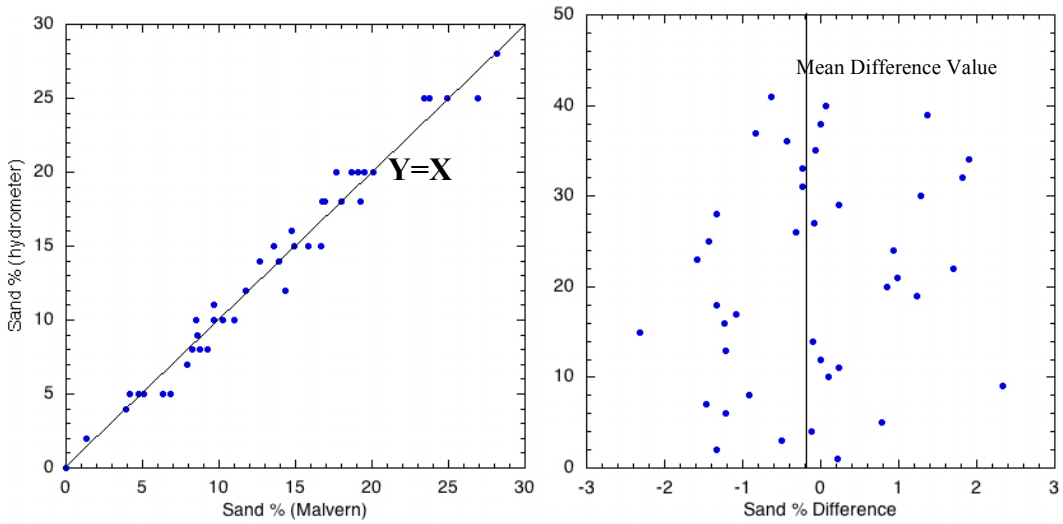

Figure 3.2: Graphs showing the comparison of sand percentages determined from the hydrometer method to the Malvern (laser diffraction) method. For the direct comparison graph (left) the Y=X line is displayed for reference purposes to the ideal comparison. The graph on the right plots the difference in percentage between the two methods (Malvern – hydrometer) versus an arbitrary sample number. The mean difference in the methods (~ -0.2) is plotted as a vertical line for reference, suggesting an slight bias of the Malvern method to under estimate sand percentages. There is a good correlation between the two methods concerning the percentage of sand, with no sample with more than a 3% difference between the methods.

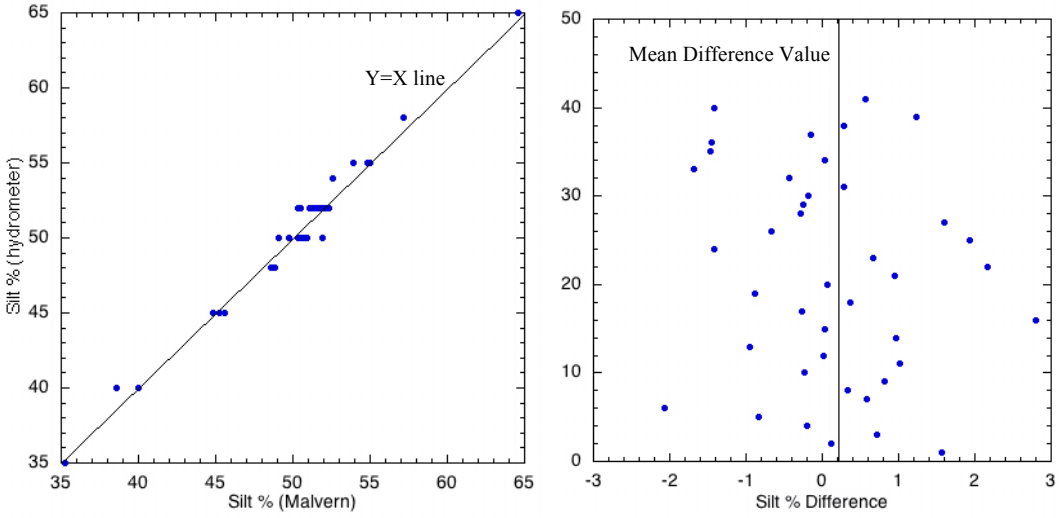

Figure 3.3: Graphs showing the comparison of silt percentages determined from the hydrometer method to the Malvern (laser diffraction) method. For the direct comparison graph (left) the Y=X line is displayed for reference purposes to the ideal comparison. The graph on the right plots the difference in percentage between the two methods (Malvern – hydrometer) versus an arbitrary sample number. The mean difference in the methods (~ 0.2) is plotted as a vertical line for reference, suggesting an slight bias of the Malvern method to over estimate silt percentages. There is a good correlation between the two methods concerning the percentage of sand, with no sample with more than a 3% difference between the methods.

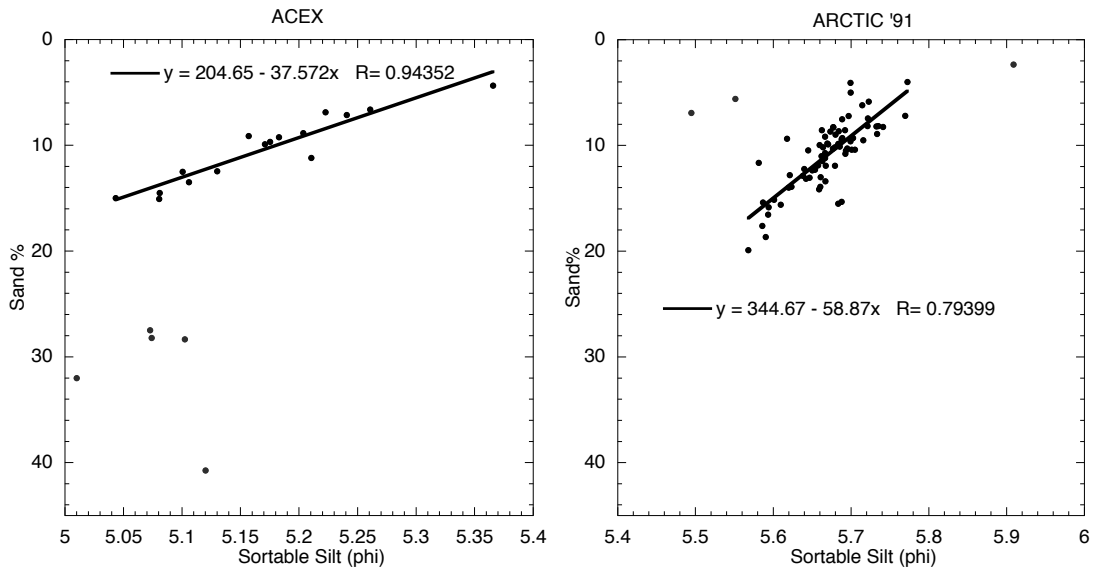

Figure 3.4: Graphs of sortable silt versus Sand % (IRD) for sediment samples taken from the late Pleistocene of the ACEX and Arctic ’91 cores. The sediments from both coring projects show a strong linear relationship between the two variables. Significant outliers from the line indicate significant changes in the paleo- ice environment, altering the depositional regime. Larger sortable silt values indicate finer mean silt fractions, corresponding to weaker current speeds over the Lomonosov Ridge. Using these linear relationships, the paleo- bottom current speeds and –ice climate can be decoupled.

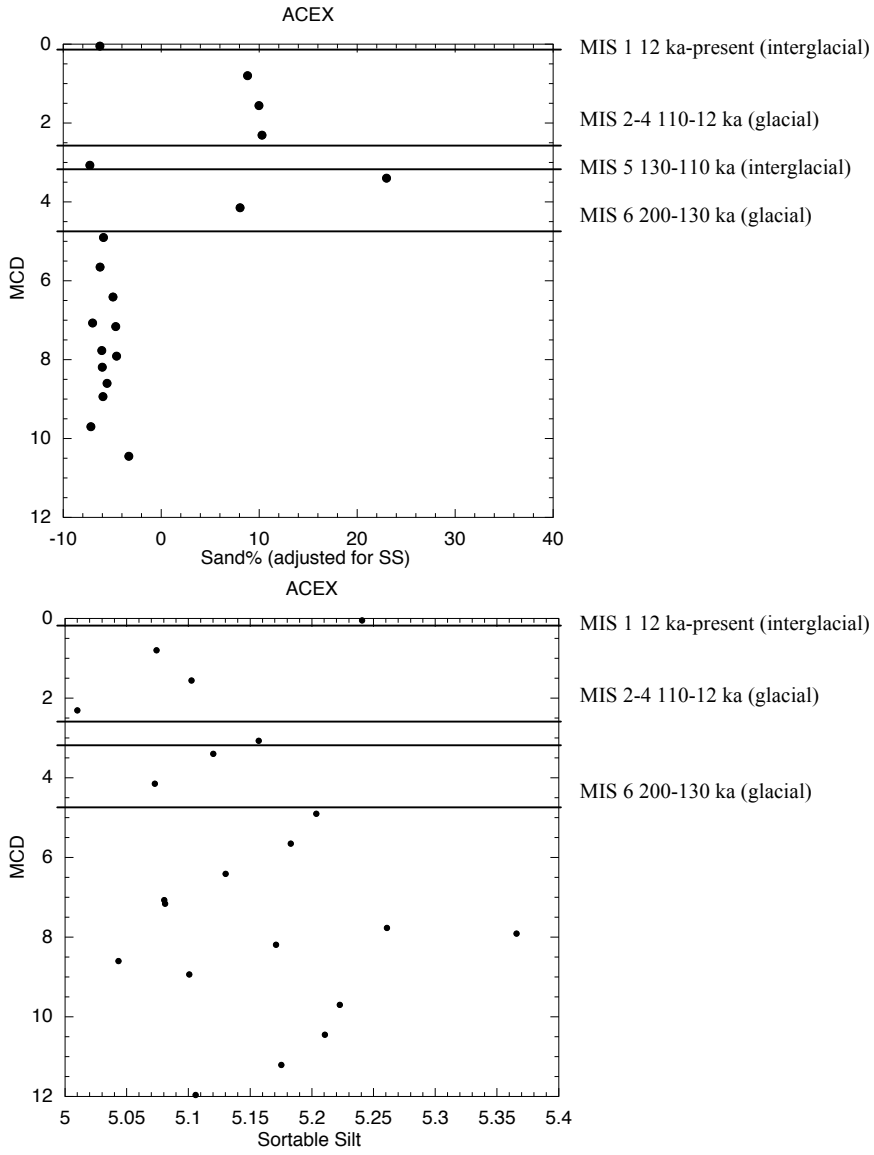

Figure 3.5: Graphs covering the late Pleistocene as gained from the ACEX core sediments. The boundary of MIS 6 (~200 ka) is found at ~4.85 MCD. The graph of sand% after it has been decoupled from winnowing affects of paleo- bottom currents, as previously established in the linear relationship, shows a significant increase in sand % (IRD) after the MIS 6 boundary. This indicates a strengthening paleo- ice climate and corresponds to the presence of 'mega-iceburgs' in the central Arctic Ocean. The variation in the adjusted sand % from the beginning of MIS 6 to present corresponds to marine isotope stages with interglacials showing decreased sand % and glacials increased sand %. While paleo- bottom currents have varied over time for the ~500ka shown in the graph of sortable silt, the range of current speeds has not deviated greatly and shows no significant strengthening or weakening after the MIS 6 boundary. The larger sortable silt phi sizes correspond to finer silt fractions, indicating weaker bottom current speeds. The two most recent interglacials do show possible current strengthening.

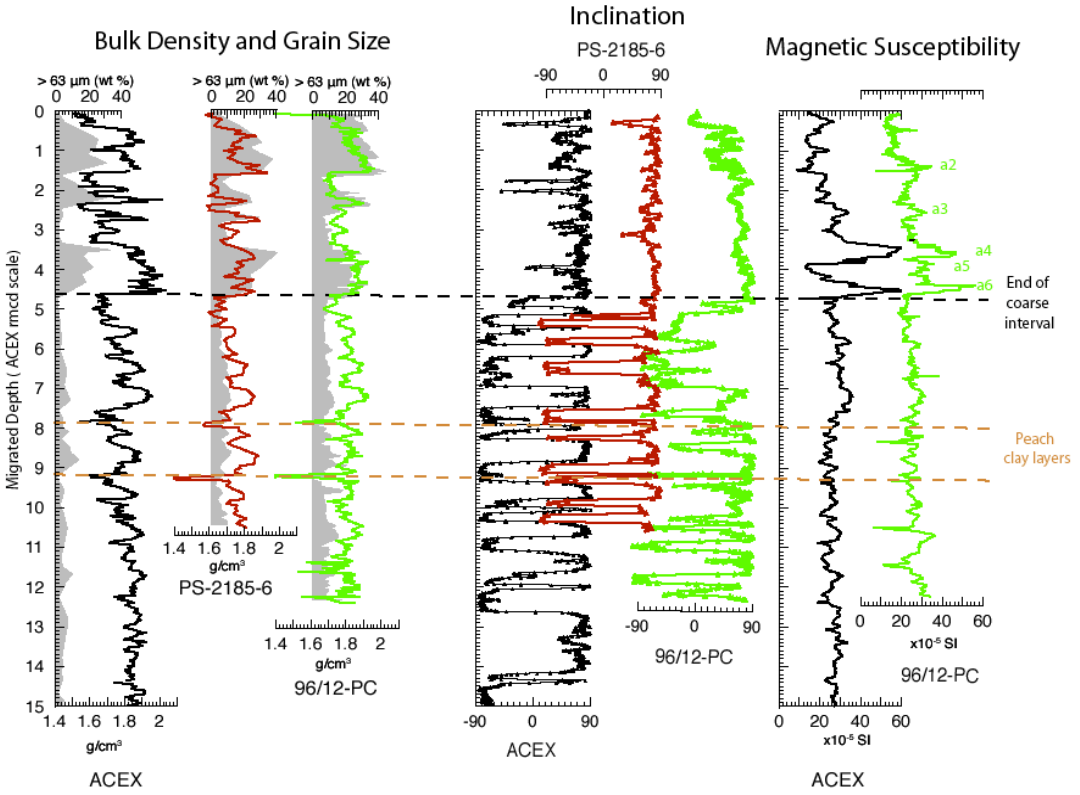

Figure 3.6: The graphs are of some of the physical properties of the ACEX cores and two previous studies of the Lomonosov Ridge, Arctic Ocean. Coring sites are shown on the Figure 3.1 map. The bulk density, inclination, and magnetic susceptibility of these studies all show a change in deposition occurring at ~4.7 on the migrated depth scale, a depth which corresponds to MIS 6. This change is more clearly visible in the transformed sand percentages in this study. Mean silt size (SS) shows no such change.

APPENDIX I: Data and statistical variables for IODP Exp. 302, ACEX, samples taken from neogene sediments. Samples exclusively contained sand, silt, and clay. Sample identifications are the expedition-site-core-section. The samples are presented in descending order.

	Sample ID:	302-4-C-1-H-1
	ANALYST:	Cristin Ashmankas,
	SAMPLE TYPE:	Unimodal, Very Poorly Sorted
	TEXTURAL GROUP:	Mud
	SEDIMENT NAME:	Fine Silt
METHOD OF	MEAN	49.36690952
MOMENTS	SORTING	204.3603811
Arithmetic (mm)	SKEWNESS	6.469754885
	KURTOSIS	46.88074205
METHOD OF	MEAN	7.64100207
MOMENTS	SORTING	4.474920979
Geometric (mm)	SKEWNESS	1.174749516
	KURTOSIS	4.83101554
METHOD OF	MEAN	6.983862503
MOMENTS	SORTING	2.20651326
Logarithmic (f)	SKEWNESS	-1.207156871
	KURTOSIS	4.826836511
FOLK AND	MEAN	7.050178415
WARD METHOD	SORTING	4.13454464
(mm)	SKEWNESS	0.249468594
	KURTOSIS	1.200840024
FOLK AND	MEAN	7.148124517
WARD METHOD	SORTING	2.047728446
(f)	SKEWNESS	-0.249468594
	KURTOSIS	1.200840024
FOLK AND	MEAN:	Fine Silt
WARD METHOD	SORTING:	Very Poorly Sorted
(Description)	SKEWNESS:	Coarse Skewed
	KURTOSIS:	Leptokurtic
	MODE 1 (mm):	4.7
	MODE 2 (mm):	
	MODE 1 (f):	7.754331413
	MODE 2 (f):	
	D10 (mm):	1.520351238
	D50 (mm):	6.0080573
	D90 (mm):	56.8317893
	(D90 / D10) (mm):	37.38069723
	(D90 - D10) (mm):	55.31143806
	(D75 / D25) (mm):	5.472098723
	(D75 - D25) (mm):	12.71296791
	D10 (f):	4.137158052
	D50 (f):	7.378885713
	D90 (f):	9.361379625
	(D90 / D10) (f):	2.262756102
	(D90 - D10) (f):	5.224221573
	(D75 / D25) (f):	1.408246023
	(D75 - D25) (f):	2.452094258
	% SAND:	0.092973514
	% MUD:	0.907026486
	% V COARSE SAND:	0.021663056
	% COARSE SAND:	0.008431928
	% MEDIUM SAND:	0.010031661
	% FINE SAND:	0.016330612
	% V FINE SAND:	0.036516257
	% V COARSE SILT:	0.057591605
	% COARSE SILT:	0.098564448
	% MEDIUM SILT:	0.168562812
	% FINE SILT:	0.225825001
	% V FINE SILT:	0.205324218
	% CLAY:	0.151158402

302-4-C-1-H-1	302-4-C-1-H-2	302-4-C-1-H-2
Cristin Ashmankas,	Cristin Ashmankas,	Cristin Ashmankas,
Bimodal, Very Poorly Sorted	Bimodal, Very Poorly Sorted	Bimodal, Very Poorly Sorted
Sandy Mud	Sandy Mud	Sandy Mud
Fine Sandy Medium Silt	Fine Sandy Fine Silt	Fine Sandy Fine Silt
92.33996366	105.2323342	94.90165134
172.3019746	228.2781555	178.8473685
4.201910948	4.496879479	5.130996209
29.42318937	27.64541096	39.93201769
22.22836522	21.2832317	24.57791066
6.118025196	6.512392595	6.10634554
0.128310655	0.238456562	-0.011054926
1.984590606	2.068992395	1.927514307
5.47882933	5.499666602	5.315607701
2.615491539	2.714127979	2.614425535
-0.13154039	-0.245680866	0.002846258
1.988328047	2.071393536	1.938701065
22.45133942	21.81369851	24.59678616
6.530817962	6.869703164	6.306267767
0.116712457	0.168868383	0.015787715
0.75528595	0.754981323	0.718202463
5.477054673	5.51862179	5.345386366
2.707263696	2.780247762	2.656786429
-0.116712457	-0.168868383	-0.015787715
0.75528595	0.754981323	0.718202463
Coarse Silt	Coarse Silt	Coarse Silt
Very Poorly Sorted	Very Poorly Sorted	Very Poorly Sorted
Coarse Skewed	Coarse Skewed	Symmetrical
Platykurtic	Platykurtic	Platykurtic
9.4	9.4	215
215	215	9.4
6.754331413	6.754331413	2.236965594
2.236965594	2.236965594	6.754331413
2.168489233	2.096708015	2.250364648
18.49915578	16.68555342	23.28006978
270.8224202	295.7171223	250.2124551
124.8899077	141.0387713	111.1875159
268.653931	293.6204143	247.9620904
21.31890603	23.3584567	22.80455626
104.926868	108.5746915	120.5151553
1.884580917	1.757710315	1.998774489
5.756396756	5.905256652	5.424760807
8.849094005	8.897658317	8.795625491
4.695523512	5.06207322	4.400509182
6.964513088	7.139948002	6.796851002
2.386659767	2.44767684	2.509778588
4.414061503	4.545873053	4.511250193
0.328979141	0.324909855	0.374136545
0.671020859	0.675090145	0.625863455
0.007067609	0.022430343	0.011947013
0.022069609	0.020763898	0.011047238
0.082210961	0.080222637	0.077130717
0.118415789	0.11255166	0.151662084
0.099215172	0.088941317	0.122349492
0.08762136	0.078020213	0.085260073
0.112890465	0.108294702	0.102161461
0.137668671	0.140116882	0.124122157
0.136870991	0.142761295	0.127574628
0.110600702	0.116339903	0.105750503
0.085368671	0.08955715	0.080994633

302-4-C-1-H-3	302-4-C-2-H-1	302-4-C-2-H-1
Cristin Ashmankas,	Cristin Ashmankas,	Cristin Ashmankas,
Unimodal, Very Poorly Sorted	Bimodal, Very Poorly Sorted	Trimodal, Very Poorly Sorted
Sandy Mud	Sandy Mud	Sandy Mud
Very Fine Sandy Fine Silt	Medium Sandy Medium Sil	Fine Sandy Medium Silt
55.0519548	138.3480623	86.68912036
207.9441421	181.2225702	161.0614094
6.350507922	1.525974789	4.873520794
45.21027651	4.949705609	39.58508177
9.761820052	35.85874746	23.74420207
4.771020313	6.972303159	5.614953235
0.804251489	-0.156661269	0.046449373
3.745719669	1.733944741	2.084072117
6.627140809	4.801531094	5.378010919
2.292126939	2.8016353	2.492239256
-0.840734115	0.156661269	-0.054200547
3.776486354	1.733944741	2.091836302
9.429477341	35.30227864	24.23951115
4.576579464	7.206534167	5.995267563
0.184175601	-0.032091566	0.060685641
0.992324791	0.671600427	0.790513238
6.728606478	4.824094882	5.366495586
2.194269731	2.849305592	2.583824141
-0.184175601	0.032091566	-0.060685641
0.992324791	0.671600427	0.790513238
Medium Silt	Very Coarse Silt	Coarse Silt
Very Poorly Sorted	Very Poorly Sorted	Very Poorly Sorted
Coarse Skewed	Symmetrical	Symmetrical
Mesokurtic	Platykurtic	Platykurtic
4.7	302.5	9.4
	9.4	215
7.754331413	1.747054535	6.754331413
	6.754331413	2.236965594
1.604188914	2.55701715	2.45994288
8.030388446	34.85965456	21.57917001
82.65857942	406.9160232	247.5246445
51.52671155	159.1369941	100.6221106
81.05439051	404.3590061	245.0647016
7.784846857	33.76287441	16.78812465
21.84563024	224.011565	97.8842648
3.59669162	1.297197004	2.014355922
6.960314509	4.842297917	5.534216814
9.283940237	8.611322448	8.667159468
2.581244437	6.638407598	4.302695155
5.687248617	7.314125444	6.652803546
1.55670931	3.400669526	2.246675034
2.960668659	5.077365828	4.069369175
0.128553537	0.440961421	0.327874525
0.871446463	0.559038579	0.672125475
0.022734849	0.0001	0.007066431
0.008867258	0.05115	0.014499517
0.005933729	0.17865	0.076630779
0.02520168	0.13915	0.120495983
0.065816021	0.071911421	0.109181814
0.08575708	0.071008992	0.105231985
0.124396308	0.097137373	0.130691598
0.168412478	0.118460873	0.142281904
0.190315123	0.113277482	0.126080834
0.168078537	0.089722173	0.095449921
0.134486937	0.069431687	0.072389233

302-4-C-2-H-2	302-4-C-2-H-2	302-4-C-2-H-3
Cristin Ashmankas,	Cristin Ashmankas,	Cristin Ashmankas,
Unimodal, Very Poorly Sorted	Unimodal, Very Poorly Sorted	Unimodal, Very Poorly Sorted
Sandy Mud	Sandy Mud	Sandy Mud
Very Fine Sandy Fine Silt	Very Fine Sandy Fine Silt	Very Fine Sandy Fine Silt
57.47639901	54.77045138	57.16564748
224.9020751	210.5975862	191.069294
5.904668035	6.393406287	6.574711446
38.83438898	45.33570893	50.11798035
8.313261954	9.603109769	11.49459294
4.874041581	4.748896525	4.978759736
1.05342518	0.822360583	0.609925243
4.280752375	3.810461376	3.091681122
6.853910009	6.650123129	6.407689549
2.331572081	2.286551045	2.337615088
-1.079293592	-0.859618669	-0.63387582
4.262047669	3.840409416	3.12392308
7.824758403	9.227873282	11.37411901
4.569956772	4.559145945	5.003443479
0.255948006	0.185824905	0.186913638
1.109196613	1.016187481	0.949823568
6.997738077	6.759786092	6.458101384
2.192180519	2.188763593	2.322921331
-0.255948006	-0.185824905	-0.186913638
1.109196613	1.016187481	0.949823568
Medium Silt	Medium Silt	Medium Silt
Very Poorly Sorted	Very Poorly Sorted	Very Poorly Sorted
Coarse Skewed	Coarse Skewed	Coarse Skewed
Mesokurtic	Mesokurtic	Mesokurtic
3.35	4.7	4.7
8.241333809	7.754331413	7.754331413
1.481105269	1.591882302	1.708617673
6.396187458	7.911986688	9.355975124
76.6950044	82.86093438	111.8123857
51.78227775	52.05217387	65.44026055
75.21389913	81.26905208	110.103768
6.740060672	7.520170948	9.21558231
16.25087689	20.86550276	29.07922984
3.70472358	3.593164101	3.160848087
7.288572063	6.981744286	6.739896259
9.399110102	9.295050612	9.192954674
2.537061105	2.586870611	2.908382314
5.694386521	5.701886511	6.032106587
1.481956166	1.541348329	1.648840623
2.752761578	2.910765457	3.204075329
0.114873975	0.126128756	0.166257888
0.885126025	0.873871244	0.833742112
0.026893725	0.02390239	0.018099397
0.008864598	0.00610061	0.007399753
0.005898624	0.00540054	0.012499583
0.025227447	0.029936327	0.049365021
0.047989581	0.060788888	0.078894134
0.064818958	0.081751512	0.089658351
0.103904996	0.124535455	0.124890297
0.159159252	0.170913374	0.164539192
0.206594608	0.192358731	0.180013359
0.194283701	0.16832016	0.153498995
0.15636451	0.135992013	0.121141918

302-3-A-1-H-3	302-4-C-2-H-3	302-3-A-1-H-3
Cristin Ashmankas,	Cristin Ashmankas,	Cristin Ashmankas,
Bimodal, Very Poorly Sorted	Bimodal, Very Poorly Sorted	Unimodal, Poorly Sorted
Sandy Mud	Sandy Mud	Mud
Very Fine Sandy Fine Silt	Very Fine Sandy Fine Silt	Fine Silt
57.8401145	59.59132141	45.038319
170.4603	188.3723836	192.5850721
6.990858	6.802515775	7.016581812
58.83002586	53.529977	54.2031639
13.81872119	13.22490129	8.089600694
5.005573968	5.042143083	4.292971205
0.374917658	0.437808476	0.996358967
2.644315655	2.779167841	4.571307541
6.153647174	6.201735268	6.90885199
2.335508036	2.354565259	2.139481041
-0.392775407	-0.464986277	-1.039596332
2.673461873	2.819180776	4.617816772
13.88365124	13.3049467	7.550738103
5.126657799	5.123988611	3.970945616
0.131382564	0.144623889	0.1753284
0.870263202	0.877059911	1.079905126
6.17046916	6.231893459	7.049166606
2.358018602	2.357267269	1.989482603
-0.131382564	-0.144623889	-0.1753284
0.870263202	0.877059911	1.079905126
Medium Silt	Medium Silt	Fine Silt
Very Poorly Sorted	Very Poorly Sorted	Poorly Sorted
Coarse Skewed	Coarse Skewed	Coarse Skewed
Platykurtic	Platykurtic	Mesokurtic
6.65	6.65	4.7
107.5	107.5	
7.254331413	7.254331413	7.754331413
3.236965594	3.236965594	
1.871704266	1.826905463	1.551038644
11.8355974	11.20994369	6.76682399
127.7940093	123.5093686	55.58486274
68.27681681	67.60577989	35.83718751
125.922305	121.6824632	54.03382409
11.0533894	10.9042057	5.91960645
40.94366215	38.89973367	14.7582603
2.968107887	3.017307615	4.169164138
6.400723661	6.479077159	7.207305421
9.061431781	9.096382304	9.332549653
3.052932078	3.014734811	2.238470193
6.093323894	6.079074689	5.163385515
1.774893771	1.758320521	1.441158342
3.466416919	3.446812778	2.565501265
0.202220186	0.195854638	0.090395019
0.797779814	0.804145362	0.909604981
0.013566214	0.01829878	0.019568624
0.0059998	0.00419972	0.006333967
0.015466151	0.013365776	0.00270027
0.067431086	0.062429171	0.019168584
0.099756935	0.097561191	0.042623575
0.105851042	0.102948224	0.06584981
0.131826507	0.129218217	0.118835553
0.156538576	0.157226791	0.181377622
0.163297973	0.166053112	0.213341887
0.134363714	0.139156981	0.186539473
0.105902002	0.109542037	0.143660636

302-4-C-2-H-4	302-4-C-3-H-1	302-3-A-1-H-CC
Cristin Ashmankas,	Cristin Ashmankas,	Cristin Ashmankas,
Unimodal, Poorly Sorted	Unimodal, Very Poorly Sorted	Bimodal, Very Poorly Sorted
Mud	Sandy Mud	Sandy Mud
Fine Silt	Very Fine Sandy Fine Silt	Very Fine Sandy Fine Silt
36.71471681	58.92352752	58.80228192
177.4364134	221.846489	179.8512113
7.801261242	5.954462299	6.806558929
65.97874816	39.68728563	54.39222353
7.02335757	9.241653535	13.50560578
3.847463425	4.912573561	5.052487387
1.105225295	0.944236292	0.396865805
5.481221861	3.937433013	2.676058407
7.118408612	6.703148211	6.183058935
1.982528787	2.337571606	2.351098573
-1.164684861	-0.971590496	-0.41652059
5.566496151	3.936382581	2.707574616
6.515503653	8.883532113	13.55120035
3.47619822	4.705729355	5.112457686
0.125861058	0.247361975	0.138525379
1.078702235	1.075228283	0.836473066
7.26190758	6.814650875	6.20543554
1.79751035	2.234418348	2.354016998
-0.125861058	-0.247361975	-0.138525379
1.078702235	1.075228283	0.836473066
Fine Silt	Medium Silt	Medium Silt
Poorly Sorted	Very Poorly Sorted	Very Poorly Sorted
Coarse Skewed	Coarse Skewed	Coarse Skewed
Mesokurtic	Mesokurtic	Platykurtic
4.7	4.7	6.65
		107.5
7.754331413	7.754331413	7.254331413
		3.236965594
1.50780015	1.578929644	1.829007867
6.176962343	7.155751442	11.32886611
35.40783328	88.98175228	122.1021384
23.48310769	56.3557424	66.75867318
33.90003313	87.40282264	120.2731306
5.05745503	7.150065927	11.76959439
11.63426631	18.86846581	42.43949497
4.819787626	3.490346681	3.033839628
7.338886749	7.126681009	6.463852718
9.373339065	9.306837398	9.094723004
1.944761842	2.666450714	2.997759974
4.553551438	5.816490717	6.060883376
1.38286667	1.51500662	1.802869816
2.338411587	2.837956544	3.556992697
0.059244192	0.130798954	0.206261524
0.940755808	0.869201046	0.793738476
0.016734449	0.026069274	0.015666144
0.004933662	0.008367503	0.007099763
0.001033402	0.00720072	0.008233059
0.009867324	0.030769744	0.065164495
0.026675354	0.058391714	0.110098063
0.05219443	0.07064122	0.102920218
0.119517384	0.108209294	0.123367427
0.193520731	0.165280049	0.153656789
0.226037019	0.203422574	0.165887018
0.197607277	0.182362345	0.138529324
0.151878967	0.139285565	0.1093777

302-4-C-3-H-1	302-4-C-3-H-2	302-4-C-3-H-2
Cristin Ashmankas,	Cristin Ashmankas,	Cristin Ashmankas,
Bimodal, Very Poorly Sorted	Unimodal, Very Poorly Sorted	Unimodal, Very Poorly Sorted
Sandy Mud	Mud	Sandy Mud
Very Fine Sandy Fine Silt	Fine Silt	Very Fine Sandy Fine Silt
57.22002117	49.98322229	65.6725685
196.4684113	207.7410735	224.5584796
6.61954541	6.514375888	5.457132844
49.69523382	46.74329302	34.60355418
11.59685611	8.352898491	10.19922126
4.935471722	4.454880499	5.183390057
0.593233648	1.017508581	0.883207965
3.102828148	4.518176741	3.656317853
6.388933282	6.854678291	6.572876508
2.328561517	2.197924354	2.402582877
-0.622477668	-1.057983073	-0.899486425
3.142215787	4.539853501	3.648348712
11.61507689	7.860341575	9.635952507
4.924836188	4.111423264	5.115219457
0.180039434	0.198019969	0.241081303
0.913046117	1.052972199	1.114725917
6.427857485	6.991192278	6.697357002
2.300075738	2.039637902	2.354796137
-0.180039434	-0.198019969	-0.241081303
0.913046117	1.052972199	1.114725917
Medium Silt	Medium Silt	Medium Silt
Very Poorly Sorted	Very Poorly Sorted	Very Poorly Sorted
Coarse Skewed	Coarse Skewed	Coarse Skewed
Mesokurtic	Mesokurtic	Leptokurtic
4.7	4.7	4.7
107.5		
7.754331413	7.754331413	7.754331413
3.236965594		
1.736058558	1.566961009	1.601316114
9.474428376	6.811374743	7.952026114
109.3014549	59.40044478	105.6166187
62.95954384	37.90805543	65.95613306
107.5653963	57.83348377	104.0153026
9.506095277	6.350467049	7.733857328
30.59273703	16.08823103	21.51762762
3.19361549	4.073382456	3.243091235
6.721745381	7.197838277	6.97446179
9.169968673	9.317815004	9.286526148
2.871343999	2.287488372	2.863479771
5.976353183	5.244432547	6.043434913
1.667072956	1.466997886	1.552803733
3.248852861	2.6668627	2.95118815
0.171028279	0.095210641	0.141616988
0.828971721	0.904789359	0.858383012
0.020131991	0.023031798	0.0244
0.005932938	0.006832878	0.0149
0.006499567	0.004466369	0.014966667
0.050196654	0.01679888	0.033166667
0.08826713	0.044080716	0.054183655
0.091317686	0.07443967	0.073011605
0.12238685	0.118327257	0.119294674
0.163794368	0.171560158	0.170723094
0.180905746	0.210251931	0.190308801
0.152299502	0.188336216	0.169861998
0.118267569	0.141874128	0.13518284

302-4-C-3-H-3	302-4-C-3-H-3	302-4-C-4-H-1
Cristin Ashmankas,	Cristin Ashmankas,	Cristin Ashmankas,
Unimodal, Very Poorly Sorted	Bimodal, Very Poorly Sorted	Unimodal, Very Poorly Sorted
Sandy Mud	Sandy Mud	Sandy Mud
Very Fine Sandy Fine Silt	Very Fine Sandy Fine Silt	Very Fine Sandy Fine Silt
54.82864055	58.94971333	63.53195903
202.0973882	194.8252303	214.6770528
6.436303114	6.586088369	5.939069062
46.66152543	49.8488854	40.45231533
10.27597616	11.9953131	11.26151232
4.74295273	5.048714278	5.160235874
0.753786987	0.564507077	0.705758989
3.618483791	2.970508383	3.244549666
6.563058024	6.34052566	6.424282834
2.275192775	2.359897936	2.397071172
-0.785530996	-0.590958125	-0.72972965
3.651669571	3.006255814	3.261115215
9.896572287	12.02710045	11.10545345
4.587167073	5.105622056	5.135049501
0.172484092	0.186614548	0.215531185
0.994429262	0.913204398	0.976783929
6.658855356	6.377567317	6.492587889
2.197603454	2.352086746	2.360378184
-0.172484092	-0.186614548	-0.215531185
0.994429262	0.913204398	0.976783929
Medium Silt	Medium Silt	Medium Silt
Very Poorly Sorted	Very Poorly Sorted	Very Poorly Sorted
Coarse Skewed	Coarse Skewed	Coarse Skewed
Mesokurtic	Mesokurtic	Mesokurtic
4.7	4.7	4.7
	107.5	
7.754331413	7.754331413	7.754331413
	3.236965594	
1.666777927	1.742509792	1.68364999
8.557305685	9.740663899	8.905574642
87.06130322	118.8808734	116.6993045
52.23329504	68.22393417	69.31328079
85.39452529	117.1383636	115.0156545
7.824387674	10.05611487	9.157210446
22.98472744	32.78939199	27.95233111
3.521824574	3.072411475	3.099132132
6.868627657	6.681764179	6.811075579
9.228722385	9.164617521	9.214192034
2.620437842	2.982874395	2.973152367
5.706897811	6.092206046	6.115059902
1.565770698	1.696723187	1.639742253
2.967977853	3.330001129	3.194908178
0.132779793	0.179534502	0.165920085
0.867220207	0.820465498	0.834079915
0.021065964	0.019633333	0.02370237
0.007966401	0.005333333	0.008767543
0.006399787	0.011966667	0.012867953
0.03269891	0.056766667	0.047438077
0.064648731	0.085834502	0.073144141
0.088158713	0.091746996	0.084619647
0.130818897	0.122245962	0.119994242
0.17207274	0.16077832	0.162152973
0.187011262	0.176983852	0.183289915
0.162697085	0.151103204	0.159751624
0.12646151	0.117607164	0.124271514

302-3-A-2-H-2	302-4-C-4-H-1	302-3-A-2-H-3
Cristin Ashmankas,	Cristin Ashmankas,	Cristin Ashmankas,
Unimodal, Very Poorly Sorted	Unimodal, Very Poorly Sorted	Unimodal, Very Poorly Sorted
Sandy Mud	Sandy Mud	Sandy Mud
Very Fine Sandy Fine Silt	Very Fine Sandy Fine Silt	Very Fine Sandy Fine Silt
57.50915519	56.01081241	54.51014465
178.046783	219.3656382	202.8680599
6.80100816	6.120814588	6.374478447
54.67119516	41.41418794	45.63326603
13.1569865	9.49323275	10.34451964
4.979777123	4.624910771	4.663797946
0.422093651	0.903255404	0.748133542
2.775005663	4.198408558	3.728015976
6.222781288	6.664731987	6.557788901
2.329693837	2.250921262	2.248031126
-0.441388214	-0.942854766	-0.779145729
2.805502483	4.210919565	3.759557812
13.01880056	8.962845709	9.832467031
5.024486347	4.343564796	4.457981037
0.128581155	0.1647364	0.147440245
0.874774113	1.065126184	0.99901537
6.263259652	6.801827423	6.668230841
2.328976117	2.118879559	2.15639048
-0.128581155	-0.1647364	-0.147440245
0.874774113	1.065126184	0.99901537
Medium Silt	Medium Silt	Medium Silt
Very Poorly Sorted	Very Poorly Sorted	Very Poorly Sorted
Coarse Skewed	Coarse Skewed	Coarse Skewed
Platykurtic	Mesokurtic	Mesokurtic
6.65	6.65	6.65
7.254331413	7.254331413	7.254331413
1.809890418	1.634320662	1.678445063
11.25084444	8.027879438	8.791724417
116.4085273	71.60449245	80.48705677
64.31799747	43.8130008	47.95334595
114.5986369	69.97017179	78.8086117
10.75037296	6.738005191	7.586872061
38.10256404	18.98559852	22.81576573
3.102731351	3.803806085	3.63509939
6.473822902	6.960765334	6.82963812
9.109881935	9.25709321	9.218658968
2.936084664	2.433639624	2.536012906
6.007150584	5.453287125	5.583559578
1.749230672	1.501591404	1.556867317
3.426314807	2.75232154	2.923505209
0.188581318	0.11091987	0.124003204
0.811418682	0.88908013	0.875996796
0.014932836	0.025869254	0.020963871
0.007699743	0.00750075	0.008765498
0.011966268	0.00410041	0.004266098
0.055531482	0.023235657	0.029662712
0.098450989	0.0502138	0.060345025
0.110282267	0.081163863	0.09407781
0.131005499	0.133074485	0.138493885
0.155069784	0.18244491	0.174828353
0.165155727	0.197745966	0.187935398
0.138926136	0.16463737	0.156260593
0.110979269	0.130013536	0.124400757

302-4-C-4-H-2	302-3-A-2-H-3	302-3-A-2-H-CC
Cristin Ashmankas,	Cristin Ashmankas,	Cristin Ashmankas,
Unimodal, Very Poorly Sorted	Unimodal, Very Poorly Sorted	Unimodal, Very Poorly Sorted
Sandy Mud	Sandy Mud	Mud
Very Fine Sandy Fine Silt	Very Fine Sandy Fine Silt	Fine Silt
60.0290278	54.225003	51.75378275
214.0564784	202.303739	209.8967804
6.108227932	6.575543368	6.248617829
41.9654812	48.26809305	43.29858377
10.90688967	10.29006225	8.768341921
4.960851515	4.745144603	4.452334541
0.697339491	0.721015187	0.99098151
3.422443132	3.559388993	4.519963069
6.469782473	6.556428141	6.792955406
2.342311283	2.27903474	2.18871758
-0.72807156	-0.757296865	-1.025430522
3.448390468	3.600761457	4.535682097
10.6329755	10.00422475	8.21678345
4.834865456	4.616688446	4.059544531
0.173379212	0.16900408	0.169616675
0.960717825	0.975269042	1.034536576
6.555310817	6.643246815	6.927210539
2.273475743	2.206858376	2.02131787
-0.173379212	-0.16900408	-0.169616675
0.960717825	0.975269042	1.034536576
Medium Silt	Medium Silt	Medium Silt
Very Poorly Sorted	Very Poorly Sorted	Very Poorly Sorted
Coarse Skewed	Coarse Skewed	Coarse Skewed
Mesokurtic	Mesokurtic	Mesokurtic
4.7	4.7	4.7
7.754331413	7.754331413	7.754331413
1.658884447	1.649160417	1.607910711
9.01057775	8.597192913	7.277976765
98.0364264	87.36476309	59.34753156
59.0978031	52.97529712	36.9097184
96.37754196	85.71560267	57.73962085
8.774440568	8.073510966	6.373810326
26.72059519	23.84418121	16.92726071
3.350538293	3.516804676	4.074668165
6.794164671	6.861918605	7.102246839
9.235570889	9.244052545	9.28059699
2.756443914	2.628537379	2.277632586
5.885032596	5.727247869	5.205928826
1.620292788	1.57952219	1.473929645
3.133307146	3.013196202	2.672156088
0.14994616	0.135402757	0.094823951
0.85005384	0.864597243	0.905176049
0.024100803	0.021734058	0.022598493
0.00810027	0.006133538	0.010232651
0.006266876	0.005666856	0.000999933
0.03690123	0.0330011	0.015065662
0.074576981	0.068867206	0.04592721
0.094193017	0.091227732	0.079456479
0.127223281	0.128724914	0.126111011
0.164552335	0.169479933	0.178530552
0.181687735	0.186788526	0.20847891
0.155874878	0.160277973	0.177781585
0.126522594	0.128098165	0.134817512

302-4-C-4-H-2	302-4-C-4-H-3	302-3-A-3-H-2
Cristin Ashmankas,	Cristin Ashmankas,	Cristin Ashmankas,
Unimodal, Very Poorly Sorted	Unimodal, Very Poorly Sorted	Unimodal, Very Poorly Sorted
Sandy Mud	Sandy Mud	Sandy Mud
Very Fine Sandy Fine Silt	Very Fine Sandy Fine Silt	Very Fine Sandy Fine Silt
60.00855917	55.7055555	62.32564208
229.188982	220.7733318	229.0000835
5.785088169	5.932698758	5.614937586
37.17793695	39.14435108	35.51443594
9.481339402	8.693820532	9.567591995
4.79715562	4.636338563	4.985212266
0.940975691	1.030311025	0.927969815
4.141538956	4.480437328	3.939957696
6.664220628	6.799286977	6.658470435
2.304461472	2.251315107	2.353439397
-0.972976272	-1.060227847	-0.950900337
4.134513463	4.474622816	3.931047026
8.95081268	8.0966778	9.007311651
4.497895092	4.260503466	4.72869886
0.1966416	0.195765719	0.222884556
1.058025771	1.082733233	1.063079529
6.803765608	6.948454217	6.794687705
2.169250012	2.091023924	2.241443269
-0.1966416	-0.195765719	-0.222884556
1.058025771	1.082733233	1.063079529
Medium Silt	Medium Silt	Medium Silt
Very Poorly Sorted	Very Poorly Sorted	Very Poorly Sorted
Coarse Skewed	Coarse Skewed	Coarse Skewed
Mesokurtic	Mesokurtic	Mesokurtic
4.7	4.7	4.7
7.754331413	7.754331413	7.754331413
1.613566853	1.561631791	1.573509568
7.724794842	7.07367202	7.527885588
77.39513508	64.88817356	86.78781255
47.9652485	41.55151933	55.15556711
75.78156823	63.32654177	85.21430298
7.084946831	6.429612195	7.487654231
19.48369621	16.60111932	20.24849966
3.691613306	3.945900631	3.526363728
7.016287667	7.143324956	7.053539583
9.275530932	9.322729956	9.311798334
2.512595487	2.362636779	2.640623331
5.583917626	5.376829325	5.785434606
1.517158093	1.473606821	1.535964865
2.824757027	2.684731723	2.904513815
0.118189504	0.102855536	0.127648806
0.881810496	0.897144464	0.872351194
0.0281	0.025233333	0.027029729
0.009	0.0108	0.011731769
0.004333333	0.0018	0.005132649
0.023233333	0.019	0.028696174
0.053522838	0.046022203	0.055058484
0.080244287	0.071903332	0.077692775
0.124614269	0.119730911	0.11818151
0.173788674	0.176168645	0.166129464
0.197568636	0.207489393	0.197092721
0.171977276	0.180351197	0.174083212
0.133617353	0.141500986	0.139171512

302-4-C-4-H-3	302-3-A-3-H-2	302-4-C-5-X-1
Cristin Ashmankas,	Cristin Ashmankas,	Cristin Ashmankas,
Unimodal, Very Poorly Sorted	Unimodal, Very Poorly Sorted	Unimodal, Very Poorly Sorted
Sandy Mud	Sandy Mud	Sandy Mud
Very Fine Sandy Fine Silt	Very Fine Sandy Fine Silt	Very Fine Sandy Fine Silt
54.20884719	55.21434416	64.3335421
205.7651768	174.6541936	228.0061677
6.493172985	7.070831896	5.562994651
46.87354597	58.03890715	35.6895928
10.037578	13.42046345	8.890221467
4.703255669	4.854361184	5.259039697
0.767042026	0.336886598	1.038413161
3.703108216	2.774119506	3.888401873
6.591281472	6.194832872	6.757095913
2.2678569	2.292450426	2.43693002
-0.804110704	-0.358972741	-1.052065052
3.740791314	2.810900945	3.856075466
9.673337245	13.2849458	8.407599385
4.530061087	4.845042117	5.132939157
0.171122714	0.067228098	0.311129914
0.988067974	0.844749801	1.198967849
6.691770588	6.234063848	6.894090357
2.179530505	2.276509207	2.35978516
-0.171122714	-0.067228098	-0.311129914
0.988067974	0.844749801	1.198967849
Medium Silt	Medium Silt	Medium Silt
Very Poorly Sorted	Very Poorly Sorted	Very Poorly Sorted
Coarse Skewed	Symmetrical	Very Coarse Skewed
Mesokurtic	Platykurtic	Leptokurtic
4.7	6.65	4.7
7.754331413	7.254331413	7.754331413
1.647910839	1.809883221	1.507403846
8.373890892	12.25120937	6.462099458
83.11221718	106.5990947	111.6516665
50.43489926	58.89832749	74.06884811
81.46430634	104.7892114	110.1442627
7.784641588	10.83719622	6.90518152
22.57985588	39.60655047	16.99864354
3.588795626	3.229732909	3.162923309
6.899886164	6.350932019	7.273781329
9.245146097	9.109887671	9.373718306
2.576113844	2.8206319	2.963624909
5.656350471	5.880154762	6.210794996
1.561740256	1.760863506	1.493155534
2.960630618	3.437919649	2.78767934
0.128244311	0.186750548	0.137166546
0.871755689	0.813249452	0.862833454
0.022562906	0.014637237	0.026464902
0.006265622	0.007835423	0.01109926
0.004965839	0.004734596	0.020031998
0.030428262	0.048646306	0.035230985
0.064021682	0.110896987	0.044339401
0.089645367	0.124329654	0.055903457
0.130059295	0.137213751	0.094527357
0.170114461	0.152169981	0.157332692
0.189244548	0.156312542	0.209323579
0.164012045	0.132488905	0.193925259
0.128679973	0.110734619	0.151821109

302-3-A-3-H-3	302-3-A-3-H-3	302-2-A-5-X-1
Cristin Ashmankas,	Cristin Ashmankas,	Cristin Ashmankas,
Bimodal, Very Poorly Sorted	Bimodal, Very Poorly Sorted	Bimodal, Very Poorly Sorted
Sandy Mud	Sandy Mud	Sandy Mud
Very Fine Sandy Fine Silt	Very Fine Sandy Fine Silt	Very Fine Sandy Fine Silt
85.8520282	86.28624725	91.83171566
261.7317647	267.9362292	289.807729
4.785874343	4.589283547	4.340125012
26.35953768	24.39545201	21.61723388
14.01731698	12.28170751	12.03713953
5.77297517	5.922617082	5.888018676
0.565874904	0.710107872	0.809929855
2.948475198	3.132036321	3.408778268
6.083888455	6.27956415	6.281707575
2.561823493	2.601141006	2.607123163
-0.584712437	-0.720846897	-0.819583068
2.938217275	3.103749768	3.336745672
13.81260181	11.86750199	11.45702368
6.237142003	6.507666967	6.456538527
0.19621467	0.257345467	0.261787109
1.000599152	1.079721877	1.169253046
6.177871091	6.396839898	6.447623882
2.640885106	2.702140422	2.690760916
-0.19621467	-0.257345467	-0.261787109
1.000599152	1.079721877	1.169253046
Medium Silt	Medium Silt	Medium Silt
Very Poorly Sorted	Very Poorly Sorted	Very Poorly Sorted
Coarse Skewed	Coarse Skewed	Coarse Skewed
Mesokurtic	Mesokurtic	Leptokurtic
4.7	4.7	4.7
1200	1200	1200
7.754331413	7.754331413	7.754331413
-0.242713414	-0.242713414	-0.242713414
1.736436495	1.579200045	1.626234494
11.70406494	9.528515269	9.517449331
148.2239515	143.1627973	136.6189271
85.3609976	90.65526416	84.00936494
146.487515	141.5835972	134.9926926
12.403464	11.58317644	10.33733502
43.6485374	35.46792243	31.8990747
2.754149504	2.804271457	2.871770727
6.416846511	6.713532853	6.7152093
9.169654635	9.306590348	9.264248983
3.329396107	3.318719493	3.225970965
6.415505132	6.502318892	6.392478256
1.826235792	1.753978313	1.698611058
3.632671183	3.533959032	3.3697924
0.210855447	0.187549778	0.171495728
0.789144553	0.812450222	0.828504272
0.03660366	0.037307461	0.045690862
0.01460146	0.018403681	0.018196361
0.00970097	0.0105021	0.00979804
0.055405541	0.043908782	0.030993801
0.094543816	0.077427753	0.066816663
0.10322596	0.093361908	0.096939575
0.126555696	0.116882804	0.124382899
0.148265452	0.147152108	0.153397588
0.156609606	0.168002858	0.17094159
0.137092836	0.151408284	0.152652642
0.117395003	0.135642259	0.130189978

302-2-A-5-X-1	302-2-A-5-X-2	302-4-A-2-X-2
Cristin Ashmankas,	Cristin Ashmankas,	Cristin Ashmankas,
Trimodal, Very Poorly Sorted	Bimodal, Very Poorly Sorted	Unimodal, Very Poorly Sorted
Sandy Mud	Sandy Mud	Sandy Mud
Fine Sandy Medium Silt	Very Fine Sandy Fine Silt	Very Fine Sandy Fine Silt
86.6341875	72.52290881	53.90889717
203.7479528	190.2238061	201.0177917
5.194011186	5.963583704	6.452820568
35.38838587	44.68724233	46.74588726
19.65379173	16.41665616	10.1280803
5.773278615	5.461905799	4.708476608
0.235022891	0.322119949	0.755631444
2.270798665	2.427346376	3.657522619
5.63516485	5.894482311	6.588129356
2.538339804	2.462342414	2.262244013
-0.246863884	-0.338432658	-0.785616631
2.28136972	2.447335809	3.69060703
19.99338127	16.51179616	9.746891813
6.040401947	5.619711714	4.528507764
0.101768779	0.13953796	0.172554501
0.810327256	0.833234666	0.982333891
5.644333709	5.920359124	6.680842054
2.594644554	2.490496123	2.179035731
-0.101768779	-0.13953796	-0.172554501
0.810327256	0.833234666	0.982333891
Coarse Silt	Coarse Silt	Medium Silt
Very Poorly Sorted	Very Poorly Sorted	Very Poorly Sorted
Coarse Skewed	Coarse Skewed	Coarse Skewed
Platykurtic	Platykurtic	Mesokurtic
9.4	6.65	4.7
107.5	107.5	
6.754331413	7.254331413	7.754331413
3.236965594	3.236965594	
2.139700922	2.012406608	1.651223089
17.33913826	13.8289274	8.372250357
222.8012306	173.8047594	83.64329716
104.127277	86.36662132	50.65535828
220.6615297	171.7923528	81.99207407
16.20449541	13.99106016	7.806207911
75.49106217	57.58985881	22.81483243
2.166170894	2.524460506	3.579606257
5.84982399	6.176166927	6.900168831
8.868375127	8.956862453	9.242249236
4.094033002	3.548030335	2.581917835
6.702204234	6.432401947	5.662642979
2.105254237	1.948985518	1.564033084
4.018322192	3.806433381	2.964621888
0.284752121	0.248880701	0.129827307
0.715247879	0.751119299	0.870172693
0.0179	0.016398907	0.020646903
0.0138	0.009832678	0.008448733
0.0514	0.033031131	0.003749438
0.101	0.083461103	0.030445433
0.100652121	0.106156883	0.066536801
0.106538245	0.103861072	0.090152081
0.128603605	0.122495876	0.128246978
0.139078107	0.147530387	0.169876934
0.138610248	0.155357396	0.19129592
0.115783097	0.126626422	0.162639575
0.086634578	0.095248145	0.127961206

302-2-A-6-X-1	302-4-C-6-X-1	302-4-A-2-X-3
Cristin Ashmankas,	Cristin Ashmankas,	Cristin Ashmankas,
Unimodal, Very Poorly Sorted	Unimodal, Very Poorly Sorted	Unimodal, Very Poorly Sorted
Sandy Mud	Sandy Mud	Sandy Mud
Very Fine Sandy Fine Silt	Very Fine Sandy Fine Silt	Very Fine Sandy Fine Silt
61.95497567	62.72473318	56.26468548
203.6352946	174.5232326	190.8372938
6.275568216	6.517327159	6.528577614
45.26784036	53.1706772	49.33084237
12.57526997	14.52546412	11.45319581
5.029223088	5.165056799	4.835874538
0.546398492	0.391553046	0.646897939
3.05290265	2.581639408	3.241288341
6.268420788	6.078033934	6.416545556
2.355371872	2.381499421	2.293806984
-0.575469009	-0.408693561	-0.670589829
3.085398897	2.606643175	3.271746462
12.42655545	14.52688894	11.20895718
5.023964637	5.2892548	4.786073293
0.153158599	0.150453497	0.183680891
0.931418268	0.872332957	0.971874287
6.330429743	6.105130419	6.479204126
2.328826309	2.403064476	2.25884249
-0.153158599	-0.150453497	-0.183680891
0.931418268	0.872332957	0.971874287
Medium Silt	Medium Silt	Medium Silt
Very Poorly Sorted	Very Poorly Sorted	Very Poorly Sorted
Coarse Skewed	Coarse Skewed	Coarse Skewed
Mesokurtic	Platykurtic	Mesokurtic
6.65	6.65	6.65
7.254331413	7.254331413	7.254331413
1.80023552	1.946709252	1.780888409
10.63145239	12.19916182	9.365245616
115.6252138	145.4973882	104.8295976
64.22782603	74.74017399	58.86365316
113.8249783	143.550679	103.0487092
9.746182376	11.69228152	8.44571313
33.61360064	44.30554815	27.16367492
3.112472062	2.780934839	3.25388199
6.555517489	6.357074163	6.738467453
9.117598622	9.004746856	9.133187165
2.929375249	3.238028712	2.80685876
6.00512656	6.223812017	5.879305176
1.693204382	1.812267969	1.6131461
3.284837219	3.547484566	3.078219245
0.175609943	0.21233127	0.156310144
0.824390057	0.78766873	0.843689856
0.021333333	0.013399107	0.017734516
0.007366667	0.008666089	0.008567238
0.013	0.027198187	0.010634042
0.0491	0.066628891	0.04440296
0.084809943	0.096438997	0.074971388
0.103084552	0.106825127	0.09149139
0.13400983	0.128568646	0.129831692
0.162935875	0.15326458	0.16935488
0.170568064	0.162850531	0.185765543
0.141970566	0.135659832	0.153197512
0.111821171	0.100500012	0.114048838

302-4-A-3-X-1	302-2-A-6-X-1	302-4-C-6-X-1
Cristin Ashmankas,	Cristin Ashmankas,	Cristin Ashmankas,
Unimodal, Very Poorly Sorted	Unimodal, Very Poorly Sorted	Unimodal, Very Poorly Sorted
Sandy Mud	Sandy Mud	Sandy Mud
Very Fine Sandy Fine Silt	ery Fine Sandy Medium Si	Very Fine Sandy Fine Silt
57.38449267	54.24183105	54.3304305
169.7224077	189.3556851	199.6083858
6.858126518	6.39855573	6.478032238
57.50276839	47.75335127	47.39859756
13.72430474	11.25663969	10.49053412
4.867219575	4.565680154	4.676775147
0.436154052	0.69387812	0.734973088
2.79397724	3.674626529	3.641129305
6.16420182	6.445167398	6.535237111
2.295041512	2.20955788	2.253265827
-0.45474561	-0.719967555	-0.767576871
2.822087016	3.703098437	3.67651711
13.62418863	10.46276526	10.0263529
4.945281398	4.407323701	4.510120126
0.142086944	0.11247415	0.152913255
0.924423115	1.061930993	0.997031948
6.197685875	6.57859199	6.640059271
2.306052616	2.139902861	2.17316586
-0.142086944	-0.11247415	-0.152913255
0.924423115	1.061930993	0.997031948
Medium Silt	Medium Silt	Medium Silt
Very Poorly Sorted	Very Poorly Sorted	Very Poorly Sorted
Coarse Skewed	Coarse Skewed	Coarse Skewed
Mesokurtic	Mesokurtic	Mesokurtic
9.4	9.4	4.7
6.754331413	6.754331413	7.754331413
1.972406402	1.821607794	1.706216897
11.74546037	10.03015929	8.930977155
123.5769208	77.46353819	83.3631207
62.65286946	42.52481707	48.85845456
121.6045144	75.6419304	81.65690381
9.633605086	7.127033207	7.724325127
36.43776406	23.53572431	23.30161769
3.016518763	3.690338791	3.584446904
6.411752928	6.639511672	6.806966253
8.985827444	9.100571916	9.194983229
2.97887338	2.466053236	2.565244646
5.96930868	5.410233125	5.610536325
1.707328391	1.545821838	1.564652358
3.268075784	2.833301646	2.949408891
0.18575656	0.117623136	0.127893064
0.81424344	0.882376864	0.872106936
0.012866667	0.016604981	0.020366667
0.007566667	0.011603481	0.008133333
0.020566667	0.013904171	0.007566667
0.0576	0.027008102	0.030466667
0.08715656	0.0485024	0.06135973
0.108557659	0.103632689	0.093797455
0.140277839	0.161861318	0.138761996
0.165310771	0.184718618	0.174693536
0.168581262	0.178184664	0.183861232
0.133149611	0.143856193	0.159101624
0.098366297	0.110123382	0.121891092

302-2-A-6-X-2	302-2-A-6-X-2	302-4-A-3-X-2
Cristin Ashmankas,	Cristin Ashmankas,	Cristin Ashmankas,
Bimodal, Very Poorly Sorted	Unimodal, Very Poorly Sorted	Unimodal, Very Poorly Sorted
Sandy Mud	Sandy Mud	Sandy Mud
ery Fine Sandy Medium Si	ery Fine Sandy Medium Si	Very Fine Sandy Fine Silt
76.08885611	69.27433943	52.3520429
242.8913614	212.2814669	199.5646497
5.212742117	5.767523594	6.458121005
31.12447682	39.07312449	46.95879727
13.58819995	14.01137804	9.431140116
5.289752349	5.167061274	4.667986575
0.600827231	0.522946718	0.842794455
3.190405017	2.96144397	3.852457497
6.137727195	6.114400178	6.693138486
2.434489002	2.390107555	2.250006571
-0.628787748	-0.546558819	-0.870648337
3.192397855	2.980418768	3.880914025
13.26199783	13.92964598	8.941914909
5.296570252	5.180103193	4.437482841
0.154234842	0.150292722	0.19430859
0.987036656	0.948320264	1.009959203
6.236558065	6.165697597	6.805200467
2.405058457	2.372980838	2.149741541
-0.154234842	-0.150292722	-0.19430859
0.987036656	0.948320264	1.009959203
Medium Silt	Medium Silt	Medium Silt
Very Poorly Sorted	Very Poorly Sorted	Very Poorly Sorted
Coarse Skewed	Coarse Skewed	Coarse Skewed
Mesokurtic	Mesokurtic	Mesokurtic
9.4	9.4	4.7
1200		
6.754331413	6.754331413	7.754331413
-0.242713414		
1.869525715	1.943986984	1.604423998
11.68341415	11.95257934	7.616762528
123.1215951	138.8272721	76.47904085
65.8571284	71.41368393	47.66759969
121.2520693	136.8832851	74.87461685
9.893317026	9.831948573	7.369315204
36.26349807	37.0326164	20.18479643
3.021844268	2.848637087	3.70879176
6.419394266	6.386534208	7.036606368
9.063111969	9.006765725	9.283728835
2.999198889	3.161780686	2.503167995
6.041267702	6.158128638	5.574937075
1.713889467	1.71679396	1.531628592
3.306454308	3.29747737	2.881530563
0.182771581	0.191406885	0.118374141
0.817228419	0.808593115	0.881625859
0.03109689	0.02240224	0.019967332
0.01269873	0.01020102	0.009166972
0.01149885	0.01890189	0.005000167
0.0429957	0.058105811	0.026200873
0.08448141	0.081795923	0.058038796
0.110827498	0.104006142	0.084189491
0.140117051	0.14218185	0.123536861
0.163135243	0.165672782	0.1668344
0.16310139	0.163138206	0.197722175
0.133985644	0.132915852	0.174383173
0.106061593	0.100678283	0.134959759

302-2-A-6-X-3	302-2-A-6-X-3	302-2-A-6-X-4
Cristin Ashmankas,	Cristin Ashmankas,	Cristin Ashmankas,
Bimodal, Very Poorly Sorted	Bimodal, Very Poorly Sorted	Bimodal, Very Poorly Sorted
Sandy Mud	Sandy Mud	Sandy Mud
Very Fine Sandy Fine Silt	Very Fine Sandy Fine Silt	Very Fine Sandy Fine Silt
84.09688731	84.10180604	89.71565437
271.219425	250.2093489	268.6675401
4.836702795	4.89207584	4.600769162
26.47184459	27.93944008	24.59954167
12.84923618	14.47020509	14.12772749
5.626341795	5.714326476	5.840590797
0.682586552	0.538038632	0.611011266
3.235865422	2.87584215	2.986052035
6.170567965	6.05095817	6.068605575
2.54727409	2.540565935	2.5797633
-0.709589229	-0.555543226	-0.627235266
3.194391944	2.873412465	2.964221464
12.7082187	14.23384654	13.81846147
6.19057664	5.915286631	6.364873089
0.222768314	0.175931087	0.220136859
1.092336192	0.954331909	1.047177159
6.298094367	6.134530603	6.177259193
2.6300738	2.564448077	2.670131748
-0.222768314	-0.175931087	-0.220136859
1.092336192	0.954331909	1.047177159
Medium Silt	Medium Silt	Medium Silt
Very Poorly Sorted	Very Poorly Sorted	Very Poorly Sorted
Coarse Skewed	Coarse Skewed	Coarse Skewed
Mesokurtic	Mesokurtic	Mesokurtic
4.7	6.65	6.65
1700	1200	1200
7.754331413	7.254331413	7.254331413
-0.742713414	-0.242713414	-0.242713414
1.745829817	1.795706426	1.778658797
10.84080894	12.04472111	11.52490942
138.3046404	156.8381678	161.2130901
79.22000133	87.34065076	90.63744569
136.5588106	155.0424614	159.4344313
10.80033388	12.16582604	11.88078895
36.26707528	44.22853858	42.17932944
2.854078532	2.672651401	2.632959203
6.527383775	6.375455201	6.439100777
9.161871352	9.121232777	9.134994502
3.210097848	3.412803021	3.46947818
6.30779282	6.448581375	6.502035299
1.739071528	1.82392039	1.804094315
3.433004007	3.604762376	3.570558738
0.185495833	0.212609244	0.206884105
0.814504167	0.787390756	0.793115895
0.04219578	0.032209663	0.038192362
0.01129887	0.015104531	0.016796641
0.01239876	0.016304891	0.015596881
0.04109589	0.057917375	0.050689862
0.078506532	0.091072783	0.08560836
0.103986227	0.105201695	0.103292391
0.131955327	0.128413173	0.126529202
0.153837105	0.149295414	0.150912059
0.162073545	0.157643101	0.160661347
0.145463157	0.134827146	0.138060365
0.117188806	0.112010228	0.113660532

302-2-A-7-X-1	302-2-A-7-X-1	302-2-A-7-X-2
Cristin Ashmankas,	Cristin Ashmankas,	Cristin Ashmankas,
Bimodal, Very Poorly Sorted	Bimodal, Very Poorly Sorted	Bimodal, Very Poorly Sorted
Sandy Mud	Sandy Mud	Sandy Mud
Very Fine Sandy Fine Silt	Very Fine Sandy Fine Silt	Very Fine Sandy Fine Silt
79.5504781	69.10304933	87.23502
223.2105209	196.6291866	273.6091518
5.503740214	6.028714685	4.572383802
35.70524761	44.11865127	24.00509614
16.97014704	14.54456762	12.83672045
5.502300406	5.386032533	5.712595395
0.31765232	0.444983912	0.727607307
2.586147256	2.611672502	3.266312838
5.828027901	6.067498957	6.207831987
2.478680779	2.445452055	2.551909465
-0.341113385	-0.46231904	-0.743011922
2.60626742	2.63189011	3.23016816
16.99423779	14.73568748	12.48855926
5.542194416	5.52401587	6.306211895
0.08628214	0.183986938	0.254527812
0.844374725	0.868219289	1.126791302
5.878810533	6.08454182	6.32324914
2.47045732	2.465717464	2.656773647
-0.08628214	-0.183986938	-0.254527812
0.844374725	0.868219289	1.126791302
Coarse Silt	Medium Silt	Medium Silt
Very Poorly Sorted	Very Poorly Sorted	Very Poorly Sorted
Symmetrical	Coarse Skewed	Coarse Skewed
Platykurtic	Platykurtic	Leptokurtic
9.4	6.65	6.65
107.5	107.5	1200
6.754331413	7.254331413	7.254331413
3.236965594	3.236965594	-0.242713414
2.017714595	1.912040045	1.731081772
15.37677952	11.67176618	10.18651111
164.5005478	160.7390133	137.8700499
81.52815476	84.06676091	79.64386899
162.4828332	158.8269733	136.1389681
13.4822698	12.34538295	10.42207223
57.81056498	46.30982885	34.81721374
2.603835707	2.637207963	2.858619007
6.02310281	6.420833303	6.617196178
8.953062164	9.030671546	9.174110409
3.438412854	3.424330455	3.209280561
6.349226458	6.393463582	6.315491402
1.937933686	1.841144981	1.719708198
3.752991496	3.625899684	3.381570253
0.249848603	0.22216336	0.185833071
0.750151397	0.77783664	0.814166929
0.025705141	0.0184	0.03980398
0.00940188	0.008333333	0.0170017
0.020804161	0.026633333	0.00780078
0.079715943	0.076333333	0.04270427
0.114221477	0.09246336	0.07852234
0.116141567	0.094158046	0.094720672
0.130798967	0.121876757	0.125477571
0.143497957	0.155488878	0.158038481
0.14493877	0.166829917	0.17280517
0.119712138	0.136541668	0.144918444
0.095062	0.102941373	0.118206592

302-2-A-7-X-2	302-2-A-7-X-3	302-2-A-8-X-1
Cristin Ashmankas,	Cristin Ashmankas,	Cristin Ashmankas,
Unimodal, Very Poorly Sorted	Unimodal, Very Poorly Sorted	Unimodal, Very Poorly Sorted
Sandy Mud	Sandy Mud	Sandy Mud
Very Fine Sandy Fine Silt	Very Fine Sandy Fine Silt	Very Fine Sandy Fine Silt
68.5259711	75.0213261	71.65526903
225.9282114	226.3804777	226.3328236
5.602261577	5.48054292	5.485839988
35.96980929	34.93815606	34.87250946
12.68493746	14.75460607	13.39090672
5.09522346	5.392857592	5.24496696
0.633988863	0.454009798	0.584405569
3.27213263	2.833661823	3.081251352
6.245922488	6.030884251	6.171771956
2.379067244	2.453828315	2.416611376
-0.66351973	-0.477918915	-0.608896067
3.285886393	2.850547943	3.093340742
12.31819983	14.65589966	13.1303787
4.994776937	5.399784322	5.213763304
0.156902985	0.120682301	0.171831308
0.970711843	0.896561727	0.948824176
6.343064752	6.092374659	6.250947663
2.32042025	2.432901784	2.382325088
-0.156902985	-0.120682301	-0.171831308
0.970711843	0.896561727	0.948824176
Medium Silt	Medium Silt	Medium Silt
Very Poorly Sorted	Very Poorly Sorted	Very Poorly Sorted
Coarse Skewed	Coarse Skewed	Coarse Skewed
Mesokurtic	Platykurtic	Mesokurtic
6.65	9.4	6.65
7.254331413	6.754331413	7.254331413
1.845860804	1.878161484	1.872137361
10.74279935	12.91563161	11.07279897
113.1504264	142.5542828	124.8011285
61.29954444	75.90097232	66.66237804
111.3045656	140.6761214	122.9289911
9.252849672	11.61213212	10.13204439
32.2615834	44.4324801	36.57019958
3.143686074	2.810416711	3.002297115
6.540486211	6.274737993	6.496836239
9.081490521	9.056463173	9.061097994
2.888803242	3.222462753	3.018055058
5.937804447	6.246046462	6.058800878
1.670260026	1.810935103	1.72261664
3.209897752	3.537560987	3.340853397
0.167840046	0.211459719	0.186464107
0.832159954	0.788540281	0.813535893
0.02640264	0.026292112	0.0260026
0.01190119	0.011196641	0.01260126
0.01080108	0.014895531	0.01340134
0.04040404	0.060981705	0.04780478
0.078331095	0.098093729	0.086654126
0.106547942	0.112369278	0.105669234
0.139613845	0.135807985	0.132187691
0.164760114	0.151419174	0.160547117
0.171419937	0.154260709	0.171215724
0.141720944	0.129350504	0.138028472
0.108097172	0.105332632	0.105887656

302-2-A-8-X-1	302-2-A-8-X-2	302-2-A-8-X-3
Cristin Ashmankas,	Cristin Ashmankas,	Cristin Ashmankas,
Trimodal, Very Poorly Sorted	Unimodal, Very Poorly Sorted	Bimodal, Very Poorly Sorted
Sandy Mud	Sandy Mud	Sandy Mud
Very Fine Sandy Fine Silt	Very Fine Sandy Fine Silt	Very Fine Sandy Fine Silt
91.6820027	57.66341377	76.34648144
257.6503323	179.6049321	239.1107587
4.662474476	7.076388939	5.204300486
25.66913885	57.97763803	31.26602062
15.97739366	14.15220882	13.83596227
5.983577184	4.814420241	5.337933651
0.447619167	0.367003389	0.575132509
2.657752572	2.777445763	3.094698357
5.906030063	6.109279712	6.118611188
2.603749384	2.284214357	2.443504064
-0.461887593	-0.396130185	-0.599667792
2.655538095	2.821478388	3.09964644
15.71331008	14.23416336	13.49972456
6.387426601	4.831397677	5.356547264
0.171939686	0.106934066	0.161044805
0.928997699	0.858919619	0.965385249
5.991869067	6.134498492	6.210926218
2.675234808	2.272440607	2.421303365
-0.171939686	-0.106934066	-0.161044805
0.928997699	0.858919619	0.965385249
Coarse Silt	Medium Silt	Medium Silt
Very Poorly Sorted	Very Poorly Sorted	Very Poorly Sorted
Coarse Skewed	Coarse Skewed	Coarse Skewed
Mesokurtic	Platykurtic	Mesokurtic
4.7	9.4	6.65
107.5		1200
7.754331413	6.754331413	7.254331413
3.236965594		-0.242713414
1.824888617	2.008626312	1.872426963
13.40530038	12.49875185	11.68874702
173.8216332	117.4035188	125.2080836
95.25054381	58.44965692	66.86940856
171.9967446	115.3948925	123.3356566
14.76665423	10.4385176	10.424524
56.64947473	41.13817158	38.53946723
2.524320449	3.090452445	2.997600388
6.221052643	6.322072158	6.418735902
9.097975873	8.959575097	9.06087484
3.604128737	2.899114371	3.02270939
6.573655424	5.869122652	6.063274452
1.961303663	1.759034027	1.742945415
3.884271077	3.383844941	3.381909604
0.24581	0.198902427	0.1908782
0.75419	0.801097573	0.8091218
0.03390339	0.016365576	0.029408823
0.01770177	0.005032998	0.014204261
0.01730173	0.008932738	0.011503451
0.069706971	0.059929338	0.045013504
0.107196138	0.108641778	0.090748161
0.104986547	0.114677125	0.111361553
0.119663102	0.136292452	0.133966913
0.140162313	0.161832073	0.159387262
0.150705755	0.1636733	0.165158398
0.129295787	0.129137619	0.13344639
0.109376497	0.095485003	0.105801284

302-2-A-9-X-1	302-2-A-9-X-1	302-2-A-9-X-2
Cristin Ashmankas,	Cristin Ashmankas,	Cristin Ashmankas,
Bimodal, Very Poorly Sorted	Unimodal, Very Poorly Sorted	Unimodal, Very Poorly Sorted
Sandy Mud	Sandy Mud	Sandy Mud
Very Fine Sandy Fine Silt	Very Fine Sandy Fine Silt	Very Fine Sandy Fine Silt
75.2958955	68.0956995	57.11235126
198.5215139	219.7964266	201.5287364
5.816627837	5.551754068	6.382170159
41.50105573	36.07061838	46.48627842
17.49422158	12.28940592	11.34131872
5.429419722	5.109097564	4.696354404
0.258860958	0.716280838	0.710168218
2.440640146	3.325472443	3.5552873
5.803094051	6.299601828	6.419087042
2.452391884	2.379595014	2.259573636
-0.275822531	-0.739233734	-0.7442348
2.460219776	3.331765858	3.58786726
17.41668009	11.95950505	10.90639808
5.495430569	5.080730438	4.580596003
0.08695888	0.205581641	0.164441145
0.814759673	1.049430575	1.030527119
5.843386541	6.385698506	6.518681471
2.458232521	2.345035923	2.195535326
-0.08695888	-0.205581641	-0.164441145
0.814759673	1.049430575	1.030527119
Coarse Silt	Medium Silt	Medium Silt
Very Poorly Sorted	Very Poorly Sorted	Very Poorly Sorted
Symmetrical	Coarse Skewed	Coarse Skewed
Platykurtic	Mesokurtic	Mesokurtic
9.4	9.4	6.65
107.5		
6.754331413	6.754331413	7.254331413
3.236965594		
2.063105221	1.860670141	1.843840032
15.55348606	9.951941324	9.611791409
166.4039613	124.3264428	92.71348729
80.65704048	66.81809962	50.28282588
164.3408561	122.4657727	90.86964726
14.19774091	8.251087333	7.545113709
62.45921275	28.00977617	24.89101803
2.587238317	3.007794921	3.431076963
6.006618216	6.650806305	6.700978945
8.920966882	9.069961967	9.083070789
3.448065384	3.015485499	2.647294388
6.333728565	6.062167046	5.651993826
1.98254892	1.61240279	1.569096622
3.827589487	3.044584251	2.915542643
0.262067555	0.165099054	0.138063683
0.737932445	0.834900946	0.861936317
0.0184	0.0238	0.02069793
0.0107	0.0137	0.00806586
0.0245	0.0165	0.01253208
0.0872	0.0455	0.0343299
0.121267555	0.065599054	0.062437912
0.111329692	0.087672505	0.096035689
0.12570045	0.134387011	0.142174419
0.144257147	0.178109635	0.180233951
0.146611645	0.182018632	0.1868928
0.11819495	0.145721047	0.148214345
0.091838561	0.106992116	0.108385113

302-2-A-9-X-2	302-2-A-9-X-3	302-2-A-10-X-1
Cristin Ashmankas,	Cristin Ashmankas,	Cristin Ashmankas,
Bimodal, Very Poorly Sorted	Bimodal, Very Poorly Sorted	Bimodal, Very Poorly Sorted
Sandy Mud	Sandy Mud	Sandy Mud
Very Fine Sandy Fine Silt	Very Fine Sandy Fine Silt	Very Fine Sandy Fine Silt
83.90004899	91.00421608	81.11429693
238.1522131	265.8862042	251.7342512
5.072943012	4.529427899	4.914930157
30.51450343	24.22861745	28.00451113
16.01738729	13.88421337	13.1671029
5.675919352	5.99765985	5.584452632
0.418869391	0.634205973	0.663799726
2.695839011	2.922242005	3.116662365
5.906433138	6.101653712	6.184127519
2.526730142	2.614898625	2.512413245
-0.438752569	-0.645120829	-0.681825555
2.703937476	2.899568975	3.104335702
15.943566	13.70968694	12.93170563
5.818687999	6.505181952	5.795107448
0.126876337	0.243027925	0.2233963
0.90766927	1.042998168	1.020292454
5.970881846	6.188660562	6.272943617
2.54069389	2.70158941	2.534835411
-0.126876337	-0.243027925	-0.2233963
0.90766927	1.042998168	1.020292454
Coarse Silt	Medium Silt	Medium Silt
Very Poorly Sorted	Very Poorly Sorted	Very Poorly Sorted
Coarse Skewed	Coarse Skewed	Coarse Skewed
Mesokurtic	Mesokurtic	Mesokurtic
9.4	4.7	6.65
1200	1200	1200
6.754331413	7.754331413	7.254331413
-0.242713414	-0.242713414	-0.242713414
1.902350082	1.726713534	1.780480329
14.06474528	10.85460479	10.47129642
170.3637127	183.662474	144.8223773
89.55434351	106.3653411	81.33893702
168.4613626	181.9357605	143.041897
12.84662211	11.85864722	10.50891013
51.36373309	40.51108653	36.10949945
2.553310019	2.44487121	2.787643556
6.151772765	6.52554899	6.57741612
9.038001521	9.177755528	9.133517788
3.5397196	3.753880978	3.276429573
6.484691501	6.732884318	6.345874232
1.884096662	1.793133639	1.730230896
3.683317162	3.567867538	3.393541151
0.232257919	0.207460443	0.191229171
0.767742081	0.792539557	0.808770829
0.028691393	0.03619638	0.03280328
0.014295711	0.01879812	0.01520152
0.023193042	0.02219778	0.01420142
0.067179846	0.055594441	0.04990499
0.098897927	0.074673722	0.07911796
0.112467103	0.092942084	0.094525092
0.133612871	0.123851812	0.126175311
0.146427658	0.151121074	0.159139057
0.147166098	0.164070551	0.172309312
0.124543586	0.141974221	0.143020794
0.103524765	0.118579815	0.113601263

302-2-A-9-X-5	302-2-A-10-X-1	302-2-A-10-X-2
Cristin Ashmankas,	Cristin Ashmankas,	Cristin Ashmankas,
Bimodal, Very Poorly Sorted	Bimodal, Very Poorly Sorted	Bimodal, Very Poorly Sorted
Sandy Mud	Sandy Mud	Sandy Mud
Very Fine Sandy Fine Silt	Very Fine Sandy Fine Silt	Very Fine Sandy Fine Silt
84.53965157	68.92612461	61.06718511
244.3538177	204.2158086	153.7813023
5.012033392	5.799017386	7.042427304
29.46019905	40.2234194	63.92992388
15.78382794	14.41742668	16.79680604
5.657296589	5.192440082	5.007972753
0.448045357	0.481880561	0.182564339
2.75221969	2.848027623	2.352154856
5.923633548	6.080162093	5.880722082
2.524006699	2.393191498	2.330041477
-0.468975621	-0.501914423	-0.194247159
2.757654624	2.8670099	2.371046036
15.69092644	14.36517504	16.74691253
5.756446956	5.234293837	5.136050028
0.138707301	0.150514637	0.049889621
0.90657107	0.924938618	0.806912275
5.993925654	6.121280618	5.899961046
2.525178614	2.387994915	2.360659255
-0.138707301	-0.150514637	-0.049889621
0.90657107	0.924938618	0.806912275
Coarse Silt	Medium Silt	Coarse Silt
Very Poorly Sorted	Very Poorly Sorted	Very Poorly Sorted
Coarse Skewed	Coarse Skewed	Symmetrical
Mesokurtic	Mesokurtic	Platykurtic
9.4	9.4	4.7
1200	107.5	107.5
6.754331413	6.754331413	7.754331413
-0.242713414	3.236965594	3.236965594
1.923687223	1.962945208	2.103165292
13.6512191	12.20799617	15.74313694
164.2478236	140.8817328	142.5166855
85.38177183	71.77058853	67.76295046
162.3241363	138.9187876	140.4135202
12.76571538	10.38858587	12.93780002
50.70719294	39.91443452	55.58763584
2.606053841	2.827443535	2.810797259
6.194826395	6.356029775	5.989133152
9.021910038	8.992764381	8.893222046
3.461904698	3.180528371	3.163950021
6.415856196	6.165320846	6.082424787
1.878159576	1.750273898	1.911297025
3.674202483	3.376927378	3.693520413
0.230285979	0.201532316	0.243323033
0.769714021	0.798467684	0.756676967
0.030893821	0.01970197	0.00963237
0.013797241	0.01230123	0.00683265
0.018996201	0.01950195	0.02143119
0.065586883	0.060206021	0.079425391
0.101011834	0.089821145	0.126001432
0.111599312	0.104202385	0.126695469
0.130308651	0.138271064	0.131424548
0.147728998	0.162467338	0.139727541
0.15137578	0.163133082	0.146044765
0.126663651	0.131220108	0.124376012
0.102037628	0.099173707	0.088408632

302-2-A-10-X-2	302-2-A-10-X-3	302-2-A-11-X-1
Cristin Ashmankas,	Cristin Ashmankas,	Cristin Ashmankas,
Bimodal, Very Poorly Sorted	Bimodal, Very Poorly Sorted	Trimodal, Very Poorly Sorted
Sandy Mud	Sandy Mud	Sandy Mud
Very Fine Sandy Fine Silt	Very Fine Sandy Fine Silt	Very Fine Sandy Fine Silt
82.3099715	77.12486251	92.27739978
203.0287071	222.097451	270.1002555
5.612873969	5.467958483	4.472334812
39.16564197	35.2049519	23.53256415
19.44935712	15.62872705	14.0691125
5.663190801	5.553707777	5.979349543
0.174716376	0.376249622	0.632182609
2.256207295	2.618496174	2.950334056
5.648253309	5.953817889	6.079592738
2.511396536	2.491801143	2.611287758
-0.189404322	-0.395555362	-0.643816639
2.273275816	2.636140044	2.925006034
19.31290244	15.51411948	13.9082189
5.725011775	5.559570353	6.585284263
0.055258063	0.10347536	0.243419805
0.766690077	0.836247847	1.060654892
5.694291193	6.010274372	6.167918511
2.51727866	2.474973395	2.719245718
-0.055258063	-0.10347536	-0.243419805
0.766690077	0.836247847	1.060654892
Coarse Silt	Medium Silt	Medium Silt
Very Poorly Sorted	Very Poorly Sorted	Very Poorly Sorted
Symmetrical	Coarse Skewed	Coarse Skewed
Platykurtic	Platykurtic	Mesokurtic
107.5	4.7	6.65
6.65	107.5	107.5
3.236965594	7.754331413	7.254331413
7.254331413	3.236965594	3.236965594
2.10898322	1.880443886	1.742420373
17.82559943	13.80264225	11.0893221
185.8626204	153.2130833	176.1558446
88.12901813	81.47708335	101.0983614
183.7536372	151.3326394	174.4134242
17.21643233	13.79938431	11.83871937
79.06372109	52.96506936	41.56611341
2.427691442	2.706388597	2.505075753
5.809905598	6.17891172	6.494685015
8.889236669	9.054711029	9.164691557
3.661600694	3.345680306	3.65844887
6.461545227	6.348322432	6.659615804
2.1486088	1.916772461	1.799223836
4.105714306	3.786531995	3.565441123
0.301764433	0.235459548	0.211009007
0.698235567	0.764540452	0.788990993
0.01940194	0.02479752	0.037688693
0.01020102	0.01159884	0.019594122
0.02960296	0.01629837	0.018194542
0.109410941	0.071692831	0.055183445
0.133147571	0.111071987	0.080348205
0.106160763	0.114347672	0.090578956
0.114652707	0.126247064	0.124274057
0.132268976	0.138453549	0.156983501
0.13971071	0.147969366	0.16305807
0.116796755	0.132261571	0.137249085
0.088645655	0.10526123	0.116847324

302-2-A-11-X-2	302-2-A-11-X-3	302-2-A-12-X-2
Cristin Ashmankas,	Cristin Ashmankas,	Cristin Ashmankas,
Unimodal, Very Poorly Sorted	Unimodal, Very Poorly Sorted	Trimodal, Very Poorly Sorted
Sandy Mud	Sandy Mud	Sandy Mud
Very Fine Sandy Fine Silt	Very Fine Sandy Fine Silt	Very Fine Sandy Fine Silt
70.01045141	60.45144762	82.96069193
233.8942214	194.9380139	234.2295697
5.360648362	6.187082378	5.21781364
32.99613226	45.06019087	32.06547081
11.42673231	12.13744858	16.51732705
5.233038254	4.971046607	5.615697464
0.789075481	0.639057526	0.392745459
3.434810115	3.119869475	2.617173836
6.398635198	6.333165923	5.863076661
2.419334805	2.331911601	2.510109744
-0.809703171	-0.659146177	-0.413869211
3.42916171	3.142401113	2.629450545
11.16035353	11.89912864	16.47142712
5.166146021	4.953570769	5.649824462
0.234125355	0.196759847	0.135066239
1.026715088	0.963520091	0.845789525
6.485473461	6.393000259	5.923890631
2.369088422	2.308468863	2.498206044
-0.234125355	-0.196759847	-0.135066239
1.026715088	0.963520091	0.845789525
Medium Silt	Medium Silt	Coarse Silt
Very Poorly Sorted	Very Poorly Sorted	Very Poorly Sorted
Coarse Skewed	Coarse Skewed	Coarse Skewed
Mesokurtic	Mesokurtic	Platykurtic
6.65	4.7	6.65
		107.5
7.254331413	7.754331413	7.254331413
		3.236965594
1.735009741	1.842434069	2.012670252
8.889779339	9.772982092	14.07432375
117.1675994	117.758941	167.4052976
67.53137843	63.91487378	83.17572014
115.4325897	115.9165069	165.3926274
8.632267893	8.977544858	13.98963559
26.96278755	29.85804124	57.83943751
3.093354421	3.086091492	2.578582911
6.813636676	6.676985437	6.150790585
9.170840522	9.084171291	8.956673458
2.964691165	2.943584567	3.473486704
6.077486101	5.998079798	6.378090547
1.617592823	1.646800361	1.950429858
3.109739638	3.166320957	3.806286477
0.164046265	0.16839707	0.249491548
0.835953735	0.83160293	0.750508452
0.027894421	0.018066064	0.02829717
0.013397321	0.010399653	0.01179882
0.01009798	0.01439952	0.01939806
0.042091582	0.050764975	0.077992201
0.070564962	0.074766858	0.112005297
0.082379219	0.092068559	0.107311303
0.11919769	0.129531285	0.122253927
0.168151318	0.167076322	0.145827658
0.190241457	0.182213907	0.153984602
0.157290888	0.151977754	0.125886877
0.118693163	0.108735103	0.095244085

302-2-A-12-X-3	302-2-A-13-X-1	302-2-A-13-X-1
Cristin Ashmankas,	Cristin Ashmankas,	Cristin Ashmankas,
Unimodal, Very Poorly Sorted	Unimodal, Very Poorly Sorted	Unimodal, Very Poorly Sorted
Sandy Mud	Sandy Mud	Sandy Mud
Very Fine Sandy Fine Silt	Very Fine Sandy Fine Silt	Very Fine Sandy Fine Silt
59.3519974	76.68924235	62.96633142
171.5094087	233.0573958	216.1898889
6.732366816	5.299574052	5.704915645
54.95195388	32.6800378	37.78594656
14.75569641	14.29065715	10.63742176
4.875828114	5.439151823	4.995983993
0.360317723	0.528217711	0.847202998
2.690214553	2.897284302	3.647919472
6.062648622	6.073961152	6.510855295
2.29513223	2.468349756	2.349872493
-0.376734486	-0.55057961	-0.869082127
2.714766346	2.90691197	3.650417241
14.68673724	14.16137562	10.07285332
4.930377559	5.464210232	4.889732359
0.105750025	0.170002813	0.22353732
0.868309559	0.907652454	1.092984045
6.089342263	6.141894776	6.633383779
2.30169813	2.450012991	2.289755501
-0.105750025	-0.170002813	-0.22353732
0.868309559	0.907652454	1.092984045
Medium Silt	Medium Silt	Medium Silt
Very Poorly Sorted	Very Poorly Sorted	Very Poorly Sorted
Coarse Skewed	Coarse Skewed	Coarse Skewed
Platykurtic	Mesokurtic	Mesokurtic
9.4	6.65	4.7
6.754331413	7.254331413	7.754331413
2.043100063	1.890767253	1.713202964
13.04363694	11.80276599	8.454616271
124.34805	141.6136697	102.8061054
60.86243756	74.89746264	60.00812958
122.30495	139.7229024	101.0929025
10.5907469	11.66426052	7.553887983
42.27540471	43.43981946	22.4976911
3.007544211	2.819967562	3.282002149
6.260509999	6.404731193	6.886045008
8.935024421	9.046812501	9.189088206
2.970870516	3.208126442	2.799842227
5.92748021	6.226844939	5.907086057
1.770136213	1.806279386	1.553634968
3.404732433	3.544022942	2.91721939
0.203412677	0.2101986	0.140015153
0.796587323	0.7898014	0.859984847
0.013102621	0.027805561	0.022901527
0.00880176	0.013202641	0.013167545
0.014102821	0.013602721	0.015434362
0.063212643	0.057711542	0.034135609
0.104192833	0.097876136	0.05437611
0.116238408	0.103921104	0.079597652
0.140303668	0.126159994	0.126652906
0.158192977	0.155163026	0.175004533
0.159343514	0.164431955	0.194127799
0.129829972	0.135630453	0.163264279
0.092678784	0.104494868	0.121337678

302-2-A-14-X-1	302-2-A-14-X-2	302-2-A-14-X-3
Cristin Ashmankas,	Cristin Ashmankas,	Cristin Ashmankas,
Bimodal, Very Poorly Sorted	Bimodal, Very Poorly Sorted	Unimodal, Very Poorly Sorted
Sandy Mud	Sandy Mud	Sandy Mud
Very Fine Sandy Fine Silt	Very Fine Sandy Fine Silt	Very Fine Sandy Fine Silt
81.70394271	78.17444189	57.49548662
253.9843309	254.3011009	202.2340812
4.941765335	4.936668209	6.289696783
28.08740482	27.92099372	45.08802356
13.7003143	12.10579277	11.01649567
5.571558575	5.497103262	4.834614937
0.601091537	0.718076629	0.707085484
3.052822336	3.339146016	3.425999178
6.120897037	6.303368074	6.464331661
2.510395959	2.49406746	2.299573579
-0.622879355	-0.737719838	-0.735355107
3.045542372	3.321058926	3.455322554
13.41495452	11.69076562	10.72465236
5.788621383	5.797048102	4.715930524
0.194132907	0.21480594	0.182889535
0.986674457	1.082612947	0.973667047
6.220014027	6.418486776	6.542925306
2.533219797	2.535318457	2.237542464
-0.194132907	-0.21480594	-0.182889535
0.986674457	1.082612947	0.973667047
Medium Silt	Medium Silt	Medium Silt
Very Poorly Sorted	Very Poorly Sorted	Very Poorly Sorted
Coarse Skewed	Coarse Skewed	Coarse Skewed
Mesokurtic	Mesokurtic	Mesokurtic
4.7	6.65	4.7
1200	1200	
7.754331413	7.254331413	7.754331413
-0.242713414	-0.242713414	
1.803115225	1.658101515	1.742884428
11.30748676	9.906746845	9.03092305
136.8982206	119.2430374	97.52265647
75.92316826	71.91540227	55.95474659
135.0951054	117.5849359	95.77977204
11.3465168	9.783761993	8.303369159
40.21828392	31.35198143	25.82267687
2.8688244	3.068023065	3.358118765
6.466577883	6.657372898	6.790910832
9.115292692	9.236251948	9.164307379
3.177361672	3.010489737	2.729000378
6.246468292	6.168228884	5.806188614
1.778204559	1.679867728	1.599930664
3.504177576	3.290389308	3.05369684
0.199025635	0.171053138	0.147958254
0.800974365	0.828946862	0.852041746
0.034093181	0.033706741	0.02069793
0.014497101	0.015803161	0.00936573
0.0104979	0.00840168	0.00746592
0.048590282	0.037207441	0.0376629
0.09134717	0.075934114	0.072765773
0.105735889	0.095316649	0.091606627
0.127243251	0.129487518	0.128775022
0.153007447	0.162461225	0.169191629
0.16385931	0.17053597	0.186696342
0.139566189	0.145420715	0.15779829
0.111562279	0.125724785	0.117973836

302-2-A-15-X-1	302-2-A-15-X-1	302-2-A-15-X-2
Cristin Ashmankas,	Cristin Ashmankas,	Cristin Ashmankas,
Bimodal, Very Poorly Sorted	Bimodal, Very Poorly Sorted	Unimodal, Very Poorly Sorted
Sandy Mud	Sandy Mud	Sandy Mud
Very Fine Sandy Fine Silt	Very Fine Sandy Fine Silt	Very Fine Sandy Fine Silt
76.46873863	59.25025682	70.17527731
247.6690791	179.2743863	217.3122366
5.06863079	6.789054512	5.887566785
29.4164158	54.84872835	39.74153569
12.58688265	13.81467313	14.69197562
5.424187056	4.943540689	5.199934049
0.652860787	0.428992122	0.428841321
3.263087967	2.760608996	2.8302772
6.253142921	6.147427232	6.036346566
2.470531219	2.320959314	2.402198559
-0.674559009	-0.451810665	-0.458613135
3.257258393	2.794155003	2.858897137
12.13330334	13.84665354	14.72907562
5.462948731	5.022879437	5.164090615
0.165667153	0.137510464	0.111664034
1.011996401	0.890140887	0.862925742
6.364883806	6.174318842	6.085189299
2.449679884	2.328514647	2.368514316
-0.165667153	-0.137510464	-0.111664034
1.011996401	0.890140887	0.862925742
Medium Silt	Medium Silt	Medium Silt
Very Poorly Sorted	Very Poorly Sorted	Very Poorly Sorted
Coarse Skewed	Coarse Skewed	Coarse Skewed
Mesokurtic	Platykurtic	Platykurtic
9.4	9.4	9.4
1200	107.5	
6.754331413	6.754331413	6.754331413
-0.242713414	3.236965594	
1.687281288	1.949616149	1.952866444
10.63800138	11.87788028	12.96895919
119.5333497	125.2785385	132.0499185
70.84375945	64.25805332	67.61850965
117.8460684	123.3289223	130.097052
9.884459806	10.37617459	11.55026115
32.9648833	38.77102839	44.91546685
3.06451491	2.996788808	2.920844684
6.554629061	6.395578793	6.268793487
9.211083778	9.002594178	9.000190998
3.00572327	3.004080286	3.081365828
6.146568868	6.00580537	6.079346314
1.693044402	1.742999135	1.812207989
3.305162124	3.375202755	3.529853566
0.172868237	0.195302807	0.212298192
0.827131763	0.804697193	0.787701808
0.03179682	0.015498967	0.02496417
0.01449855	0.006466236	0.00769923
0.00859914	0.016532231	0.01076559
0.04039596	0.061729218	0.062493751
0.077577766	0.095076156	0.106375451
0.102910606	0.106107679	0.112946347
0.137344004	0.136958403	0.134817506
0.161134512	0.160973693	0.153112228
0.164193362	0.164030317	0.156090291
0.139373806	0.13632501	0.130713507
0.122175472	0.100302091	0.100021929

302-2-A-15-X-2	302-2-A-15-X-3	302-2-A-15-X-3
Cristin Ashmankas,	Cristin Ashmankas,	Cristin Ashmankas,
Unimodal, Very Poorly Sorted	Unimodal, Very Poorly Sorted	Unimodal, Very Poorly Sorted
Sandy Mud	Sandy Mud	Sandy Mud
Very Fine Sandy Fine Silt	Very Fine Sandy Fine Silt	Very Fine Sandy Fine Silt
60.62938404	74.21127358	54.51888737
196.261429	227.1814013	191.8645729
6.401795987	5.528180306	6.568880245
47.48339133	35.23159378	49.16405477
12.91824671	14.77353728	11.40163873
4.917317046	5.311797314	4.668590461
0.540594507	0.460958767	0.644214977
3.03787789	2.862816279	3.381158169
6.236246286	6.028683144	6.422725548
2.31892807	2.43229475	2.243773449
-0.567968815	-0.486717886	-0.672272371
3.07081474	2.881509435	3.418106936
12.77325357	14.70550927	11.07200201
4.910367742	5.243494461	4.535094885
0.151279764	0.120003114	0.149356287
0.935344062	0.870197901	0.943376255
6.290730139	6.087499442	6.49694008
2.295831073	2.390528598	2.181132736
-0.151279764	-0.120003114	-0.149356287
0.935344062	0.870197901	0.943376255
Medium Silt	Medium Silt	Medium Silt
Very Poorly Sorted	Very Poorly Sorted	Very Poorly Sorted
Coarse Skewed	Coarse Skewed	Coarse Skewed
Mesokurtic	Platykurtic	Mesokurtic
9.4	9.4	4.7
6.754331413	6.754331413	7.754331413
1.897345563	1.936291132	1.817501549
10.97204639	12.86321632	9.650879949
117.5179804	135.0699104	91.34563997
61.93810065	69.7570258	50.25890625
115.6206349	133.1336193	89.52813842
9.331319674	11.68946268	8.28914735
33.2748959	45.1863417	26.96325379
3.089046587	2.888221774	3.452520321
6.510023563	6.28060477	6.695123794
9.041801824	9.012488399	9.103827691
2.927052594	3.120428105	2.636864332
5.952755238	6.124266625	5.65130737
1.678920894	1.817510363	1.606920282
3.222081127	3.547136711	3.051223709
0.175340501	0.213518117	0.144577005
0.824659499	0.786481883	0.855422995
0.019332045	0.026735116	0.018199393
0.007632824	0.010900727	0.009566348
0.012665822	0.010167344	0.004399853
0.053129791	0.060370691	0.035498817
0.082580019	0.105344239	0.076912594
0.103142003	0.111564104	0.102103151
0.139779963	0.133459504	0.137866994
0.166266664	0.15263492	0.169690054
0.170895904	0.156548428	0.182083683
0.140465161	0.131068696	0.152774762
0.104109804	0.10120623	0.110904353

302-2-A-16-X-2	302-2-A-16-X-3	302-2-A-17-X-1
Cristin Ashmankas,	Cristin Ashmankas,	Cristin Ashmankas,
Unimodal, Very Poorly Sorted	Bimodal, Very Poorly Sorted	Unimodal, Very Poorly Sorted
Sandy Mud	Sandy Mud	Sandy Mud
Very Fine Sandy Fine Silt	Very Fine Sandy Fine Silt	Very Fine Sandy Fine Silt
61.00329561	53.94366109	58.67080672
188.0355279	161.1590696	207.9550123
6.520351182	7.422870517	6.079508233
50.28649349	66.01525379	42.16351488
13.42097496	13.59582238	10.90502167
5.032016825	4.844618	4.807344402
0.468375333	0.356416135	0.751497311
2.829263547	2.639334285	3.583019741
6.185481914	6.180430359	6.478333329
2.348796655	2.287107289	2.292199125
-0.491529318	-0.374435066	-0.779617148
2.860654289	2.671353348	3.605635041
13.34466803	13.61836689	10.46186281
5.091965627	4.911698743	4.634870634
0.144845418	0.12121589	0.178618604
0.905905797	0.843768468	0.990984469
6.227592773	6.198302483	6.578716433
2.34822268	2.296222076	2.212529072
-0.144845418	-0.12121589	-0.178618604
0.905905797	0.843768468	0.990984469
Medium Silt	Medium Silt	Medium Silt
Very Poorly Sorted	Very Poorly Sorted	Very Poorly Sorted
Coarse Skewed	Coarse Skewed	Coarse Skewed
Mesokurtic	Platykurtic	Mesokurtic
6.65	6.65	4.7
	107.5	
7.254331413	7.254331413	7.754331413
	3.236965594	
1.875919963	1.910288849	1.752385391
11.43088628	11.71876438	8.986622513
125.1806905	117.0815945	89.72129551
66.73029392	61.28999526	51.19952266
123.3047705	115.1713056	87.96891012
10.32960141	10.97299608	8.050364674
37.21759806	40.52582478	24.97352189
2.997916056	3.094413797	3.478405738
6.450918924	6.415035728	6.798005282
9.058186009	9.031993485	9.156464192
3.021494211	2.918805977	2.632373818
6.060269953	5.937579688	5.678058455
1.732173813	1.770172814	1.586320173
3.368712681	3.455885589	3.009054137
0.189242149	0.197134433	0.138247418
0.810757851	0.802865567	0.861752582
0.017167239	0.011932538	0.02160144
0.007466916	0.006232918	0.011167411
0.017367246	0.009466036	0.00810054
0.058135271	0.062229185	0.030068671
0.089105478	0.107273757	0.067309355
0.105987568	0.111256474	0.095694324
0.136054252	0.130131334	0.132520191
0.158156674	0.155362112	0.169924379
0.165569391	0.16551702	0.18815856
0.13927073	0.137494657	0.158394728
0.105719236	0.10310397	0.117060399

302-2-A-17-X-1	302-2-A-17-X-2	302-2-A-18-X-1
Cristin Ashmankas,	Cristin Ashmankas,	Cristin Ashmankas,
Unimodal, Very Poorly Sorted	Unimodal, Very Poorly Sorted	Bimodal, Very Poorly Sorted
Sandy Mud	Sandy Mud	Sandy Mud
Very Fine Sandy Fine Silt	Very Fine Sandy Fine Silt	Very Fine Sandy Fine Silt
52.96364792	54.74322872	67.54835111
167.3944671	200.7356381	190.7655071
7.155163039	6.4450314	6.050861673
60.85983455	46.77083968	44.88056388
12.69172408	10.72310679	14.80849169
4.735811298	4.672064599	5.267079577
0.458231731	0.707719925	0.417267254
2.909899798	3.596852735	2.642970105
6.28136657	6.504928514	6.048203391
2.254428155	2.250378061	2.410135459
-0.475671395	-0.739962093	-0.433440698
2.939124982	3.633015653	2.662636101
12.48680776	10.34391376	14.84331857
4.736238739	4.488691734	5.370374423
0.130542996	0.15147571	0.154989476
0.904128619	0.964230242	0.881218549
6.323451489	6.595074038	6.074042514
2.243741805	2.166295021	2.425022677
-0.130542996	-0.15147571	-0.154989476
0.904128619	0.964230242	0.881218549
Medium Silt	Medium Silt	Medium Silt
Very Poorly Sorted	Very Poorly Sorted	Very Poorly Sorted
Coarse Skewed	Coarse Skewed	Coarse Skewed
Mesokurtic	Mesokurtic	Platykurtic
6.65	6.65	6.65
		107.5
7.254331413	7.254331413	7.254331413
		3.236965594
1.879592539	1.731987615	1.950196525
10.88653733	9.063401939	12.33785759
106.0603333	83.91540261	151.1668147
56.42730064	48.45034796	77.51363145
104.1807408	82.183415	149.2166182
9.381143967	7.965231586	11.69515694
33.31822303	24.70994842	45.15405849
3.237042908	3.574920549	2.725786632
6.521311039	6.785731619	6.340764291
9.055364338	9.173355671	9.00216477
2.797418693	2.566030642	3.302593337
5.818321431	5.598435122	6.276378138
1.6806771	1.581844269	1.817465652
3.22976386	2.993716308	3.547839316
0.169845202	0.132555143	0.216625671
0.830154798	0.867444857	0.783374329
0.012499167	0.020468031	0.016463923
0.007766149	0.009067271	0.010464923
0.011532564	0.004400293	0.024895851
0.047763482	0.028601907	0.06902183
0.09028384	0.07001764	0.095779145
0.109821626	0.099278507	0.103263368
0.138169165	0.135621828	0.129420265
0.16429547	0.171328976	0.155779994
0.172190384	0.186632888	0.162977029
0.140269763	0.155726712	0.131685558
0.10540839	0.118855945	0.100248114

302-2-A-18-X-1	302-2-A-18-X-2	302-2-A-19-X-1
Cristin Ashmankas,	Cristin Ashmankas,	Cristin Ashmankas,
Unimodal, Very Poorly Sorted	Unimodal, Very Poorly Sorted	Bimodal, Very Poorly Sorted
Sandy Mud	Sandy Mud	Sandy Mud
Very Fine Sandy Fine Silt	Very Fine Sandy Fine Silt	Very Fine Sandy Fine Silt
56.56953502	62.12649857	72.80472332
185.9243925	208.4555134	171.8625894
6.259224589	6.156538851	6.422451328
46.15429164	43.24151537	53.25833948
11.84488948	12.49645515	18.85759613
4.800434961	4.965462819	5.503863436
0.617012429	0.561603441	0.113952252
3.239944083	3.15540559	2.163967211
6.374345641	6.274504708	5.704127322
2.278773906	2.33898744	2.46776269
-0.637000842	-0.593908933	-0.126400388
3.265495603	3.188772083	2.182980257
11.35925185	12.21119935	18.86663071
4.699576214	4.879684933	5.597537141
0.155608395	0.139291368	0.039908977
0.960846395	0.920450133	0.746225158
6.459988371	6.355651285	5.728019387
2.232530667	2.286788	2.484792196
-0.155608395	-0.139291368	-0.039908977
0.960846395	0.920450133	0.746225158
Medium Silt	Medium Silt	Coarse Silt
Very Poorly Sorted	Very Poorly Sorted	Very Poorly Sorted
Coarse Skewed	Coarse Skewed	Symmetrical
Mesokurtic	Mesokurtic	Platykurtic
6.65	6.65	107.5
		4.7
7.254331413	7.254331413	3.236965594
		7.754331413
1.817207228	1.817361933	2.0618497
9.917163253	10.69229194	17.53535492
98.66183278	105.89025	176.3827889
54.29311047	58.26591175	85.54590029
96.84462555	104.072888	174.3209392
8.61982785	9.688142395	17.28824328
28.66148771	33.49145524	77.49089647
3.341364102	3.239358338	2.503218303
6.65585678	6.547285055	5.833589559
9.104061336	9.10393852	8.921845114
2.724654081	2.810414153	3.56414984
5.762697234	5.864580182	6.418626811
1.628210691	1.690764389	2.140918072
3.107659057	3.27622007	4.111719374
0.149752344	0.168015656	0.298270132
0.850247656	0.831984344	0.701729868
0.015966134	0.0224985	0.013100437
0.012699577	0.0089994	0.005866862
0.01019966	0.009532698	0.029934331
0.0389987	0.039964002	0.114370479
0.071888272	0.087021055	0.134998023
0.106370922	0.112363052	0.10605573
0.136896633	0.135399917	0.115516024
0.167786546	0.160162102	0.130532667
0.179954768	0.170948749	0.139329283
0.148543279	0.142662351	0.118452033
0.110695507	0.110448173	0.091844131

302-2-A-20-X-1	302-2-A-20-X-1	302-2-A-20-X-2
Cristin Ashmankas,	Cristin Ashmankas,	Cristin Ashmankas,
Bimodal, Very Poorly Sorted	Unimodal, Very Poorly Sorted	Unimodal, Very Poorly Sorted
Sandy Mud	Sandy Mud	Sandy Mud
Very Fine Sandy Fine Silt	Very Fine Sandy Fine Silt	Very Fine Sandy Fine Silt
67.07341044	63.54088555	62.16406714
201.3275307	186.3375019	201.5771528
5.867110845	6.294032808	6.203482204
41.27318498	47.97815925	44.6384912
13.39678481	14.03571269	12.52668381
5.298889284	5.166516926	5.089718947
0.527795931	0.427241813	0.540618697
2.804794309	2.695949274	2.9988628
6.186094958	6.124196204	6.279651591
2.423831617	2.384062847	2.369464651
-0.545783468	-0.446125212	-0.5650869
2.823950769	2.721631471	3.027457302
13.27095233	13.8983475	12.29059197
5.349414796	5.228632943	5.078719905
0.190146186	0.146254066	0.157826651
0.890592853	0.873111377	0.912079517
6.235584287	6.168942832	6.346301786
2.419381075	2.386433795	2.34446491
-0.190146186	-0.146254066	-0.157826651
0.890592853	0.873111377	0.912079517
Medium Silt	Medium Silt	Medium Silt
Very Poorly Sorted	Very Poorly Sorted	Very Poorly Sorted
Coarse Skewed	Coarse Skewed	Coarse Skewed
Platykurtic	Platykurtic	Mesokurtic
4.7	6.65	4.7
107.5		
7.754331413	7.254331413	7.754331413
3.236965594		
1.832074201	1.884140275	1.762693186
10.67506113	11.78255051	10.43217561
135.3230728	131.3932168	114.1605929
73.86331446	69.7364302	64.76486878
133.4909986	129.5090765	112.3978997
11.43668366	11.56360202	10.29671927
39.98150117	42.61256346	34.8595653
2.885520253	2.928037297	3.130863362
6.549611858	6.407204323	6.582816129
9.09230635	9.051877906	9.148002903
3.151011101	3.091448977	2.921878678
6.206786097	6.12384061	6.017139541
1.779076506	1.798608867	1.71654462
3.515596863	3.531518958	3.364112836
0.201702451	0.205258016	0.177935818
0.798297549	0.794741984	0.822064182
0.018932071	0.015931209	0.020167339
0.012932471	0.010565258	0.009333644
0.018365442	0.019397414	0.01290043
0.057429505	0.059025463	0.046534884
0.094042961	0.100338672	0.08899952
0.097051944	0.108968588	0.105760488
0.120586361	0.126940946	0.128338522
0.154575158	0.152117145	0.157167616
0.171436606	0.164334818	0.171160106
0.145260741	0.137350019	0.144340016
0.109386741	0.105030468	0.115297434

302-2-A-20-X-2	302-2-A-20-X-3	302-2-A-20-X-3
Cristin Ashmankas,	Cristin Ashmankas,	Cristin Ashmankas,
Unimodal, Very Poorly Sorted	Bimodal, Very Poorly Sorted	Unimodal, Very Poorly Sorted
Sandy Mud	Sandy Mud	Sandy Mud
Very Fine Sandy Fine Silt	Very Fine Sandy Fine Silt	Very Fine Sandy Fine Silt
60.99604697	64.52266208	61.22298117
194.8396619	205.1146174	201.0864438
6.257187324	6.131271798	6.223769732
45.79977057	43.35051216	44.8931854
12.74376588	13.08906223	12.12599159
5.012057139	5.216407771	5.039186628
0.534879432	0.486117929	0.603924914
2.979743207	2.835747764	3.070840739
6.263835984	6.213971734	6.326222519
2.342190076	2.404769984	2.356172458
-0.555287486	-0.509905625	-0.628462945
3.005422146	2.864867307	3.098636637
12.52456777	13.01098948	11.92312091
4.990075531	5.196915972	5.014420451
0.157562052	0.154804643	0.188701526
0.904655177	0.848528208	0.920699223
6.319095374	6.264125507	6.390094276
2.319061653	2.377655733	2.326082969
-0.157562052	-0.154804643	-0.188701526
0.904655177	0.848528208	0.920699223
Medium Silt	Medium Silt	Medium Silt
Very Poorly Sorted	Very Poorly Sorted	Very Poorly Sorted
Coarse Skewed	Coarse Skewed	Coarse Skewed
Mesokurtic	Platykurtic	Mesokurtic
4.7	4.7	4.7
	76.5	
7.754331413	7.754331413	7.754331413
	3.731217775	
1.829288518	1.774858844	1.795038624
10.60210716	10.79720807	9.794700881
114.2357923	120.7807701	113.3683999
62.44820932	68.05091597	63.15652401
112.4065038	119.0059112	111.5733613
10.11106777	11.91160109	9.91674709
34.87210485	41.01712138	32.70411856
3.129913349	3.049537318	3.140909532
6.559505162	6.53319788	6.67378285
9.094501647	9.138079994	9.121769398
2.905672021	2.996546374	2.904180876
5.964588298	6.088542676	5.980859866
1.711464436	1.797633433	1.692290975
3.337863455	3.574295441	3.309866963
0.179339483	0.200574293	0.173291444
0.820660517	0.799425707	0.826708556
0.018099397	0.021332622	0.020133333
0.010266324	0.009233026	0.009166667
0.011532949	0.007899737	0.0128
0.048698377	0.056298123	0.046433333
0.090742436	0.105810785	0.08475811
0.104319868	0.102985771	0.099533938
0.130240803	0.119830973	0.124003475
0.159993172	0.151087879	0.15811538
0.171252108	0.166475198	0.179237321
0.14526389	0.144787519	0.152976322
0.109590676	0.114258367	0.11284212

302-2-A-20-X-4	302-2-A-21-X-1	302-2-A-21-X-1
Cristin Ashmankas,	Cristin Ashmankas,	Cristin Ashmankas,
Unimodal, Very Poorly Sorted	Unimodal, Very Poorly Sorted	Unimodal, Very Poorly Sorted
Sandy Mud	Sandy Mud	Sandy Mud
Very Fine Sandy Fine Silt	Very Fine Sandy Fine Silt	Very Fine Sandy Fine Silt
62.2010513	52.29759393	56.24744641
218.8475072	199.3599309	160.6879333
5.912135058	6.368225338	6.890927831
39.51612819	45.8357815	58.76484579
11.07989683	9.627738205	14.04567833
4.967737525	4.543475769	4.881481685
0.742342233	0.870173767	0.369621615
3.475220623	4.026699537	2.650635868
6.446084481	6.664700316	6.139777326
2.344432583	2.209999555	2.294407647
-0.771298509	-0.899258075	-0.381395208
3.492638475	4.053291269	2.670309466
10.76804341	9.090662388	13.91405941
4.829599444	4.266930963	4.947700166
0.198053797	0.177552048	0.117400678
0.972098145	1.022008853	0.864953159
6.537100059	6.781398865	6.167312804
2.27190354	2.093198768	2.306758075
-0.198053797	-0.177552048	-0.117400678
0.972098145	1.022008853	0.864953159
Medium Silt	Medium Silt	Medium Silt
Very Poorly Sorted	Very Poorly Sorted	Very Poorly Sorted
Coarse Skewed	Coarse Skewed	Coarse Skewed
Mesokurtic	Mesokurtic	Platykurtic
4.7	4.7	6.65
7.754331413	7.754331413	7.254331413
1.734605842	1.686601332	1.95751807
8.931343449	7.933002039	12.21609149
99.60287995	71.14082808	120.0852498
57.4210449	42.17999045	61.34566607
97.86827411	69.45422675	118.1277318
8.675837178	6.910728001	10.76261242
26.8768197	19.66618443	40.47685002
3.327668732	3.813178422	3.05786914
6.806907083	6.977917365	6.355073418
9.171176411	9.211665286	8.996758659
2.756036477	2.415744627	2.942166014
5.843507679	5.398486863	5.938889519
1.618352994	1.51240558	1.764133503
3.117002978	2.788837697	3.427956402
0.151276852	0.111596894	0.196277057
0.848723148	0.888403106	0.803722943
0.024965834	0.019535287	0.010767026
0.009399687	0.011234457	0.009033634
0.007633079	0.00430043	0.015433848
0.035532149	0.021468814	0.059001967
0.073746103	0.055057907	0.102040582
0.094186984	0.086377949	0.11488362
0.124348036	0.129530452	0.135461485
0.164097955	0.176674561	0.155659075
0.187428745	0.200989356	0.161604455
0.15977607	0.170142119	0.13650162
0.118885359	0.124688669	0.099612688

302-2-A-21-X-2	302-2-A-21-X-2	302-2-A-21-X-3
Cristin Ashmankas,	Cristin Ashmankas,	Cristin Ashmankas,
Unimodal, Very Poorly Sorted	Unimodal, Very Poorly Sorted	Unimodal, Very Poorly Sorted
Sandy Mud	Sandy Mud	Sandy Mud
Very Fine Sandy Fine Silt	Very Fine Sandy Fine Silt	Very Fine Sandy Fine Silt
63.10853626	60.25789067	64.82924509
194.9494712	207.3951107	205.6997321
6.238265965	6.254305451	5.975410906
45.83404103	44.31651288	41.72529036
13.68834727	12.03505196	12.83518264
5.052068181	4.886268735	5.148795495
0.463699037	0.606787958	0.562825042
2.859855784	3.242269453	2.976266813
6.157026516	6.331435597	6.244217467
2.354079694	2.315640381	2.385561303
-0.486280417	-0.638885409	-0.585232312
2.888065032	3.276542825	2.999277547
13.50294735	11.74601975	12.62276928
5.04389794	4.763322109	5.132766738
0.13477644	0.151636802	0.175706925
0.885217654	0.91427372	0.909093161
6.210581844	6.411684221	6.307827735
2.334539084	2.251968111	2.359736698
-0.13477644	-0.151636802	-0.175706925
0.885217654	0.91427372	0.909093161
Medium Silt	Medium Silt	Medium Silt
Very Poorly Sorted	Very Poorly Sorted	Very Poorly Sorted
Coarse Skewed	Coarse Skewed	Coarse Skewed
Platykurtic	Mesokurtic	Mesokurtic
6.65	4.7	4.7
7.254331413	7.754331413	7.754331413
1.90075089	1.816366391	1.821242675
11.69731708	10.13276595	10.47566899
119.424793	100.5335632	120.5830269
62.8303233	55.3487246	66.20920351
117.5240421	98.71719677	118.7617843
10.74021051	9.409077032	10.47878877
39.41681936	31.57100083	35.90817032
3.065825719	3.314250869	3.051901245
6.417678522	6.624828148	6.57681381
9.039214818	9.104729037	9.100861115
2.948378559	2.747145403	2.982030015
5.973389099	5.790478168	6.04895987
1.757054481	1.670527127	1.728144293
3.424950366	3.234053211	3.389400062
0.192936193	0.161295778	0.184443186
0.807063807	0.838704222	0.815556814
0.018198787	0.022333333	0.020735407
0.010432638	0.007833333	0.011067773
0.013599093	0.008666667	0.013468013
0.051496567	0.036566667	0.050238357
0.099209108	0.085895778	0.088933635
0.112200956	0.108819511	0.102769632
0.132247022	0.131929976	0.126653388
0.15646592	0.16202687	0.155909904
0.164520192	0.176253003	0.172829655
0.137824467	0.148840412	0.147052293
0.103805251	0.110834449	0.110341942

302-2-A-22-X-1	302-2-A-23-X-2	302-2-A-24-X-1
Cristin Ashmankas,	Cristin Ashmankas,	Cristin Ashmankas,
Unimodal, Very Poorly Sorted	Unimodal, Very Poorly Sorted	Unimodal, Very Poorly Sorted
Sandy Mud	Sandy Mud	Sandy Mud
Very Fine Sandy Fine Silt	Very Fine Sandy Fine Silt	Very Fine Sandy Fine Silt
65.6079979	59.24503917	61.20845978
212.1236634	197.9159262	212.7182871
5.683788714	6.158725314	5.945212943
38.00489168	44.19684754	40.47713625
11.73376035	11.68274537	10.95159408
5.176733097	4.899718082	4.957904264
0.716130394	0.661938879	0.763879604
3.224008711	3.275584409	3.472870263
6.375654222	6.386917615	6.469528805
2.394274603	2.312780928	2.337760668
-0.734017327	-0.684251603	-0.788965569
3.23403917	3.29942746	3.489331399
11.40654668	11.32316341	10.5679005
5.15403921	4.820857592	4.839168636
0.227562462	0.181995783	0.213958003
0.994286037	0.97009829	0.988264902
6.453994107	6.464579123	6.564167402
2.365703513	2.269289813	2.274759215
-0.227562462	-0.181995783	-0.213958003
0.994286037	0.97009829	0.988264902
Medium Silt	Medium Silt	Medium Silt
Very Poorly Sorted	Very Poorly Sorted	Very Poorly Sorted
Coarse Skewed	Coarse Skewed	Coarse Skewed
Mesokurtic	Mesokurtic	Mesokurtic
4.7	6.65	4.7
7.754331413	7.254331413	7.754331413
1.764351681	1.796806586	1.738657198
9.124883967	9.550729294	8.677250887
119.2146561	103.3783214	99.09162948
67.56853376	57.53447378	56.99319542
117.4503044	101.5815148	97.35297228
9.112118223	8.688849445	8.533738405
28.858432	28.28865357	26.07983625
3.068366485	3.273994413	3.335092995
6.775978071	6.710173383	6.848546242
9.146646129	9.120349164	9.167810772
2.980949692	2.785694786	2.748892095
6.078279644	5.846354751	5.832717777
1.644367551	1.627947941	1.608760336
3.187786465	3.119165152	3.093177886
0.167064556	0.156328637	0.148562428
0.832935444	0.843671363	0.851437572
0.021399287	0.018669156	0.022667422
0.013666211	0.011734898	0.011000367
0.016332789	0.011368182	0.01050035
0.043831872	0.038838512	0.034101137
0.071834397	0.075717889	0.070293152
0.087931377	0.097069981	0.092368538
0.121620524	0.130228648	0.12257683
0.162363592	0.16790226	0.163071024
0.18665993	0.18344475	0.190930643
0.158444769	0.152404134	0.16372336
0.11591525	0.11262159	0.118767176

302-2-A-24-X-1	302-2-A-24-X-2	302-2-A-24-X-2
Cristin Ashmankas,	Cristin Ashmankas,	Cristin Ashmankas,
Unimodal, Very Poorly Sorted	Unimodal, Very Poorly Sorted	Unimodal, Very Poorly Sorted
Sandy Mud	Sandy Mud	Sandy Mud
Very Fine Sandy Fine Silt	Very Fine Sandy Fine Silt	Very Fine Sandy Fine Silt
59.37352631	58.2890047	63.26354326
196.9078825	183.5737903	203.4042368
6.296700201	6.363264117	6.154509921
45.94424609	48.24093322	43.85322127
12.14597875	12.58135038	12.77109491
4.928791977	4.911458456	5.114288382
0.580410873	0.55146462	0.540249827
3.133451313	2.993050355	2.947101117
6.329497161	6.288984508	6.251436439
2.321222292	2.309648472	2.376068498
-0.604502958	-0.568900145	-0.564078972
3.162623192	3.017080776	2.974752944
11.81283513	12.3061309	12.60848593
4.856413401	4.890463349	5.091232547
0.15527327	0.167802935	0.169575012
0.925411551	0.916138539	0.88730168
6.40350093	6.344478947	6.309461147
2.279891236	2.28997116	2.348014964
-0.15527327	-0.167802935	-0.169575012
0.925411551	0.916138539	0.88730168
Medium Silt	Medium Silt	Medium Silt
Very Poorly Sorted	Very Poorly Sorted	Very Poorly Sorted
Coarse Skewed	Coarse Skewed	Coarse Skewed
Mesokurtic	Mesokurtic	Platykurtic
4.7	6.65	4.7
7.754331413	7.254331413	7.754331413
1.795488146	1.862447707	1.812297435
10.15898886	10.34862453	10.45977559
104.7441216	110.8639264	117.8591595
58.33740635	59.5259271	65.03301127
102.9486334	109.0014787	116.0468621
9.485402229	9.650103299	10.75689557
31.75200523	33.30101837	36.7409341
3.255058816	3.173138086	3.084864212
6.621099374	6.594417162	6.579004291
9.121408157	9.068584366	9.107964534
2.802225297	2.857923015	2.952468539
5.866349341	5.89544628	6.023100322
1.673903347	1.688468572	1.740901858
3.245708953	3.270544386	3.427189873
0.164074966	0.173332283	0.186252789
0.835925034	0.826667717	0.813747211
0.01883145	0.015132829	0.020670112
0.01016565	0.011899603	0.009234872
0.01076559	0.012399587	0.011268545
0.04036263	0.046065131	0.05104184
0.083949645	0.087835133	0.09403742
0.106625486	0.103798539	0.104080461
0.132503252	0.130003046	0.12466617
0.16101496	0.162483928	0.15348625
0.175367868	0.176848816	0.17263509
0.147858859	0.146608847	0.147761818
0.112554609	0.106924541	0.111117422

302-2-A-24-X-3	302-2-A-24-X-3	302-2-A-25-X-1
Cristin Ashmankas,	Cristin Ashmankas,	Cristin Ashmankas,
Unimodal, Very Poorly Sorted	Unimodal, Very Poorly Sorted	Unimodal, Very Poorly Sorted
Sandy Mud	Sandy Mud	Sandy Mud
Very Fine Sandy Fine Silt	Very Fine Sandy Fine Silt	Very Fine Sandy Fine Silt
64.19759488	57.62330917	55.16658475
198.141659	185.0424116	194.9388519
5.908332459	6.605324497	6.603848057
41.96914928	51.52625484	49.34496093
12.29661888	11.98437198	11.40248152
5.240969627	5.010986821	4.755115677
0.61936506	0.573568598	0.608759015
2.953372444	2.953975652	3.291896458
6.315444995	6.352140142	6.419129823
2.406775015	2.343222735	2.272231909
-0.634537892	-0.594172259	-0.638410669
2.969057462	2.983656302	3.331698374
12.0861704	11.83118468	11.14021787
5.289775143	5.052367176	4.634702688
0.219541464	0.194103566	0.148675114
0.93803462	0.92011479	0.916487608
6.370499002	6.401261649	6.488078742
2.403206398	2.336959489	2.212476794
-0.219541464	-0.194103566	-0.148675114
0.93803462	0.92011479	0.916487608
Medium Silt	Medium Silt	Medium Silt
Very Poorly Sorted	Very Poorly Sorted	Very Poorly Sorted
Coarse Skewed	Coarse Skewed	Coarse Skewed
Mesokurtic	Mesokurtic	Mesokurtic
4.7	4.7	4.7
7.754331413	7.754331413	7.754331413
1.764913765	1.766305711	1.763356265
9.534484926	9.607349369	9.602538359
127.9303071	115.7309014	93.0936881
72.48530188	65.52144436	52.79346547
126.1653933	113.9645957	91.33033184
10.28351115	9.940208319	8.915873819
33.41027578	32.29478633	28.79383296
2.966570011	3.111153964	3.425172836
6.712629282	6.701645833	6.702368463
9.14618659	9.145049219	9.147460301
3.083084692	2.939439618	2.67065656
6.179616579	6.033895255	5.722287465
1.706955327	1.690325208	1.638106972
3.36226103	3.313276087	3.156376199
0.18235997	0.174378159	0.150545461
0.81764003	0.825621841	0.849454539
0.017776778	0.0163	0.0192
0.013026303	0.008133333	0.0083
0.019851985	0.0158	0.0043
0.051280128	0.050666667	0.0355
0.080424776	0.083478159	0.083245461
0.091055559	0.095852115	0.105414401
0.118404851	0.122368044	0.131917806
0.156421667	0.157612896	0.163672212
0.180932693	0.180034837	0.180681368
0.155100106	0.154208583	0.152111146
0.115725154	0.115545366	0.115657607

302-2-A-25-X-1	302-2-A-25-X-2	302-2-A-25-X-2
Cristin Ashmankas,	Cristin Ashmankas,	Cristin Ashmankas,
Unimodal, Very Poorly Sorted	Unimodal, Very Poorly Sorted	Unimodal, Very Poorly Sorted
Sandy Mud	Sandy Mud	Sandy Mud
Very Fine Sandy Fine Silt	Very Fine Sandy Fine Silt	Very Fine Sandy Fine Silt
60.09948675	58.521988	60.3359379
185.3935034	213.8418623	186.5443825
6.5521595	6.028300497	6.595505798
50.75914085	41.2441135	51.26552364
13.40771791	10.08491416	13.51714478
5.026111673	4.78338094	5.012158488
0.440391961	0.881756547	0.438768058
2.798178004	3.86809282	2.80419472
6.190900118	6.583157236	6.17584425
2.345083669	2.292658076	2.342648314
-0.46160224	-0.911680896	-0.462433778
2.828775351	3.878740884	2.837689834
13.24064423	9.527727498	13.40381316
5.052409763	4.598113766	5.04540956
0.132613605	0.214381901	0.13394442
0.878611069	1.074052907	0.883552535
6.238882871	6.713652133	6.221212708
2.33697165	2.201042162	2.334971384
-0.132613605	-0.214381901	-0.13394442
0.878611069	1.074052907	0.883552535
Medium Silt	Medium Silt	Medium Silt
Very Poorly Sorted	Very Poorly Sorted	Very Poorly Sorted
Coarse Skewed	Coarse Skewed	Coarse Skewed
Platykurtic	Mesokurtic	Platykurtic
4.7	4.7	6.65
7.754331413	7.754331413	7.254331413
1.849705961	1.715222237	1.876469033
11.45714737	8.101143584	11.57734257
118.6337065	86.65420573	120.0356112
64.1365217	50.52068698	63.96887404
116.7840006	84.93898349	118.1591422
10.84249001	7.199918375	10.71769982
38.86825281	20.96312593	38.99498475
3.075414125	3.528586418	3.058465618
6.447608307	6.947658707	6.43255205
9.078488334	9.18738877	9.057763803
2.951956376	2.603702356	2.96153854
6.00307421	5.658802352	5.999298184
1.756462624	1.531312792	1.753850654
3.438624209	2.847980551	3.42192341
0.19087355	0.127193204	0.191976688
0.80912645	0.872806796	0.808023312
0.016330612	0.023466667	0.016867791
0.00869855	0.0098	0.00780052
0.013997667	0.010966667	0.014900993
0.053824363	0.0295	0.05490366
0.098022359	0.053459871	0.097503723
0.111994013	0.081644869	0.11146617
0.131510585	0.126640527	0.132300453
0.153453104	0.174322163	0.155387641
0.164761982	0.20009933	0.165271785
0.13964102	0.168661172	0.137977755
0.107765745	0.121438736	0.105619507

302-2-A-25-X-3	302-2-A-26-X-1	302-2-A-26-X-1
Cristin Ashmankas,	Cristin Ashmankas,	Cristin Ashmankas,
Bimodal, Very Poorly Sorted	Unimodal, Very Poorly Sorted	Bimodal, Very Poorly Sorted
Sandy Mud	Sandy Mud	Sandy Mud
Very Fine Sandy Fine Silt	Very Fine Sandy Fine Silt	Very Fine Sandy Fine Silt
64.79503683	62.15660293	70.97934596
201.447541	184.5785954	186.2809513
6.012099196	6.399835004	5.994418782
42.58328677	49.64800999	45.58560994
12.60262855	13.42836142	15.84001924
5.283727125	5.159942348	5.503658342
0.568710808	0.477226381	0.337090278
2.85502696	2.738509514	2.406562463
6.279903989	6.189667326	5.948721681
2.41801482	2.38221957	2.472950359
-0.584057787	-0.49482774	-0.351734979
2.872766823	2.762818904	2.426053539
12.4689701	13.33295661	15.83108528
5.310386417	5.256624449	5.662604596
0.207541543	0.174110962	0.147642096
0.890781894	0.8977375	0.831349499
6.325513882	6.228859454	5.981096029
2.408816844	2.394136668	2.501465794
-0.207541543	-0.174110962	-0.147642096
0.890781894	0.8977375	0.831349499
Medium Silt	Medium Silt	Coarse Silt
Very Poorly Sorted	Very Poorly Sorted	Very Poorly Sorted
Coarse Skewed	Coarse Skewed	Coarse Skewed
Platykurtic	Platykurtic	Platykurtic
4.7	4.7	4.7
107.5		107.5
7.754331413	7.754331413	7.754331413
3.236965594		3.236965594
1.762134453	1.848272838	1.943594179
9.79265147	10.94824669	13.19440642
132.4864767	134.7687437	170.5054418
75.18522577	72.91604406	87.72687408
130.7243422	132.9204709	168.5618477
11.18822919	10.95922754	14.31183892
36.73628896	38.84494898	55.74699267
2.916082988	2.891442157	2.55211031
6.674084746	6.513156342	6.243929741
9.148460277	9.079606544	9.007057268
3.137242772	3.140165375	3.529258603
6.232377289	6.188164387	6.454946958
1.752208944	1.759456192	1.945492451
3.483909807	3.454074209	3.83913715
0.191727604	0.196936846	0.243655715
0.808272396	0.803063154	0.756344285
0.019365376	0.015635939	0.015267685
0.009532698	0.00870145	0.010567371
0.015732285	0.022503751	0.033668911
0.061095927	0.060410068	0.078271885
0.08600132	0.089685637	0.105879863
0.094901145	0.100984214	0.106416858
0.116227389	0.126340672	0.117510591
0.149668032	0.155655762	0.141078924
0.177276798	0.169714933	0.157223475
0.154260952	0.142428413	0.133404404
0.115938079	0.10793916	0.100710033

302-2-A-26-X-2	302-2-A-27-X-1	302-2-A-27-X-1
Cristin Ashmankas,	Cristin Ashmankas,	Cristin Ashmankas,
Bimodal, Very Poorly Sorted	Unimodal, Very Poorly Sorted	Unimodal, Very Poorly Sorted
Sandy Mud	Sandy Mud	Sandy Mud
Very Fine Sandy Fine Silt	Very Fine Sandy Fine Silt	Very Fine Sandy Fine Silt
62.63947665	65.05542262	58.4795956
202.5596161	207.2456418	182.9461777
6.216768708	6.128858505	6.526079311
45.00440993	43.07700687	50.68106748
12.22671078	14.01734944	12.50258646
5.103454005	5.002091816	5.024687431
0.62198034	0.454280151	0.525053333
3.041328927	2.953493814	2.888380194
6.30963673	6.116119146	6.297043243
2.376682876	2.342571127	2.342994575
-0.646892877	-0.482117786	-0.541981052
3.066969652	2.984136681	2.913045859
12.18683315	13.87054797	12.31026961
5.141624424	4.932486889	5.069051912
0.208687021	0.108166787	0.169756467
0.949907726	0.885248629	0.912564432
6.358532911	6.171831406	6.343993831
2.362224231	2.302315216	2.341715939
-0.208687021	-0.108166787	-0.169756467
0.949907726	0.885248629	0.912564432
Medium Silt	Medium Silt	Medium Silt
Very Poorly Sorted	Very Poorly Sorted	Very Poorly Sorted
Coarse Skewed	Coarse Skewed	Coarse Skewed
Mesokurtic	Platykurtic	Mesokurtic
4.7	9.4	4.7
107.5		
7.754331413	6.754331413	7.754331413
3.236965594		
1.810998176	1.949164185	1.78972212
9.736440077	12.38203757	10.27724637
126.5915043	116.5266914	118.9582962
69.90150844	59.78290196	66.46746715
124.7805061	114.5775272	117.1685741
9.586339947	10.41347816	10.13812316
31.87880305	39.73162296	33.97312056
2.981747508	3.101267641	3.071472206
6.682389907	6.335607448	6.604402421
9.108999191	9.002928665	9.126048679
3.054919696	2.902983459	2.971229452
6.127251684	5.901661024	6.054576474
1.67763133	1.749876426	1.706547967
3.260980101	3.380380113	3.34171869
0.178364936	0.192156443	0.178512316
0.821635064	0.807843557	0.821487684
0.020800693	0.02189781	0.015435906
0.007266909	0.00816585	0.008768128
0.0180006	0.00979902	0.0156026
0.055035168	0.050294971	0.054275713
0.077261566	0.101998793	0.084429969
0.089664181	0.118158701	0.100299442
0.123541157	0.138507083	0.128574127
0.163911372	0.15777346	0.158457316
0.181855494	0.161225595	0.172145877
0.151321454	0.131855933	0.148856138
0.111341406	0.100322784	0.113154783

302-2-A-27-X-2	302-2-A-27-X-2	302-2-A-27-X-3
Cristin Ashmankas,	Cristin Ashmankas,	Cristin Ashmankas,
Unimodal, Very Poorly Sorted	Unimodal, Very Poorly Sorted	Unimodal, Very Poorly Sorted
Sandy Mud	Sandy Mud	Sandy Mud
Very Fine Sandy Fine Silt	Very Fine Sandy Fine Silt	Very Fine Sandy Fine Silt
61.93474551	58.60549048	60.48492448
211.5481879	162.6494564	179.6607173
6.058104562	7.21584709	6.79963037
41.88325203	63.12147309	54.65464254
11.63647249	15.83374595	14.92504362
4.984124115	4.893511059	4.910947411
0.677702653	0.203030419	0.325496363
3.300567925	2.511046323	2.694171818
6.378032601	5.963247949	6.036548981
2.346040633	2.298459201	2.309721719
-0.706307557	-0.218378349	-0.349355286
3.324504042	2.53603364	2.728916949
11.3993703	15.74571136	14.88993221
4.905942084	4.940294546	4.935781554
0.190296821	0.038658291	0.084319235
0.963983123	0.817920558	0.851563731
6.454902058	5.988897252	6.069519004
2.294530203	2.304597059	2.303278546
-0.190296821	-0.038658291	-0.084319235
0.963983123	0.817920558	0.851563731
Medium Silt	Coarse Silt	Medium Silt
Very Poorly Sorted	Very Poorly Sorted	Very Poorly Sorted
Coarse Skewed	Symmetrical	Symmetrical
Mesokurtic	Platykurtic	Platykurtic
4.7	9.4	9.4
7.754331413	6.754331413	6.754331413
1.779381575	2.039430602	2.019595885
9.468116775	14.96481696	13.50126819
107.9710889	123.3060677	122.1701597
60.67899679	60.4610265	60.49237903
106.1917073	121.2666371	120.1505639
8.932039281	11.89010673	11.03292721
28.87274454	50.01879004	44.65660164
3.211283037	3.019684301	3.033036147
6.722706785	6.062281557	6.210761263
9.134408366	8.937617869	8.951717642
2.844473147	2.95978552	2.951404865
5.923125328	5.917933568	5.918681495
1.639102844	1.851488487	1.796645732
3.158989596	3.571689761	3.463743707
0.161407627	0.224404262	0.208873974
0.838592373	0.775595738	0.791126026
0.023032566	0.011866271	0.015603641
0.009033032	0.006366454	0.00720168
0.010132996	0.01229959	0.012102824
0.042198593	0.067031099	0.061447671
0.077010441	0.126840847	0.112518157
0.094349749	0.131688913	0.121229349
0.127312491	0.135107508	0.13814204
0.165738531	0.145432629	0.155131335
0.183375721	0.147602067	0.155517394
0.153576831	0.122453357	0.126429175
0.11423905	0.093311265	0.094676734

302-2-A-29-X-1	302-2-A-29-X-1	302-2-A-29-X-2
Cristin Ashmankas,	Cristin Ashmankas,	Cristin Ashmankas,
Bimodal, Very Poorly Sorted	Unimodal, Very Poorly Sorted	Bimodal, Very Poorly Sorted
Sandy Mud	Sandy Mud	Sandy Mud
Very Fine Sandy Fine Silt	Very Fine Sandy Fine Silt	Very Fine Sandy Fine Silt
92.59134058	58.54942354	66.6642035
201.5271105	191.9352858	175.6544938
4.547807929	6.576381019	6.566871692
29.3644321	49.83212922	53.30937769
19.58287	12.8515107	16.65783413
6.248106619	4.862297874	5.299334507
0.238010587	0.502178383	0.198451803
2.11414806	3.012864657	2.354636944
5.646361637	6.245711629	5.881412126
2.650559871	2.301875096	2.415735159
-0.24386284	-0.53059282	-0.214420553
2.120088375	3.051124105	2.379368969
19.46289696	12.70894235	16.59785942
6.565017343	4.807217749	5.369122282
0.141740794	0.13628446	0.051751093
0.79206774	0.892914113	0.791568017
5.683129725	6.298012217	5.912858997
2.714798822	2.265202154	2.424686263
-0.141740794	-0.13628446	-0.051751093
0.79206774	0.892914113	0.791568017
Coarse Silt	Medium Silt	Coarse Silt
Very Poorly Sorted	Very Poorly Sorted	Very Poorly Sorted
Coarse Skewed	Coarse Skewed	Symmetrical
Platykurtic	Platykurtic	Platykurtic
4.7	6.65	4.7
107.5		107.5
7.754331413	7.254331413	7.754331413
3.236965594		3.236965594
1.992002828	1.885037492	1.968320493
16.12648012	10.96871864	15.50101341
252.7589333	108.7172547	149.239236
126.8868346	57.67378907	75.82059759
250.7669305	106.8322172	147.2709155
20.11609878	9.77871501	14.4842558
85.00132113	34.94907929	59.4906423
1.984166012	3.201347163	2.744301215
5.954424609	6.51046119	6.011493652
8.971564589	9.051191066	8.988819137
4.521579613	2.827306944	3.27544917
6.987398577	5.849843903	6.244517922
2.243329521	1.702470285	1.971882415
4.330278638	3.289644898	3.856413655
0.305249565	0.17646548	0.254068859
0.694750435	0.82353452	0.745931141
0.014032398	0.018398773	0.014066667
0.026764882	0.008266116	0.0077
0.060262649	0.00839944	0.020533333
0.092160523	0.046696887	0.0821
0.112029113	0.094704264	0.129668859
0.097053737	0.109822314	0.12328802
0.102582057	0.134389417	0.121194491
0.127558531	0.162723629	0.132695293
0.144965493	0.171256026	0.14431703
0.125741104	0.140334275	0.125679451
0.096849513	0.105008859	0.098756855

302-2-A-29-X-3	302-2-A-30-X-1	302-2-A-30-X-1
Cristin Ashmankas,	Cristin Ashmankas,	Cristin Ashmankas,
Trimodal, Very Poorly Sorted	Unimodal, Very Poorly Sorted	Bimodal, Very Poorly Sorted
Sandy Mud	Sandy Mud	Sandy Mud
y Fine Sandy Very Coarse	Very Fine Sandy Fine Silt	Very Fine Sandy Fine Silt
75.84386802	56.28782141	59.82287853
147.0583369	189.4647099	193.7117444
6.580728236	6.76197007	6.501777718
62.04498185	52.11985541	48.71824174
24.56868513	12.56385152	12.8347724
5.267836498	4.773720663	4.987751915
-0.23868863	0.500056815	0.498396127
2.200608274	3.057073635	2.912088955
5.33208487	6.28003049	6.248583691
2.399433967	2.27516099	2.337800898
0.229416346	-0.529838498	-0.523317195
2.214347542	3.099882409	2.946380429
24.64810541	12.3978911	12.78473462
5.379801566	4.704412087	4.968969146
-0.212952408	0.126817745	0.153044861
0.790083281	0.885271364	0.869046354
5.342379432	6.333761452	6.289433976
2.42755296	2.23401444	2.312946584
0.212952408	-0.126817745	-0.153044861
0.790083281	0.885271364	0.869046354
Coarse Silt	Medium Silt	Medium Silt
Very Poorly Sorted	Very Poorly Sorted	Very Poorly Sorted
Fine Skewed	Coarse Skewed	Coarse Skewed
Platykurtic	Platykurtic	Platykurtic
107.5	6.65	6.65
9.4		76.5
3.236965594	7.254331413	7.254331413
6.754331413		3.731217775
2.28732037	1.867783533	1.833328931
32.15401924	10.81634387	10.67925111
177.1380406	102.203242	114.6197396
77.44347619	54.71899726	62.52000811
174.8507202	100.3354585	112.7864107
14.49247488	9.616448554	10.60044282
86.93733815	33.95719273	37.03254998
2.497054029	3.290487134	3.125072571
4.958857105	6.530643267	6.549045709
8.772125836	9.064457021	9.091318631
3.512990001	2.754746229	2.909154404
6.275071807	5.773969888	5.96624606
2.127604527	1.691590892	1.738501937
3.85723208	3.265504191	3.406052628
0.35634555	0.169713765	0.188000207
0.64365445	0.830286235	0.811999793
0.007967729	0.018166061	0.018767918
0.006634218	0.007233092	0.00810054
0.035171356	0.005899803	0.007233816
0.119549273	0.042631912	0.053370225
0.187022973	0.095782896	0.100527709
0.149246938	0.112725902	0.102897473
0.110845936	0.134685174	0.126052763
0.104346159	0.163061134	0.158401923
0.105182399	0.171994422	0.171667864
0.093128667	0.141437821	0.14374822
0.080904351	0.106381783	0.109231551

302-2-A-30-X-2	302-2-A-30-X-2	302-2-A-30-X-3
Cristin Ashmankas,	Cristin Ashmankas,	Cristin Ashmankas,
Unimodal, Very Poorly Sorted	Unimodal, Very Poorly Sorted	Unimodal, Very Poorly Sorted
Sandy Mud	Sandy Mud	Sandy Mud
Very Fine Sandy Fine Silt	Very Fine Sandy Fine Silt	Very Fine Sandy Fine Silt
59.93946283	65.36486483	59.20304813
193.4385679	196.9077398	174.7295578
6.645995559	6.005642976	6.775586798
50.8041175	43.19713942	55.18670728
12.98177168	13.2821472	14.30866791
5.018312196	5.277446033	4.983445254
0.471810882	0.507858877	0.337499982
2.853857813	2.775093465	2.660060237
6.225180415	6.202476225	6.102054022
2.349993743	2.416203143	2.329278314
-0.501158284	-0.524769557	-0.356852182
2.895021399	2.795565878	2.690340098
12.92435663	13.09603877	14.11835419
5.048542991	5.32196832	5.00203049
0.142368691	0.180564115	0.086828233
0.873878657	0.878598913	0.846750682
6.273763724	6.254725692	6.14628427
2.335867086	2.411959923	2.322513851
-0.142368691	-0.180564115	-0.086828233
0.873878657	0.878598913	0.846750682
Medium Silt	Medium Silt	Medium Silt
Very Poorly Sorted	Very Poorly Sorted	Very Poorly Sorted
Coarse Skewed	Coarse Skewed	Symmetrical
Platykurtic	Platykurtic	Platykurtic
4.7	4.7	4.7
7.754331413	7.754331413	7.754331413
1.820210369	1.801257154	1.906686468
11.0344597	10.65392397	12.84827635
117.6796761	131.0776719	117.8841807
64.65168974	72.77010483	61.82672542
115.8594657	129.2764148	115.9774942
10.8435617	11.65102061	11.49778451
37.79610029	40.14497659	43.50933535
3.087062915	2.93150614	3.084557964
6.5018402	6.5524713	6.28228136
9.101679086	9.116780124	9.034716656
2.948329638	3.109930421	2.929015036
6.014616172	6.185273984	5.950158692
1.749834821	1.785595312	1.802340064
3.4387668	3.542384433	3.523283992
0.188657265	0.200066964	0.201899867
0.811342735	0.799933036	0.798100133
0.0194	0.017933931	0.013899073
0.005533333	0.012033734	0.009132724
0.0118	0.01740058	0.01409906
0.055	0.057201907	0.0539964
0.096923932	0.095496812	0.110772609
0.107581725	0.100710951	0.125037663
0.129646131	0.120209021	0.13318529
0.154408908	0.150662275	0.146917279
0.165687889	0.169812754	0.156347083
0.143591453	0.146436429	0.133281726
0.110426629	0.112101606	0.103331091

302-2-A-31-X-1	302-2-A-32-X-1	302-2-A-32-X-1
Cristin Ashmankas,	Cristin Ashmankas,	Cristin Ashmankas,
Bimodal, Very Poorly Sorted	Unimodal, Very Poorly Sorted	Unimodal, Very Poorly Sorted
Sandy Mud	Sandy Mud	Sandy Mud
Very Fine Sandy Fine Silt	Very Fine Sandy Fine Silt	Very Fine Sandy Fine Silt
61.94937275	46.47953632	58.04291883
173.8990807	156.8213248	184.6014246
6.758060564	8.035233364	6.835492152
55.11618016	74.80099714	53.75406809
15.08641617	11.49743515	13.64749841
5.188121302	4.578685564	4.912190072
0.277501677	0.484061632	0.370861638
2.434448456	2.914385421	2.770642888
6.0276817	6.418957654	6.163329151
2.385384841	2.210437244	2.312921325
-0.292846748	-0.510117524	-0.396947132
2.459904612	2.966537396	2.811246774
14.99636427	11.4877435	13.54850887
5.215243191	4.621400028	4.86580527
0.099581495	0.149909106	0.088702149
0.780934676	0.876272754	0.824082511
6.059243415	6.443760747	6.20572211
2.382734528	2.208329974	2.282678585
-0.099581495	-0.149909106	-0.088702149
0.780934676	0.876272754	0.824082511
Medium Silt	Medium Silt	Medium Silt
Very Poorly Sorted	Very Poorly Sorted	Very Poorly Sorted
Symmetrical	Coarse Skewed	Symmetrical
Platykurtic	Platykurtic	Platykurtic
4.7	4.7	4.7
107.5		
7.754331413	7.754331413	7.754331413
3.236965594		
1.90926453	1.800031229	1.871801689
13.07981575	9.722070839	12.14401406
131.3298477	96.36066705	110.3005358
68.78556931	53.53277514	58.92746888
129.4205831	94.56063582	108.4287341
14.11221605	9.329648041	11.4015191
53.92225362	30.34069698	41.88820024
2.928733256	3.375411809	3.180488296
6.256513971	6.684520638	6.363610824
9.032767282	9.117762348	9.06135669
3.084189133	2.701229617	2.849045759
6.104034025	5.742350539	5.880868394
1.92985786	1.660340162	1.789932186
3.818872648	3.221822657	3.511154152
0.237387262	0.160576747	0.195962975
0.762612738	0.839423253	0.804037025
0.013868516	0.0120004	0.017
0.008234431	0.005233508	0.007566667
0.010934791	0.00480016	0.004433333
0.073443126	0.042768092	0.050866667
0.130906398	0.095774587	0.116096308
0.114344192	0.102176965	0.121853691
0.11498991	0.128374364	0.130406601
0.138186857	0.16302718	0.148817758
0.156860255	0.178153507	0.160021223
0.135076988	0.155039313	0.136925581
0.103154537	0.112651924	0.106012171

302-2-A-32-X-2	302-2-A-32-X-2	302-2-A-32-X-3
Cristin Ashmankas,	Cristin Ashmankas,	Cristin Ashmankas,
Bimodal, Very Poorly Sorted	Unimodal, Very Poorly Sorted	Unimodal, Very Poorly Sorted
Sandy Mud	Sandy Mud	Sandy Mud
Very Fine Sandy Fine Silt	Very Fine Sandy Fine Silt	Very Fine Sandy Fine Silt
70.87122229	58.52600213	59.59303707
207.8108436	179.2684052	202.1701322
5.88326679	6.685598298	6.20545192
40.48439057	53.02117397	44.35031809
15.93887972	13.62499246	11.58633996
5.212220539	4.946603272	4.890889877
0.325389007	0.402899791	0.683702666
2.666930386	2.776459908	3.328826914
5.934101604	6.172022765	6.394885206
2.396998357	2.31972898	2.312808991
-0.347702167	-0.422880833	-0.708291654
2.692313455	2.80689083	3.352997851
15.66865948	13.44680584	11.27202726
5.137667337	4.946645518	4.815531981
0.058855289	0.109441729	0.188851049
0.824457665	0.864709374	0.998426116
5.995974433	6.216592675	6.471109184
2.361113479	2.306450518	2.267695184
-0.058855289	-0.109441729	-0.188851049
0.824457665	0.864709374	0.998426116
Coarse Silt	Medium Silt	Medium Silt
Very Poorly Sorted	Very Poorly Sorted	Very Poorly Sorted
Symmetrical	Coarse Skewed	Coarse Skewed
Platykurtic	Platykurtic	Mesokurtic
4.7	6.65	6.65
53.5		
7.754331413	7.254331413	7.254331413
4.247428514		
1.995385599	1.876304382	1.801758769
14.74152933	11.91400133	9.445789959
129.4151984	114.8865057	108.2972212
64.85723788	61.230207	60.10639329
127.4198128	113.0102013	106.4954624
12.65550695	10.79513619	8.238065387
51.60754138	39.5373893	26.86817037
2.949921039	3.121718743	3.20693187
6.083969988	6.391198165	6.726112829
8.969116717	9.057890398	9.116378418
3.040459931	2.901571584	2.84271035
6.019195679	5.936171655	5.909446548
1.880739657	1.759294232	1.604681052
3.661693395	3.432309539	3.042305577
0.229458181	0.190798933	0.155535296
0.770541819	0.809201067	0.844464704
0.021265958	0.014866171	0.020302707
0.011032966	0.009499683	0.008967862
0.010599647	0.011066298	0.01140152
0.060931302	0.052531582	0.045339379
0.125628308	0.102835198	0.069523828
0.129636729	0.117547669	0.090943133
0.129587119	0.134318484	0.130910013
0.139928465	0.152813906	0.172927258
0.148253651	0.162187917	0.186987872
0.126581333	0.136692288	0.150646302
0.096554522	0.105640803	0.112050126

302-2-A-32-X-3	302-2-A-32-X-4	302-2-A-33-X-1
Cristin Ashmankas,	Cristin Ashmankas,	Cristin Ashmankas,
Unimodal, Very Poorly Sorted	Unimodal, Very Poorly Sorted	Unimodal, Very Poorly Sorted
Sandy Mud	Sandy Mud	Sandy Mud
Very Fine Sandy Fine Silt	Very Fine Sandy Fine Silt	Very Fine Sandy Fine Silt
45.6676364	51.041571	47.95948553
168.3511058	172.880931	165.6591899
7.320901299	6.943160294	7.523227694
61.96927159	56.38383525	65.76541214
10.10872076	11.36267027	11.25048526
4.380526553	4.638780886	4.565401288
0.709035643	0.604389675	0.541534439
3.627843211	3.225271864	3.133892443
6.605668899	6.443276829	6.44862399
2.148353446	2.224517399	2.207711736
-0.735611456	-0.620087892	-0.568734364
3.673287902	3.250831516	3.183292821
9.626546212	11.07089887	10.79808455
4.225379971	4.575663576	4.494903828
0.150744718	0.159111738	0.129928836
0.97623731	0.949313788	0.905410862
6.698766	6.497083828	6.533080772
2.079081083	2.193980982	2.168290248
-0.150744718	-0.159111738	-0.129928836
0.97623731	0.949313788	0.905410862
Medium Silt	Medium Silt	Medium Silt
Very Poorly Sorted	Very Poorly Sorted	Very Poorly Sorted
Coarse Skewed	Coarse Skewed	Coarse Skewed
Mesokurtic	Mesokurtic	Mesokurtic
4.7	6.65	4.7
7.754331413	7.254331413	7.754331413
1.749519166	1.804234059	1.774162194
8.571624826	9.49309425	9.684016927
70.34297971	93.68156855	86.52494523
40.20703578	51.9231793	48.76946737
68.59346054	91.87733449	84.75078304
7.299660862	8.233719619	8.935629362
21.945782	26.6726236	28.5327972
3.829449741	3.416090958	3.530740067
6.866215579	6.718905878	6.690178684
9.158825815	9.114397776	9.138646378
2.391681947	2.668078189	2.588309025
5.329376074	5.698306818	5.607906311
1.54136984	1.603278749	1.637008626
2.867829439	3.041544322	3.159569346
0.111244061	0.147849266	0.134609708
0.888755939	0.852150734	0.865390292
0.01313202	0.0133	0.013065796
0.00883245	0.009433333	0.007032864
0.00826584	0.007833333	0.008599427
0.0246642	0.0385	0.035930938
0.056349551	0.078782599	0.069980683
0.101183625	0.09728529	0.120700946
0.136299582	0.132665577	0.136575929
0.176320989	0.173643745	0.160750728
0.194363484	0.184099689	0.176469448
0.162804814	0.152449122	0.155615439
0.117783445	0.112007312	0.115277801

302-2-A-33-X-1	302-2-A-33-X-2	302-2-A-33-X-2
Cristin Ashmankas,	Cristin Ashmankas,	Cristin Ashmankas,
Unimodal, Very Poorly Sorted	Unimodal, Very Poorly Sorted	Unimodal, Very Poorly Sorted
Sandy Mud	Sandy Mud	Sandy Mud
Very Fine Sandy Fine Silt	Very Fine Sandy Fine Silt	Very Fine Sandy Fine Silt
58.69239349	60.3290708	69.19041747
211.4375571	195.1476061	196.5250024
6.110545296	6.400360829	5.866269632
42.13929318	47.35182467	42.17630969
10.79511861	12.95721298	14.72817623
4.822838307	4.961790706	5.327656912
0.742692242	0.499755873	0.428261311
3.582444478	2.944440521	2.665696026
6.488957323	6.234222734	6.050731646
2.299662512	2.330484022	2.428983323
-0.773421939	-0.525519366	-0.446095605
3.607188989	2.978602461	2.6857615
10.46464596	12.74283447	14.61159981
4.642020348	4.913087534	5.442600451
0.174416176	0.132428066	0.147990733
0.97233935	0.874103384	0.890392579
6.578332686	6.294169968	6.096742044
2.214752847	2.296629943	2.44429613
-0.174416176	-0.132428066	-0.147990733
0.97233935	0.874103384	0.890392579
Medium Silt	Medium Silt	Medium Silt
Very Poorly Sorted	Very Poorly Sorted	Very Poorly Sorted
Coarse Skewed	Coarse Skewed	Coarse Skewed
Mesokurtic	Platykurtic	Platykurtic
6.65	4.7	4.7
7.254331413	7.754331413	7.754331413
1.717735483	1.85033351	1.912293243
8.912238887	11.09377719	12.45516616
90.0753573	111.5205014	148.6841802
52.43843316	60.27048682	77.75176782
88.35762182	109.6701679	146.771887
8.174390523	10.49165141	11.90255095
25.17704605	36.50879832	44.94676919
3.47272372	3.164619142	2.74967694
6.809996381	6.494105534	6.327111922
9.185276394	9.077998955	9.030480513
2.644977584	2.868591305	3.284196911
5.712552674	5.913379813	6.280803573
1.591610372	1.73225993	1.821607545
3.031111168	3.391169875	3.5731989
0.141203681	0.180712866	0.2138756
0.858796319	0.819287134	0.7861244
0.022936392	0.01890063	0.017465502
0.00990132	0.009166972	0.013132458
0.005567409	0.008500283	0.024698353
0.030270703	0.048368279	0.062229185
0.072527858	0.095776702	0.096350102
0.09449594	0.11263529	0.108551528
0.127761549	0.133378466	0.130329206
0.171188879	0.154189254	0.150441683
0.187813242	0.165422544	0.159183332
0.157102422	0.145660847	0.134685467
0.120434287	0.108000732	0.102933183

302-2-A-33-X-3	302-2-A-34-X-1	302-2-A-34-X-1
Cristin Ashmankas,	Cristin Ashmankas,	Cristin Ashmankas,
Bimodal, Very Poorly Sorted	Bimodal, Very Poorly Sorted	Unimodal, Very Poorly Sorted
Sandy Mud	Sandy Mud	Sandy Mud
Very Fine Sandy Fine Silt	Very Fine Sandy Fine Silt	Very Fine Sandy Fine Silt
60.76338829	58.63290924	48.95108341
178.3473134	169.2466436	165.8244934
6.787555051	7.231530531	7.153907099
55.03242034	61.61459059	60.18678636
14.45419227	15.65946247	11.20850491
5.039326881	4.887654176	4.591831676
0.360004296	0.204273882	0.582617617
2.629581806	2.521846005	3.196944813
6.083795808	5.971907868	6.465641525
2.346847752	2.300015804	2.208276666
-0.380593102	-0.226048631	-0.596758252
2.660746098	2.557356352	3.221810288
14.50775193	15.6210805	10.87342203
5.118442558	4.883033994	4.529764794
0.122706564	0.028935126	0.149481545
0.85059282	0.790984016	0.940353105
6.107032208	6.000361943	6.52305014
2.355704893	2.287777821	2.179436141
-0.122706564	-0.028935126	-0.149481545
0.85059282	0.790984016	0.940353105
Medium Silt	Medium Silt	Medium Silt
Very Poorly Sorted	Very Poorly Sorted	Very Poorly Sorted
Coarse Skewed	Symmetrical	Coarse Skewed
Platykurtic	Platykurtic	Mesokurtic
6.65	6.65	6.65
107.5	76.5	
7.254331413	7.254331413	7.254331413
3.236965594	3.731217775	
1.94687576	2.02043294	1.77677697
12.49565161	14.89271376	9.430222013
130.6909643	119.2469059	89.82787982
67.12855899	59.02047208	50.55664347
128.7440886	117.226473	88.05110285
11.60692014	12.35463792	8.275092259
44.63660451	51.24568505	26.52276449
2.935768695	3.067976262	3.476692907
6.322430055	6.069249523	6.728492548
9.004623463	8.951119817	9.136521686
3.067211486	2.917597482	2.627934629
6.068854768	5.883143555	5.659828779
1.812028906	1.870895944	1.603620463
3.536913303	3.626980825	3.048775397
0.211763971	0.227870778	0.143082483
0.788236029	0.772129222	0.856917517
0.015202027	0.01379954	0.011834122
0.006434191	0.006566448	0.00960064
0.015635418	0.005599813	0.007267151
0.067775703	0.064864505	0.036469098
0.106716632	0.137040472	0.077911472
0.110333714	0.131852857	0.100712515
0.130179985	0.130753831	0.134996588
0.154364997	0.14232823	0.16989741
0.160458609	0.147960493	0.184002485
0.1324177	0.124584095	0.152792392
0.100481023	0.094649717	0.114516126

302-2-A-34-X-2	302-2-A-34-X-2	302-2-A-35-X-1
Cristin Ashmankas,	Cristin Ashmankas,	Cristin Ashmankas,
Unimodal, Very Poorly Sorted	Unimodal, Very Poorly Sorted	Unimodal, Very Poorly Sorted
Sandy Mud	Sandy Mud	Sandy Mud
Very Fine Sandy Fine Silt	Very Fine Sandy Fine Silt	Very Fine Sandy Fine Silt
70.42026867	56.20254517	55.1643579
197.4399097	173.3861209	187.8228547
5.800795394	7.050020413	6.76840194
41.93115755	58.48548989	52.49870066
14.27570815	13.74856745	11.8350637
5.429402966	4.846618272	4.797093027
0.503503963	0.362358358	0.565809986
2.659969555	2.737707651	3.127977475
6.091759511	6.15932655	6.367572759
2.458539631	2.290125411	2.282643214
-0.520280364	-0.384377852	-0.593242862
2.676469803	2.773621455	3.167647155
14.23803765	13.59880328	11.7104682
5.611996606	4.830135187	4.748413883
0.209238326	0.088437669	0.158089494
0.909319504	0.84366466	0.914494365
6.134105869	6.200376493	6.416057432
2.488514136	2.272063568	2.247445689
-0.209238326	-0.088437669	-0.158089494
0.909319504	0.84366466	0.914494365
Medium Silt	Medium Silt	Medium Silt
Very Poorly Sorted	Very Poorly Sorted	Very Poorly Sorted
Coarse Skewed	Symmetrical	Coarse Skewed
Mesokurtic	Platykurtic	Mesokurtic
6.65	4.7	6.65
7.254331413	7.754331413	7.254331413
1.911278312	1.912500278	1.797862192
11.22594551	12.30965916	9.877527197
168.5478014	110.8734454	102.1950473
88.18590171	57.9730349	56.84253652
166.636523	108.9609451	100.3971851
11.88760874	10.87905462	9.144797419
43.52063502	40.35718959	30.54721914
2.568770287	3.173014219	3.290602815
6.477019228	6.344065374	6.661634371
9.031246412	9.030324327	9.119501844
3.515785922	2.845976634	2.77137727
6.462476125	5.857310108	5.828899029
1.812530983	1.766594155	1.656210445
3.571386633	3.443481288	3.192951211
0.213656665	0.190340111	0.163951335
0.786343335	0.809659889	0.836048665
0.017666667	0.014234282	0.01759824
0.011666667	0.0075005	0.00763257
0.036266667	0.009533969	0.00709929
0.061833333	0.051036736	0.04269573
0.086223332	0.108034624	0.088925504
0.094908013	0.124532562	0.100077919
0.120467594	0.135738141	0.129110653
0.157416933	0.149370365	0.166596236
0.169160767	0.160430521	0.180375752
0.141305142	0.136637556	0.147602055
0.103084887	0.102950745	0.112286051

302-2-A-35-X-2	302-2-A-35-X-3	302-2-A-35-X-3
Cristin Ashmankas,	Cristin Ashmankas,	Cristin Ashmankas,
Unimodal, Very Poorly Sorted	Unimodal, Very Poorly Sorted	Unimodal, Very Poorly Sorted
Sandy Mud	Sandy Mud	Sandy Mud
Very Fine Sandy Fine Silt	Very Fine Sandy Fine Silt	Very Fine Sandy Fine Silt
54.24977568	61.71371159	54.6010179
204.6814506	184.1784852	180.0494425
6.36129339	6.480415342	6.99901428
45.28811691	50.07268717	56.37917594
10.52078376	14.10783607	12.70424452
4.540108591	5.056467672	4.747408107
0.758707441	0.4034318	0.461186085
3.871683026	2.71616826	2.979657111
6.528760502	6.119789307	6.269975118
2.212565939	2.351659084	2.263625403
-0.796831336	-0.422595402	-0.487267573
3.907920564	2.743505923	3.020345472
10.04230753	14.05148449	12.59337922
4.270676996	5.092454777	4.723757535
0.128147029	0.13007616	0.121193774
0.978882396	0.861106564	0.89145495
6.637765379	6.153133636	6.311190732
2.094464787	2.348361263	2.239934915
-0.128147029	-0.13007616	-0.121193774
0.978882396	0.861106564	0.89145495
Medium Silt	Medium Silt	Medium Silt
Very Poorly Sorted	Very Poorly Sorted	Very Poorly Sorted
Coarse Skewed	Coarse Skewed	Coarse Skewed
Mesokurtic	Platykurtic	Platykurtic
6.65	6.65	6.65
7.254331413	7.254331413	7.254331413
1.764199795	1.915776155	1.86983666
9.129031698	12.04532586	11.01445736
74.53174808	124.8025267	104.8303913
42.2467729	65.1446289	56.06392984
72.76754829	122.8867505	102.9605547
7.367432259	11.29878982	9.504451261
22.94141582	42.53376388	34.02860043
3.746001092	3.002280952	3.253871066
6.775322441	6.375382766	6.504457769
9.14677033	9.027855282	9.062872036
2.441742569	3.006998821	2.785258497
5.400769238	6.02557433	5.80900097
1.550317742	1.79114632	1.68874157
2.88116189	3.498096353	3.248603335
0.118094	0.205013189	0.172322806
0.881906	0.794986811	0.827677194
0.021531898	0.015832278	0.015967731
0.009832678	0.009399373	0.007033802
0.00329978	0.013265782	0.0060004
0.021131925	0.061262582	0.047569838
0.06229772	0.105253173	0.095751034
0.100632701	0.109790288	0.11042326
0.144057736	0.129718986	0.137412926
0.179313208	0.154962604	0.165215264
0.187357126	0.163555763	0.170454479
0.154807283	0.134294848	0.138052314
0.115737945	0.102664322	0.106118951

302-2-A-35-X-4	302-2-A-35-X-4	302-2-A-35-X-5
Cristin Ashmankas,	Cristin Ashmankas,	Cristin Ashmankas,
Unimodal, Very Poorly Sorted	Unimodal, Very Poorly Sorted	Unimodal, Very Poorly Sorted
Sandy Mud	Sandy Mud	Sandy Mud
Very Fine Sandy Fine Silt	Very Fine Sandy Fine Silt	Very Fine Sandy Fine Silt
53.042433	57.39103794	56.93853369
177.7448974	200.714772	186.9337932
7.097505713	6.307427288	6.641035927
57.84840731	45.56682514	51.31591607
12.4283314	11.00833496	11.70238536
4.69492252	4.849081816	5.045325985
0.462220592	0.699021287	0.558849802
3.019001602	3.41477985	2.930734924
6.302649732	6.468050601	6.387153214
2.247521996	2.302146413	2.35305112
-0.488886961	-0.725430441	-0.579070882
3.062016006	3.442614171	2.961606243
12.21654933	10.57918987	11.59721332
4.640539154	4.740059736	5.05244044
0.111300762	0.17540882	0.190331901
0.886736144	0.988220758	0.879926898
6.355019349	6.562627036	6.430078006
2.214292433	2.244905241	2.33698041
-0.111300762	-0.17540882	-0.190331901
0.886736144	0.988220758	0.879926898
Medium Silt	Medium Silt	Medium Silt
Very Poorly Sorted	Very Poorly Sorted	Very Poorly Sorted
Coarse Skewed	Coarse Skewed	Coarse Skewed
Platykurtic	Mesokurtic	Platykurtic
6.65	4.7	4.7
7.254331413	7.754331413	7.754331413
1.847894127	1.7200383	1.697462237
10.86730729	9.097087209	9.301187184
98.17555749	96.67466601	110.9134671
53.12834542	56.20494963	65.34075671
96.32766337	94.95462771	109.2160048
9.435240205	8.313821837	10.61842893
33.15608662	25.70530558	33.56684474
3.348492304	3.370718315	3.172493547
6.523861677	6.780379601	6.748369414
9.079902183	9.183343595	9.202404805
2.711638958	2.724447058	2.900685113
5.731409878	5.81262528	6.029911258
1.681273239	1.599483927	1.716956432
3.238059247	3.055511832	3.40849842
0.163622896	0.143322935	0.177577348
0.836377104	0.856677065	0.822422652
0.015501033	0.020068674	0.016868354
0.007167144	0.009067573	0.008234157
0.005733716	0.01040104	0.00990099
0.041202747	0.037437077	0.049138247
0.094018255	0.066348571	0.0934356
0.116483698	0.094751942	0.096514739
0.138421441	0.133931918	0.114664049
0.162152585	0.166640584	0.152750325
0.170844257	0.184263356	0.179810945
0.140583929	0.156892498	0.15621908
0.107891194	0.120196768	0.122463514

302-2-A-37-X-1	302-2-A-37-X-1	302-2-A-38-X-1
Cristin Ashmankas,	Cristin Ashmankas,	Cristin Ashmankas,
Unimodal, Very Poorly Sorted	Unimodal, Very Poorly Sorted	Bimodal, Very Poorly Sorted
Sandy Mud	Sandy Mud	Sandy Mud
Very Fine Sandy Fine Silt	Very Fine Sandy Fine Silt	Very Fine Sandy Fine Silt
63.40946265	61.53067314	83.39433243
220.0433753	199.7960897	161.8443204
5.699908004	6.231255393	4.975958217
37.33255599	45.160747	38.61321913
10.32615363	12.60518487	20.61050833
5.133703691	5.051765457	6.118347143
0.829206492	0.520141781	0.075045117
3.531675058	3.002448771	1.915070517
6.553037902	6.268980559	5.590509321
2.389847868	2.359521324	2.61547744
-0.849122345	-0.546954891	-0.077880897
3.534992939	3.034757916	1.920229711
9.904649963	12.25679818	20.22943255
5.027675625	5.018931264	6.294800297
0.244502975	0.134668382	0.061837224
1.023812091	0.90391948	0.720172528
6.657678294	6.350274034	5.627400338
2.329891573	2.327380188	2.654160609
-0.244502975	-0.134668382	-0.061837224
1.023812091	0.90391948	0.720172528
Medium Silt	Medium Silt	Coarse Silt
Very Poorly Sorted	Very Poorly Sorted	Very Poorly Sorted
Coarse Skewed	Coarse Skewed	Symmetrical
Mesokurtic	Mesokurtic	Platykurtic
4.7	4.7	107.5
		4.7
7.754331413	7.754331413	3.236965594
		7.754331413
1.622156581	1.765498315	1.970701149
7.895865791	10.80667392	18.30966148
102.4828148	108.2037154	220.7153811
63.17689431	61.28791769	111.9984028
100.8606583	106.4382171	218.7446799
8.492592086	10.442568	23.05524168
24.13185898	35.30614338	98.27734043
3.286546088	3.208178057	2.179740924
6.984686817	6.531933632	5.771251072
9.2678712	9.145708841	8.987075272
2.819942564	2.850748518	4.123001579
5.981325113	5.937530784	6.807334348
1.594395165	1.723362526	2.378918543
3.086204957	3.384404633	4.527022884
0.146763213	0.173167702	0.342733117
0.853236787	0.826832298	0.657266883
0.024134138	0.019666011	0.00720072
0.012133738	0.010532982	0.01580158
0.012033734	0.013132896	0.055605561
0.034667822	0.039698677	0.127912791
0.06379378	0.090137136	0.136212465
0.083343386	0.115494846	0.089446798
0.11361979	0.13297239	0.08945379
0.158923889	0.153077148	0.116739475
0.193549003	0.165011996	0.138477981
0.17134724	0.145048999	0.124582718
0.132453479	0.115226919	0.098566122

302-2-A-38-X-2	302-2-A-38-X-2	302-2-A-38-X-3
Cristin Ashmankas,	Cristin Ashmankas,	Cristin Ashmankas,
Bimodal, Very Poorly Sorted	Unimodal, Very Poorly Sorted	Unimodal, Very Poorly Sorted
Sandy Mud	Sandy Mud	Sandy Mud
Very Fine Sandy Fine Silt	Very Fine Sandy Fine Silt	Very Fine Sandy Fine Silt
80.1290291	44.26264526	67.9276015
249.0836661	164.311611	216.0763068
4.940523768	7.479975814	5.784710406
28.31680156	65.02837602	38.57119571
12.94187698	9.173996443	13.28352823
5.714319326	4.606542109	5.317202926
0.602512607	0.708754334	0.459600509
3.000379344	3.420631127	2.880205898
6.212020594	6.74032695	6.187378613
2.544341106	2.226003656	2.434408792
-0.619326635	-0.737049181	-0.484417345
2.995769254	3.474994955	2.906173118
12.45979817	8.849928236	12.91480319
6.022391565	4.49347527	5.247205137
0.199109582	0.183784864	0.101273405
0.981216784	0.945488997	0.861278999
6.326575491	6.820118528	6.274830532
2.590336512	2.167831662	2.391549193
-0.199109582	-0.183784864	-0.101273405
0.981216784	0.945488997	0.861278999
Medium Silt	Medium Silt	Medium Silt
Very Poorly Sorted	Very Poorly Sorted	Very Poorly Sorted
Coarse Skewed	Coarse Skewed	Coarse Skewed
Mesokurtic	Mesokurtic	Platykurtic
4.7	3.35	4.7
1200		
7.754331413	8.241333809	7.754331413
-0.242713414		
1.635952543	1.529080952	1.691955125
10.54749977	7.493489837	11.71004761
128.0246177	75.748359	114.895901
78.2569264	49.53848839	67.90717985
126.3886652	74.21927805	113.2039459
12.28363444	8.136071437	12.07161772
39.69876831	21.33310536	41.10601406
2.965506843	3.722641555	3.121600765
6.566955134	7.060146524	6.416109248
9.255653387	9.353119497	9.20709298
3.121103365	2.512495323	2.949478063
6.290146543	5.630477942	6.085492214
1.798424746	1.564076947	1.802175152
3.618665578	3.024332347	3.593547119
0.19418376	0.119875418	0.192282989
0.80581624	0.880124582	0.807717011
0.03159684	0.01270127	0.0236
0.01729827	0.00950095	0.0123
0.01119888	0.00650065	0.0081
0.04169583	0.02610261	0.0443
0.092393938	0.065069937	0.103982989
0.106822377	0.090028599	0.122472056
0.12026201	0.120329032	0.12854405
0.144822635	0.159025072	0.14205901
0.159663539	0.184868181	0.153384163
0.14565403	0.178584973	0.139166945
0.128591649	0.147288726	0.122090788

302-2-A-38-X-3	302-2-A-38-X-3	302-2-A-38-X-4
Cristin Ashmankas,	Cristin Ashmankas,	Cristin Ashmankas,
Bimodal, Very Poorly Sorted	Unimodal, Very Poorly Sorted	Bimodal, Very Poorly Sorted
Sandy Mud	Sandy Mud	Sandy Mud
ery Fine Sandy Very Fine S	Very Fine Sandy Fine Silt	Very Coarse Sandy Fine Sil
92.52587859	60.26270123	81.03205671
284.3342622	182.2572731	288.603733
4.297186945	5.977816591	4.439425917
21.61411687	44.34471195	22.22193787
10.86107676	11.30151296	8.330007087
6.34952406	5.345045114	5.500468089
0.856780111	0.644502549	1.244805243
3.219758829	2.871046516	4.609493429
6.438974735	6.448407171	6.820755567
2.71440144	2.429722917	2.525005457
-0.854564646	-0.653499296	-1.241017588
3.150089709	2.883444589	4.440841035
10.49369457	10.99151179	7.626588402
6.8883639	5.416332579	5.884372822
0.332598512	0.250355828	0.356871298
1.113723524	0.926411623	1.402233102
6.574333485	6.50746636	7.034746443
2.78416136	2.437316328	2.556888656
-0.332598512	-0.250355828	-0.356871298
1.113723524	0.926411623	1.402233102
Medium Silt	Medium Silt	Fine Silt
Very Poorly Sorted	Very Poorly Sorted	Very Poorly Sorted
Very Coarse Skewed	Coarse Skewed	Very Coarse Skewed
Leptokurtic	Mesokurtic	Leptokurtic
3.35	3.35	3.35
1200		1200
8.241333809	8.241333809	8.241333809
-0.242713414		-0.242713414
1.449384997	1.615845126	1.440798269
7.60867939	8.345096929	6.029135104
174.2955443	125.9307734	77.45542741
120.2548285	77.93492791	53.75868994
172.8461593	124.3149283	76.01462914
11.61411664	10.83772127	7.146941416
30.46347271	31.51444361	16.54287929
2.520392406	2.989297221	3.690489856
7.038138212	6.904855478	7.373833226
9.430343419	9.273495358	9.438915932
3.741617137	3.102232623	2.557632266
6.909951013	6.284198137	5.748426076
1.720989111	1.709130276	1.497760014
3.537807523	3.437989543	2.837325963
0.179852662	0.176343576	0.114321796
0.820147338	0.823656424	0.885678204
0.04240424	0.01349865	0.04490449
0.02110211	0.01459854	0.01850185
0.01880188	0.02209779	0.00040004
0.03720372	0.050394961	0.01120112
0.060340711	0.075753635	0.039314295
0.077907517	0.087568105	0.069304365
0.101425606	0.107986555	0.098355631
0.134626358	0.142891154	0.146283273
0.171737522	0.18080646	0.203799272
0.174862592	0.170565224	0.202297745
0.159587742	0.133838925	0.165637919

302-2-A-38-X-4	302-2-A-38-X-5	302-2-A-38-X-5
Cristin Ashmankas,	Cristin Ashmankas,	Cristin Ashmankas,
Unimodal, Very Poorly Sorted	Unimodal, Very Poorly Sorted	Unimodal, Very Poorly Sorted
Sandy Mud	Sandy Mud	Sandy Mud
Very Fine Sandy Fine Silt	Very Fine Sandy Fine Silt	Very Fine Sandy Fine Silt
56.6986745	58.47252075	58.15932357
215.2684025	227.221057	204.3117635
6.023968072	5.743757836	6.134081087
40.92024129	36.7353716	43.13552898
9.046165604	8.999115925	11.17803125
4.773811634	4.764695226	4.763485068
0.999393245	0.975078214	0.719941499
4.111407007	4.274150248	3.553998286
6.735659221	6.745180589	6.445323883
2.296434462	2.292364844	2.276789398
-1.028378895	-1.004779975	-0.748124206
4.111080887	4.266904854	3.579408985
8.601150968	8.455119183	10.64353013
4.519795406	4.373389567	4.589660939
0.243932084	0.19175487	0.158825583
1.092346402	1.005585565	0.988961157
6.861254557	6.885959194	6.553879463
2.176257469	2.128751865	2.198387579
-0.243932084	-0.19175487	-0.158825583
1.092346402	1.005585565	0.988961157
Medium Silt	Medium Silt	Medium Silt
Very Poorly Sorted	Very Poorly Sorted	Very Poorly Sorted
Coarse Skewed	Coarse Skewed	Coarse Skewed
Mesokurtic	Mesokurtic	Mesokurtic
4.7	3.35	4.7
7.754331413	8.241333809	7.754331413
1.613128146	1.555155232	1.786895244
7.067717168	7.290559147	9.418613745
82.57572229	66.74555627	87.74579659
51.18980938	42.91890281	49.10517104
80.96259415	65.19040103	85.95890134
6.702824348	7.332759366	8.07337823
17.49749826	19.08903595	25.62813365
3.598138506	3.9051844	3.510526174
7.144539977	7.099754819	6.730269549
9.275923235	9.32872569	9.128329225
2.577978368	2.388805427	2.600273797
5.677784729	5.42354129	5.617803051
1.489821148	1.522649178	1.591356767
2.744769128	2.874356196	3.013172482
0.122717023	0.105786255	0.135136492
0.877282977	0.894213745	0.864863508
0.0241	0.02679732	0.02049795
0.0109	0.01239876	0.01159884
0.0062	0.00079992	0.00919908
0.0273	0.0149985	0.02919708
0.054217023	0.050791755	0.064643541
0.067832059	0.087175182	0.102323247
0.108763521	0.123997111	0.141357223
0.171755137	0.164387607	0.168820235
0.205545036	0.193026665	0.183163983
0.187403934	0.182063999	0.155496387
0.135983291	0.143563181	0.113702433

302-2-A-39-X-1	302-2-A-39-X-1	302-2-A-40-X-1
Cristin Ashmankas,	Cristin Ashmankas,	Cristin Ashmankas,
Unimodal, Very Poorly Sorted	Unimodal, Very Poorly Sorted	Unimodal, Very Poorly Sorted
Sandy Mud	Sandy Mud	Sandy Mud
Very Fine Sandy Fine Silt	Very Fine Sandy Fine Silt	Very Fine Sandy Fine Silt
37.57064006	76.95892189	65.91211308
112.7533947	255.5609642	243.2131903
8.124090577	4.86578144	5.282957933
85.63079458	27.30054309	31.49243244
10.05990247	10.27996586	8.644166116
4.433004281	5.672129624	5.195333597
0.514044221	0.886662402	1.058444562
2.876259617	3.496332982	4.133262701
6.635239872	6.538239962	6.794274739
2.148284756	2.545273789	2.423078744
-0.514044221	-0.897066386	-1.073917847
2.876259617	3.456747556	4.087205101
9.766217066	9.823652113	8.080136939
4.487262346	5.985983247	5.006070694
0.163401269	0.304837208	0.289615408
0.925365184	1.116586263	1.117070111
6.677984441	6.669524814	6.951404541
2.165835533	2.581588241	2.323678665
-0.163401269	-0.304837208	-0.289615408
0.925365184	1.116586263	1.117070111
Medium Silt	Medium Silt	Medium Silt
Very Poorly Sorted	Very Poorly Sorted	Very Poorly Sorted
Coarse Skewed	Very Coarse Skewed	Coarse Skewed
Mesokurtic	Leptokurtic	Leptokurtic
3.35	3.35	3.35
8.241333809	8.241333809	8.241333809
1.641744117	1.517807912	1.465332185
8.36836953	7.536089913	6.409533989
82.21899013	115.9290484	82.16975147
50.08027091	76.37926213	56.07585248
80.57724601	114.4112405	80.70441929
8.353287909	9.736825824	7.656095346
23.98186452	25.99161583	18.3952437
3.604384538	3.108685986	3.605248787
6.900837725	7.051968107	7.285564816
9.250554999	9.363795064	9.414556529
2.566472834	3.012139246	2.611347257
5.646170461	6.255109078	5.809307743
1.589143729	1.642621075	1.527921063
3.062344164	3.283451535	2.936608797
0.130732001	0.158001534	0.121545991
0.869267999	0.841998466	0.878454009
0.00370037	0.03350335	0.030793841
0.00780078	0.01790179	0.013797241
0.00910091	0.01130113	0.00639872
0.03690369	0.03080308	0.021295741
0.07322625	0.064492183	0.049260448
0.095697981	0.081426995	0.073779163
0.12858738	0.10584189	0.104054123
0.161939337	0.145713493	0.147656348
0.183978339	0.181845054	0.196057847
0.168704485	0.1783826	0.195927991
0.130360477	0.148788433	0.160978537

302-2-A-40-X-1	302-2-A-40-X-2	302-2-A-40-X-2
Cristin Ashmankas,	Cristin Ashmankas,	Cristin Ashmankas,
Unimodal, Very Poorly Sorted	Unimodal, Very Poorly Sorted	Unimodal, Very Poorly Sorted
Sandy Mud	Sandy Mud	Sandy Mud
Very Fine Sandy Fine Silt	Very Fine Sandy Fine Silt	Very Fine Sandy Fine Silt
56.22596581	49.02267746	60.27017448
189.803908	175.519793	212.9789746
6.245487517	7.278885921	5.861018009
46.44593764	60.21877673	39.21418728
9.772849213	10.96088223	10.38149607
5.103068688	4.598054292	4.978653457
0.824453035	0.574748655	0.797451339
3.324293474	3.228094744	3.553530262
6.647113678	6.48359365	6.55297211
2.372615199	2.220139134	2.340910116
-0.839538684	-0.603501008	-0.818394733
3.340583228	3.277801897	3.56652183
9.585537855	10.71414729	9.982476424
5.09661653	4.515756838	4.782132536
0.292200058	0.140410988	0.214784122
1.01420362	0.904323731	0.975916202
6.704924899	6.544339155	6.646386525
2.349539809	2.174967803	2.257654115
-0.292200058	-0.140410988	-0.214784122
1.01420362	0.904323731	0.975916202
Medium Silt	Medium Silt	Medium Silt
Very Poorly Sorted	Very Poorly Sorted	Very Poorly Sorted
Coarse Skewed	Coarse Skewed	Coarse Skewed
Mesokurtic	Mesokurtic	Mesokurtic
4.7	4.7	4.7
7.754331413	7.754331413	7.754331413
1.583833683	1.741237426	1.647243114
7.064739627	9.342021967	8.116861815
107.800424	86.41295489	95.07151845
68.06296972	49.62732458	57.71553553
106.2165904	84.67171747	93.42427534
8.456126915	8.765000297	8.431426192
22.7008713	27.35095564	24.37301736
3.213565242	3.532608575	3.394842987
7.145147894	6.742049447	6.944862232
9.302363437	9.16567135	9.245730789
2.894717467	2.594590133	2.723463449
6.088798195	5.633062776	5.850887802
1.583383827	1.624166646	1.594188361
3.07999703	3.13175414	3.075776686
0.153368485	0.140928375	0.14371576
0.846631515	0.859071625	0.85628424
0.016296741	0.015296941	0.02229777
0.012597481	0.00709858	0.0129987
0.015696861	0.00389922	0.00459954
0.040991802	0.033593281	0.03369663
0.067785602	0.081040352	0.07012312
0.072314818	0.107005524	0.087078591
0.096606763	0.133564675	0.11867492
0.149528026	0.162597611	0.160079653
0.202758836	0.179238999	0.1923272
0.186071634	0.158365822	0.168893341
0.139351438	0.118298995	0.129230534

302-2-A-40-X-3	302-2-A-40-X-3	302-2-A-40-X-4
Cristin Ashmankas,	Cristin Ashmankas,	Cristin Ashmankas,
Bimodal, Very Poorly Sorted	Unimodal, Very Poorly Sorted	Unimodal, Very Poorly Sorted
Sandy Mud	Sandy Mud	Sandy Mud
Very Fine Sandy Fine Silt	Very Fine Sandy Fine Silt	Very Fine Sandy Fine Silt
76.14258174	61.04858922	53.08425365
263.1353019	231.585689	191.0082324
4.822810037	5.565909634	6.399037949
26.40296996	34.64024786	47.6899558
10.01820895	9.568101607	9.147193381
5.409706288	4.799788559	4.896365013
0.971396627	0.918077346	0.887943274
3.893056172	4.194182323	3.625382597
6.571478068	6.657712685	6.739574621
2.481610276	2.300100735	2.317011477
-0.98494033	-0.9475561	-0.907625155
3.832966236	4.186447068	3.645800578
9.515354483	8.941788768	8.780977839
5.8098142	4.372269726	4.755295074
0.297629873	0.152301465	0.265565399
1.240095712	0.983027474	1.046899314
6.715526881	6.805220819	6.831402679
2.538492026	2.128382404	2.249534866
-0.297629873	-0.152301465	-0.265565399
1.240095712	0.983027474	1.046899314
Medium Silt	Medium Silt	Medium Silt
Very Poorly Sorted	Very Poorly Sorted	Very Poorly Sorted
Coarse Skewed	Coarse Skewed	Coarse Skewed
Leptokurtic	Mesokurtic	Mesokurtic
4.7	4.7	3.35
1200		
7.754331413	7.754331413	8.241333809
-0.242713414		
1.563939456	1.581319045	1.558514203
7.63411084	8.010704963	6.87325748
100.8650039	67.41888149	93.070663
64.49418713	42.63458515	59.71755844
99.30106446	65.83756244	91.5121488
8.083651647	7.619037638	7.472763054
22.15518245	20.99415178	19.16213066
3.309502391	3.890703497	3.425529705
7.033324151	6.963855076	7.184790279
9.320599622	9.304655811	9.325612982
2.816314515	2.391509869	2.72238567
6.011097231	5.413952314	5.900083277
1.568258332	1.545461457	1.527730692
3.015007152	2.929608782	2.901641778
0.142509327	0.107098169	0.134405681
0.857490673	0.892901831	0.865594319
0.03639636	0.027505501	0.017196561
0.01689831	0.014302861	0.01189762
0.00419958	0.00070014	0.01009798
0.02539746	0.0115023	0.035492901
0.059617616	0.053087367	0.059720618
0.077109995	0.095901604	0.069186627
0.111163463	0.135633976	0.104975349
0.162857483	0.167759024	0.156144403
0.194634423	0.187207165	0.19997197
0.171687004	0.168524161	0.191050909
0.140038305	0.137875901	0.144265061

302-2-A-40-X-4	302-2-A-41-X-1	302-2-A-42-X-1
Cristin Ashmankas,	Cristin Ashmankas,	Cristin Ashmankas,
Bimodal, Very Poorly Sorted	Unimodal, Very Poorly Sorted	Unimodal, Poorly Sorted
Sandy Mud	Mud	Mud
Very Fine Sandy Fine Silt	Fine Silt	Fine Silt
75.382523	66.137304	43.94809269
261.4628959	262.5228131	190.205195
4.875691461	4.967377567	6.873239683
26.8999653	27.47315338	52.39280809
10.48279205	7.759266615	7.878449441
5.320318716	4.556947661	4.184329834
0.90343193	1.507897935	1.033728926
3.852083083	6.132031183	4.880222182
6.506072676	6.939106917	6.953992286
2.456170911	2.251550423	2.097360623
-0.92254853	-1.519931493	-1.073608495
3.804065145	5.918150495	4.920058011
9.831596142	6.873343284	7.31229202
5.685437151	4.705360346	3.797027661
0.247237325	0.28329883	0.140023383
1.198348013	1.590084897	1.042289908
6.66835863	7.184772269	7.095460598
2.507271282	2.234305212	1.924870509
-0.247237325	-0.28329883	-0.140023383
1.198348013	1.590084897	1.042289908
Medium Silt	Fine Silt	Fine Silt
Very Poorly Sorted	Very Poorly Sorted	Poorly Sorted
Coarse Skewed	Coarse Skewed	Coarse Skewed
Leptokurtic	Very Leptokurtic	Mesokurtic
4.7	4.7	4.7
1200		
7.754331413	7.754331413	7.754331413
-0.242713414		
1.590285174	1.613480681	1.534436872
8.483709538	6.310857059	6.78199979
92.11876868	39.92608276	44.7635523
57.92594321	24.74531193	29.17262555
90.52848351	38.31260208	43.22911543
8.520271413	4.983533061	5.869534791
24.28432418	11.95440641	14.37979675
3.440361062	4.646524657	4.481531661
6.881089057	7.307948338	7.204073545
9.296498788	9.275607981	9.348074991
2.702186956	1.99624637	2.085910733
5.856137726	4.629083323	4.86654333
1.596270952	1.38216972	1.436426173
3.090899388	2.317168899	2.553246163
0.136350111	0.071930658	0.073036463
0.863649889	0.928069342	0.926963537
0.0361	0.0365	0.01819818
0.0164	0.0161	0.00969903
0.004	0.0011	0.00119988
0.0212	0.0033	0.01249875
0.058650111	0.014930658	0.031440623
0.09177787	0.051017048	0.069190598
0.129251084	0.116340209	0.12970711
0.163024541	0.18982812	0.186261664
0.179675313	0.234133857	0.207551763
0.163781165	0.199749112	0.187081172
0.136139917	0.137000995	0.14717123

302-2-A-42-X-1	302-2-A-42-X-2	302-2-A-42-X-2
Cristin Ashmankas,	Cristin Ashmankas,	Cristin Ashmankas,
Bimodal, Very Poorly Sorted	Unimodal, Poorly Sorted	Unimodal, Very Poorly Sorted
Sandy Mud	Mud	Sandy Mud
Very Fine Sandy Fine Silt	Fine Silt	Very Fine Sandy Fine Silt
80.1410446	48.68728423	46.3203845
271.2921623	211.2837724	154.5412102
4.698954815	6.300174511	7.916227759
24.98361088	43.6055357	73.3298612
10.6384587	7.714649775	11.0725662
5.62505386	4.269749524	4.710478939
0.847805991	1.15683525	0.486832661
3.5926823	5.21955574	2.847542307
6.478819507	6.975326463	6.476934998
2.538063043	2.134967713	2.249241193
-0.862155615	-1.195594933	-0.507154468
3.543184235	5.219827382	2.889907732
10.09891224	7.22925694	11.03663799
6.218909737	3.760762183	4.768978932
0.269383984	0.170710743	0.168367818
1.155752737	1.034904289	0.863520117
6.629656281	7.111936917	6.501555429
2.636661678	1.911025078	2.253680409
-0.269383984	-0.170710743	-0.168367818
1.155752737	1.034904289	0.863520117
Medium Silt	Fine Silt	Medium Silt
Very Poorly Sorted	Poorly Sorted	Very Poorly Sorted
Coarse Skewed	Coarse Skewed	Coarse Skewed
Leptokurtic	Mesokurtic	Platykurtic
3.35	4.7	4.7
1200		
8.241333809	7.754331413	7.754331413
-0.242713414		
1.515707876	1.536205731	1.683649685
8.374023359	6.393772839	9.069018047
102.4486915	47.0994708	96.87924351
67.59131695	30.65961145	57.54121202
100.9329836	45.56326507	95.19559383
10.11787042	5.690996498	9.999714117
27.99828422	13.72441538	30.88981581
3.287026538	4.40814534	3.36766859
6.899863342	7.289116796	6.784837934
9.365792557	9.346412848	9.214192295
2.84932064	2.120259685	2.736074542
6.078766019	4.938267509	5.846523705
1.666649326	1.424601126	1.682853017
3.338833762	2.508681292	3.32188685
0.153256452	0.073357657	0.162652121
0.846743548	0.926642343	0.837347879
0.03930393	0.02310231	0.0112
0.01710171	0.01030103	0.0066
0.0010001	0.00030003	0.0037
0.02430243	0.0040004	0.0439
0.071548281	0.035653887	0.097252121
0.09589415	0.074484649	0.101164392
0.118796466	0.113693189	0.117793761
0.147742576	0.175756875	0.154007306
0.171271013	0.2213518	0.180957147
0.16597454	0.1940463	0.159100406
0.147064803	0.14730953	0.124324868

302-2-A-42-X-3	302-2-A-42-X-3	302-2-A-42-X-4
Cristin Ashmankas,	Cristin Ashmankas,	Cristin Ashmankas,
Bimodal, Very Poorly Sorted	Unimodal, Very Poorly Sorted	Bimodal, Very Poorly Sorted
Sandy Mud	Sandy Mud	Sandy Mud
Very Fine Sandy Fine Silt	Very Fine Sandy Fine Silt	Very Fine Sandy Fine Silt
81.87631313	74.1205014	75.8081865
278.9411164	268.8738866	261.7319722
4.575438398	4.735245555	4.873254771
23.66781149	25.40138377	26.87605604
10.22497058	7.93839551	10.49087215
5.645659505	5.349511605	5.393256649
0.915628872	1.289243418	0.882769377
3.760244267	4.700299671	3.757314217
6.530031893	6.905197543	6.503964502
2.548585142	2.476789723	2.476041731
-0.926939873	-1.288333346	-0.901039802
3.687516311	4.563313449	3.712281349
9.642598002	7.188411466	9.91521736
6.232172857	5.525787234	5.815507412
0.28062133	0.351966509	0.262264475
1.202567934	1.498645497	1.174791028
6.696362381	7.120111293	6.656139885
2.639735249	2.466180013	2.539905075
-0.28062133	-0.351966509	-0.262264475
1.202567934	1.498645497	1.174791028
Medium Silt	Fine Silt	Medium Silt
Very Poorly Sorted	Very Poorly Sorted	Very Poorly Sorted
Coarse Skewed	Very Coarse Skewed	Coarse Skewed
Leptokurtic	Leptokurtic	Leptokurtic
3.35	3.35	4.7
1200		1200
8.241333809	8.241333809	7.754331413
-0.242713414		-0.242713414
1.490304308	1.432493593	1.56859374
7.990427318	5.759594103	8.302777042
98.3485766	85.95086204	95.22044687
65.99227825	60.00087012	60.70433944
96.85827229	84.51836844	93.65185313
9.560105238	5.921906554	8.992184077
25.66770577	13.10718678	25.53422583
3.345952017	3.540344081	3.39258479
6.967511626	7.439817141	6.912190327
9.390177337	9.447255598	9.316312536
2.806429168	2.668456902	2.746080971
6.04422532	5.906911517	5.923727746
1.635578893	1.428630395	1.61871898
3.257026499	2.566061725	3.168671569
0.144893459	0.118184717	0.142596729
0.855106541	0.881815283	0.857403271
0.04190419	0.037892422	0.0362
0.01770177	0.017296541	0.0167
0.00040004	0.00519896	0.003
0.02050205	0.019796041	0.0219
0.064385408	0.038000754	0.064796729
0.091397142	0.04866494	0.093635839
0.118553294	0.084471372	0.121967924
0.150338177	0.156883701	0.15651243
0.174270847	0.218143648	0.182258544
0.169174766	0.206158897	0.164288618
0.151372315	0.167492725	0.138739917

302-2-A-43-X-1	302-2-A-43-X-1	302-2-A-43-X-2
Cristin Ashmankas,	Cristin Ashmankas,	Cristin Ashmankas,
Unimodal, Very Poorly Sorted	Unimodal, Very Poorly Sorted	Bimodal, Very Poorly Sorted
Sandy Mud	Sandy Mud	Sandy Mud
Very Fine Sandy Fine Silt	Very Fine Sandy Fine Silt	Very Fine Sandy Fine Silt
43.59770373	68.55384488	82.53835783
122.0393154	227.1124659	258.7530503
6.813132798	5.515041107	4.716188534
60.72388186	34.85364023	25.91027446
10.68378418	12.04993431	11.7076132
4.76583323	5.217054972	5.834563683
0.536406933	0.670740782	0.778513063
2.729065232	3.229225731	3.168636432
6.548433452	6.328983716	6.351644557
2.252728468	2.40942796	2.580039384
-0.536406933	-0.692446359	-0.78844971
2.729065232	3.238942024	3.14057797
10.54113039	11.69344803	11.2974959
4.874709775	5.103666222	6.247522786
0.21656798	0.188819297	0.306960276
0.90323087	0.928008353	1.038531658
6.567826605	6.418155792	6.467853156
2.285316328	2.35153398	2.643284258
-0.21656798	-0.188819297	-0.306960276
0.90323087	0.928008353	1.038531658
Medium Silt	Medium Silt	Medium Silt
Very Poorly Sorted	Very Poorly Sorted	Very Poorly Sorted
Coarse Skewed	Coarse Skewed	Very Coarse Skewed
Mesokurtic	Mesokurtic	Mesokurtic
4.7	4.7	3.35
		1200
7.754331413	7.754331413	8.241333809
		-0.242713414
1.65485949	1.742052483	1.631310302
8.265175153	9.686381148	8.40989336
101.8009029	110.6161101	135.6198806
61.51634234	63.49757611	83.13555086
100.1460434	108.8740576	133.9885703
9.524366439	10.1434845	11.725202
27.90795546	32.65531333	34.61019292
3.296177738	3.17636658	2.882359415
6.918738892	6.689826512	6.893696778
9.239075558	9.164996196	9.259753052
2.802966434	2.885371057	3.21256017
5.942897821	5.988629616	6.377393637
1.649915278	1.698270384	1.751799819
3.251623128	3.342481428	3.551540873
0.160578451	0.171529316	0.185377412
0.839421549	0.828470684	0.814622588
0.00419958	0.0260026	0.034093181
0.01069893	0.01310131	0.019596081
0.01249875	0.00770077	0.01219756
0.04729527	0.03890389	0.039792042
0.08588592	0.085820745	0.079698548
0.089132357	0.100880035	0.089905604
0.112174456	0.123927515	0.101993258
0.151483308	0.154638607	0.138967402
0.187813678	0.176483645	0.18107994
0.170183173	0.154514392	0.170950862
0.128634577	0.118026491	0.131725522

302-2-A-43-X-2	302-2-A-43-X-3	302-2-A-43-X-3
Cristin Ashmankas,	Cristin Ashmankas,	Cristin Ashmankas,
Bimodal, Very Poorly Sorted	Unimodal, Very Poorly Sorted	Unimodal, Poorly Sorted
Sandy Mud	Sandy Mud	Mud
Very Fine Sandy Fine Silt	Very Fine Sandy Fine Silt	Fine Silt
83.2844335	43.4305335	35.08465743
279.4211016	174.9294543	155.4845458
4.521736034	7.383672627	8.618420177
23.2539365	61.03250716	83.2419299
10.25459936	8.939778049	7.658595293
5.746725929	4.325709267	4.024236317
0.911241201	0.810735441	0.860853278
3.686907461	3.921908976	4.296650684
6.527858788	6.779634232	6.993817259
2.572338138	2.135013772	2.043639979
-0.919922725	-0.842075237	-0.919060674
3.615919738	3.976371423	4.420763737
9.636881851	8.555882692	7.288612821
6.300051292	4.119865024	3.782933017
0.28527706	0.178520928	0.147629001
1.193122257	0.975942126	0.977844136
6.697217867	6.868867582	7.10014002
2.655363574	2.042597072	1.919505231
-0.28527706	-0.178520928	-0.147629001
1.193122257	0.975942126	0.977844136
Medium Silt	Medium Silt	Fine Silt
Very Poorly Sorted	Very Poorly Sorted	Poorly Sorted
Coarse Skewed	Coarse Skewed	Coarse Skewed
Leptokurtic	Mesokurtic	Mesokurtic
3.35	4.7	3.35
1200		
8.241333809	7.754331413	8.241333809
-0.242713414		
1.473140936	1.624521311	1.511496715
7.900463199	7.351134475	6.575130852
103.9751956	63.48434822	45.56954253
70.58061656	39.07880296	30.14862163
102.5020546	61.85982691	44.05804582
9.764247252	6.924885659	6.242055713
25.91869746	18.67700179	15.05050355
3.265688696	3.977455244	4.455786302
6.983847045	7.087817371	7.248764679
9.406888824	9.265769615	9.369806442
2.880522211	2.329572314	2.102840174
6.141200128	5.288314371	4.914020139
1.642846872	1.505979977	1.455351646
3.287508828	2.79179025	2.642021234
0.148150111	0.101621252	0.070068775
0.851849889	0.898378748	0.929931225
0.0416	0.0151	0.012502501
0.019	0.0078	0.00590118
0.0022	0.0015	0.00620124
0.0224	0.0205	0.01070214
0.062950111	0.056721252	0.034761713
0.089432916	0.088748013	0.078792189
0.117129576	0.124022376	0.129068563
0.147824541	0.168086811	0.17293444
0.173149694	0.204538049	0.203980708
0.169853329	0.179818796	0.193024345
0.154459833	0.133164702	0.152130979

302-2-A-44-X-1	302-2-A-44-X-1	302-2-A-44-X-2
Cristin Ashmankas,	Cristin Ashmankas,	Cristin Ashmankas,
Unimodal, Poorly Sorted	Unimodal, Very Poorly Sorted	Unimodal, Poorly Sorted
Mud	Sandy Mud	Mud
Very Fine Silt	Very Fine Sandy Fine Silt	Fine Silt
26.68546341	54.5464405	42.59337067
111.2204538	179.4911554	173.3920916
6.196361835	6.318380177	7.561470158
41.8789539	47.94170894	63.47029039
4.864744739	10.83394797	9.549787745
3.809137452	4.860149821	4.136499107
1.498362979	0.722125172	0.764712329
6.16112385	3.255389311	3.959964088
7.683420178	6.509362132	6.682405839
1.929464348	2.293715439	2.071624892
-1.498362979	-0.735618171	-0.80491847
6.16112385	3.274201207	4.032178652
4.290335621	10.43135892	9.262797031
3.301329661	4.78766323	3.918275061
0.247845513	0.222430539	0.149586933
1.25204411	0.966023837	0.91792933
7.864693774	6.582929075	6.754336384
1.723047209	2.259321675	1.970218678
-0.247845513	-0.222430539	-0.149586933
1.25204411	0.966023837	0.91792933
Fine Silt	Medium Silt	Medium Silt
Poorly Sorted	Very Poorly Sorted	Poorly Sorted
Coarse Skewed	Coarse Skewed	Coarse Skewed
Leptokurtic	Mesokurtic	Mesokurtic
3.35	4.7	4.7
8.241333809	7.754331413	7.754331413
1.206400441	1.733937785	1.797297932
3.829964215	8.416973302	8.105695823
23.48474502	99.78001968	61.63042023
19.46679082	57.54532863	34.29059765
22.27834458	98.04608189	59.8331223
4.076571699	8.576380016	6.98649832
6.259525593	25.63082188	20.47263189
5.41213226	3.325105236	4.020213562
8.028453372	6.892482743	6.946848247
9.695075424	9.17173215	9.119954706
1.791359664	2.758328383	2.268524934
4.282943164	5.846626914	5.099741144
1.293237618	1.607068381	1.520588844
2.027356389	3.100368832	2.804569548
0.052573631	0.149750111	0.09803621
0.947426369	0.850249889	0.90196379
0	0.0135	0.015103021
0.022195561	0.0145	0.00780156
0.00319936	0.0119	0.00030006
0.00679864	0.0376	0.01140228
0.020380069	0.072250111	0.063429288
0.028436314	0.088553558	0.104115229
0.057502584	0.119797754	0.132588053
0.124292083	0.160498922	0.17522931
0.228901757	0.191546899	0.20179937
0.273254195	0.169807971	0.174458978
0.235039437	0.120044785	0.113772851

302-2-A-44-X-2	302-2-A-44-X-3	302-2-A-44-X-3
Cristin Ashmankas,	Cristin Ashmankas,	Cristin Ashmankas,
Polymodal, Very Poorly Sorted	Unimodal, Very Poorly Sorted	Bimodal, Very Poorly Sorted
Sandy Mud	Sandy Mud	Sandy Mud
Very Fine Sandy Fine Silt	ery Fine Sandy Medium Si	ery Fine Sandy Medium Si
95.4501495	57.41924192	75.29182895
271.6036583	166.7682164	218.8727215
4.190259724	6.167621741	5.185749562
21.53104121	48.61092249	32.9214124
11.22386423	13.84929699	15.16453724
6.613119455	4.521021713	5.100310694
0.875706723	0.640529316	0.570622593
2.998147369	3.219464195	3.131840187
6.409519394	6.163079986	6.001310975
2.761408827	2.182612719	2.369014622
-0.869662217	-0.65089248	-0.593171277
2.944058952	3.231608552	3.137962468
11.40647121	13.31069908	14.26681129
7.11058433	4.510584725	5.160268298
0.393995647	0.193993235	0.144773066
1.074515351	1.066093031	1.081105476
6.454003651	6.231269846	6.131193269
2.829968122	2.173314468	2.367446078
-0.393995647	-0.193993235	-0.144773066
1.074515351	1.066093031	1.081105476
Medium Silt	Medium Silt	Medium Silt
Very Poorly Sorted	Very Poorly Sorted	Very Poorly Sorted
Very Coarse Skewed	Coarse Skewed	Coarse Skewed
Mesokurtic	Mesokurtic	Mesokurtic
3.35	9.4	9.4
107.5		215
8.241333809	6.754331413	6.754331413
3.236965594		2.236965594
1.512929566	2.3641149	2.144757819
7.060536421	11.30708561	13.20195864
249.6200759	116.4184482	141.0635211
164.9912075	49.24398901	65.77130521
248.1071464	114.0543333	138.9187633
11.73367748	6.96563393	8.56813246
31.33190247	28.32424869	35.94137954
2.002194126	3.102608403	2.825583138
7.146006489	6.466629066	6.243104206
9.36843946	8.72448413	8.864969533
4.679086478	2.811983659	3.13739469
7.366245334	5.621875727	6.039386395
1.729825962	1.569361206	1.670896032
3.552583338	2.800254656	3.098980784
0.200043767	0.161999609	0.175581477
0.799956233	0.838000391	0.824418523
0.0353	0.00980098	0.021393582
0.028	0.01530153	0.020393882
0.0366	0.02440244	0.031290613
0.0452	0.04380438	0.032490253
0.054943767	0.068690278	0.070013147
0.057863572	0.096869396	0.127317561
0.079784915	0.152484586	0.155991589
0.135950945	0.198429012	0.173010833
0.19029473	0.191476907	0.16190127
0.185176125	0.127194774	0.120085429
0.150885947	0.071545716	0.086111842

302-2-A-44-X-4	302-2-A-45-X-1	302-2-A-45-X-1
Cristin Ashmankas,	Cristin Ashmankas,	Cristin Ashmankas,
Trimodal, Very Poorly Sorted	Bimodal, Very Poorly Sorted	Bimodal, Very Poorly Sorted
Sandy Mud	Sandy Mud	Sandy Mud
Very Fine Sandy Fine Silt	Medium Sandy Fine Silt	Fine Sandy Fine Silt
90.78763674	104.2748915	122.099865
255.2795452	246.1419792	270.4751563
4.426818889	3.575987592	3.680086396
24.15453049	17.82867707	18.35313486
12.31286192	14.65718282	18.70741935
6.320840671	6.763985428	7.374782961
0.788377949	0.691413923	0.422328777
2.876253757	2.563755432	2.105306063
6.286890767	6.066342494	5.680456907
2.688415533	2.768153367	2.897649717
-0.789170341	-0.690496557	-0.419118121
2.845587465	2.550530402	2.090027618
12.62974845	16.01394301	19.5570997
6.810150501	7.596387717	8.053565385
0.357801237	0.342404144	0.269982572
1.027518267	1.033579654	0.769525716
6.307030285	5.964527613	5.676163754
2.767686681	2.925313542	3.009627619
-0.357801237	-0.342404144	-0.269982572
1.027518267	1.033579654	0.769525716
Medium Silt	Coarse Silt	Coarse Silt
Very Poorly Sorted	Very Poorly Sorted	Very Poorly Sorted
Very Coarse Skewed	Very Coarse Skewed	Coarse Skewed
Mesokurtic	Mesokurtic	Platykurtic
4.7	4.7	3.35
107.5	427.5	215
7.754331413	7.754331413	8.241333809
3.236965594	1.247054535	2.236965594
1.63775014	1.72098183	1.790409926
8.106161593	9.699081811	12.83293626
229.5005585	375.349778	367.7022151
140.1316067	218.1021156	205.3731995
227.8628084	373.6287962	365.9118051
11.85945198	11.96474123	28.71522675
35.074645	38.5694901	105.8738929
2.12343043	1.413692465	1.443390227
6.946765349	6.687936107	6.284004883
9.254069013	9.182552419	9.125494345
4.358074972	6.495438467	6.322264188
7.130638582	7.768859954	7.682104117
1.758118664	1.783444697	2.519156035
3.56796544	3.580717289	4.843744049
0.208725114	0.218166835	0.297871697
0.791274886	0.781833165	0.702128303
0.03049695	0.020195961	0.03179682
0.02449755	0.050589882	0.03769623
0.03789621	0.065486903	0.079492051
0.056994301	0.042191562	0.088491151
0.058840103	0.039702528	0.060395444
0.060104883	0.064982039	0.067824761
0.091793589	0.115078959	0.099407365
0.14814498	0.152288028	0.130517079
0.188614064	0.173232748	0.14935013
0.171278637	0.155554646	0.141744199
0.131338733	0.120696745	0.113284771

302-2-A-46-X-1
Cristin Ashmankas,
Bimodal, Very Poorly Sorted
Sandy Mud
Very Fine Sandy Fine Silt
64.18248825
176.9936098
5.502937289
40.57795547
12.01646725
5.460312957
0.659504369
2.799680587
6.360906755
2.459121071
-0.666498548
2.807372895
11.67708638
5.662540857
0.261680033
0.988928059
6.420175847
2.501449555
-0.261680033
0.988928059
Medium Silt
Very Poorly Sorted
Coarse Skewed
Mesokurtic
3.35
215
8.241333809
2.236965594
1.693127508
8.90245635
163.8722034
96.78668773
162.1790759
10.33122949
31.20876093
2.609356935
6.811580828
9.206093659
3.528108223
6.596736724
1.693906833
3.36894005
0.18045437
0.81954563
0.01069893
0.01849815
0.04039596
0.04889511
0.061966218
0.082484932
0.114535553
0.153294771
0.177637054
0.166860565
0.124732754

APENDIX II: Data and statistical variables for IODP Exp. 302, ACEX, samples taken from paleogene sediments. Samples exclusively contained sand, silt, and clay. Sample identifications are the expedition-site-core-section. The samples are presented in descending order.

	Sample ID:	**302-2-A-46-X-1**
	ANALYST:	Cristin Ashmankas,
	SAMPLE TYPE:	Bimodal, Very Poorly Sorted
	TEXTURAL GROUP:	Sandy Mud
	SEDIMENT NAME:	Very Fine Sandy Fine Silt
METHOD OF	MEAN	73.95
MOMENTS	SORTING	211.2
Arithmetic (mm)	SKEWNESS	4.910
	KURTOSIS	30.92
METHOD OF	MEAN	11.77
MOMENTS	SORTING	5.671
Geometric (mm)	SKEWNESS	0.799
	KURTOSIS	3.042
METHOD OF	MEAN	6.380
MOMENTS	SORTING	2.520
Logarithmic (f)	SKEWNESS	-0.805
	KURTOSIS	3.036
FOLK AND	MEAN	11.41
WARD METHOD	SORTING	5.863
(mm)	SKEWNESS	0.313
	KURTOSIS	1.078
FOLK AND	MEAN	6.454
WARD METHOD	SORTING	2.552
(f)	SKEWNESS	-0.313
	KURTOSIS	1.078
FOLK AND	MEAN:	Medium Silt
WARD METHOD	SORTING:	Very Poorly Sorted
(Description)	SKEWNESS:	Very Coarse Skewed
	KURTOSIS:	Mesokurtic
	MODE 1 (mm):	4.700
	MODE 2 (mm):	215.0
	MODE 1 (f):	7.754
	MODE 2 (f):	2.237
	D10 (mm):	1.707
	D50 (mm):	8.261
	D90 (mm):	183.1
	(D90 / D10) (mm):	107.3
	(D90 - D10) (mm):	181.4
	(D75 / D25) (mm):	9.356
	(D75 - D25) (mm):	27.90
	D10 (f):	2.450
	D50 (f):	6.919
	D90 (f):	9.194
	(D90 / D10) (f):	3.754
	(D90 - D10) (f):	6.745
	(D75 / D25) (f):	1.645
	(D75 - D25) (f):	3.226
	% SAND:	17.8%
	% MUD:	82.2%
	% V COARSE SAND:	1.7%
	% COARSE SAND:	2.5%
	% MEDIUM SAND:	3.9%
	% FINE SAND:	4.1%
	% V FINE SAND:	5.6%
	% V COARSE SILT:	7.2%
	% COARSE SILT:	10.5%
	% MEDIUM SILT:	15.9%
	% FINE SILT:	19.2%
	% V FINE SILT:	17.1%
	% CLAY:	12.3%

302-2-A-46-X-2	302-2-A-46-X-2	302-2-A-46-X-3
Cristin Ashmankas,	Cristin Ashmankas,	Cristin Ashmankas,
Bimodal, Very Poorly Sorted	Trimodal, Very Poorly Sorted	Unimodal, Very Poorly Sorted
Sandy Mud	Sandy Mud	Mud
Very Fine Sandy Fine Silt	Fine Sandy Fine Silt	Fine Silt
87.58	103.1	58.79
245.4	229.3	207.9
4.357	3.711	5.274
24.14	19.61	34.11
11.98	16.45	7.794
5.986	6.918	4.674
0.915	0.490	1.494
3.187	2.235	5.393
6.335	5.908	6.977
2.607	2.796	2.248
-0.916	-0.490	-1.498
3.150	2.231	5.340
12.12	16.97	6.377
6.260	7.593	4.176
0.360	0.299	0.266
1.218	0.839	1.646
6.366	5.881	7.293
2.646	2.925	2.062
-0.360	-0.299	-0.266
1.218	0.839	1.646
Medium Silt	Coarse Silt	Fine Silt
Very Poorly Sorted	Very Poorly Sorted	Very Poorly Sorted
Very Coarse Skewed	Coarse Skewed	Coarse Skewed
Leptokurtic	Platykurtic	Very Leptokurtic
6.650	6.650	4.700
427.5	215.0	
7.254	7.254	7.754
1.247	2.237	
1.766	1.693	1.651
8.119	10.73	5.986
259.1	328.0	42.27
146.8	193.7	25.60
257.4	326.3	40.62
7.859	20.53	4.222
23.99	72.59	9.714
1.948	1.608	4.564
6.944	6.542	7.384
9.146	9.206	9.243
4.694	5.725	2.025
7.197	7.598	4.678
1.574	2.174	1.330
2.974	4.360	2.078
18.5%	26.8%	9.1%
81.5%	73.2%	90.9%
2.6%	1.7%	1.7%
3.1%	4.2%	2.2%
4.5%	6.9%	3.1%
3.7%	7.2%	1.8%
4.6%	6.8%	0.3%
5.2%	6.3%	2.3%
9.1%	9.3%	8.5%
18.4%	14.9%	20.3%
20.9%	16.5%	25.9%
16.4%	13.9%	20.8%
11.6%	12.2%	13.2%

302-2-A-46-X-3	302-2-A-47-X-1	302-2-A-47-X-2
Cristin Ashmankas,	Cristin Ashmankas,	Cristin Ashmankas,
Unimodal, Poorly Sorted	Unimodal, Poorly Sorted	Unimodal, Poorly Sorted
Mud	Mud	Mud
Fine Silt	Fine Silt	Fine Silt
51.00	54.41	39.83
215.0	226.2	188.1
5.959	5.726	7.102
39.88	36.73	55.30
7.366	7.428	7.273
4.198	4.281	3.660
1.450	1.485	1.430
6.088	6.146	6.677
7.044	7.023	7.069
2.110	2.147	1.910
-1.475	-1.508	-1.480
6.022	6.039	6.692
6.477	6.512	6.710
3.632	3.840	3.124
0.194	0.219	0.167
1.290	1.382	1.137
7.270	7.263	7.219
1.861	1.941	1.643
-0.194	-0.219	-0.167
1.290	1.382	1.137
Fine Silt	Fine Silt	Fine Silt
Poorly Sorted	Poorly Sorted	Poorly Sorted
Coarse Skewed	Coarse Skewed	Coarse Skewed
Leptokurtic	Leptokurtic	Leptokurtic
4.700	4.700	4.700
7.754	7.754	7.754
1.613	1.620	1.810
6.094	6.118	6.178
37.12	36.65	33.50
23.01	22.63	18.51
35.51	35.03	31.69
4.523	4.553	4.128
10.50	10.62	10.02
4.752	4.770	4.900
7.359	7.353	7.339
9.276	9.270	9.110
1.952	1.943	1.859
4.524	4.500	4.211
1.350	1.353	1.328
2.177	2.187	2.046
7.3%	7.3%	5.4%
92.7%	92.7%	94.6%
2.3%	2.6%	1.8%
1.3%	1.3%	0.9%
0.6%	0.8%	0.2%
0.9%	1.0%	0.4%
2.1%	1.6%	2.1%
3.9%	3.8%	5.3%
10.1%	10.4%	10.3%
20.0%	19.9%	20.1%
24.6%	24.5%	27.0%
20.4%	20.4%	20.7%
13.7%	13.6%	11.3%

302-2-A-47-X-2	302-2-A-47-X-3	302-2-A-47-X-3
Cristin Ashmankas,	Cristin Ashmankas,	Cristin Ashmankas,
Unimodal, Poorly Sorted	Unimodal, Poorly Sorted	Unimodal, Poorly Sorted
Sandy Mud	Mud	Mud
Very Fine Sandy Medium Silt	Fine Silt	Fine Silt
61.37	43.05	7.404
217.4	195.5	6.765
5.767	6.872	1.938
37.89	51.58	7.635
13.03	8.197	5.055
4.142	3.842	2.399
0.916	1.107	-0.032
4.547	5.684	2.443
6.220	6.893	7.628
2.076	1.979	1.262
-0.961	-1.165	0.032
4.553	5.727	2.443
12.14	7.631	5.077
3.752	3.318	2.473
0.115	0.060	0.000
1.156	0.947	0.942
6.364	7.034	7.622
1.908	1.730	1.306
-0.115	-0.060	0.000
1.156	0.947	0.942
Medium Silt	Fine Silt	Fine Silt
Poorly Sorted	Poorly Sorted	Poorly Sorted
Coarse Skewed	Symmetrical	Symmetrical
Leptokurtic	Mesokurtic	Mesokurtic
13.30	4.700	4.700
6.254	7.754	7.754
2.655	1.736	1.553
11.71	7.487	5.043
76.18	35.26	16.28
28.70	20.31	10.48
73.53	33.52	14.73
5.169	5.531	3.546
21.34	14.78	6.921
3.714	4.826	5.941
6.416	7.061	7.632
8.557	9.170	9.331
2.304	1.900	1.571
4.843	4.344	3.390
1.452	1.426	1.273
2.370	2.468	1.826
11.7%	5.1%	0.0%
88.3%	94.9%	100.0%
2.3%	2.0%	0.0%
1.5%	0.9%	0.0%
0.6%	0.0%	0.0%
1.9%	0.6%	0.0%
5.4%	1.7%	0.0%
9.3%	6.5%	1.0%
19.4%	17.4%	9.8%
22.5%	19.7%	21.6%
19.1%	20.8%	28.3%
12.1%	18.4%	24.2%
5.8%	12.1%	15.1%

302-2-A-47-X-4	302-2-A-47-X-4	302-2-A-47-X-5
Cristin Ashmankas,	Cristin Ashmankas,	Cristin Ashmankas,
Unimodal, Poorly Sorted	Unimodal, Very Poorly Sorted	Unimodal, Very Poorly Sorted
Mud	Sandy Mud	Sandy Mud
Very Fine Silt	Very Coarse Sandy Very Fine Silt	Very Fine Sandy Fine Silt
51.83	86.46	46.83
215.4	275.8	158.6
5.659	4.232	6.009
36.75	21.46	46.48
5.987	7.689	7.118
4.382	6.182	5.031
1.768	1.364	1.101
6.728	4.217	3.941
7.351	6.956	7.124
2.168	2.679	2.340
-1.770	-1.343	-1.106
6.615	4.077	3.945
5.021	7.192	6.485
3.779	6.073	4.875
0.311	0.468	0.313
1.617	1.572	1.293
7.638	7.119	7.269
1.918	2.602	2.285
-0.311	-0.468	-0.313
1.617	1.572	1.293
Fine Silt	Fine Silt	Fine Silt
Poorly Sorted	Very Poorly Sorted	Very Poorly Sorted
Very Coarse Skewed	Very Coarse Skewed	Very Coarse Skewed
Very Leptokurtic	Very Leptokurtic	Leptokurtic
3.350	3.350	4.700
8.241	8.241	7.754
1.459	1.398	1.265
4.501	4.700	5.150
33.95	196.2	85.74
23.27	140.4	67.78
32.49	194.8	84.48
3.825	5.525	5.820
6.907	10.71	11.22
4.880	2.350	3.544
7.796	7.733	7.601
9.421	9.483	9.627
1.930	4.035	2.716
4.541	7.133	6.083
1.287	1.394	1.409
1.936	2.466	2.541
7.4%	14.6%	11.9%
92.6%	85.4%	88.1%
2.1%	3.7%	0.8%
1.8%	2.8%	1.8%
0.9%	2.5%	2.3%
0.8%	2.7%	2.8%
1.7%	2.9%	4.1%
3.0%	3.1%	4.3%
5.2%	5.0%	6.4%
13.9%	11.7%	14.6%
26.4%	22.2%	21.9%
26.6%	24.7%	20.8%
17.4%	18.8%	20.2%

302-2-A-47-X-5	302-2-A-48-X-1	302-2-A-48-X-1
Cristin Ashmankas,	Cristin Ashmankas,	Cristin Ashmankas,
Unimodal, Very Poorly Sorted	Unimodal, Poorly Sorted	Trimodal, Very Poorly Sorted
Sandy Mud	Mud	Sandy Mud
Very Fine Sandy Fine Silt	Fine Silt	Very Fine Sandy Coarse Silt
52.51	47.76	83.55
191.7	200.6	224.2
6.439	6.253	4.851
48.01	44.57	29.33
10.37	7.384	18.92
4.398	4.088	4.955
0.913	1.475	0.465
4.090	6.117	3.032
6.559	7.046	5.686
2.161	2.068	2.321
-0.943	-1.500	-0.489
4.115	6.073	3.036
9.803	6.549	17.80
4.157	3.640	5.020
0.200	0.234	0.085
1.115	1.360	1.083
6.673	7.255	5.812
2.056	1.864	2.328
-0.200	-0.234	-0.085
1.115	1.360	1.083
Medium Silt	Fine Silt	Coarse Silt
Very Poorly Sorted	Poorly Sorted	Very Poorly Sorted
Coarse Skewed	Coarse Skewed	Symmetrical
Leptokurtic	Leptokurtic	Mesokurtic
6.650	4.700	26.50
		9.400
7.254	7.754	5.259
		6.754
1.954	1.699	2.712
8.558	5.994	17.80
76.19	36.56	166.3
38.99	21.52	61.33
74.24	34.86	163.6
5.984	4.285	8.313
18.70	10.07	43.67
3.714	4.774	2.588
6.868	7.382	5.812
8.999	9.201	8.526
2.423	1.928	3.295
5.285	4.428	5.938
1.471	1.336	1.705
2.581	2.099	3.055
11.7%	6.9%	20.2%
88.3%	93.1%	79.8%
1.7%	1.9%	2.2%
1.2%	1.4%	2.5%
1.2%	1.1%	3.4%
2.3%	0.9%	3.4%
5.3%	1.6%	8.7%
7.9%	4.3%	15.8%
13.3%	9.7%	17.2%
19.9%	19.2%	15.9%
21.1%	26.2%	14.6%
16.1%	21.0%	10.3%
10.0%	12.6%	6.0%

302-2-A-48-X-2	302-2-A-48-X-2	302-2-A-48-X-3
Cristin Ashmankas,	Cristin Ashmankas,	Cristin Ashmankas,
Unimodal, Very Poorly Sorted	Unimodal, Poorly Sorted	Unimodal, Poorly Sorted
Sandy Mud	Mud	Mud
Very Coarse Sandy Fine Silt	Fine Silt	Fine Silt
74.70	38.63	6.227
257.9	182.3	6.744
4.672	7.065	2.960
25.69	55.90	15.14
7.833	5.600	4.031
5.352	4.028	2.491
1.431	1.523	0.110
4.882	6.476	2.649
6.933	7.451	7.955
2.471	2.047	1.317
-1.422	-1.551	-0.110
4.735	6.462	2.649
6.651	4.856	3.976
4.951	3.444	2.547
0.353	0.189	0.010
1.616	1.282	0.975
7.232	7.686	7.974
2.308	1.784	1.349
-0.353	-0.189	-0.010
1.616	1.282	0.975
Fine Silt	Fine Silt	Fine Silt
Very Poorly Sorted	Poorly Sorted	Poorly Sorted
Very Coarse Skewed	Coarse Skewed	Symmetrical
Very Leptokurtic	Leptokurtic	Mesokurtic
4.700	4.700	3.350
7.754	7.754	8.241
1.515	1.289	1.199
5.510	4.643	3.990
105.7	28.15	13.46
69.80	21.84	11.23
104.2	26.86	12.26
4.891	4.276	3.612
10.67	7.484	5.460
3.241	5.151	6.215
7.504	7.751	7.970
9.367	9.599	9.704
2.890	1.864	1.561
6.125	4.449	3.489
1.368	1.314	1.263
2.290	2.096	1.853
11.5%	6.3%	0.0%
88.5%	93.7%	100.0%
3.2%	1.6%	0.0%
2.2%	1.0%	0.0%
2.4%	0.5%	0.0%
1.7%	1.0%	0.0%
1.8%	2.2%	0.0%
3.3%	3.0%	1.4%
7.2%	5.7%	5.8%
16.4%	16.3%	16.6%
24.0%	25.0%	27.1%
22.0%	23.3%	26.5%
15.5%	20.2%	22.7%

302-2-A-48-X-3	302-2-A-48-X-4	302-2-A-48-X-4
Cristin Ashmankas,	Cristin Ashmankas,	Cristin Ashmankas,
Unimodal, Poorly Sorted	Unimodal, Very Poorly Sorted	Unimodal, Poorly Sorted
Mud	Mud	Mud
Fine Silt	Very Fine Silt	Very Fine Silt
12.43	59.13	8.390
21.38	244.6	9.956
5.385	5.207	2.294
43.41	30.55	8.655
6.097	5.964	4.865
3.076	4.548	2.747
0.374	1.777	0.308
2.831	6.925	2.449
7.358	7.335	7.683
1.621	2.244	1.458
-0.374	-1.772	-0.308
2.831	6.687	2.449
6.021	5.118	4.875
3.119	4.313	2.872
0.118	0.325	0.149
0.966	1.708	0.969
7.376	7.610	7.680
1.641	2.109	1.522
-0.118	-0.325	-0.149
0.966	1.708	0.969
Fine Silt	Fine Silt	Fine Silt
Poorly Sorted	Very Poorly Sorted	Poorly Sorted
Coarse Skewed	Very Coarse Skewed	Coarse Skewed
Mesokurtic	Very Leptokurtic	Mesokurtic
4.700	3.350	3.350
7.754	8.241	8.241
1.493	1.393	1.387
5.492	4.572	4.376
28.79	30.34	21.97
19.28	21.79	15.84
27.30	28.95	20.58
4.737	4.166	4.157
10.20	7.545	7.299
5.118	5.043	5.508
7.509	7.773	7.836
9.387	9.488	9.494
1.834	1.882	1.723
4.269	4.445	3.985
1.358	1.309	1.307
2.244	2.059	2.056
2.4%	6.6%	0.0%
97.6%	93.4%	100.0%
0.0%	3.0%	0.0%
0.0%	1.8%	0.0%
0.0%	0.6%	0.0%
0.8%	0.6%	0.0%
1.6%	0.7%	0.0%
6.3%	3.2%	4.6%
12.1%	6.9%	11.0%
17.5%	14.3%	14.3%
24.1%	25.2%	24.5%
21.9%	25.2%	26.3%
15.8%	18.6%	19.2%

302-2-A-49-X-1	302-2-A-49-X-2	302-2-A-49-X-2
Cristin Ashmankas,	Cristin Ashmankas,	Cristin Ashmankas,
Unimodal, Very Poorly Sorted	Unimodal, Poorly Sorted	Unimodal, Poorly Sorted
Mud	Mud	Mud
Fine Silt	Very Fine Silt	Very Fine Silt
67.34	7.614	6.659
271.1	9.581	9.022
4.752	2.870	3.567
25.28	13.07	18.93
6.031	4.400	3.895
4.654	2.739	2.644
1.889	0.286	0.374
7.304	2.652	2.992
7.302	7.828	8.004
2.293	1.454	1.402
-1.866	-0.286	-0.374
6.914	2.652	2.992
5.085	4.315	3.778
4.633	2.826	2.680
0.341	0.092	0.082
1.899	1.021	1.075
7.619	7.856	8.048
2.212	1.499	1.422
-0.341	-0.092	-0.082
1.899	1.021	1.075
Fine Silt	Fine Silt	Very Fine Silt
Very Poorly Sorted	Poorly Sorted	Poorly Sorted
Very Coarse Skewed	Symmetrical	Symmetrical
Very Leptokurtic	Mesokurtic	Mesokurtic
3.350	3.350	3.350
8.241	8.241	8.241
1.421	1.213	1.140
4.622	4.126	3.679
29.35	18.34	14.27
20.66	15.12	12.52
27.93	17.12	13.13
4.096	3.967	3.584
7.487	6.302	5.096
5.091	5.769	6.131
7.757	7.921	8.086
9.459	9.688	9.777
1.858	1.679	1.595
4.368	3.919	3.646
1.306	1.288	1.258
2.034	1.988	1.842
6.8%	0.2%	0.2%
93.2%	99.8%	99.8%
3.8%	0.0%	0.0%
1.9%	0.0%	0.0%
0.1%	0.0%	0.0%
0.1%	0.0%	0.0%
0.9%	0.2%	0.2%
2.7%	3.7%	3.0%
6.6%	8.2%	5.5%
15.1%	14.9%	13.0%
25.4%	25.2%	25.6%
25.3%	25.7%	28.0%
18.1%	22.2%	24.6%

302-2-A-49-X-3	302-2-A-49-X-3	302-2-A-49-X-4
Cristin Ashmankas,	Cristin Ashmankas,	Cristin Ashmankas,
Unimodal, Poorly Sorted	Unimodal, Very Poorly Sorted	Unimodal, Poorly Sorted
Mud	Sandy Mud	Mud
Fine Silt	Very Fine Sandy Fine Silt	Fine Silt
6.271	76.05	42.79
6.676	247.4	184.1
2.849	4.959	6.545
13.98	28.58	49.37
4.109	11.17	6.205
2.453	5.455	4.250
0.123	0.881	1.422
2.677	3.474	5.835
7.927	6.426	7.309
1.294	2.482	2.113
-0.123	-0.894	-1.439
2.677	3.445	5.823
4.049	10.85	5.452
2.504	5.669	3.746
0.018	0.309	0.225
0.987	1.113	1.327
7.948	6.526	7.519
1.324	2.503	1.905
-0.018	-0.309	-0.225
0.987	1.113	1.327
Fine Silt	Medium Silt	Fine Silt
Poorly Sorted	Very Poorly Sorted	Poorly Sorted
Symmetrical	Very Coarse Skewed	Coarse Skewed
Mesokurtic	Leptokurtic	Leptokurtic
3.350	4.700	4.700
8.241	7.754	7.754
1.257	1.728	1.356
4.054	8.147	4.982
13.50	124.5	33.83
10.74	72.02	24.94
12.24	122.7	32.47
3.490	8.841	4.457
5.388	26.31	8.490
6.211	3.006	4.886
7.946	6.939	7.649
9.635	9.177	9.526
1.551	3.053	1.950
3.424	6.170	4.640
1.256	1.620	1.331
1.803	3.144	2.156
0.0%	16.7%	6.9%
100.0%	83.3%	93.1%
0.0%	3.1%	1.5%
0.0%	1.8%	1.4%
0.0%	1.3%	0.9%
0.0%	3.8%	1.2%
0.0%	6.7%	1.9%
1.4%	7.6%	3.6%
5.9%	11.0%	7.7%
16.4%	15.8%	16.2%
27.9%	19.7%	24.7%
27.0%	17.3%	22.5%
21.5%	12.1%	18.4%

302-2-A-49-X-4	302-2-A-49-X-5	302-2-A-49-X-5
Cristin Ashmankas,	Cristin Ashmankas,	Cristin Ashmankas,
Unimodal, Poorly Sorted	Bimodal, Very Poorly Sorted	Unimodal, Poorly Sorted
Mud	Mud	Mud
Very Fine Silt	Fine Silt	Very Fine Silt
6.706	80.27	5.298
8.488	295.1	6.059
3.059	4.348	3.839
14.08	21.29	24.22
4.014	7.579	3.520
2.603	5.084	2.359
0.375	1.585	0.267
2.844	5.865	2.932
7.961	6.951	8.150
1.380	2.424	1.238
-0.375	-1.566	-0.267
2.844	5.538	2.932
3.888	6.611	3.454
2.654	5.188	2.370
0.100	0.351	0.030
1.058	1.709	0.985
8.007	7.241	8.177
1.408	2.375	1.245
-0.100	-0.351	-0.030
1.058	1.709	0.985
Very Fine Silt	Fine Silt	Very Fine Silt
Poorly Sorted	Very Poorly Sorted	Poorly Sorted
Coarse Skewed	Very Coarse Skewed	Symmetrical
Mesokurtic	Very Leptokurtic	Mesokurtic
3.350	4.700	3.350
	1200.0	
8.241	7.754	8.241
	-0.243	
1.199	1.541	1.154
3.755	5.676	3.435
14.97	49.13	10.64
12.49	31.88	9.217
13.77	47.59	9.485
3.579	4.995	3.261
5.220	11.23	4.309
6.062	4.347	6.554
8.057	7.461	8.185
9.704	9.342	9.759
1.601	2.149	1.489
3.643	4.994	3.204
1.259	1.377	1.233
1.840	2.321	1.705
0.0%	8.8%	0.0%
100.0%	91.2%	100.0%
0.0%	4.7%	0.0%
0.0%	2.0%	0.0%
0.0%	0.1%	0.0%
0.0%	0.4%	0.0%
0.0%	1.6%	0.0%
3.0%	4.7%	1.1%
6.4%	9.4%	3.6%
13.1%	16.6%	12.5%
25.8%	23.9%	26.7%
28.1%	21.6%	30.3%
23.7%	15.0%	25.8%

302-2-A-50-X-1	302-2-A-50-X-1	302-2-A-50-X-2
Cristin Ashmankas,	Cristin Ashmankas,	Cristin Ashmankas,
Unimodal, Poorly Sorted	Unimodal, Poorly Sorted	Unimodal, Poorly Sorted
Mud	Mud	Mud
Fine Silt	Fine Silt	Fine Silt
38.67	6.430	26.66
167.1	6.932	96.98
6.553	2.773	7.568
50.53	14.12	73.84
6.036	4.073	6.022
4.008	2.574	3.811
1.493	0.078	1.311
6.315	2.496	5.002
7.362	7.940	7.375
2.015	1.364	1.930
-1.504	-0.078	-1.311
6.314	2.496	5.002
5.286	4.025	5.246
3.346	2.646	3.479
0.187	0.007	0.268
1.211	0.940	1.386
7.563	7.957	7.575
1.742	1.404	1.799
-0.187	-0.007	-0.268
1.211	0.940	1.386
Fine Silt	Fine Silt	Fine Silt
Poorly Sorted	Poorly Sorted	Poorly Sorted
Coarse Skewed	Symmetrical	Coarse Skewed
Leptokurtic	Mesokurtic	Leptokurtic
3.350	3.350	3.350
8.241	8.241	8.241
1.404	1.151	1.481
4.918	4.034	4.702
28.46	14.38	36.01
20.27	12.49	24.31
27.06	13.23	34.52
4.293	3.941	3.981
8.151	5.967	7.470
5.135	6.120	4.796
7.668	7.954	7.733
9.476	9.763	9.399
1.846	1.595	1.960
4.341	3.643	4.603
1.321	1.284	1.300
2.102	1.979	1.993
5.6%	0.0%	7.7%
94.4%	100.0%	92.3%
1.0%	0.0%	0.2%
1.8%	0.0%	0.9%
0.9%	0.0%	1.3%
0.2%	0.0%	2.5%
1.7%	0.0%	2.9%
3.6%	1.3%	3.0%
7.6%	7.0%	5.8%
16.9%	17.4%	15.1%
24.9%	25.6%	26.0%
23.4%	25.0%	25.6%
17.9%	23.7%	16.9%

302-2-A-50-X-2	302-2-A-51-X-1	302-2-A-51-X-1
Cristin Ashmankas,	Cristin Ashmankas,	Cristin Ashmankas,
Unimodal, Very Poorly Sorted	Unimodal, Poorly Sorted	Unimodal, Poorly Sorted
Sandy Mud	Mud	Sandy Mud
Very Coarse Sandy Very Fine Silt	Fine Silt	Very Fine Sandy Coarse Silt
85.38	16.25	59.20
285.7	81.58	208.8
4.194	8.431	6.356
20.74	76.41	44.93
6.837	4.550	14.61
5.944	2.847	4.248
1.531	1.604	0.455
4.972	8.989	3.730
7.117	7.780	6.045
2.635	1.509	2.114
-1.501	-1.604	-0.521
4.747	8.989	3.791
5.478	4.244	14.18
5.280	2.430	3.890
0.370	0.040	-0.071
1.763	1.012	0.899
7.512	7.880	6.140
2.400	1.281	1.960
-0.370	-0.040	0.071
1.763	1.012	0.899
Fine Silt	Fine Silt	Medium Silt
Very Poorly Sorted	Poorly Sorted	Poorly Sorted
Very Coarse Skewed	Symmetrical	Symmetrical
Very Leptokurtic	Mesokurtic	Platykurtic
3.350	3.350	26.50
8.241	8.241	5.259
1.279	1.411	2.324
4.599	4.208	15.32
169.2	13.66	76.56
132.3	9.678	32.94
167.9	12.25	74.24
4.777	3.297	7.227
8.543	5.348	32.92
2.563	6.194	3.707
7.765	7.892	6.028
9.611	9.469	8.749
3.750	1.529	2.360
7.048	3.275	5.042
1.345	1.245	1.606
2.256	1.721	2.853
12.0%	1.8%	13.3%
88.0%	98.2%	86.7%
4.1%	0.0%	2.3%
2.7%	1.2%	1.0%
2.1%	0.4%	0.4%
1.8%	0.1%	0.8%
1.4%	0.1%	8.8%
1.9%	0.9%	17.1%
5.1%	4.8%	19.1%
13.7%	16.8%	16.9%
23.1%	29.0%	14.7%
23.7%	27.9%	11.3%
20.4%	18.8%	7.6%

302-2-A-51-X-2	302-2-A-51-X-2	302-2-A-52-X-1
Cristin Ashmankas,	Cristin Ashmankas,	Cristin Ashmankas,
Unimodal, Poorly Sorted	Unimodal, Poorly Sorted	Unimodal, Poorly Sorted
Mud	Sandy Mud	Sandy Mud
Coarse Silt	Very Fine Sandy Coarse Silt	Very Fine Sandy Medium Silt
45.42	53.27	49.35
160.8	185.5	146.7
7.533	6.891	6.649
65.33	53.55	55.69
13.82	14.40	14.15
3.770	4.146	4.141
0.348	0.356	0.418
3.992	3.602	3.418
6.168	6.085	6.137
1.920	2.069	2.053
-0.368	-0.404	-0.427
4.021	3.663	3.432
13.13	13.96	13.49
3.412	3.861	3.992
-0.202	-0.095	0.023
0.905	0.892	1.020
6.251	6.163	6.211
1.771	1.949	1.997
0.202	0.095	-0.023
0.905	0.892	1.020
Medium Silt	Medium Silt	Medium Silt
Poorly Sorted	Poorly Sorted	Poorly Sorted
Fine Skewed	Symmetrical	Symmetrical
Mesokurtic	Platykurtic	Mesokurtic
26.50	26.50	18.80
5.259	5.259	5.754
2.296	2.220	2.370
15.74	15.28	13.61
54.70	72.94	77.96
23.83	32.85	32.90
52.41	70.72	75.59
5.892	7.135	6.478
27.06	32.59	29.00
4.192	3.777	3.681
5.990	6.032	6.200
8.767	8.815	8.721
2.091	2.334	2.369
4.575	5.038	5.040
1.518	1.600	1.554
2.559	2.835	2.696
7.0%	12.7%	12.8%
93.0%	87.3%	87.2%
1.1%	1.7%	0.7%
1.0%	1.0%	1.6%
0.9%	0.5%	1.6%
0.2%	0.4%	1.9%
3.8%	9.0%	7.0%
19.4%	17.5%	14.4%
23.8%	19.3%	19.0%
17.6%	17.5%	19.1%
13.6%	14.0%	16.4%
10.8%	10.9%	10.8%
7.8%	8.2%	7.5%

302-2-A-52-X-1	302-2-A-52-X-2	302-2-A-53-X-1
Cristin Ashmankas,	Cristin Ashmankas,	Cristin Ashmankas,
Bimodal, Poorly Sorted	Unimodal, Poorly Sorted	Unimodal, Poorly Sorted
Mud	Sandy Mud	Mud
Coarse Silt	Very Fine Sandy Coarse Silt	Coarse Silt
17.37	41.48	29.02
17.85	134.3	106.5
1.526	9.421	12.72
5.163	102.5	178.1
9.607	16.09	12.55
3.180	3.438	3.260
-0.172	0.155	-0.044
2.060	3.741	3.517
6.702	5.935	6.303
1.669	1.794	1.716
0.172	-0.224	-0.016
2.060	3.849	3.657
9.735	15.97	12.58
3.313	3.271	3.200
-0.067	-0.120	-0.201
0.794	0.958	0.888
6.683	5.969	6.313
1.728	1.710	1.678
0.067	0.120	0.201
0.794	0.958	0.888
Medium Silt	Coarse Silt	Medium Silt
Poorly Sorted	Poorly Sorted	Poorly Sorted
Symmetrical	Fine Skewed	Fine Skewed
Platykurtic	Mesokurtic	Platykurtic
26.50	26.50	26.50
4.700		
5.259	5.259	5.259
7.754		
1.950	3.145	2.375
10.19	17.50	14.61
42.61	66.55	48.86
21.85	21.16	20.57
40.66	63.40	46.48
6.654	5.178	5.436
21.53	29.80	24.50
4.553	3.909	4.355
6.616	5.836	6.097
9.002	8.313	8.718
1.977	2.126	2.002
4.449	4.403	4.363
1.516	1.499	1.483
2.734	2.372	2.443
2.7%	11.0%	4.6%
97.3%	89.0%	95.4%
0.0%	0.9%	0.6%
0.0%	0.6%	0.3%
0.0%	0.6%	0.1%
0.0%	0.7%	0.0%
2.7%	8.3%	3.7%
15.9%	19.2%	18.9%
20.5%	23.5%	24.5%
17.6%	19.2%	19.1%
17.6%	13.8%	14.8%
15.6%	8.5%	10.8%
10.0%	4.7%	7.4%

302-2-A-53-X-2	302-2-A-53-X-2	302-2-A-53-X-3
Cristin Ashmankas,	Cristin Ashmankas,	Cristin Ashmankas,
Unimodal, Poorly Sorted	Unimodal, Poorly Sorted	Trimodal, Very Poorly Sorted
Mud	Sandy Mud	Sandy Mud
Coarse Silt	Very Fine Sandy Very Coarse Silt	Very Fine Sandy Coarse Silt
43.35	44.64	71.19
172.1	152.1	213.6
7.530	9.000	4.938
63.00	89.12	30.01
12.94	16.66	13.83
3.388	3.595	4.926
0.668	0.010	0.682
5.343	3.629	3.458
6.248	5.873	6.156
1.778	1.863	2.311
-0.735	-0.102	-0.694
5.425	3.763	3.461
12.53	16.68	12.37
2.960	3.422	4.935
-0.098	-0.213	0.109
1.015	0.920	1.138
6.318	5.905	6.337
1.566	1.775	2.303
0.098	0.213	-0.109
1.015	0.920	1.138
Medium Silt	Coarse Silt	Medium Silt
Poorly Sorted	Poorly Sorted	Very Poorly Sorted
Symmetrical	Fine Skewed	Coarse Skewed
Mesokurtic	Mesokurtic	Leptokurtic
18.80	37.50	26.50
		6.650
5.754	4.759	5.259
		7.254
2.895	2.850	2.039
13.34	19.71	12.63
45.56	69.22	87.24
15.73	24.29	42.78
42.66	66.37	85.20
4.309	5.728	7.948
20.34	33.93	29.89
4.456	3.853	3.519
6.228	5.665	6.307
8.432	8.455	8.938
1.892	2.195	2.540
3.976	4.602	5.419
1.402	1.547	1.614
2.107	2.518	2.991
5.4%	12.1%	13.0%
94.6%	87.9%	87.0%
1.4%	1.3%	1.8%
0.9%	0.4%	2.8%
0.4%	0.2%	2.4%
0.2%	0.2%	1.4%
2.5%	10.0%	4.5%
13.9%	22.5%	14.2%
24.9%	22.3%	18.0%
24.1%	16.4%	15.8%
16.9%	12.1%	16.2%
9.1%	8.7%	13.5%
5.7%	5.8%	9.3%

302-2-A-53-X-3	302-2-A-53-X-4	302-2-A-53-X-4
Cristin Ashmankas,	Cristin Ashmankas,	Cristin Ashmankas,
Unimodal, Poorly Sorted	Unimodal, Poorly Sorted	Unimodal, Poorly Sorted
Mud	Mud	Mud
Coarse Silt	Coarse Silt	Medium Silt
45.19	26.10	21.76
156.2	105.2	63.38
7.564	12.50	11.40
66.22	175.0	157.5
14.91	10.65	10.05
3.506	3.136	3.126
0.407	0.236	0.068
4.473	4.092	3.585
6.060	6.540	6.636
1.815	1.661	1.645
-0.429	-0.298	-0.068
4.502	4.255	3.585
14.20	10.52	9.997
3.120	3.008	3.033
-0.180	-0.130	-0.115
1.002	0.905	0.934
6.138	6.571	6.644
1.642	1.589	1.601
0.180	0.130	0.115
1.002	0.905	0.934
Medium Silt	Medium Silt	Medium Silt
Poorly Sorted	Poorly Sorted	Poorly Sorted
Fine Skewed	Fine Skewed	Fine Skewed
Mesokurtic	Mesokurtic	Mesokurtic
26.50	18.80	18.80
5.259	5.754	5.754
2.923	2.317	2.135
16.46	11.59	10.74
52.90	39.83	38.17
18.10	17.19	17.88
49.97	37.51	36.03
4.681	4.950	4.832
24.63	18.86	17.84
4.241	4.650	4.712
5.925	6.431	6.541
8.418	8.754	8.872
1.985	1.882	1.883
4.178	4.104	4.160
1.446	1.427	1.415
2.227	2.308	2.272
6.8%	3.1%	2.5%
93.2%	96.9%	97.5%
1.0%	0.6%	0.1%
1.0%	0.3%	0.4%
0.9%	0.3%	0.5%
0.9%	0.2%	0.3%
3.0%	1.7%	1.2%
18.3%	12.8%	12.1%
26.9%	24.0%	22.7%
19.7%	22.4%	23.1%
13.9%	17.6%	18.9%
8.9%	12.7%	11.9%
5.5%	7.4%	8.7%

302-2-A-54-X-1	302-2-A-54-X-1	302-2-A-55-X-1
Cristin Ashmankas,	Cristin Ashmankas,	Cristin Ashmankas,
Unimodal, Poorly Sorted	Unimodal, Poorly Sorted	Unimodal, Poorly Sorted
Sandy Mud	Mud	Mud
Very Fine Sandy Coarse Silt	Coarse Silt	Coarse Silt
44.26	50.82	39.55
103.7	192.9	164.6
6.427	6.667	8.709
52.87	49.61	81.70
16.68	13.54	11.80
3.878	3.689	3.595
0.060	0.637	0.509
2.959	4.900	4.249
5.906	6.174	6.357
1.955	1.904	1.882
-0.060	-0.704	-0.626
2.959	4.959	4.449
16.16	12.90	11.54
3.782	3.211	3.370
-0.142	-0.134	-0.042
0.927	0.996	0.932
5.951	6.276	6.437
1.919	1.683	1.753
0.142	0.134	0.042
0.927	0.996	0.932
Coarse Silt	Medium Silt	Medium Silt
Poorly Sorted	Poorly Sorted	Poorly Sorted
Fine Skewed	Fine Skewed	Symmetrical
Mesokurtic	Mesokurtic	Mesokurtic
26.50	18.80	18.80
5.259	5.754	5.754
2.603	2.599	2.362
18.61	14.46	12.13
80.27	51.34	52.53
30.83	19.75	22.24
77.67	48.74	50.16
6.645	4.883	5.692
35.50	23.08	22.76
3.639	4.284	4.251
5.748	6.112	6.365
8.585	8.588	8.726
2.359	2.005	2.053
4.946	4.304	4.475
1.596	1.448	1.484
2.732	2.288	2.509
14.5%	6.7%	7.3%
85.5%	93.3%	92.7%
0.2%	1.8%	1.6%
1.2%	1.1%	0.2%
1.5%	0.5%	0.3%
1.7%	0.1%	1.1%
9.8%	3.2%	4.2%
19.6%	15.7%	13.9%
20.9%	25.1%	21.4%
15.8%	21.1%	19.9%
13.1%	15.0%	17.8%
9.7%	10.0%	12.5%
6.5%	6.5%	7.1%

302-2-A-55-X-2	302-2-A-55-X-2	302-2-A-55-X-3
Cristin Ashmankas,	Cristin Ashmankas,	Cristin Ashmankas,
Bimodal, Very Poorly Sorted	Unimodal, Very Poorly Sorted	Unimodal, Poorly Sorted
Sandy Mud	Sandy Mud	Mud
Very Fine Sandy Medium Silt	Very Fine Sandy Coarse Silt	Coarse Silt
66.88	65.02	33.61
220.4	232.6	113.7
5.493	5.460	9.179
35.39	33.71	99.28
13.20	12.40	12.98
4.617	4.454	3.308
0.774	0.812	0.256
3.860	4.291	4.097
6.198	6.281	6.268
2.232	2.187	1.726
-0.807	-0.857	-0.256
3.863	4.290	4.097
12.02	11.46	12.61
4.508	4.188	3.070
0.121	0.065	-0.185
1.187	1.098	0.927
6.378	6.447	6.309
2.172	2.066	1.618
-0.121	-0.065	0.185
1.187	1.098	0.927
Medium Silt	Medium Silt	Medium Silt
Very Poorly Sorted	Very Poorly Sorted	Poorly Sorted
Coarse Skewed	Symmetrical	Fine Skewed
Leptokurtic	Mesokurtic	Mesokurtic
18.80	18.80	26.50
9.400		
5.754	5.754	5.259
6.754		
2.189	2.095	2.623
11.93	11.82	14.51
84.79	64.78	46.49
38.74	30.92	17.73
82.60	62.68	43.87
6.551	6.564	4.930
25.52	24.63	22.53
3.560	3.948	4.427
6.389	6.403	6.107
8.836	8.899	8.575
2.482	2.254	1.937
5.276	4.950	4.148
1.537	1.532	1.447
2.712	2.715	2.301
12.2%	10.4%	5.1%
87.8%	89.6%	94.9%
2.3%	2.7%	0.4%
1.6%	1.6%	0.8%
2.1%	0.6%	0.5%
2.1%	0.7%	0.5%
4.1%	4.7%	2.8%
11.8%	12.7%	16.1%
18.7%	19.4%	26.5%
18.7%	18.6%	20.1%
17.5%	17.0%	15.3%
12.8%	13.2%	10.6%
8.2%	8.8%	6.3%

302-2-A-55-X-3	302-2-A-55-X-4	302-2-A-55-X-4
Cristin Ashmankas,	Cristin Ashmankas,	Cristin Ashmankas,
Unimodal, Poorly Sorted	Unimodal, Poorly Sorted	Bimodal, Poorly Sorted
Mud	Mud	Sandy Mud
Medium Silt	Coarse Silt	Very Fine Sandy Coarse Silt
59.82	24.38	43.76
227.3	45.18	137.4
5.715	13.25	7.600
36.46	248.9	71.67
12.15	13.01	13.12
4.014	3.170	3.987
0.947	-0.276	0.439
5.207	2.747	3.348
6.311	6.264	6.244
2.040	1.664	2.000
-1.010	0.276	-0.453
5.197	2.747	3.374
11.27	13.09	12.45
3.566	3.200	3.765
0.015	-0.215	-0.001
1.144	0.906	0.891
6.472	6.256	6.328
1.834	1.678	1.912
-0.015	0.215	0.001
1.144	0.906	0.891
Medium Silt	Medium Silt	Medium Silt
Poorly Sorted	Poorly Sorted	Poorly Sorted
Symmetrical	Fine Skewed	Symmetrical
Leptokurtic	Mesokurtic	Platykurtic
18.80	26.50	26.50
		6.650
5.754	5.259	5.259
		7.254
2.372	2.483	2.294
11.89	15.50	12.74
49.06	50.57	64.69
20.68	20.37	28.20
46.69	48.08	62.39
5.028	5.355	7.189
20.43	24.85	28.88
4.349	4.306	3.950
6.394	6.012	6.295
8.720	8.654	8.768
2.005	2.010	2.220
4.370	4.348	4.818
1.440	1.481	1.581
2.330	2.421	2.846
7.1%	5.6%	10.5%
92.9%	94.4%	89.5%
2.7%	0.0%	0.7%
1.3%	0.2%	1.1%
0.6%	0.1%	1.5%
0.5%	0.5%	1.3%
2.1%	4.7%	5.9%
11.7%	18.6%	16.5%
22.2%	25.6%	18.4%
22.3%	18.3%	16.4%
17.8%	14.6%	17.7%
11.5%	10.5%	13.1%
7.3%	6.9%	7.5%

302-2-A-55-X-5	302-2-A-55-X-5	302-2-A-56-X-1
Cristin Ashmankas,	Cristin Ashmankas,	Cristin Ashmankas,
Unimodal, Poorly Sorted	Unimodal, Poorly Sorted	Unimodal, Poorly Sorted
Mud	Mud	Mud
Coarse Silt	Coarse Silt	Coarse Silt
47.30	32.52	42.16
154.1	87.41	158.3
7.390	11.68	8.440
65.70	177.5	77.96
14.72	14.61	15.15
3.794	3.407	3.345
0.370	-0.153	0.218
3.887	3.256	4.565
6.070	6.091	6.020
1.933	1.772	1.756
-0.403	0.131	-0.297
3.932	3.301	4.677
13.89	14.37	14.91
3.433	3.273	3.072
-0.165	-0.285	-0.216
0.971	0.910	0.992
6.169	6.121	6.068
1.779	1.710	1.619
0.165	0.285	0.216
0.971	0.910	0.992
Medium Silt	Medium Silt	Medium Silt
Poorly Sorted	Poorly Sorted	Poorly Sorted
Fine Skewed	Fine Skewed	Fine Skewed
Mesokurtic	Mesokurtic	Mesokurtic
26.50	26.50	26.50
5.259	5.259	5.259
2.574	2.533	2.967
16.45	18.23	17.45
57.62	54.37	54.32
22.38	21.46	18.31
55.04	51.83	51.36
5.630	5.538	4.579
27.40	28.09	25.85
4.117	4.201	4.202
5.926	5.777	5.841
8.602	8.625	8.397
2.089	2.053	1.998
4.484	4.424	4.194
1.508	1.507	1.446
2.493	2.469	2.195
8.3%	6.5%	6.8%
91.7%	93.5%	93.2%
1.0%	0.3%	1.3%
1.1%	0.3%	0.6%
1.7%	1.1%	0.0%
0.9%	0.5%	0.0%
3.7%	4.3%	4.8%
18.9%	22.1%	20.3%
24.5%	26.6%	27.1%
17.3%	15.3%	19.3%
14.3%	12.9%	12.8%
10.1%	9.7%	8.4%
6.6%	6.9%	5.5%

302-2-A-56-X-1	302-2-A-56-X-2	302-2-A-56-X-2
Cristin Ashmankas,	Cristin Ashmankas,	Cristin Ashmankas,
Unimodal, Poorly Sorted	Unimodal, Poorly Sorted	Unimodal, Poorly Sorted
Sandy Mud	Sandy Mud	Mud
Very Fine Sandy Coarse Silt	Very Fine Sandy Coarse Silt	Coarse Silt
47.84	48.23	26.47
145.1	174.4	29.13
8.479	7.751	3.870
83.78	65.81	30.92
18.38	15.60	15.43
3.595	3.697	3.082
-0.015	0.219	-0.482
3.691	3.958	2.723
5.745	5.971	6.018
1.854	1.903	1.624
-0.037	-0.290	0.482
3.757	4.052	2.723
18.18	15.39	15.51
3.384	3.431	3.119
-0.232	-0.184	-0.258
1.009	0.925	0.944
5.782	6.022	6.010
1.759	1.779	1.641
0.232	0.184	0.258
1.009	0.925	0.944
Coarse Silt	Medium Silt	Medium Silt
Poorly Sorted	Poorly Sorted	Poorly Sorted
Fine Skewed	Fine Skewed	Fine Skewed
Mesokurtic	Mesokurtic	Mesokurtic
26.50	26.50	26.50
5.259	5.259	5.259
3.078	2.683	2.982
21.90	17.82	18.93
72.65	64.35	56.29
23.60	23.98	18.87
69.58	61.66	53.30
5.080	5.750	4.944
33.89	31.14	28.26
3.783	3.958	4.151
5.513	5.810	5.723
8.344	8.542	8.389
2.206	2.158	2.021
4.561	4.584	4.238
1.513	1.534	1.478
2.345	2.524	2.306
12.9%	10.6%	7.2%
87.1%	89.4%	92.8%
1.0%	1.6%	0.0%
0.7%	0.6%	0.0%
0.9%	0.1%	0.2%
0.6%	0.1%	0.9%
9.7%	8.1%	6.2%
23.5%	20.7%	22.7%
24.4%	22.8%	26.7%
15.5%	17.3%	16.7%
10.8%	13.1%	12.8%
7.5%	9.2%	8.6%
5.4%	6.3%	5.3%

302-2-A-56-X-3	302-2-A-56-X-3	302-2-A-57-X-1
Cristin Ashmankas,	Cristin Ashmankas,	Cristin Ashmankas,
Unimodal, Poorly Sorted	Unimodal, Poorly Sorted	Unimodal, Poorly Sorted
Mud	Mud	Mud
Coarse Silt	Coarse Silt	Coarse Silt
39.08	19.93	52.16
138.4	20.28	190.4
9.085	2.157	6.510
93.18	10.78	48.37
14.65	11.41	12.49
3.391	3.151	4.053
0.166	-0.408	0.668
4.094	2.485	4.211
6.087	6.454	6.292
1.766	1.656	2.039
-0.186	0.408	-0.713
4.128	2.485	4.257
14.28	11.66	11.72
3.182	3.218	3.659
-0.206	-0.184	-0.032
0.965	0.884	0.971
6.130	6.423	6.415
1.670	1.686	1.872
0.206	0.184	0.032
0.965	0.884	0.971
Medium Silt	Medium Silt	Medium Silt
Poorly Sorted	Poorly Sorted	Poorly Sorted
Fine Skewed	Fine Skewed	Symmetrical
Mesokurtic	Platykurtic	Mesokurtic
26.50	26.50	18.80
5.259	5.259	5.754
2.742	2.215	2.228
16.77	13.32	12.59
54.76	44.62	58.65
19.97	20.14	26.32
52.01	42.40	56.42
4.949	5.601	6.177
26.10	22.99	24.07
4.191	4.486	4.092
5.898	6.230	6.311
8.510	8.818	8.810
2.031	1.966	2.153
4.320	4.332	4.718
1.468	1.482	1.513
2.307	2.486	2.627
7.0%	3.8%	9.0%
93.0%	96.2%	91.0%
0.8%	0.0%	1.7%
0.6%	0.0%	1.4%
0.4%	0.0%	0.6%
0.0%	0.2%	0.9%
5.1%	3.5%	4.5%
19.5%	17.2%	13.4%
26.0%	24.5%	21.5%
19.0%	18.8%	18.6%
13.2%	16.1%	16.5%
9.2%	11.2%	13.0%
6.1%	8.3%	7.9%

302-2-A-57-X-2	302-2-A-57-X-2	302-2-A-57-X-3
Cristin Ashmankas,	Cristin Ashmankas,	Cristin Ashmankas,
Unimodal, Poorly Sorted	Unimodal, Poorly Sorted	Unimodal, Poorly Sorted
Mud	Mud	Mud
Coarse Silt	Coarse Silt	Coarse Silt
49.33	49.92	40.29
187.1	176.7	157.2
7.006	6.378	8.681
54.18	48.14	81.84
14.61	12.52	13.80
3.544	3.822	3.451
0.492	0.810	0.255
4.919	4.731	4.262
6.065	6.305	6.153
1.844	1.945	1.804
-0.570	-0.835	-0.334
4.998	4.755	4.390
13.96	11.51	13.49
3.132	3.438	3.245
-0.200	-0.010	-0.196
1.012	1.105	0.946
6.162	6.441	6.212
1.647	1.782	1.698
0.200	0.010	0.196
1.012	1.105	0.946
Medium Silt	Medium Silt	Medium Silt
Poorly Sorted	Poorly Sorted	Poorly Sorted
Fine Skewed	Symmetrical	Fine Skewed
Mesokurtic	Mesokurtic	Mesokurtic
26.50	18.80	26.50
5.259	5.754	5.259
2.826	2.481	2.556
16.55	12.31	15.90
52.47	49.31	53.79
18.57	19.87	21.05
49.65	46.83	51.24
4.573	4.948	5.155
23.84	20.51	25.16
4.252	4.342	4.216
5.917	6.344	5.975
8.467	8.655	8.612
1.991	1.993	2.043
4.215	4.313	4.396
1.436	1.437	1.473
2.193	2.307	2.366
6.8%	7.2%	6.9%
93.2%	92.8%	93.1%
1.8%	1.2%	1.3%
1.0%	1.7%	0.5%
0.1%	1.3%	0.0%
0.1%	0.7%	0.1%
3.8%	2.3%	5.0%
17.3%	11.7%	18.1%
28.2%	23.1%	25.7%
19.6%	22.3%	19.2%
12.8%	17.4%	13.3%
9.6%	11.6%	10.4%
5.6%	6.7%	6.5%

302-2-A-57-X-3	302-2-A-57-X-4	302-2-A-57-X-4
Cristin Ashmankas,	Cristin Ashmankas,	Cristin Ashmankas,
Unimodal, Poorly Sorted	Unimodal, Poorly Sorted	Unimodal, Poorly Sorted
Mud	Mud	Sandy Mud
Coarse Silt	Coarse Silt	Very Fine Sandy Coarse Silt
44.43	35.85	42.68
154.6	104.9	137.2
7.946	8.798	9.895
72.61	97.27	108.1
14.74	13.95	18.35
3.527	3.417	3.300
0.412	0.285	-0.104
4.272	3.720	3.857
6.065	6.164	5.742
1.830	1.773	1.734
-0.461	-0.285	0.014
4.341	3.720	3.983
14.17	13.45	18.46
3.207	3.228	3.148
-0.109	-0.074	-0.248
1.002	1.003	0.979
6.141	6.216	5.759
1.681	1.691	1.654
0.109	0.074	0.248
1.002	1.003	0.979
Medium Silt	Medium Silt	Coarse Silt
Poorly Sorted	Poorly Sorted	Poorly Sorted
Fine Skewed	Symmetrical	Fine Skewed
Mesokurtic	Mesokurtic	Mesokurtic
26.50	18.80	26.50
5.259	5.754	5.259
2.967	2.892	3.424
15.63	14.46	22.19
57.88	56.37	67.45
19.51	19.49	19.70
54.92	53.47	64.03
4.874	4.940	4.734
25.21	23.99	32.59
4.111	4.149	3.890
5.999	6.112	5.494
8.397	8.434	8.190
2.043	2.033	2.105
4.286	4.285	4.300
1.459	1.456	1.488
2.285	2.304	2.243
8.5%	8.2%	11.5%
91.5%	91.8%	88.5%
1.1%	0.3%	1.0%
0.9%	0.7%	0.4%
0.7%	1.0%	0.1%
1.1%	1.7%	0.4%
4.8%	4.5%	9.7%
16.9%	15.5%	24.7%
24.6%	23.8%	25.3%
20.7%	21.2%	15.7%
14.9%	16.2%	11.0%
9.1%	9.7%	7.5%
5.2%	5.4%	4.1%

302-2-A-57-X-5	302-2-A-57-X-5	302-2-A-58-X-1
Cristin Ashmankas,	Cristin Ashmankas,	Cristin Ashmankas,
Unimodal, Poorly Sorted	Unimodal, Poorly Sorted	Unimodal, Poorly Sorted
Mud	Sandy Mud	Sandy Mud
Coarse Silt	Very Fine Sandy Coarse Silt	Very Fine Sandy Coarse Silt
21.41	49.16	39.32
18.40	147.7	110.3
1.415	7.666	9.745
5.460	71.66	115.4
13.63	16.76	17.32
2.837	3.694	3.257
-0.565	0.339	0.026
2.647	3.708	3.776
6.198	5.884	5.847
1.505	1.892	1.705
0.565	-0.371	-0.041
2.647	3.750	3.800
13.90	16.08	17.09
2.898	3.536	3.090
-0.257	-0.044	-0.160
0.922	1.069	1.017
6.169	5.959	5.870
1.535	1.822	1.628
0.257	0.044	0.160
0.922	1.069	1.017
Medium Silt	Coarse Silt	Coarse Silt
Poorly Sorted	Poorly Sorted	Poorly Sorted
Fine Skewed	Symmetrical	Fine Skewed
Mesokurtic	Mesokurtic	Mesokurtic
26.50	26.50	26.50
5.259	5.259	5.259
2.966	3.180	3.538
16.64	17.35	19.24
45.45	75.66	62.95
15.32	23.79	17.79
42.48	72.48	59.41
4.528	5.224	4.520
23.42	29.78	28.93
4.460	3.724	3.990
5.909	5.849	5.700
8.397	8.297	8.143
1.883	2.228	2.041
3.937	4.573	4.153
1.431	1.501	1.458
2.179	2.385	2.176
3.3%	12.3%	10.2%
96.7%	87.7%	89.8%
0.0%	0.9%	0.5%
0.0%	1.0%	0.6%
0.0%	1.5%	0.7%
0.0%	2.4%	1.4%
3.3%	6.6%	7.0%
20.0%	17.6%	21.0%
29.2%	23.5%	26.3%
19.0%	19.2%	18.7%
14.0%	14.2%	12.5%
9.4%	8.5%	7.2%
5.1%	4.6%	4.1%

302-2-A-58-X-1	302-2-A-58-X-2	302-2-A-58-X-2
Cristin Ashmankas,	Cristin Ashmankas,	Cristin Ashmankas,
Bimodal, Poorly Sorted	Unimodal, Poorly Sorted	Unimodal, Poorly Sorted
Mud	Mud	Mud
Coarse Silt	Coarse Silt	Medium Silt
45.09	44.53	39.05
174.9	172.7	164.7
7.425	7.504	8.375
61.34	62.97	76.39
12.44	12.29	11.30
3.785	3.747	3.517
0.495	0.535	0.611
4.253	4.393	4.789
6.303	6.319	6.435
1.939	1.925	1.841
-0.551	-0.592	-0.697
4.334	4.474	4.928
11.90	11.69	10.97
3.426	3.373	3.208
-0.157	-0.140	-0.034
0.897	0.935	0.990
6.393	6.419	6.510
1.776	1.754	1.682
0.157	0.140	0.034
0.897	0.935	0.990
Medium Silt	Medium Silt	Medium Silt
Poorly Sorted	Poorly Sorted	Poorly Sorted
Fine Skewed	Fine Skewed	Symmetrical
Platykurtic	Mesokurtic	Mesokurtic
26.50	26.50	13.30
4.700		
5.259	5.259	6.254
7.754		
2.200	2.247	2.398
13.95	13.54	11.35
51.17	48.53	46.04
23.26	21.59	19.20
48.97	46.28	43.64
6.092	5.695	4.960
24.18	22.83	19.67
4.289	4.365	4.441
6.163	6.207	6.462
8.828	8.798	8.704
2.059	2.015	1.960
4.540	4.433	4.263
1.510	1.485	1.432
2.607	2.510	2.310
6.7%	6.4%	6.1%
93.3%	93.6%	93.9%
1.5%	1.5%	1.5%
0.9%	0.8%	0.4%
0.3%	0.6%	0.3%
0.5%	0.9%	1.0%
3.5%	2.6%	3.0%
15.5%	14.2%	12.0%
24.6%	25.1%	21.3%
17.6%	18.8%	22.8%
14.7%	15.2%	18.8%
12.7%	12.4%	11.8%
8.1%	7.8%	7.2%

302-2-A-58-X-3	302-2-A-58-X-3	302-2-A-58-X-4
Cristin Ashmankas,	Cristin Ashmankas,	Cristin Ashmankas,
Unimodal, Poorly Sorted	Unimodal, Poorly Sorted	Unimodal, Poorly Sorted
Mud	Sandy Mud	Mud
Coarse Silt	Very Fine Sandy Very Coarse Silt	Coarse Silt
37.94	32.22	22.20
92.49	24.21	20.05
5.829	1.073	1.526
41.94	4.134	5.776
14.00	21.75	13.55
3.710	2.756	2.994
0.242	-0.993	-0.548
3.333	3.648	2.572
6.159	5.523	6.206
1.891	1.463	1.582
-0.242	0.993	0.548
3.333	3.648	2.572
13.33	22.97	13.70
3.555	2.726	3.082
-0.073	-0.306	-0.270
1.007	1.187	0.935
6.230	5.444	6.189
1.830	1.447	1.624
0.073	0.306	0.270
1.007	1.187	0.935
Medium Silt	Coarse Silt	Medium Silt
Poorly Sorted	Poorly Sorted	Poorly Sorted
Symmetrical	Very Fine Skewed	Fine Skewed
Mesokurtic	Leptokurtic	Mesokurtic
26.50	37.50	26.50
5.259	4.759	5.259
2.548	4.641	2.621
14.65	26.87	16.79
60.67	64.82	48.75
23.81	13.97	18.60
58.12	60.18	46.13
5.677	3.307	4.828
26.42	30.89	24.44
4.043	3.947	4.358
6.093	5.218	5.896
8.616	7.751	8.575
2.131	1.964	1.968
4.574	3.804	4.217
1.505	1.384	1.452
2.505	1.726	2.271
9.4%	11.0%	4.6%
90.6%	89.0%	95.4%
0.0%	0.0%	0.0%
1.2%	0.0%	0.0%
1.8%	0.0%	0.0%
1.7%	0.1%	0.0%
4.8%	10.9%	4.6%
16.3%	31.8%	19.9%
22.4%	28.7%	28.3%
19.1%	13.2%	18.3%
15.6%	6.9%	12.7%
10.4%	5.2%	9.8%
6.7%	3.3%	6.4%

302-2-A-58-X-4	302-2-A-59-X-1	302-2-A-59-X-1
Cristin Ashmankas,	Cristin Ashmankas,	Cristin Ashmankas,
Unimodal, Poorly Sorted	Unimodal, Poorly Sorted	Trimodal, Very Poorly Sorted
Mud	Mud	Sandy Mud
Coarse Silt	Coarse Silt	Very Fine Sandy Fine Silt
20.28	34.04	72.12
15.40	93.68	233.7
0.895	6.892	5.074
3.495	57.74	30.16
13.46	11.87	12.13
2.768	3.772	5.265
-0.755	0.299	0.669
2.787	3.287	3.432
6.215	6.396	6.324
1.469	1.915	2.419
0.755	-0.299	-0.687
2.787	3.287	3.431
13.71	11.37	11.16
2.835	3.620	5.380
-0.342	-0.057	0.135
0.954	0.941	1.103
6.188	6.459	6.485
1.503	1.856	2.428
0.342	0.057	-0.135
0.954	0.941	1.103
Medium Silt	Medium Silt	Medium Silt
Poorly Sorted	Poorly Sorted	Very Poorly Sorted
Very Fine Skewed	Symmetrical	Coarse Skewed
Mesokurtic	Mesokurtic	Mesokurtic
26.50	18.80	4.700
		26.50
5.259	5.754	7.754
		5.259
2.836	2.075	1.663
17.33	12.22	10.82
41.43	56.28	93.83
14.61	27.12	56.43
38.60	54.21	92.17
4.181	6.228	9.082
22.17	23.78	29.26
4.593	4.151	3.414
5.851	6.354	6.531
8.462	8.913	9.232
1.842	2.147	2.704
3.869	4.761	5.818
1.405	1.513	1.646
2.064	2.639	3.183
0.9%	8.4%	13.9%
99.1%	91.6%	86.1%
0.0%	0.1%	2.6%
0.0%	1.2%	2.1%
0.0%	1.0%	1.3%
0.0%	1.4%	2.1%
0.9%	4.7%	5.8%
20.6%	13.8%	12.1%
33.1%	20.9%	16.0%
18.3%	19.1%	15.1%
12.2%	16.3%	16.1%
9.2%	12.5%	14.3%
5.7%	9.1%	12.4%

302-2-A-59-X-2	302-2-A-59-X-2	302-2-A-59-X-3
Cristin Ashmankas,	Cristin Ashmankas,	Cristin Ashmankas,
Unimodal, Very Poorly Sorted	Unimodal, Poorly Sorted	Unimodal, Poorly Sorted
Mud	Mud	Sandy Mud
Coarse Silt	Coarse Silt	Very Fine Sandy Coarse Silt
66.67	31.00	49.42
231.7	77.22	156.1
5.319	10.33	8.334
32.42	130.5	77.91
12.66	14.44	18.73
4.527	3.287	3.619
0.782	-0.094	-0.050
4.219	3.356	3.729
6.256	6.114	5.712
2.206	1.717	1.867
-0.820	0.094	-0.017
4.216	3.356	3.812
11.55	14.23	18.53
4.497	3.231	3.460
0.062	-0.166	-0.225
1.205	1.035	1.049
6.436	6.135	5.754
2.169	1.692	1.791
-0.062	0.166	0.225
1.205	1.035	1.049
Medium Silt	Medium Silt	Coarse Silt
Very Poorly Sorted	Poorly Sorted	Poorly Sorted
Symmetrical	Fine Skewed	Fine Skewed
Leptokurtic	Mesokurtic	Mesokurtic
18.80	26.50	26.50
5.754	5.259	5.259
2.063	2.804	2.989
12.49	16.31	22.25
61.47	56.81	77.34
29.79	20.26	25.88
59.40	54.01	74.35
6.573	4.713	4.915
24.79	24.87	34.39
4.024	4.138	3.693
6.323	5.938	5.490
8.921	8.478	8.386
2.217	2.049	2.271
4.897	4.341	4.694
1.533	1.449	1.507
2.716	2.237	2.297
9.8%	8.2%	14.3%
90.2%	91.8%	85.7%
2.6%	0.2%	1.2%
1.9%	0.5%	0.6%
0.9%	0.1%	0.1%
0.9%	1.7%	1.2%
3.5%	5.7%	11.1%
13.3%	17.1%	22.5%
20.9%	26.3%	25.2%
18.1%	20.1%	15.2%
15.9%	13.4%	9.6%
13.0%	8.7%	7.6%
9.1%	6.1%	5.6%

302-2-A-59-X-3	302-2-A-60-X-1	302-2-A-60-X-1
Cristin Ashmankas,	Cristin Ashmankas,	Cristin Ashmankas,
Unimodal, Poorly Sorted	Unimodal, Poorly Sorted	Bimodal, Very Poorly Sorted
Sandy Mud	Mud	Sandy Mud
Very Fine Sandy Coarse Silt	Coarse Silt	Very Fine Sandy Coarse Silt
35.89	36.85	58.69
86.19	109.1	148.0
14.20	9.380	5.477
241.1	116.2	41.51
19.28	13.63	16.11
3.023	3.612	4.474
-0.374	0.223	0.420
3.613	3.504	3.062
5.692	6.179	5.951
1.598	1.864	2.164
0.350	-0.270	-0.425
3.653	3.596	3.068
19.57	13.23	15.20
2.978	3.455	4.488
-0.209	-0.088	0.068
1.107	1.000	1.120
5.675	6.240	6.040
1.574	1.789	2.166
0.209	0.088	-0.068
1.107	1.000	1.120
Coarse Silt	Medium Silt	Medium Silt
Poorly Sorted	Poorly Sorted	Very Poorly Sorted
Fine Skewed	Symmetrical	Symmetrical
Mesokurtic	Mesokurtic	Leptokurtic
26.50	18.80	18.80
		215.0
5.259	5.754	5.754
		2.237
3.953	2.538	2.534
22.37	14.48	15.19
68.14	60.75	128.0
17.24	23.93	50.50
64.19	58.22	125.4
3.874	5.365	6.674
29.96	25.06	31.81
3.875	4.041	2.966
5.482	6.110	6.041
7.983	8.622	8.624
2.060	2.134	2.907
4.107	4.581	5.658
1.422	1.483	1.578
1.954	2.424	2.739
11.6%	9.5%	16.2%
88.4%	90.5%	83.8%
0.3%	0.4%	0.5%
0.1%	0.9%	1.9%
0.1%	1.2%	3.3%
1.4%	1.1%	4.4%
9.6%	5.9%	6.1%
23.6%	15.1%	12.8%
28.9%	23.0%	20.2%
16.6%	20.3%	18.1%
9.4%	15.0%	15.3%
6.2%	10.4%	10.6%
3.6%	6.7%	6.7%

302-2-A-60-X-2	302-2-A-60-X-2	302-2-A-60-X-3
Cristin Ashmankas,	Cristin Ashmankas,	Cristin Ashmankas,
Unimodal, Poorly Sorted	Unimodal, Poorly Sorted	Unimodal, Poorly Sorted
Sandy Mud	Mud	Sandy Mud
Very Fine Sandy Coarse Silt	Coarse Silt	Very Fine Sandy Coarse Silt
31.75	26.53	50.85
27.96	26.24	183.8
1.736	1.918	7.144
7.018	7.850	56.49
20.15	15.60	14.86
2.905	3.069	3.842
-0.769	-0.464	0.373
3.256	2.624	3.887
5.633	6.002	6.042
1.538	1.618	1.958
0.769	0.464	-0.431
3.256	2.624	3.961
20.57	15.69	14.46
2.937	3.173	3.493
-0.270	-0.202	-0.169
1.170	0.969	0.839
5.603	5.994	6.112
1.554	1.666	1.805
0.270	0.202	0.169
1.170	0.969	0.839
Coarse Silt	Coarse Silt	Medium Silt
Poorly Sorted	Poorly Sorted	Poorly Sorted
Fine Skewed	Fine Skewed	Fine Skewed
Leptokurtic	Mesokurtic	Platykurtic
26.50	26.50	37.50
5.259	5.259	4.759
3.940	3.018	2.584
24.43	18.36	16.90
67.34	60.04	62.66
17.09	19.89	24.25
63.40	57.02	60.08
3.556	4.815	6.752
30.06	28.37	31.67
3.892	4.058	3.996
5.355	5.767	5.887
7.987	8.372	8.596
2.052	2.063	2.151
4.095	4.314	4.600
1.400	1.472	1.580
1.830	2.268	2.755
11.5%	9.0%	10.1%
88.5%	91.0%	89.9%
0.0%	0.0%	1.7%
0.0%	0.0%	0.8%
0.0%	0.0%	0.2%
1.1%	0.7%	0.1%
10.4%	8.2%	7.2%
26.6%	20.7%	20.8%
30.1%	26.2%	21.3%
13.7%	18.2%	15.3%
8.2%	12.0%	14.8%
6.3%	8.9%	11.6%
3.6%	5.0%	6.1%

302-2-A-60-X-3	302-2-A-60-X-4	302-2-A-61-X-1
Cristin Ashmankas,	Cristin Ashmankas,	Cristin Ashmankas,
Unimodal, Poorly Sorted	Bimodal, Poorly Sorted	Unimodal, Poorly Sorted
Sandy Mud	Mud	Mud
Very Fine Sandy Coarse Silt	Coarse Silt	Coarse Silt
40.03	48.15	42.98
85.34	187.8	154.8
7.565	7.278	8.027
77.13	57.40	72.76
17.66	14.09	13.83
3.525	3.736	3.658
-0.087	0.280	0.299
3.175	4.337	4.087
5.823	6.111	6.162
1.818	1.925	1.880
0.087	-0.367	-0.334
3.175	4.445	4.140
17.36	13.58	13.39
3.476	3.343	3.342
-0.137	-0.310	-0.176
1.036	0.883	0.960
5.848	6.202	6.223
1.797	1.741	1.741
0.137	0.310	0.176
1.036	0.883	0.960
Coarse Silt	Medium Silt	Medium Silt
Poorly Sorted	Poorly Sorted	Poorly Sorted
Fine Skewed	Very Fine Skewed	Fine Skewed
Mesokurtic	Platykurtic	Mesokurtic
26.50	26.50	26.50
	3.350	
5.259	5.259	5.259
	8.241	
3.163	2.314	2.550
19.72	17.95	15.76
79.15	52.15	54.33
25.02	22.53	21.31
75.98	49.83	51.78
5.124	5.897	5.469
32.00	27.21	25.54
3.659	4.261	4.202
5.664	5.800	5.988
8.304	8.755	8.615
2.269	2.055	2.050
4.645	4.494	4.413
1.507	1.519	1.490
2.357	2.560	2.451
13.6%	6.0%	7.4%
86.4%	94.0%	92.6%
0.1%	1.9%	1.1%
0.7%	0.7%	0.8%
0.9%	0.0%	0.3%
2.9%	0.0%	1.4%
8.9%	3.5%	3.8%
19.3%	20.8%	17.6%
25.1%	28.3%	25.3%
16.8%	14.2%	17.7%
12.2%	12.0%	15.1%
7.9%	11.0%	10.2%
5.0%	7.6%	6.8%

302-4-A-4-X-1	302-2-A-61-X-1	302-2-A-61-X-2
Cristin Ashmankas,	Cristin Ashmankas,	Cristin Ashmankas,
Unimodal, Poorly Sorted	Unimodal, Poorly Sorted	Unimodal, Poorly Sorted
Mud	Mud	Mud
Coarse Silt	Coarse Silt	Coarse Silt
44.76	51.99	24.40
172.0	185.6	16.82
7.767	6.856	0.790
65.89	53.15	3.426
15.07	14.07	17.09
3.351	3.953	2.626
0.325	0.448	-1.023
4.988	4.111	3.503
6.025	6.121	5.870
1.761	2.000	1.393
-0.413	-0.499	1.023
5.095	4.168	3.503
14.63	13.39	17.47
2.996	3.605	2.629
-0.249	-0.125	-0.394
1.019	1.007	1.157
6.095	6.223	5.839
1.583	1.850	1.394
0.249	0.125	0.394
1.019	1.007	1.157
Medium Silt	Medium Silt	Coarse Silt
Poorly Sorted	Poorly Sorted	Poorly Sorted
Fine Skewed	Fine Skewed	Very Fine Skewed
Mesokurtic	Mesokurtic	Leptokurtic
26.50	26.50	26.50
5.259	5.259	5.259
2.955	2.463	3.739
17.55	15.69	22.15
50.79	57.36	46.89
17.19	23.29	12.54
47.84	54.89	43.15
4.233	5.903	3.121
23.97	27.08	23.12
4.299	4.124	4.414
5.832	5.994	5.497
8.403	8.665	8.063
1.954	2.101	1.827
4.103	4.541	3.649
1.417	1.519	1.337
2.082	2.561	1.642
5.7%	8.3%	2.4%
94.3%	91.7%	97.6%
1.5%	1.7%	0.0%
0.7%	0.9%	0.0%
0.0%	0.8%	0.0%
0.0%	1.5%	0.0%
3.4%	3.4%	2.4%
19.4%	18.1%	27.0%
29.7%	23.7%	36.4%
19.2%	16.9%	14.5%
11.9%	15.4%	9.2%
8.7%	10.5%	6.7%
5.4%	7.1%	3.8%

302-2-A-61-X-2	302-2-A-62-X-1	302-4-A-5-X-1
Cristin Ashmankas,	Cristin Ashmankas,	Cristin Ashmankas,
Unimodal, Poorly Sorted	Unimodal, Poorly Sorted	Unimodal, Poorly Sorted
Sandy Mud	Mud	Mud
Very Fine Sandy Coarse Silt	Coarse Silt	Coarse Silt
48.94	43.70	21.74
110.9	135.0	16.87
8.365	8.145	0.979
95.71	79.13	3.734
21.65	17.70	14.20
3.433	3.271	2.844
-0.050	0.076	-0.786
3.412	4.485	2.885
5.525	5.819	6.138
1.781	1.710	1.508
0.038	-0.079	0.786
3.425	4.489	2.885
20.94	16.88	14.45
3.355	2.936	2.903
-0.143	-0.316	-0.349
1.123	1.078	0.980
5.577	5.889	6.113
1.746	1.554	1.537
0.143	0.316	0.349
1.123	1.078	0.980
Coarse Silt	Coarse Silt	Medium Silt
Poorly Sorted	Poorly Sorted	Poorly Sorted
Fine Skewed	Very Fine Skewed	Very Fine Skewed
Leptokurtic	Mesokurtic	Mesokurtic
26.50	26.50	26.50
5.259	5.259	5.259
4.083	3.322	2.877
24.33	21.28	18.44
87.85	54.81	43.90
21.52	16.50	15.26
83.77	51.49	41.02
4.577	3.916	4.200
35.55	26.55	23.50
3.509	4.189	4.510
5.361	5.554	5.761
7.936	8.234	8.441
2.262	1.965	1.872
4.427	4.045	3.931
1.492	1.409	1.413
2.194	1.969	2.070
15.7%	6.6%	2.2%
84.3%	93.4%	97.8%
0.4%	0.6%	0.0%
0.6%	1.2%	0.0%
1.7%	0.9%	0.0%
3.8%	0.2%	0.0%
9.2%	3.8%	2.2%
24.2%	24.3%	22.2%
25.0%	31.6%	32.7%
14.9%	15.3%	16.8%
10.9%	10.2%	11.6%
6.1%	7.4%	8.7%
3.3%	4.6%	5.8%

302-2-A-62-X-1	302-4-A-5-X-1	302-2-A-62-X-2
Cristin Ashmankas,	Cristin Ashmankas,	Cristin Ashmankas,
Unimodal, Poorly Sorted	Unimodal, Poorly Sorted	Unimodal, Poorly Sorted
Mud	Mud	Mud
Coarse Silt	Coarse Silt	Coarse Silt
40.37	20.76	38.37
140.1	21.32	151.6
8.402	2.043	8.740
82.35	9.360	83.81
13.39	11.69	13.51
3.624	3.205	3.274
0.330	-0.389	0.341
3.992	2.447	4.804
6.217	6.418	6.191
1.861	1.680	1.724
-0.345	0.389	-0.409
4.019	2.447	4.915
12.86	11.93	13.23
3.354	3.267	2.977
-0.124	-0.181	-0.222
0.992	0.866	0.954
6.281	6.389	6.240
1.746	1.708	1.574
0.124	0.181	0.222
0.992	0.866	0.954
Medium Silt	Medium Silt	Medium Silt
Poorly Sorted	Poorly Sorted	Poorly Sorted
Fine Skewed	Fine Skewed	Fine Skewed
Mesokurtic	Platykurtic	Mesokurtic
26.50	26.50	26.50
5.259	5.259	5.259
2.508	2.239	2.800
14.47	13.65	15.56
54.15	47.65	45.44
21.59	21.28	16.23
51.64	45.41	42.64
5.276	5.864	4.552
24.11	24.21	22.41
4.207	4.391	4.460
6.111	6.195	6.006
8.639	8.803	8.480
2.054	2.005	1.902
4.432	4.412	4.021
1.473	1.501	1.427
2.399	2.552	2.187
7.6%	4.6%	4.6%
92.4%	95.4%	95.4%
0.8%	0.0%	1.1%
0.8%	0.0%	0.6%
0.6%	0.0%	0.1%
1.5%	0.3%	0.3%
3.9%	4.3%	2.4%
15.7%	18.0%	17.0%
24.4%	23.8%	28.3%
19.5%	18.0%	20.5%
15.5%	16.0%	14.2%
10.3%	11.5%	9.8%
6.9%	8.1%	5.7%

302-4-A-5-X-2	302-4-A-5-X-2	302-2-A-62-X-2
Cristin Ashmankas,	Cristin Ashmankas,	Cristin Ashmankas,
Unimodal, Poorly Sorted	Unimodal, Poorly Sorted	Unimodal, Poorly Sorted
Mud	Mud	Mud
Coarse Silt	Coarse Silt	Coarse Silt
21.65	34.63	46.33
17.35	112.6	140.1
0.989	10.04	6.742
3.652	118.8	57.15
13.80	13.33	15.42
2.914	3.568	3.624
-0.694	0.034	0.376
2.647	3.533	4.153
6.180	6.229	6.019
1.543	1.835	1.858
0.694	-0.034	-0.376
2.647	3.533	4.153
14.05	13.12	14.25
2.987	3.403	3.218
-0.338	-0.188	-0.230
0.914	0.936	1.031
6.153	6.252	6.133
1.579	1.767	1.686
0.338	0.188	0.230
0.914	0.936	1.031
Medium Silt	Medium Silt	Medium Silt
Poorly Sorted	Poorly Sorted	Poorly Sorted
Very Fine Skewed	Fine Skewed	Fine Skewed
Mesokurtic	Mesokurtic	Mesokurtic
26.50	26.50	26.50
5.259	5.259	5.259
2.730	2.344	2.791
18.02	15.40	17.69
44.99	54.90	52.00
16.48	23.42	18.63
42.26	52.55	49.21
4.746	5.701	4.738
24.62	26.11	24.81
4.474	4.187	4.265
5.794	6.021	5.821
8.517	8.737	8.485
1.904	2.087	1.989
4.043	4.549	4.220
1.449	1.504	1.450
2.247	2.511	2.244
2.4%	7.3%	6.7%
97.6%	92.7%	93.3%
0.0%	0.5%	0.5%
0.0%	0.6%	1.6%
0.0%	0.4%	1.8%
0.0%	0.8%	0.9%
2.4%	5.1%	1.9%
22.5%	18.1%	18.5%
30.7%	24.2%	29.8%
16.2%	17.9%	16.9%
12.5%	14.6%	12.7%
9.6%	10.2%	9.5%
6.1%	7.7%	5.9%

302-2-A-62-X-3	302-2-A-62-X-3	302-4-A-6-X-1
Cristin Ashmankas,	Cristin Ashmankas,	Cristin Ashmankas,
Unimodal, Poorly Sorted	Unimodal, Poorly Sorted	Unimodal, Poorly Sorted
Mud	Mud	Mud
Coarse Silt	Coarse Silt	Coarse Silt
52.67	52.10	23.56
167.0	197.9	18.35
7.060	6.687	1.069
58.36	49.28	4.283
18.62	14.35	15.36
3.442	3.692	2.861
0.287	0.488	-0.811
4.640	4.862	2.931
5.729	6.089	6.025
1.791	1.905	1.516
-0.337	-0.561	0.811
4.683	4.925	2.931
17.51	13.70	15.54
2.981	3.114	2.907
-0.266	-0.282	-0.369
1.132	0.942	0.990
5.836	6.190	6.008
1.576	1.639	1.540
0.266	0.282	0.369
1.132	0.942	0.990
Coarse Silt	Medium Silt	Medium Silt
Poorly Sorted	Poorly Sorted	Poorly Sorted
Fine Skewed	Fine Skewed	Very Fine Skewed
Leptokurtic	Mesokurtic	Mesokurtic
26.50	26.50	26.50
5.259	5.259	5.259
3.533	2.611	3.027
21.55	17.11	20.16
57.86	47.90	48.24
16.37	18.34	15.94
54.32	45.29	45.22
3.839	4.950	4.155
26.96	24.50	25.35
4.111	4.384	4.374
5.536	5.869	5.632
8.145	8.581	8.368
1.981	1.957	1.913
4.033	4.197	3.994
1.406	1.459	1.419
1.941	2.307	2.055
8.1%	5.2%	3.4%
91.9%	94.8%	96.6%
1.2%	2.0%	0.0%
1.1%	0.9%	0.0%
1.4%	0.4%	0.0%
0.8%	0.6%	0.0%
3.5%	1.4%	3.4%
23.6%	19.0%	24.6%
31.4%	29.2%	32.4%
15.5%	16.9%	15.1%
10.2%	13.4%	11.0%
7.1%	9.7%	8.2%
4.2%	6.6%	5.3%

302-4-A-6-X-2	302-4-A-6-X-2	302-4-A-6-X-3
Cristin Ashmankas,	Cristin Ashmankas,	Cristin Ashmankas,
Unimodal, Poorly Sorted	Bimodal, Poorly Sorted	Unimodal, Poorly Sorted
Mud	Mud	Mud
Coarse Silt	Coarse Silt	Coarse Silt
37.51	41.90	26.95
140.5	160.1	20.56
9.376	8.411	1.276
96.66	76.83	5.226
13.95	14.83	18.45
3.401	3.442	2.653
0.138	0.107	-0.889
3.985	4.326	3.480
6.148	6.053	5.760
1.776	1.797	1.408
-0.188	-0.178	0.889
4.076	4.434	3.480
13.75	14.48	19.04
3.195	3.134	2.626
-0.248	-0.350	-0.310
0.876	0.882	1.116
6.184	6.110	5.714
1.676	1.648	1.393
0.248	0.350	0.310
0.876	0.882	1.116
Medium Silt	Medium Silt	Coarse Silt
Poorly Sorted	Poorly Sorted	Poorly Sorted
Fine Skewed	Very Fine Skewed	Very Fine Skewed
Platykurtic	Platykurtic	Leptokurtic
26.50	26.50	26.50
	4.700	
5.259	5.259	5.259
	7.754	
2.610	2.618	4.303
16.84	19.14	22.65
52.27	50.61	54.57
20.03	19.33	12.68
49.66	47.99	50.26
5.580	5.327	3.310
26.68	27.46	25.80
4.258	4.305	4.196
5.892	5.707	5.464
8.582	8.577	7.860
2.016	1.993	1.873
4.324	4.273	3.665
1.502	1.494	1.363
2.480	2.413	1.727
5.9%	4.7%	5.8%
94.1%	95.3%	94.2%
1.0%	1.3%	0.0%
0.5%	0.6%	0.0%
0.1%	0.0%	0.0%
0.0%	0.0%	0.1%
4.3%	2.8%	5.8%
20.6%	23.7%	27.3%
26.2%	28.8%	32.6%
16.3%	14.1%	16.2%
14.1%	12.3%	9.2%
10.7%	10.0%	5.6%
6.2%	6.4%	3.3%

302-4-A-6-X-3	302-4-A-6-X-4	302-4-A-6-X-4
Cristin Ashmankas,	Cristin Ashmankas,	Cristin Ashmankas,
Unimodal, Poorly Sorted	Unimodal, Poorly Sorted	Unimodal, Poorly Sorted
Mud	Mud	Mud
Coarse Silt	Coarse Silt	Coarse Silt
33.24	33.58	27.40
125.8	111.9	29.72
10.54	10.91	13.29
121.0	134.0	489.1
13.84	14.60	17.00
3.179	3.243	2.904
0.012	-0.023	-0.600
4.146	3.649	2.999
6.166	6.097	5.879
1.675	1.697	1.538
-0.052	0.023	0.600
4.224	3.649	2.999
13.77	14.48	17.46
3.012	3.115	2.931
-0.297	-0.238	-0.227
0.887	0.875	1.000
6.182	6.109	5.840
1.591	1.639	1.551
0.297	0.238	0.227
0.887	0.875	1.000
Medium Silt	Medium Silt	Coarse Silt
Poorly Sorted	Poorly Sorted	Poorly Sorted
Fine Skewed	Fine Skewed	Fine Skewed
Platykurtic	Platykurtic	Mesokurtic
26.50	26.50	26.50
5.259	5.259	5.259
2.757	2.867	3.682
17.25	17.41	20.25
46.18	53.74	58.79
16.75	18.74	15.97
43.43	50.87	55.11
5.017	5.403	4.278
24.72	27.71	28.46
4.437	4.218	4.088
5.857	5.844	5.626
8.503	8.446	8.085
1.917	2.002	1.978
4.066	4.228	3.997
1.464	1.499	1.441
2.327	2.434	2.097
3.6%	6.1%	8.3%
96.4%	93.9%	91.7%
0.8%	0.5%	0.0%
0.4%	0.4%	0.0%
0.0%	0.1%	0.0%
0.0%	0.0%	0.5%
2.5%	5.0%	7.7%
20.9%	22.1%	23.6%
29.3%	25.3%	27.6%
16.4%	16.8%	17.9%
13.8%	14.4%	11.9%
10.2%	9.9%	6.7%
5.8%	5.4%	4.0%

302-4-A-6-X-5	302-4-A-7-X-1	302-4-A-7-X-1
Cristin Ashmankas,	Cristin Ashmankas,	Cristin Ashmankas,
Unimodal, Poorly Sorted	Bimodal, Poorly Sorted	Unimodal, Poorly Sorted
Mud	Mud	Sandy Mud
Coarse Silt	Coarse Silt	Very Fine Sandy Very Coarse Silt
53.56	20.54	32.97
199.4	15.57	25.95
6.588	0.896	1.307
47.79	3.613	5.145
15.33	13.52	21.96
3.598	2.821	2.779
0.537	-0.793	-0.925
4.928	2.823	3.559
5.992	6.208	5.509
1.867	1.496	1.475
-0.618	0.793	0.925
4.992	2.823	3.559
14.68	13.75	22.82
3.120	2.877	2.755
-0.187	-0.375	-0.292
0.982	0.943	1.164
6.090	6.184	5.453
1.642	1.525	1.462
0.187	0.375	0.292
0.982	0.943	1.164
Medium Silt	Medium Silt	Coarse Silt
Poorly Sorted	Poorly Sorted	Poorly Sorted
Fine Skewed	Very Fine Skewed	Fine Skewed
Mesokurtic	Mesokurtic	Leptokurtic
26.50	26.50	37.50
	4.700	
5.259	5.259	4.759
	7.754	
2.991	2.771	4.664
17.13	17.94	26.87
55.35	41.47	67.69
18.50	14.96	14.52
52.36	38.70	63.03
4.767	4.326	3.358
25.88	22.59	31.39
4.175	4.592	3.885
5.868	5.801	5.218
8.385	8.495	7.744
2.008	1.850	1.993
4.210	3.903	3.859
1.457	1.415	1.390
2.253	2.113	1.747
7.4%	1.1%	11.9%
92.6%	98.9%	88.1%
2.0%	0.0%	0.0%
1.0%	0.0%	0.0%
0.0%	0.0%	0.0%
0.1%	0.0%	0.5%
4.3%	1.1%	11.5%
19.2%	20.6%	30.8%
26.8%	34.5%	28.8%
18.9%	16.3%	12.5%
13.6%	12.0%	7.8%
8.9%	9.4%	5.1%
5.2%	6.0%	3.0%

302-4-A-7-X-2	302-4-A-7-X-2	302-4-A-7-X-3
Cristin Ashmankas,	Cristin Ashmankas,	Cristin Ashmankas,
Unimodal, Poorly Sorted	Bimodal, Poorly Sorted	Unimodal, Poorly Sorted
Mud	Mud	Sandy Mud
Coarse Silt	Coarse Silt	Very Fine Sandy Coarse Silt
25.94	20.99	42.51
27.47	15.31	112.0
1.851	0.775	8.822
7.081	3.288	96.36
14.01	14.06	18.55
3.331	2.776	3.354
-0.309	-0.854	-0.028
2.264	2.910	3.624
6.158	6.152	5.751
1.736	1.473	1.746
0.309	0.854	0.025
2.264	2.910	3.628
14.19	14.20	18.35
3.462	2.835	3.217
-0.169	-0.393	-0.166
0.850	0.978	1.019
6.139	6.138	5.768
1.792	1.503	1.686
0.169	0.393	0.166
0.850	0.978	1.019
Medium Silt	Medium Silt	Coarse Silt
Poorly Sorted	Poorly Sorted	Poorly Sorted
Fine Skewed	Very Fine Skewed	Fine Skewed
Platykurtic	Mesokurtic	Mesokurtic
26.50	26.50	26.50
	4.700	
5.259	5.259	5.259
	7.754	
2.537	2.861	3.545
16.41	18.68	20.85
61.36	41.65	72.86
24.19	14.56	20.55
58.83	38.79	69.31
6.525	4.021	4.724
30.68	22.50	32.08
4.026	4.586	3.779
5.929	5.742	5.584
8.623	8.449	8.140
2.142	1.843	2.154
4.596	3.864	4.361
1.565	1.397	1.485
2.706	2.008	2.240
9.5%	0.9%	12.7%
90.5%	99.1%	87.3%
0.0%	0.0%	0.4%
0.0%	0.0%	0.9%
0.0%	0.0%	0.5%
0.9%	0.0%	1.4%
8.6%	0.9%	9.5%
20.3%	21.8%	21.8%
21.5%	35.6%	25.4%
16.2%	16.0%	17.3%
14.7%	11.0%	11.6%
11.2%	9.2%	7.1%
6.4%	5.6%	4.1%

302-4-A-7-X-3	302-4-A-7-X-4	302-4-A-7-X-4
Cristin Ashmankas,	Cristin Ashmankas,	Cristin Ashmankas,
Unimodal, Poorly Sorted	Unimodal, Poorly Sorted	Unimodal, Poorly Sorted
Sandy Mud	Mud	Mud
Very Fine Sandy Coarse Silt	Coarse Silt	Coarse Silt
44.36	34.39	43.68
139.1	102.6	165.8
9.133	10.56	8.108
94.01	133.2	71.80
17.89	14.93	14.63
3.485	3.355	3.508
-0.067	-0.076	0.239
3.678	3.556	4.327
5.796	6.066	6.067
1.805	1.747	1.827
0.041	0.076	-0.317
3.717	3.556	4.439
17.50	14.64	14.23
3.374	3.240	3.226
-0.240	-0.222	-0.239
1.009	0.969	0.943
5.836	6.094	6.135
1.755	1.696	1.690
0.240	0.222	0.239
1.009	0.969	0.943
Coarse Silt	Medium Silt	Medium Silt
Poorly Sorted	Poorly Sorted	Poorly Sorted
Fine Skewed	Fine Skewed	Fine Skewed
Mesokurtic	Mesokurtic	Mesokurtic
26.50	26.50	26.50
5.259	5.259	5.259
3.026	2.773	2.667
21.52	17.58	17.40
70.74	56.91	54.54
23.37	20.53	20.45
67.71	54.14	51.87
4.973	5.081	5.183
32.26	27.15	26.64
3.821	4.135	4.196
5.538	5.830	5.845
8.368	8.495	8.550
2.190	2.054	2.038
4.547	4.359	4.354
1.500	1.480	1.482
2.314	2.345	2.374
12.2%	7.9%	7.0%
87.8%	92.1%	93.0%
0.9%	0.3%	1.4%
0.6%	0.7%	0.6%
0.0%	0.1%	0.0%
1.2%	0.8%	0.2%
9.5%	6.0%	4.7%
22.5%	19.9%	20.0%
26.3%	26.5%	27.0%
14.6%	17.6%	17.2%
10.7%	12.9%	12.9%
8.4%	9.1%	9.8%
5.2%	6.1%	6.2%

302-4-A-8-X-1	302-4-A-9-X-1	302-4-A-10-X-1
Cristin Ashmankas,	Cristin Ashmankas,	Cristin Ashmankas,
Unimodal, Poorly Sorted	Unimodal, Poorly Sorted	Bimodal, Poorly Sorted
Mud	Mud	Mud
Coarse Silt	Coarse Silt	Coarse Silt
31.81	25.82	15.95
73.45	23.59	13.78
9.869	2.521	1.136
122.2	13.82	4.098
14.83	16.71	9.809
3.384	2.785	2.957
-0.147	-0.695	-0.482
3.106	3.161	2.346
6.075	5.903	6.672
1.759	1.478	1.564
0.147	0.695	0.482
3.106	3.161	2.346
14.80	16.65	10.11
3.332	2.793	2.989
-0.177	-0.312	-0.247
0.937	1.089	0.815
6.078	5.909	6.628
1.737	1.482	1.580
0.177	0.312	0.247
0.937	1.089	0.815
Medium Silt	Coarse Silt	Medium Silt
Poorly Sorted	Poorly Sorted	Poorly Sorted
Fine Skewed	Very Fine Skewed	Fine Skewed
Mesokurtic	Mesokurtic	Platykurtic
26.50	26.50	26.50
		4.700
5.259	5.259	5.259
		7.754
2.816	3.543	2.061
17.15	20.64	12.07
60.68	51.72	35.41
21.55	14.60	17.18
57.87	48.18	33.35
5.529	3.593	5.563
28.65	24.32	19.53
4.043	4.273	4.820
5.866	5.599	6.373
8.472	8.141	8.922
2.096	1.905	1.851
4.430	3.868	4.102
1.510	1.377	1.459
2.467	1.845	2.476
9.3%	5.7%	0.4%
90.7%	94.3%	99.6%
0.1%	0.0%	0.0%
0.6%	0.0%	0.0%
0.2%	0.0%	0.0%
1.2%	0.8%	0.0%
7.3%	5.0%	0.4%
19.4%	22.5%	13.1%
24.3%	34.3%	28.9%
17.4%	15.7%	18.3%
14.3%	10.5%	16.6%
9.3%	7.4%	13.7%
6.0%	3.9%	9.1%

302-4-A-10-X-1	302-4-A-10-X-2	302-4-A-10-X-2
Cristin Ashmankas,	Cristin Ashmankas,	Cristin Ashmankas,
Bimodal, Poorly Sorted	Bimodal, Poorly Sorted	Unimodal, Poorly Sorted
Mud	Mud	Mud
Coarse Silt	Coarse Silt	Coarse Silt
42.63	48.73	43.56
172.8	190.6	167.3
7.798	7.024	8.025
66.06	53.91	70.41
13.52	13.79	14.35
3.407	3.657	3.443
0.367	0.438	0.373
4.975	4.724	4.524
6.180	6.144	6.095
1.788	1.894	1.801
-0.455	-0.522	-0.453
5.094	4.815	4.637
13.08	13.09	13.93
3.040	3.215	3.152
-0.310	-0.298	-0.194
0.921	0.924	0.952
6.257	6.255	6.165
1.604	1.685	1.656
0.310	0.298	0.194
0.921	0.924	0.952
Medium Silt	Medium Silt	Medium Silt
Poorly Sorted	Poorly Sorted	Poorly Sorted
Very Fine Skewed	Fine Skewed	Fine Skewed
Mesokurtic	Mesokurtic	Mesokurtic
26.50	26.50	26.50
4.700	3.350	
5.259	5.259	5.259
7.754	8.241	
2.561	2.428	2.847
16.76	17.18	16.54
43.36	46.41	53.62
16.93	19.11	18.84
40.80	43.98	50.78
4.846	5.308	4.988
22.93	24.00	24.80
4.528	4.430	4.221
5.899	5.863	5.918
8.609	8.686	8.457
1.901	1.961	2.003
4.081	4.256	4.236
1.445	1.474	1.463
2.277	2.408	2.318
3.9%	5.6%	7.1%
96.1%	94.4%	92.9%
1.6%	1.9%	1.4%
0.7%	0.8%	0.6%
0.0%	0.0%	0.0%
0.0%	0.6%	0.3%
1.7%	2.3%	4.7%
17.4%	16.9%	17.6%
31.7%	31.6%	27.4%
17.1%	15.3%	18.0%
12.7%	12.3%	14.2%
10.8%	11.4%	10.3%
6.4%	6.9%	5.3%

302-4-A-10-X-3	302-4-A-10-X-3	302-4-A-10-X-4
Cristin Ashmankas,	Cristin Ashmankas,	Cristin Ashmankas,
Bimodal, Poorly Sorted	Unimodal, Poorly Sorted	Bimodal, Poorly Sorted
Mud	Mud	Mud
Coarse Silt	Coarse Silt	Coarse Silt
18.47	20.46	18.69
15.28	16.52	15.14
1.081	1.026	1.002
4.026	3.840	3.766
11.68	13.00	11.92
2.883	2.921	2.874
-0.552	-0.675	-0.595
2.387	2.591	2.432
6.419	6.266	6.391
1.528	1.546	1.523
0.552	0.675	0.595
2.387	2.591	2.432
11.96	13.21	12.21
2.953	3.006	2.946
-0.315	-0.342	-0.335
0.839	0.905	0.849
6.385	6.242	6.356
1.562	1.588	1.559
0.315	0.342	0.335
0.839	0.905	0.849
Medium Silt	Medium Silt	Medium Silt
Poorly Sorted	Poorly Sorted	Poorly Sorted
Very Fine Skewed	Very Fine Skewed	Very Fine Skewed
Platykurtic	Mesokurtic	Platykurtic
26.50	26.50	26.50
4.700		4.700
5.259	5.259	5.259
7.754		7.754
2.423	2.526	2.442
15.16	17.09	15.69
39.55	42.59	39.71
16.32	16.86	16.26
37.12	40.06	37.26
5.205	4.834	5.096
21.84	23.39	22.01
4.660	4.553	4.655
6.043	5.870	5.994
8.689	8.629	8.678
1.864	1.895	1.864
4.029	4.075	4.023
1.457	1.447	1.453
2.380	2.273	2.349
1.0%	1.8%	0.9%
99.0%	98.2%	99.1%
0.0%	0.0%	0.0%
0.0%	0.0%	0.0%
0.0%	0.0%	0.0%
0.0%	0.0%	0.0%
1.0%	1.8%	0.9%
17.2%	20.4%	17.8%
30.9%	31.5%	31.5%
17.4%	16.8%	17.3%
14.7%	12.5%	14.1%
12.0%	10.3%	11.6%
6.9%	6.7%	6.8%

302-4-A-10-X-4	302-4-A-11-X-1	302-4-A-11-X-1
Cristin Ashmankas,	Cristin Ashmankas,	Cristin Ashmankas,
Bimodal, Poorly Sorted	Unimodal, Poorly Sorted	Unimodal, Poorly Sorted
Mud	Mud	Mud
Coarse Silt	Coarse Silt	Coarse Silt
20.68	36.48	19.88
16.53	130.5	15.60
0.876	10.22	1.038
3.458	114.2	3.970
12.80	16.08	13.09
3.056	3.049	2.764
-0.678	-0.042	-0.669
2.402	4.641	2.651
6.288	5.944	6.255
1.612	1.617	1.467
0.678	-0.029	0.669
2.402	4.757	2.651
12.97	16.00	13.31
3.138	2.827	2.831
-0.403	-0.288	-0.326
0.827	1.004	0.913
6.269	5.966	6.232
1.650	1.499	1.501
0.403	0.288	0.326
0.827	1.004	0.913
Medium Silt	Coarse Silt	Medium Silt
Poorly Sorted	Poorly Sorted	Poorly Sorted
Very Fine Skewed	Fine Skewed	Very Fine Skewed
Platykurtic	Mesokurtic	Mesokurtic
26.50	26.50	26.50
3.350		
5.259	5.259	5.259
8.241		
2.273	3.412	2.840
18.09	19.33	16.76
42.62	51.08	41.02
18.75	14.97	14.44
40.35	47.67	38.18
5.757	4.014	4.392
25.00	25.05	21.94
4.552	4.291	4.608
5.789	5.693	5.899
8.781	8.195	8.460
1.929	1.910	1.836
4.229	3.904	3.852
1.500	1.409	1.416
2.525	2.005	2.135
1.5%	5.2%	1.3%
98.5%	94.8%	98.7%
0.0%	0.9%	0.0%
0.0%	0.4%	0.0%
0.0%	0.0%	0.0%
0.0%	0.0%	0.0%
1.5%	3.9%	1.3%
21.9%	22.5%	19.0%
32.7%	31.0%	32.8%
12.8%	17.7%	18.2%
11.6%	11.9%	13.1%
11.8%	7.4%	10.1%
7.7%	4.4%	5.4%

302-4-A-11-X-2	302-4-A-11-X-2	302-4-A-11-X-3
Cristin Ashmankas,	Cristin Ashmankas,	Cristin Ashmankas,
Unimodal, Poorly Sorted	Bimodal, Poorly Sorted	Unimodal, Poorly Sorted
Mud	Mud	Mud
Coarse Silt	Coarse Silt	Coarse Silt
45.08	18.07	20.34
175.1	16.62	16.34
7.500	1.257	1.066
61.79	4.245	3.968
13.84	10.80	13.16
3.531	2.986	2.828
0.416	-0.319	-0.654
4.621	2.154	2.636
6.150	6.533	6.248
1.836	1.578	1.500
-0.482	0.319	0.654
4.708	2.154	2.636
13.41	11.02	13.44
3.146	3.081	2.896
-0.244	-0.151	-0.317
0.886	0.803	0.905
6.220	6.503	6.217
1.653	1.623	1.534
0.244	0.151	0.317
0.886	0.803	0.905
Medium Silt	Medium Silt	Medium Silt
Poorly Sorted	Poorly Sorted	Poorly Sorted
Fine Skewed	Fine Skewed	Very Fine Skewed
Platykurtic	Platykurtic	Mesokurtic
26.50	26.50	26.50
	4.700	
5.259	5.259	5.259
	7.754	
2.620	2.314	2.811
16.39	12.26	16.89
49.92	41.44	42.27
19.05	17.91	15.04
47.30	39.13	39.46
5.373	5.912	4.608
25.18	22.37	22.81
4.324	4.593	4.564
5.931	6.350	5.888
8.576	8.755	8.475
1.983	1.906	1.857
4.252	4.163	3.910
1.484	1.492	1.432
2.426	2.564	2.204
5.5%	1.8%	1.8%
94.5%	98.2%	98.2%
1.5%	0.0%	0.0%
0.9%	0.0%	0.0%
0.0%	0.0%	0.0%
0.0%	0.0%	0.0%
3.1%	1.8%	1.8%
19.2%	17.5%	19.8%
27.1%	24.6%	31.7%
16.9%	17.1%	17.5%
14.3%	18.0%	13.5%
11.0%	13.7%	10.0%
6.1%	7.2%	5.7%

302-4-A-11-X-3	302-4-A-11-X-4	302-4-A-11-X-4
Cristin Ashmankas,	Cristin Ashmankas,	Cristin Ashmankas,
Unimodal, Poorly Sorted	Bimodal, Poorly Sorted	Unimodal, Poorly Sorted
Sandy Mud	Mud	Mud
Very Fine Sandy Coarse Silt	Coarse Silt	Coarse Silt
51.33	26.72	32.48
165.1	84.95	89.78
7.397	14.82	13.73
64.01	246.7	215.5
15.36	13.72	16.36
3.991	3.013	3.190
0.371	-0.329	-0.358
3.490	3.574	3.286
6.003	6.188	5.930
2.008	1.591	1.676
-0.408	0.329	0.340
3.539	3.574	3.321
14.62	13.63	16.26
3.876	2.971	3.184
-0.063	-0.352	-0.303
1.011	0.908	0.944
6.096	6.197	5.943
1.955	1.571	1.671
0.063	0.352	0.303
1.011	0.908	0.944
Medium Silt	Medium Silt	Coarse Silt
Poorly Sorted	Poorly Sorted	Poorly Sorted
Symmetrical	Very Fine Skewed	Very Fine Skewed
Mesokurtic	Mesokurtic	Mesokurtic
26.50	26.50	26.50
	4.700	
5.259	5.259	5.259
	7.754	
2.577	2.675	2.946
16.42	17.82	20.81
78.26	43.07	58.50
30.37	16.10	19.86
75.68	40.39	55.55
6.330	4.718	4.966
30.38	23.64	29.90
3.676	4.537	4.095
5.929	5.811	5.587
8.600	8.546	8.407
2.340	1.884	2.053
4.924	4.009	4.312
1.555	1.442	1.488
2.662	2.238	2.312
12.5%	2.3%	8.1%
87.5%	97.7%	91.9%
1.3%	0.3%	0.4%
0.8%	0.2%	0.2%
1.3%	0.1%	0.0%
2.9%	0.1%	0.2%
6.4%	1.6%	7.3%
16.6%	20.7%	24.5%
22.4%	32.6%	27.5%
16.8%	15.8%	14.4%
14.4%	12.2%	11.3%
11.0%	10.4%	9.0%
6.3%	6.0%	5.2%

302-4-A-15-X-1	302-4-A-19-X-1	302-4-A-19-X-1
Cristin Ashmankas,	Cristin Ashmankas,	Cristin Ashmankas,
Unimodal, Poorly Sorted	Unimodal, Very Poorly Sorted	Bimodal, Poorly Sorted
Sandy Mud	Muddy Sand	Sandy Mud
Very Fine Sandy Coarse Silt	Fine Silty Very Coarse Sand	Very Fine Sandy Fine Silt
38.26	678.9	24.94
34.02	577.8	33.50
1.486	0.427	2.149
5.138	1.934	8.111
23.86	223.2	10.87
2.970	9.522	3.704
-0.777	-1.276	0.216
3.387	3.355	2.036
5.390	1.516	6.524
1.571	2.549	1.889
0.777	1.523	-0.216
3.387	4.363	2.036
25.36	416.7	11.02
2.980	5.352	3.889
-0.183	-0.615	0.184
1.194	1.322	0.788
5.302	1.263	6.504
1.575	2.420	1.960
0.183	0.615	-0.184
1.194	1.322	0.788
Coarse Silt	Medium Sand	Medium Silt
Poorly Sorted	Very Poorly Sorted	Poorly Sorted
Fine Skewed	Very Fine Skewed	Coarse Skewed
Leptokurtic	Leptokurtic	Platykurtic
26.50	1200.0	4.700
		53.50
5.259	-0.243	7.754
		4.247
4.659	15.65	2.135
27.31	728.1	8.951
86.85	1825.2	72.10
18.64	116.7	33.77
82.19	1809.6	69.97
3.647	6.022	8.633
37.35	1057.0	29.34
3.525	-0.868	3.794
5.194	0.458	6.804
7.746	5.998	8.871
2.197	-6.910	2.338
4.221	6.866	5.078
1.436	-6.575	1.633
1.867	2.590	3.110
18.7%	84.1%	12.6%
81.3%	15.9%	87.4%
0.0%	36.5%	0.0%
0.0%	25.0%	0.0%
0.0%	11.5%	0.0%
2.6%	6.8%	1.9%
16.1%	4.2%	10.6%
25.2%	3.0%	13.6%
28.7%	2.9%	11.9%
12.7%	3.0%	15.4%
6.2%	3.3%	21.1%
5.2%	2.5%	17.3%
3.3%	1.2%	8.2%

302-4-A-19-X-2	302-4-A-19-X-2
Cristin Ashmankas,	Cristin Ashmankas,
Unimodal, Very Poorly Sorted	Bimodal, Very Poorly Sorted
Sandy Mud	Sandy Mud
Coarse Sandy Fine Silt	Very Fine Sandy Fine Silt
59.06	46.79
184.7	131.9
4.923	7.233
30.41	69.21
10.43	12.26
4.651	4.567
1.093	0.531
4.162	2.698
6.584	6.349
2.217	2.192
-1.093	-0.532
4.162	2.701
8.974	11.90
4.416	4.524
0.251	0.228
1.310	0.814
6.800	6.393
2.143	2.178
-0.251	-0.228
1.310	0.814
Medium Silt	Medium Silt
Very Poorly Sorted	Very Poorly Sorted
Coarse Skewed	Coarse Skewed
Leptokurtic	Platykurtic
4.700	4.700
	53.50
7.754	7.754
	4.247
1.985	2.048
8.076	9.249
81.34	96.32
40.98	47.03
79.36	94.27
5.693	10.58
16.86	35.94
3.620	3.376
6.952	6.756
8.977	8.932
2.480	2.646
5.357	5.556
1.447	1.731
2.509	3.403
11.0%	17.1%
89.0%	82.9%
1.0%	0.5%
2.9%	1.1%
2.4%	1.7%
2.2%	3.3%
2.5%	10.6%
6.0%	11.7%
14.3%	10.5%
19.6%	14.6%
21.5%	19.9%
17.9%	17.2%
9.6%	9.0%

BIBLIOGRAPHY

Aagaard, K., 1981. "On the Deep Circulation in the Arctic Ocean." *Deep-Sea Research*, Vol. 28, No. 3, pp. 251-268.

Aagaard, K., E.C. Carmack, 1989. "The Role of Sea Ice and Other Fresh Water in the Arctic Circulation." *Journal of Geophysical Research*, Vol. 94, No. C10, pp. 14485-14498.

Alley, R.B., K.M. Cuffey, E.B. Evenson, J.C. Strasser, D.E. Lawsons, and G.J. Larson, 1997. "How Glaciers Entrain and Transport Basal Sediment: Physical Constraints." *Quaternary Science Reviews*, Vol. 16, pp. 1017-1038.

Bachman, R.T., 1985. "Acoustic and Physical Property Relationships in Marine Sediments." *Journal of Accoust. Soc. Am.*, Vol. 78, No. 2, pp. 616-621.

Backman, J., M. Jakobsson, M. Frank, F. Sangiorgi, H. Brinkhuis, C. Stickley, M. O'Regan, R. Lovlie, H. Palike, D. Spofforth, J. Gattacecca, K. Moran, and C. Heil, 2008. "Age Model and Core-Seismic Integration for the Cenozoic ACEX Sediments from the Lomonosov Ridge." *Paleoceanography*, Vol. 23.

Backman, J., M. Jakobsson, R. Lovlie, L. Polyak, and L.A. Febo, 2004. "Is the Central Arctic Ocean a Sediment Starved Basin?" *Quaternary Science Reviews*, Vol. 23, pp. 1435-1454.

Backman, J., K. Moran, and D. Evans, 2004. "ACEX Arctic Coring Expedition: Paleoceanographic and tectonic evolution of the central Arctic Ocean." *IODP Expedition 302 Scientific Prospectus,* Edinburgh (Integrated Ocean Drilling Program Management International, Inc.).

Backman, J., K. Moran, D.B. McInroy, L.A. Mayer, 2006. *Proceedings of the Integrated Ocean Drilling Program, 302*, Edinburg (Integrated Ocean Drilling Program Management International, Inc.).

Barrett, L., and S.B. Treves, 1981. "Sedimentology and Petrology of Core from DVDP-15, Western McMurdo Sound." *Antarctic Research Series*, Vol. 33, pp. 281-314.

Bendat, J.S., and A.G. Piersol, 2000. Random Data: Analysis and Measurement Procedures. John Wiley & Sons Inc., NY.

Betzer, P.R., K.I. Carder, R.A. Duce, J.T. Merrill, et al., 1988. "Long-range Transport of Giant Mineral Aerosol Particles." *Nature*, Vol. 336, pp. 568-571.

Bischof, J., 2000. Ice Drift, Ocean Circulation, and Climate Change. Springer, NY.

Bischof, J., D.L. Clark, and J.S. Vincent, 1996. "Origin of Ice-Rafted Debris: Pleistocene paleoceanography in the western Arctic Ocean." *Paleoceanography*, Vol. 11, No. 6, pp. 743-756.

Bischof, J.F. and D.A. Darby, 1997. "Mid- to Late Pleistocene Ice Drift in the Western Arctic Ocean: Evidence for a different circulation in the past." *Science*, Vol. 277, pp. 74-77.

Bischof, J.F. and D.A. Darby, 1999. "Quaternary Ice Transport in the Canadian Arctic and Extent of Late Wisconsinan Glaciation in the Queen Elizabeth Islands." *Canadian Journal of Earth Science*, Vol. 36, pp. 2007-2022.

Bischof, J.F., D.A. Darby, and C. Majer, 1999. "Very High Resolution Record of Late Pleistocene to Holocene Ice Rafting and Glacio-Fluvial Meltwater Discharge from the Northern Chukchi Sea." *EOS*, AGU, Vol. 80, No. 46.

Bjork, G., Jakobsson, M., Rudels, B., et al., 2007. "Bathymetry and Deep-Water Exchange Across the Central Lomonosov Ridge at 88-89°N." *Deep-Sea Research I*, Vol. 54, pp. 1197-1208.

Boggs, S., 1995. Principles of Sedimentology and Stratigraphy. Prentice-Hall Inc., NJ.

Bouyoucos, G.J., 1962. "Hydrometer Method Improved for Making Particle Size Analysis of Soils." *Agronomy Journal*, Vol. 54, pp. 464-465.

Boyce, R. E., 1976. "Definitions and Laboratory Techniques of Compressional Sound Velocity Parameters and Wet-Water Content, Wet-Bulk Density, and Porosity Parameters by Gravimetric and Gamma Ray Attenuation Techniques." *Initial Report of the Deep Sea Drilling Program*, Vol. 33, pp. 931-958.

Broecker, W.S., 1997. "Thermohaline Circulation, the Achilles Heel of our Climate System: Will man-made CO2 upset the current balance?" *Science*, Vol. 278, pp. 1582-1588.

Clark, D.L., 1996. "The Pliocene Record in the Central Arctic." *Marine Micropaleontology*, Vol. 27, pp. 157-164.

Clark, D.L., Hanson, A., 1983. "Central Arctic Ocean Sediment Texture: a key to ice-transport mechanisms." *In*: B. Molnia (*Ed.*), Glacial-Marine Sedimentation, Plenum, New York, pp. 301-330.

Clark, P.U., N.G. Pisias, T.F. Stocker, and A.J. Weavers, 2002. "The Role of the Thermohaline Circulation in Abrupt Climate Change." *Nature*, Vol. 415, pp. 863-869.

Coachman, L.K. and K. Aagaard, 1974. Physical Oceanography of Arctic and Subarctic Seas. Marine Geology and Oceanography of the Arctic Seas, Springer-Veriag, NY.

Curry, J.A., J. Schramm, and E.E. Ebert, 1995. "On the Sea-Ice Albedo Climate Feedback Mechanism." *Journal of Climate*, Vol. 8, pp. 240-247.

Darby, D.A., 2008. "Arctic Perennial Ice Cover Over the Last 14 Million Years." *Paleoceanography,* Vol. 23, PA1S07. doi:10.1029/2007PA001479.

Darby, D.A., Naidu, S.A., Mowatt, T.C., Jones, G.A., 1989. "Sediment Composition and Sedimentary Processes in the Arctic Ocean." *In*: Herman, Y. (*Ed*.), The Arctic Seas: Climatology, Oceanography, Geology, and Biology, Van Nostrand Reinhold Co., New York, pp. 657-720.

Darby, D.A., Bischof, J.F., Jones, G.A., 1997. "Radiocarbon Chronology of Depositional Regimes in the Western Arctic Ocean." *Deep-Sea Research I*, Vol. 44, pp. 1745-1757.

Darby, D.A., J.F. Bischof, R.F. Spielhagen, S.A. Marshall, and S.W. Herman, 2002. "Arctic Ice Export Events and their Potential Impact on Global Climate during the Late Pleistocene." *Paleoceanography*, Vol. 17, No. 2.

Dethloff, K, et al., 2006. "A Dynamical Link Between the Arctic and the Global Climate System." *Geophysical Research Letters*, Vol. 33, L03703.

Dreimanis A., and V.J. Vagners, 1971. "Bimodal Distribution of Rock and Mineral Fragments in Basal Tills." In: R.P. Goldthwait (ed) *A Symposium on Till*, Univ. Press, Ohio, pp. 237-250.

Eicken, H., J. Kolatschek, F. Lindemann, I. Dmitrenko, J. Freitag, and H. Kassens, 2000. "A Key Source Area and Constraints on Entrainment for Basin-Scale Sediment Transport by Arctic Sea Ice." *Geophysical Research Letters*, Vol. 27, pp. 1919-1922.

Eldrett, J.S., I.C. Harding, P.A. Wilson, E. Butler, and A.P. Roberts, 2007. "Continental Ice in Greenland during the Eocene and Oligocene." *Nature.*

Evans, H.B., 1965. "GRAPE-A Device for Continuous Determination of Material Density and Porosity." *Transactions 6th Annual SPWIA Logging Symposium, Dallas, TX*. Vol. 2, pp. B1-B25.

Fahl, K., and E.-M. Nothig, 2007. "Lithogenic and Biogenic Particle Fluxes on the Lomonosov Ridge (central Arctic Ocean) and their Relevance for Sediment Accumulation: Vertical vs. Lateral Transport." *Deep-Sea Research I*, Vol. 54, pp. 1256-1272.

Fetter, C.W., 2001. Applied Hydrogeology. Prentice-Hall Inc., NJ.

Frank, M., J. Backman, M. Jakobsson, K. Moran, M. O'Regan, J. King, B.A. Haley, P.W. Kubik, and D. Garbe-Schonberg, 2008. "Beryllium Isotopes in Central Arctic Ocean Sediments Over the Past 12.3 Million Years: Stratigraphic and Paleoclimatic Implications." *Paleoceanography*, Vol. 23.

Goldstein, R.H., 1983. "Stratigraphy and Sedimentology of Ice-Rafted and Turbidite Sediment, Canadian Basin, Arctic Ocean." In: B Molnia (ed) *Glacial Marine Sedimentation*. Plenum Press, New York, pp. 367-401.

Goossens, D., 2008. "Techniques to Measure Grain-Size Distributions of Loamy Sediments: a comparative study of ten instruments for wet analysis." *Sedimentology*, Vol. 55, pp. 65-96.

Grosswald, M.G., Hughes, T.J., 1999. "The Case for an Ice Shelf in the Pleistocene Arctic Ocean." *Polar Geography*, Vol. 23, pp. 23-54.

Gyllencreutz, R., 2005. "Late Glacial and Holocene Paleoceanography in the Skagerrak from High-Resolution Grain Size Records." *Paleogeography, Paleoclimatology, Paleoecology*, Vol. 222, pp. 344-369.

Hald, M., H. Ebbesen, M. Forwick, F. Goftliebsen, L. Khomenko, S. Korsun, L.R. Olsen, and T.O. Vorren, 2004. "Holocene Paleoceanography and Glacial History of the West Spitsbergen Area, Euro-Arctic Margin." *Quaternary Science Reviews*, Vol. 23, pp. 2075-2088.

Haley, A.B., Frank, M., Spielhagen, R.F., Eisenhauer, A., 2008. "Influence of Brine Formation on Arctic Ocean Circulation Over the Past 15 Million Years." *Nature Geoscience*, Vol. 1, pp. 68–72.

Haley, B.A., M. Frank, R.F. Spielhagen, and J. Fietzke, 2008. "The Radiogenic Isotope Record of Arctic Ocean Circulation and Weathering Inputs of the Past 15 Million Years." *Paleoceanography*, Vol. 23.

Hall, I.R., McCave, I.N., M.R. Chapman, and Shackleton, N.J., 1998. "Coherent Deep Flow Variation in the Iceland and American Basins during the Last Interglacial." *Earth and Planetary Science Letters*, Vol. 164, pp. 15-21.

Hall, I.R., McCave, I.N., Shackleton, N.J., Weedon, and G.P., Harris, S.E., 2001. "Intensified Deep Pacific Inflow and Ventilation in Pleistocene Glacial Times." *Nature*, Vol. 412, pp. 809-811.

Hamilton, E.L., 1970. "Sound Velocity and Related Properties of Marine Sediments, North Pacific." *Journal of Geophysical Research*, Vol. 75, No. 23, pp. 4423-4446.

Hamilton, E.L., 1971. "Elastic Properties of Marine Sediments." *Journal of Geophysical Research*, Vol. 76, No. 2, pp. 579-604.

Hein, F.J., 991. "The Need for Grain Size Analyses in Marine Geotechnical Studies." *In* Syvitski, J.P.M. (*Ed*.), *Principles, Methods, and Applications of Particle Size Analysis*, Cambridge Univ. Press, NY.

Heinrich, H., 1988. "Origin and Consequences of Cyclic Ice Rafting in the Northeast Atlantic Ocean during the Past 130,000 Years." *Quaternary Research*, Vol. 29, pp. 142-152.

Herman, Y., 1974. Topography of the Arctic Ocean. Marine Geology and Oceanography of the Arctic Seas, Springer-Veriag, NY.

Hodell, D.A., Woodruff, F., 1994. "Variation in the Strontium Isotope Ratio of Seawater during the Miocene: stratigraphic and geochemical implications." *Paleoceanography*, Vol. 9, pp. 405-426.

Holland, M.M., et al., 2001. "The Role of Ice-Ocean Interactions in the Variability of the North Atlnatic Thermohaline Circulation." *Journal of Climate*, Vol. 14, pp. 656-675.

Holland, M.M., and C.M. Bitz, 2003. "Polar Amplification of Climate Change in Coupled Models." *Climate Dynamics*, Vol. 21, pp. 221-232.

Honjo, S., 1980. "Material Fluxes and Mode of Sedimentation in Mesopelagic and Bathypelagic Zones." *Journal of Marine Research*, Vol. 38, pp. 53-97.

Hughes, T.J., Denton, G.H., Grosswald, M.G., 1977. "Was There a Late Wurm Ice Sheet?" *Nature*, Vol. 266, pp. 596-602.

Hunt, A.G, and P.E. Malin, 1998. Possible Triggering of Heinrich Events by Ice-Load-Induced Earthquakes." *Nature*, Vol. 393, pp. 155-158.

Iverson, N.R., and D.J. Semmens, 1995. "Intrusion of Ice into Porous Media by Regelation: A mechanism of sediment entrainment by glaciers." *Journal of Geophysical Research*, Vol. 100, pp. 10219-10230.

Jakobsson, M., R. Lovlie, H. Al-Hanbali, et al., 2000. "Manganese and Color Cycles in Arctic Ocean Sediments Constrain Pleistocene Chronology." *Geology*, Vol. 28, No. 1, pp. 23-26.

Jakobsson, M., R. Lovlie, E.M. Arnold, J. Backman, L. Polyak, J.O. Knutsen, and E. Musatov, 2001. "Pleistocene Stratigraphy and Paleoenvironmental Variation from Lomonosov Ridge Sediments, Central Arctic Ocean." *Global and Planetary Change*, Vol. 31, pp. 1-22.

Jokat, W., G. Uenseimann-Neben, Y. Kristoffersen, and T.M. Rasmussen, 1992. "Lomonosov Ridge- A Double-sided Continental Margin." *Geology*, Vol. 20, pp. 887-890.

Jonkers, L., Prins, M.A., Brummer, G.-J.A., Koner, M., Lougheed, B.C., 2009. "Experimental Insights into Laser Diffraction Particle Sizing of Fine-Grained Sediments for Use in Paleoceanography." *Sedimentology*, Vol. 56, pp. 2192-2206.

Knies, J., Gaina, C., 2008. "Middle Miocene Ice Sheet Expansion in the Arctic: views from the Barents Sea". *Geochemistry, Geophysics, and Geosystems*, Vol. 9, Q02015. doi:10.1029/2007GC001824.

Knight, P.G., R.I. Waller, C.J. Patterson, A.P. Jones, and Z.P. Robinson, 2002. "Discharge of Debris from Ice at the Margin of the Greenland Ice Sheet." *Journal of Glaciology*, Vol. 48, No. 161, pp. 192-198.

Kotlyakov, V.M., and F.G. Gordienko, 1982. "Isotopic and Geochemical Glaciology." *Gidrometeoizdat*, Moscow.

Krissek, L.A., 1989. "Late Cenozoic Records of Ice-Rafting at ODP Sites 642, 643, and 644, Norwegian Sea: onset, chronology, and characteristics of glacial/interglacial fluctuations." *Proceedings of ODP, Scientific Results*, Edinburgh (Ocean Drilling Program Management International, Inc.).

Kristoffersen, Y., M.Y. Sorokin, W. Jokat, and O. Svendsen, 2004. A Submarine Fan in the Amundsen Basin, Arctic Ocean." *Marine Geology*, Vol. 204, pp. 317-324.

Krylov, A.A., Andreeva, I.A., Vogt, C., Backman, J., Krupskaya, V.V., Grikurov, G.E., Moran, K., Shoji, H., 2008. "A Shift in Heavy and Clay Mineral Provenance Indicates a Middle Miocene Onset of a Perennial Sea Ice Cover in the Arctic Ocean." *Paleoceanography* , Vol. 23, PA1S06. doi:10.1029/2007PA001497.

Lisiecki, L.E., Raymo, M.E., 2005. "A Pliocene-Pleistocene Stack of 57 Globally Distributed Benthic δ18O Records." *Paleoceanography*, Vol. 20, PA 1003. doi:10.1029/2004PA001071.

Lisitzin, A.P., 2002. Sea-Ice and Iceberg Sedimentation in the Ocean. Springer, NY.

Lisitzin, A.P., 1961. "Ice-Rafted Deposits and Glacial Epochs on the Polar Areas and their Importance for Paleogeography." *International Geography Congress in Stockholm*, pp. 33-43.

Lisitzin, A.P., and V.I. Chernyshova, 1970. "Rock Material from Bottom Sediments of the North Pacific." In: *The Pacific Ocean*, Nauka, Moscow, pp. 237-296.

Lisitzin, A.P., V.P. Shevchenko, M.E. Vinogradov, O.V. Severina, V.V. Vavilova, I.N. Mitzkevich, 1994. "Particle Fluxes in the Kara Sea and Ob and Yenisei Estuaries." *Oceanology*, Vol. 34, pp. 748-759.

Madureira, L.A.S., S.A. Kreveld, G. Eglington, H. Maureen, G. Ganssen, J.E. Hinte, J.J. Ottens, 1997. "Late Quaternary High-Resolution Biomarker and other Sedimentary Climate Proxies in a Northeast Atlantic Core." *Paleoceanography*, Vol. 12, pp. 255-269.

Maslin, M.A., X.S. Li, M.F. Loutre, and A. Berger, 1998. "The Contribution of Orbital Forcing to the Progressive Intensification of Northern Hemisphere Glaciation." *Quaternary Science Reviews*, Vol. 17, pp. 411-426.

McCave, I.N., 2008. "Size Sorting During Transport and Deposition of fine Sediments: Sortable Silt and Flow Speed." In: M. Rebesco, A. Camerlenghi (eds) *Contourites*. Developments in Sedimentology, Vol. 57.

McCave, I.N., and I.R. Hall, 2006. "Size Sorting in Marine Muds:Processes, pitfalls, and prospects for paleoflow-speed proxies." *Geochem. Geophys. Geosyst*., Vol. 7.

McCave, I.N., I.R. Hall, and G.G. Bianchi, 2006. "Laser vs. Settling Velocity Differences in Silt Grainsize Measurements: estimation of palaeocurrent vigour." *Sedimentology*, Vol. 53, pp. 919-928.

McCave, I.N., Manighetti, B., Robinson, S.G., 1995a. "Sortable Silt and Fine Sediment Size/Composition Slicing; Parameters for Paleocurrent Speed and Paleoceanography." *Paleoceanography,* Vol. 10, pp. 593-610.

McCave, I.N., Manighetti, B., Beveridge, N.A.S., 1995b. "Circulation in the Glacial North Atlantic Inferred from Grain Size Measurements." *Nature*, Vol. 374, pp. 149-152.

Mercer, J.H., 1970. "A Former Ice Sheet in the Arctic Ocean." *Palaeogeography, Palaeoclimatology, Palaeoecology*, Vol. 8, pp. 19-27.

Moran, K., V. Altmann, M. O'Regan, and C. Ashmankas, 2007. "Acoustic Compressional Wave Velocity as a Predictor of Glacio-marine Sediment Grain Size." *Geotechnical Testing Journal*, Vol. 30, No. 4.

Moran, K., J. Backman, H. Brinkhuis, S.C. Clemens, T. Cronin, G.R., Dickens, et al., 2006. "The Cenozoic Palaeoenvironment of the Arctic Ocean." *Nature*, Vol. 441, pp. 601-605.

Moros, M., Kuijpers, A., Snowball, I., Lassens, S., Backstrom, D., Gingele, F., McManus, J., 2002. "Were Glacial Iceberg Surges in the North Atlantic Triggered by Climatic Warming?" *Marine Geology*, Vol.192, pp. 393-417.

Mortlock, R.A., and P.N. Froelich, 1989. "A Simple Method for the Rapid Determination of Biogenic Opal in Pelagic Marine Sediments." *Deep-Sea Research*, Vol. 36, No. 9, pp. 1415-1426.

Mulholland, J.W., 1976. "Texture of Tills, Central Massachusetts." *Journal of Sedimentary Petrology*, Vol. 46, pp. 778-787.

Nam, S.I., R. Stein, H. Grobe, and H. Hubberten, 1995. "Late Quaternary Glacial-Interglacial Changes in Sediment Composition at the East Greenland Continental Margin and their Paleoceanographic Implications." *Marine Geology*, Vol. 122, pp. 243-262.

NECP, 2008. "Real-time , Global, Sea Surface Temperature Experimental Analysis: Arctic SST." < polar.ncep.noaa.gov/sst/ophi > (July 30, 2008).

Norgaard-Pedersen, N., R.F. Spielhagen, J. Thiede, and H. Kassens, 1998. "Central Arctic Surface Ocean Environment during the Past 80,000 Years." *Paleoceanography*, Vol. 13, No. 2, pp. 193-204.

Nurnberg, D., I. Wollenburg, D. Dethleff, H. Eicken, H. Kassens, T. Letzig, E. Reimnnitz, and J. Thiede, 1994. "Sediments in the Arctic Sea Ice: Implications for entrainment, transport, and release." *Marine Geology*, Vol. 119, pp. 185-214.

O'Regan, M.A., 2007. A Cenozoic History of the Central Arctic Ocean. University of Rhode Island Doctorate Dissertation.

O'Regan, M., St. John, K., Moran, K., Backman, J., King, J., Haley, B.A., Jakobsson, M., Frank, M., Rohl, U., 2010. "Plio-Pleistocene Trends in Ice Rafted Debris on the Lomonosov Ridge." *Quaternary International*, Vol. 219, pp. 168-176.

Pagani, M., Arthur, M.A., Freeman, K.H., 2000. "Variations in Miocene Phytoplankton Growth Rates in the Southwest Atlantic: Evidence for changes in ocean circulation." *Paleoceanography*, Vol. 15, pp. 486-496.

Pffirman, S.L., R. Colony, D. Nurnberg, H. Eicken, and I. Rigor, 1997. "Reconstructing the Origin and Trajectory of Drifting Arctic Sea Ice." *Journal of Geophysical Research*, Vol. 102, pp. 12575-12586.

Phillips, R.L., and A. Grantz, 1997. "Quaternary History of Sea Ice and Paleoclimate in the Amerasia Basin, Arctic Ocean, as Recorded in the Cyclical Strata of Northwind Ridge." *GSA Bulletin*, Vol. 109, No. 9, pp. 1101-1115.

Polyak, L., Darby, D.A., Bischof, J.F., Jakobsson, M., 2007. "Stratigraphic Constraints on Late Pleistocene Glacial Erosion and Deglaciation of the Chukchi Margin, Arctic Ocean." *Quaternary Research*, Vol. 67, pp. 234-245.

Poore, R.Z., R.L. Phillips, and H.J. Rieck, 1993. "Paleoclimate Record for Northwind Ridge, Western Arctic Ocean." *Paleoceanography*, Vol. 8, No. 2, pp. 149-159.

Prins, M.A., L.M. Bouwer, C.J. Beets, S.R. Troelstra, G.J. Weltje, R.W. Kruk, A. Kuijpers, and P.Z. Vroon, 2002. "Ocean Circulation and Iceberg Discharge in the Glacial North Atlantic: Inferences from unmixing of sediment size distributions." *Geology*, Vol. 30, No. 6, pp. 555-558.

Raymo, M.E., L.E. Lisiecki, and K.H. Nisancioglu, 2006. "Pli-Peistocene Ice Volume, Antarctic Climate, and the Global $\delta^{18}O$ Record." *Science*,

Reeh, N., 2004. "Holocene Climate and Fjord Glaciations in Northeast Greenland: implications for IRD deposition in the North Atlantic." *Sedimentary Geology*, Vol. 165, pp. 333-342.

Reimnitz, E., M. McCormick, K. McDougall, and E. Brouwers, 1993a. "Sediment Export by Ice-Rafting from Coastal Polynya, Arctic, Alaska, USA." *Arctic and Alpine Research*, Vol. 25, pp. 83-89.

Reimnitz, E., J.R. Clayton, E.W. Kempema, J.R. Payne, W.S. Wefer, 1993b. "Interaction of Rising Frazil with Suspended Particles: Tank experiments with application to nature." *Cold Regions Science and Technology*, Vol. 21, pp. 117-135.

Reimnitz, E., M. McCormick, J. Bischof, D.A. Darby, 1998. "Comparing Sea-Ice Sediment Load with Beaufort Sea Shelf Deposits: Is entrainment selective?" *Journal of Sedimentary Research*, Vol. 68, pp. 777-787.

Rennermalm, A.K., E.F. Wood, S.J. Dery, A.J. Weaver, and M. Eby, 2006. Sensitivity of the Thermohaline Circulation to Arctic Runoff. Geophysical Research Letters, Vol. 33, L12703.

Ruddiman, W.F., 1977a. "Late Quaternary Deposition of Ice Rafted Sand in the Subpolar North Atlantic (Lat. 40º to 65º N)." *Geological Society of America Bulletin*, Vol. 88, pp. 1813-1827.

Ruddiman, W.F., 1977b. "North Atlantic Ice Rafting: a major change at 75000 years before present." *Science*, Vol. 196, pp. 1208-1211.

Ruddiman, W.F., and L.K. Glover, 1972. "Vertical Mixing of Ice-Rafted Volcanic Ash in North Atlantic Sediments." *Geological Society of America Bulletin*, Vol. 83, pp. 2817-2836.

Ruddiman, W.F., and JOIDES NAAG-DPG, 1991. "North Atlantic-Arctic Gateways." *JOIDES Journal*, Vol. 17, pp. 38-50.

Ruddiman, W.F., and A. McIntyre, 1976. "Northeast Atlantic Paleoclimatic Changes over the Past 60000 Years." *Geological Society of America Mem*, Vol. 145, pp. 111-146.

Ruddiman, W.F., and A. McIntyre, 1977. "Late Quaternary Surface Ocean Kinematics and Climatic Change in the High-Latitude North Atlantic." *Journal of Geophysical Research*, Vol, 82, pp. 3877-3887.

Ruddiman, W.F., and A. McIntyre, 1981. "The North Atlantic Ocean during the Last Deglaciation." *Palaeogeography Palaeoclimatology Palaeoecology*, Vol. 35, pp. 145-214.

Ruddiman, W.F., and A. McIntyre, 1984. "Ice-Age Thermal Response and Climatic Role of the Surface Atlantic Ocean, 40ºN to 63ºN." *Geological Society of America Bulletin*, Vol. 95, pp. 381-396.

Ruddiman, W.F., N.J. Shackleton, and A. McIntyre, 1986. "North Atlantic Sea-Surface Temperatures for the Last 1.1 Million Years." In: M. Smmaerhayes, N.J. Shackleton (eds) *North Atlantic Palaeoceanography*. Geological Society Special Publications, Vol. 21, pp. 155-173.

Rutherford, S., and S. D'Hondt, 2000. "Early Onset and Tropical Forcing of 100,000-year Pleistocene Glacial Cycles." *Nature*, Vol. 408, pp. 72-75.

Sakamoto, T., M. Ikehara, K. Aoki, K. Iijima, N. Kimura, T. Nakatsuka, and M. Wakatsuchi, 2005. "Ice-Rafted Debris (IRD)- Based Sea-Ice Expansion Events during the Past 100 kyrs in the Okhotsk Sea." *Deep-Sea Research*, Vol. 52, pp. 2275-2301.

Schreiber, B.C., 1968. "Sound Velocity in Deep Sea Sediments." *Journal of Geophysical Research*, Vol. 73, pp. 1259-1268.

Schultheiss, P.J., and S.D. McPhail, 1989. "An Automated P-Wave Logger for Recording Fine-Scale Compressional Wave Velocity Structures in Sediments." *Proc. ODP Sci. Results*, Vol. 108, pp. 407-413.

Shackleton, N.J., J. Imbrie, and N.G. Pisias, 1988. "The Evolution of Oceanic Oxygen-Isotope Variability in the North Atlantic Over the Past Three Million Years." *Phil. Trans. R. Soc. Lond. B*, Vol. 318, pp. 679-688.

Singarayer, J.S., J.L. Bamber, and P.J. Valdes, 2006. "Twenty-First Century Climate Impacts from a Declining Arctic Sea Ice Cover." *Journal of Climate*, Vol. 19, pp. 1109-1124.

Smythe, F.W., W.F. Ruddiman, and D.N. Lumsden, 1985. "Ice-Rafted Evidence of Long-term North Atlantic Circulation." *Marine Geology*, Vol. 64, pp. 131-141.

Goossens, D., 2008. "Techniques to Measure Grain-Size Distributions of Loamy Sediments: a comparative study of ten instruments for wet analysis." *Sedimentology*, Vol. 55, pp. 65-96.

Steurer, J.F., and M.B. Underwood, 2003. "Data Report: The Relation Between Physical Properties and Grain-Size Variations in Hemipelagic Sediments from Nankai Trough." *In* Mikada, H., G.F. Moore, et al. (*Eds*.), *Proc. ODP Sci. Results*, Vol. 190/196.

Stickley, C.E., K. St John, N. Koc, et al., 2009. "Evidence for Middle Eocene Arctic Sea Ice from Diatoms and Ice-Rafted Debris." *Nature*, Vol. 460, pp. 376-390.

St. John, K., 2008. "Cenozoic Ice-Rafting History of the Central Arctic Ocean: Terrigenous Sands on the Lomonosov Ridge." *Paleoceanography*, Vol. 23.

Svendsen, J.I., Alexanderson, H., Astakhov, V.I.,, et al., 2004. "Late Quaternary Ice Sheet History of Northern Euraisa." *Quaternary Science Reviews*, Vol. 23, pp. 1229-1271.

Thiede, J., O. Eldholm, E. Taylor, 1989. "Variability of Cenozoic Norwegian-Greenland Sea Paleoceanography and Northern Hemisphere Paleoclimate." *Proceedings of ODP, Scientific Results*, Vol. 104.

Tripati, A., J. Backman, H. Elderfield, and P. Ferretti, 2005. "Eocene Bipolar Glaciation Associated with Global Carbon Cycle Changes." *Nature*, Vol. 436, pp. 341-346.

Vanney, J., and L. Dangeard, 1976. "Les deposits glacio-marins actuels et anciens." *Rev Geogr Montr*, Vol. 30, pp. 9-50.

Vorren, T.O., and J. Thiede, 1994. "The Marine Geology of the Arctic Ocean." *Marine Geology*, Vol. 119, pp. 357-361.

Wefer, G., E. Suess, W. Balzer, et al., 1982. "Fluxes of Biogenic Components from Sediment Trap Deployment in Circumpolar waters of the Antarctic sector." In: U. Bleil and J. Thiede (eds) *Geological History of the Polar Oceans: Arctic versus Antarctic*, Kluwer Academic Publishing, Dordrecht, pp. 245-254.

Wefer, G., G. Fisher, D. Futterer, R. Gersonde, S. Honjo, D. Osterman, 1990. "Particle Sedimentation and Productivity in Atlantic waters of the Atlantic sector." In: U. Bleil and J. Thiede (eds) *Geological History of the Polar Oceans: Arctic versus Antarctic*, Kluwer Academic Publishing, Dordrecht, pp. 363-380.

Weller, P., and R. Stein, 2008. "Paleogene Biomarker Records from the Central Artic Ocean (IODP Exp. 302): Organic Carbon Sources, Anoxia, and Sea Surface Temperatures. " *Paleoceanography*, Vol. 23.

Wen, B., Aydin, A., Duzgoren-Aydin, N.S., 2002. "A Comparative Study of Particle Size Analyses by Sieve-Hydrometer and Laser Diffraction Methods." *ASTM Geotechnical Testing Journal*, Vol. 25, pp. 434-442.

Winter, B.L., C.M. Johnson, and D.L. Clark, 1997. "Strontium, Neodymium, and Lead Isotope Variations of Authigenic and Silicate Sediment Components from the Late Cenozoic Arctic Ocean: Implications for Sediment Provenance and the Source of Trace Metals in Seawater." *GSA*, Vol. 61, No. 19, pp. 4181-4200.

Winton, M., 2006. "Amplified Arctic Climate Change: What does surface albedo feedback have to do with it?" *Geophysical Research Letters*, Vol. 33, L03701.

Wolf-Welling, T.C.W., M. Cremer, S. O'Connell, A. Winkler, and J. Thiede, 1996. "Cenozoic Arctic Gateway Paleoclimate Variablity Indications from Changes in Coarse-Fraction Composition." *Proceedings of the Ocean Drilling Program, Scientific Results*, Vol. 151, pp. 515-567.

Woodruff, F., Savin, S.M., 1989. "Miocene Deepwater Oceanography." *Paleoceanography*, Vol. 4, pp. 87-140.

Woods Hole Oceanographic Institution, 2008. "Image: Arctic Ocean Circlation Primer." Polar Research, <www.whoi.edu/page.do?pid=12317&tid=441&cid=41043&ct=61&article=23446>. (March 3, 2008).

Zachos, J., M. Pagani, L. Sloan, E. Thomas, and K. Billups, 2001. "Trends, Rhythms, and Aberrations in Global Climate 65 Ma to Present." *Science*, Vol. 292, pp. 686-693.